Etude du comportement à long terme des membranes échangeuses d'ions utilisées dans les procédés d'électrodialyse

Wendy Garcia-Vasquez

▶ **To cite this version:**

Wendy Garcia-Vasquez. Etude du comportement à long terme des membranes échangeuses d'ions utilisées dans les procédés d'électrodialyse. Matériaux. Université Paris-Est, 2013. Français. NNT : 2013PEST1111 . tel-01397697

HAL Id: tel-01397697

https://theses.hal.science/tel-01397697

Submitted on 16 Nov 2016

HAL is a multi-disciplinary open access archive for the deposit and dissemination of scientific research documents, whether they are published or not. The documents may come from teaching and research institutions in France or abroad, or from public or private research centers.

L'archive ouverte pluridisciplinaire **HAL**, est destinée au dépôt et à la diffusion de documents scientifiques de niveau recherche, publiés ou non, émanant des établissements d'enseignement et de recherche français ou étrangers, des laboratoires publics ou privés.

ÉCOLE DOCTORALE UNIVERSITÉ PARIS-EST
Sciences, Ingénierie et Environnement

Thèse

présentée pour obtenir le titre de DOCTEUR de l'Université Paris-Est en
Chimie et Sciences des Matériaux

Etude du comportement à long terme des membranes échangeuses d'ions utilisées dans les procédés d'électrodialyse

Wendy GARCIA-VASQUEZ

Soutenue publiquement le 27/09/2013 devant un jury composé de :

Rapporteurs	Xavier COLIN, Professeur	Arts et Métiers Paris Tech
(*Président du jury)*	Gérald POURCELLY, Professeur	Université de Montpellier II
Examinateurs	Shingjiang Jessie LUE, Professeur	Chang Gung University (Taiwan)
	Victor NIKONENKO, Professeur	Kuban State University (Russie)
	Daniel GRANDE, Chargé de recherche	ICMPE, CNRS
Invitée	Florence LUTIN, Directeur R&D	EURODIA INDUSTRIE S.A
Directeurs de thèse	Christian LARCHET, Professeur	Université Paris-Est Créteil
	Lasâad DAMMAK, Professeur	Université Paris-Est Créteil

Thèse réalisée au Institut de Chimie et des Matériaux Paris-Est
Equipe Systèmes Polymères Complexes
2-8 rue Henri Dunant
94320 Thiais

Tél : +33 (0)1 49 78 11 81
Fax : +33 (0)1 49 78 11 66

Web : http ://www.icmpe.cnrs.fr/

Sous la direction de Professeur Lasâad Dammak dammak@u-pec.fr
Co-direction Professeur Christian Larchet larchet@u-pec.fr

A Marco, Verónica, Natalie, Marco Vinicio y Chaíto

Al que vivió los desvelos, sufrió los altibajos y se ocupó de que yo no me alimentara únicamente de dulces y café, Pierrick

Avant Propos

Excepté le chapitre bibliographique, cette thèse a été rédigée sous la forme d'un recueil de quatre publications parues ou soumises dans des revues à comité de lecture. L'indulgence du lecteur est donc sollicitée pour les répétitions inhérentes à ce choix de forme de rédaction.

Remerciements

Ce travail de thèse a été réalisé au sein de l'équipe Systèmes Polymères Complexes de l'Institut de Chimie et Matériaux Paris-Est. Je remercie Valérie Langlois, son responsable, de m'y avoir accueilli.

Je tiens à remercier Professeur Lasâad Dammak et Professeur Christian Larchet, mes directeurs de thèse, pour m'avoir proposé ce sujet. Je les remercie pour leur aide et leurs conseils scientifiques toujours judicieux.

Je désire exprimer ma sincère reconnaissance au Professeur Gérald Pourcelly et au Professeur Xavier Colin, pour avoir accepté de juger ce travail ainsi qu'au Dr. Daniel Grande, au Professeur Victor Nikonenko, au Professeur Jessie Lue et au Dr. Florence Lutin pour avoir accepté de participer à ce jury de thèse.

Je tiens à témoigner ma gratitude et mon amitié aux membres de l'Institut des Membranes de l'Université de Kuban en Russie, tout particulièrement à Victor et Natalia pour leurs précieux conseils et leur accueil très chaleureux au sein de leur laboratoire, Спасибо за ваше руководство, Я никогда не сделал бы этого без тебя! Je remercie à cet égard le CNRS pour la création du Laboratoire Franco-Russe « Membranes Echangeuses d'Ions et Procédés Associés ».

Je tiens aussi à remercier EURODIA Industrie S.A. et sa directrice R&D, Mme. Florence Lutin pour leurs contributions en échantillons, équipements et matériels pour l'électrodialyse ainsi que pour leurs conseils. Leur expérience technique a été essentielle pour la bonne réalisation de ce travail.

Mes remerciements se dirigent ensuite vers Madame Shingjiang Jessie Lue et son équipe à l'Université de Chang Gung à Taiwan pour leur gentillesse, l'ambiance du laboratoire et leur aide tout au long de mon séjour. 感謝您！ 讓我在台期間， 留下許多美好回憶，也感謝您協助我的研究工作， 以及無條件的包容. Je remercie l'Université Paris-Est pour la bourse de mobilité internationale qui m'a été accordé.

Je voudrais exprimer toute ma gratitude aux membres de l'Equipe Ionique et Electrochimie de l'Institut Européen des Membranes de Montpellier tout particulièrement Stephano Deabate, Phillipe Sistat et Gérald Pourcelly pour le temps qu'il ont consacré à m'aider avec les protocoles expérimentaux et pour l'intérêt qu'ils ont porté à ce travail. Ma gratitude va également aux membres de l'équipe GPM où j'ai réalisé mon projet de fin d'études, leur influence a été déterminante dans la décision de me former dans la recherche.

Je remercie Rym Ghalloussi pour m'avoir accompagné dans le début de cette thèse et pour sa patiente ainsi qu'aux stagiaires Alejandro Bermejo et Manel Moussa pour leur précieuse contribution aux protocoles expérimentaux. Un grand merci en particulier à Alejandra Baldetti pour son travail de grande qualité.

Cette étude n'aurait pas été possible sans l'aide des chercheurs du laboratoire. Je remercie donc vivement Christine Gaillet, Pierre Dubot, Remy Pires, Olivier Rouleau et Diana Dragoe pour le temps qu'ils ont passé à réaliser les essais en RMN en phase solide, XPS, EDX, WAXS et ICP. Je voudrais ensuite remercier tous ceux qui, de près ou de loin, ont apporté leur contribution à ce travail, en particulier Nelly Lacoudre, Julien Babinot et Benjamin Villeroy qui m'ont formé sur les différentes techniques de l'institut. Ce travail a également bénéficié de discussions fructueuses avec les différents membres du laboratoire, je pense notamment à Florent Dalmas et Daniel Grande.

Merci également à David, Julien, Sandrine, Benjamin, Pierre, Gaëlle, Romain et Cédric pour tous nos bons moments au labo ou ailleurs.

Je remercie mes parents, ma sœur et mon frère pour leur soutien sans faille y por haber venido desde tan lejos para mostrarme una vez más que no importa lo que pase, ellos siempre estarán ahí…

Enfin, je souhaite remercier Pierrick pour ses encouragements permanents, sa patiente et son courage pour m'avoir supporté durant ces trois dernières années.

Table de matières

Table de Figures

Liste de Tableaux

Table 4-7. Percentage of increase or decrease in the mechanical and physic-chemical properties of AEM samples after exposure to 2 M NaOH for 700 h, 2 M HCl for 700 h and the HCl-NaOH ageing cycle for 400 h, compared to the new samples.

Introduction générale

Ce travail est dédié à l'étude du comportement à long terme des membranes échangeuses d'ions utilisées en procédés d'électrodialyse conventionnelle.

L'électrodialyse est une opération unitaire pour la séparation ou la concentration des ions en solution, basée sur l'électromigration sélective à travers les membranes échangeuses d'ions sous l'influence d'un gradient de potentiel électrique. L'intégration de cette technologie dans des procédés de purification, concentration ou déminéralisation rend le procédé plus propre et moins énergivore.

De nombreuses applications ont été développées ces dernières années dans des différents champs d'application. Il a été prouvé que l'électrodialyse est efficace pour la concentration ou la séparation de produits agroalimentaires ou pharmaceutiques contenant des espèces ioniques, ainsi que dans la fabrication de produits chimiques. En revanche, toutes les potentialités de l'électrodialyse n'ont pas encore été entièrement exploitées. Parmi les raisons on trouvera sans doute, les coûts élevés des membranes échangeuses d'ions et leurs courtes durées de vie dans les applications moins conventionnelles, en particulier celles de l'industrie agroalimentaire.

Les membranes échangeuses d'ions tendent à perdre de leurs propriétés physicochimiques et séparatives tout au long de leur utilisation. Le vieillissement de ces matériaux est accompagné d'une diminution du rendement des opérations et de l'augmentation des coûts, due à des remplacements plus fréquents des membranes échangeuses d'ions et à l'augmentation de la consommation d'énergie. Le comportement à long terme des membranes échangeuses d'ions et leurs mécanismes de vieillissement doivent encore être compris afin de surmonter de nombreux obstacles techniques qui empêchent leurs développements.

Nous nous sommes intéressés à la compréhension des causes de dégradation des membranes échangeuses d'ions ainsi qu'aux mécanismes de vieillissement. Nous avons étudié également, les différences du comportement à long terme des membranes possédant des structures distinctes : homogènes et hétérogènes.

Lors de ce travail de thèse nous avons analysé le comportement à long terme de nombreuses membranes échangeuses d'ions utilisées dans des procédés d'électrodialyse pour l'industrie agroalimentaire. Nous avons ainsi comparé leurs propriétés physico-chimiques, structurales et mécaniques à celles des mêmes membranes n'ayant jamais servies. L'approche adoptée dans notre étude est à la fois expérimentale et théorique. Les membranes étudiées sont tirées

directement d'empilements industriels après différents temps de fonctionnement (*in-situ*), ou vieillies artificiellement dans le laboratoire (*ex-situ*).

Le premier chapitre est consacré à une synthèse bibliographique sur les membranes échangeuses d'ions, sur l'électrodialyse et ses applications, ainsi que sur le vieillissement des membranes échangeuses d'ions.

Dans le second et troisième chapitre, nous avons présenté les résultats expérimentaux du vieillissement *in-situ*. Nous avons étudié, dans un premier temps, des membranes échangeuses d'ions après deux ans de service dans la purification des acides organiques (chapitre 2), ainsi que des membranes échangeuses d'anions utilisées pour la déminéralisation du lactosérum à différents moments de leur cycle de vie en électrodialyse (chapitre 3). Cela nous a permis, d'une part, d'approfondir la connaissance de leurs propriétés et de leurs microstructures, et d'autre part, de proposer des mécanismes appropriés de vieillissement.

Ensuite, dans le quatrième et cinquième chapitre, nous avons abordé l'approche du vieillissement *ex-situ*. Nous avons ainsi réalisé le vieillissement artificiel de différentes membranes échangeuses d'ions, homogènes et hétérogènes, dans l'acide chlorhydrique concentré, dans l'hydroxyde de sodium concentré, dans des cycles acide-base simulant les conditions du nettoyage classique en électrodialyse (chapitre 4), ainsi que dans l'hypochlorite de sodium (chapitre 5). Les résultats ont été corrélés aux interprétations réalisées sur le vieillissement en électrodialyse industrielle, et des mécanismes de vieillissement ont été proposés.

Enfin, le sixième chapitre présente une première approche scientifique à l'étude du nettoyage chimique des membranes échangeuses d'ions afin d'identifier les indicateurs principaux pour mieux cibler des études futures sur ce thème.

Dans chaque chapitre, l'état de l'art de chaque sujet présenté, et les méthodes expérimentales qui nous ont permis d'atteindre nos objectives sont décrits.

Chapitre 1

Synthèse bibliographique

1.1. Généralités sur les membranes échangeuses d'ions

1.1.1. Définitions

Les membranes échangeuses d'ions (MEIs) peuvent être définies comme étant des films insolubles qui contiennent des anions ou des cations fixes et d'autres mobiles et agissent comme une barrière à perméabilité sélective entre deux compartiments. Les ions mobiles sont en mesure d'être substitués d'une manière stœchiométrique par d'autres ions de même charge lorsque la membrane est en contact avec une solution d'électrolyte et aussi de permettre leur transfert d'un compartiment à l'autre sous l'action d'une force qui peut être une différence de pression, de concentration ou de potentiel.

Selon leur charge, nous pouvons classer les MEIs en deux types :

- Les membranes échangeuses de cations (MECs) qui contiennent des groupes chargés négativement tels que SO_3^-, COO^-, PO_3^{2-} et HPO_2^- fixés à une matrice de polymère. Les groupes sont également appelés sites fonctionnels ou sites fixes. Leur nombre de mole par unité de masse de la membrane caractérise la capacité d'échange du matériau.

  Dans une MEC, des anions fixes sont en équilibre électrique avec des cations mobiles dans les interstices du polymère.

  Les cations mobiles sont appelés contre-ions. Les anions mobiles sont appelés des co-ions et sont plus ou moins exclus de la matrice de la membrane en raison de leur charge électrique qui est identique à celle des ions fixes. En raison de l'exclusion des co-ions (dite exclusion de Donnan), une MEC est perméable aux cations. La Fig. 1-1a représente schématiquement la matrice d'une MEC avec les anions fixes et les cations mobiles. Le nombre et la mobilité de chaque espèce ionique échangeable dans la membrane définissent sa capacité à conduire l'électricité ; on parle alors de la conductivité électrique de ce matériau.

  Cette exclusion n'est jamais totale. On cherche alors un compromis entre la perméabilité (capacité à laisser passer les ions) et la sélectivité (capacité à ne laisser passer que les contre-ions) d'une MEI ; il s'agit de la permsélectivité de ce matériau.

- Les membranes échangeuses d'anions (MEAs) qui contiennent des groupes chargés positivement tels que RNH_2^+, R_2NH^+, R_3N^+ fixés à une matrice de polymère. Elles excluent donc les cations et sont perméables aux anions.

Les MEIs peuvent aussi être divisées en deux grandes catégories en fonction de leur structure et des procédures de leur préparation : homogènes ou hétérogènes (Fig. 1-1).

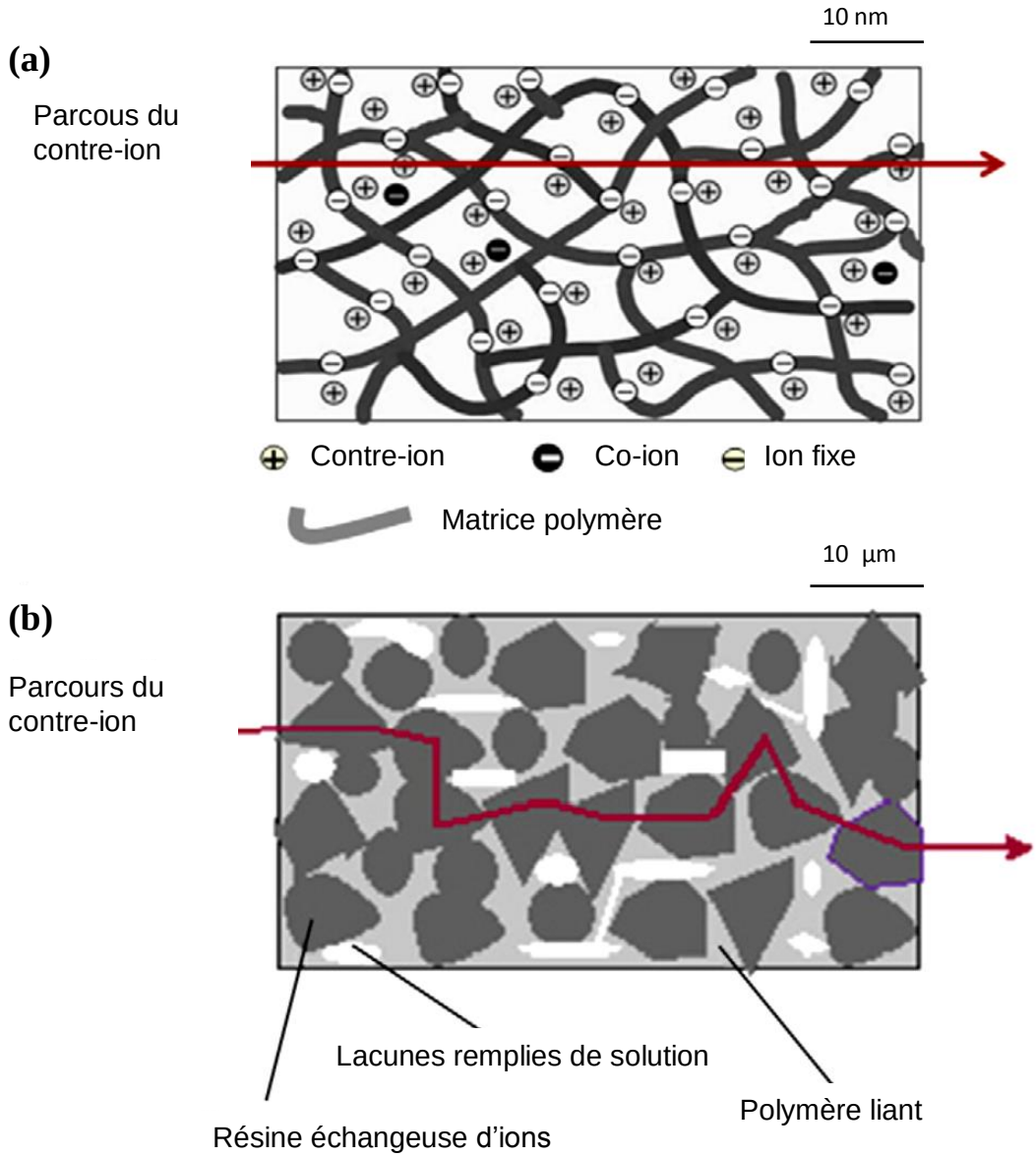

Fig. 1-1. Représentation schématique illustrant a) une membrane échangeuse de cations avec une structure homogène, et b) une membrane échangeuse d'ions avec une structure hétérogène [1].

- Les membranes hétérogènes sont souvent préparées à partir de grains de résines échangeuses d'ions dispersés dans un liant inerte pour former un film. L'intérêt de ces membranes réside dans la variété des possibilités d'association des propriétés du polymère liant avec les qualités physico-chimiques de l'échangeur d'ions.
- Les membranes homogènes sont préparées par introduction du groupement fonctionnel directement dans la structure du polymère de la membrane. Cela conduit à une distribution relativement homogène des groupes chargés sur l'ensemble de la matrice de la membrane.

Selon Molau [2], il existe plusieurs formes intermédiaires entre une MEI homogène et une MEI hétérogène. Cet auteur a proposé une classification de la morphologie de la membrane en fonction du degré d'hétérogénéité et du type et de la taille de la microphase. Toutefois, pour des raisons pratiques, nous allons juste faire la différence entre les MEIs homogènes et hétérogènes.

1.1.2. Caractéristiques attendues d'une membrane échangeuse d'ions

- Une bonne perméabilité sélective

La membrane doit être perméable aux seuls contre-ions, dans un large domaine de concentrations en électrolyte de la solution externe, et imperméable aux co-ions. Dans ce cas la membrane est dite idéalement permsélective.

- Une faible résistance électrique

Dans les cellules électrochimiques ou les modules de techniques séparatives, la résistance électrique totale est presque essentiellement due aux membranes. Pour diminuer au maximum la dépense énergétique, la résistance électrique des membranes doit être donc la plus faible possible.

Elle dépend de plusieurs caractéristiques de la membrane : capacité d'échange, taux de réticulation et structure (homogène ou hétérogène) mais aussi de la concentration et de la nature (valence et taille) des ions des solutions électrolytiques en contact avec la membrane.

- Une bonne stabilité mécanique

L'introduction des membranes dans des modules de géométrie filtre-presse nécessite une bonne tenue mécanique afin qu'elles puissent résister aux différences de pression sans se fissurer. D'autre part, une bonne stabilité dimensionnelle est requise lorsque les solutions

externes voient leurs concentrations en électrolyte varier, ce qui entraîne des variations de gonflement.

- Une bonne stabilité chimique

Suivant les applications, la membrane peut se trouver au contact de milieux agressifs tels que des acides, des bases ou des solutions oxydantes. Dans la mesure du possible, les membranes doivent être stables lors de leurs utilisations dans des conditions opératoires limites (pH fortement acide ou basique, présence d'oxydants).

- Un faible coût

La majeure partie des investissements de maintenance des procédés membranaires est consacrée au remplacement des membranes qui est souvent onéreux à cause du coût d'achat des membranes auquel vient s'ajouter la perte de productivité suite à l'arrêt de l'installation. Ainsi, plusieurs efforts doivent être faits non seulement pour réduire les coûts de fabrication mais aussi pour améliorer leur tenue, leur durée de vie, leurs résistances mécanique et chimique.

1.1.3. Préparation des membranes échangeuses d'ions

La Fig. 1-2 montre la vue de surface et la vue transversale d'une MEI hétérogène (Fig. a et b) et d'une MEI homogène avec un support mécanique (Fig. c et d). Leurs structures sont essentiellement différentes car leurs modes de préparation diffèrent fondamentalement.

Généralement, les membranes homogènes présentent de bonnes propriétés électrochimiques et une faible résistance mécanique, alors que les membranes hétérogènes ayant une très bonne résistance mécanique ont relativement une grande résistance électrique [3, 4]. Cependant, plusieurs auteurs ont constaté qu'il est possible d'avoir de bonnes membranes échangeuses d'ions par la combinaison optimale des propriétés électrochimiques et de la résistance mécanique en les préparant selon la méthode hétérogène [5-9].

1.1.3.1. Membranes hétérogènes

Les membranes échangeuses d'ions hétérogènes sont par exemple préparées par incorporation mécanique d'une poudre de résine échangeuse d'ions dans du PVC, du polyéthylène, des copolymères d'acrylonitrile ou d'une autre matrice extrudable ou moulable. Ces membranes peuvent être préparées soit par [8, 10, 11]:

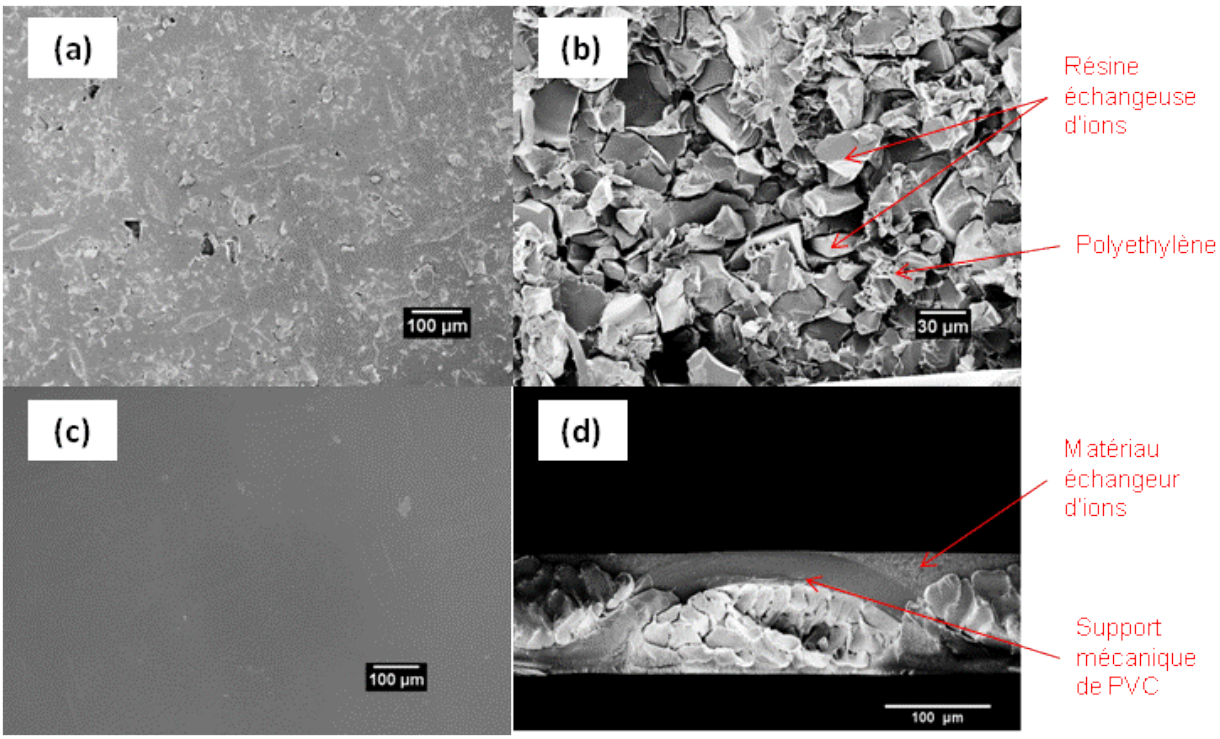

Fig. 1-2. Images MEB d'une MEI avec une structure hétérogène préparée à partir d'une poudre de résine échangeuse d'ions et d'un polymère liant a) vue de face, b) vue transversale ; MEI de type Neosepta® avec une structure homogène c) vue de face, d) vue transversale.

- Le calendrage des particules échangeuses d'ions dans un film plastique inerte.
- Le moulage à sec des films inertes formant des polymères et des particules d'échange d'ions, puis broyage du stock de moulage.
- La dispersion des particules de résine dans une solution contenant un liant pour former un film, puis l'évaporation du solvant pour former un film mince.

Cette méthode de préparation entraîne une structure dans laquelle les groupes échangeurs d'ions sont regroupés et très inégalement répartis dans la matrice de la membrane. La plupart des membranes hétérogènes, ont des coûts de production relativement faibles, mais ils ont une résistance électrique plus élevée, du fait que les ions mobiles font un chemin plus long dans la structure hétérogène (Fig. 1-1b) [12].

Vyas et al. [4] ont constaté que la quantité de résine et la répartition de la taille de ces particules affectent les propriétés mécaniques et électrochimiques des membranes. Ils ont observé qu'avec l'augmentation de la quantité en résine, les membranes deviennent de plus en plus fragiles. Après un certain point, une inversion de phase a lieu, ainsi les particules de

résines réticulées ont tendance à former une phase continue et le liant devient une phase discrète. Les particules de résine étant naturellement plus fragiles que le liant, elles ne parviennent pas à agir comme répartiteur de contrainte et la propagation des fissures est facilitée, ce qui donnera une membrane fragile.

Ces auteurs on vérifié également que plus la résine est fine, plus la membrane est flexible car le mélange sera plus homogène et ainsi on obtiendra une membrane plus souple.

La taille de la particule de résine a aussi une influence sur la capacité d'échange effective et sur la résistance électrique de la membrane [12]. Pour une quantité de résine et une épaisseur de membrane définies, la résistance électrique diminue et la capacité d'échange augmente avec la diminution de la taille des particules. Cette diminution est la cause d'une augmentation de la surface spécifique de la résine et donc du nombre de groupes fonctionnels peuvent participer au transport des contre-ions à travers la membrane, ce qui conduira à une résistance plus faible, et à une capacité d'échange d'ions plus élevée.

Oren et al. [6] ont constaté que las MEIs hétérogènes ayant des particules échangeuses d'ions hautement ordonnées sont potentiellement plus performantes que les membranes traditionnelles avec des particules dispersées de façon aléatoire en raison de la quantité réduite de matière échangeuse d'ions nécessaire pour atteindre la conductivité ionique souhaitée. Ils ont montré que la baisse de la quantité d'échangeurs d'ions entraîne une importante réduction de la quantité de l'eau dans la membrane même si la conductivité reste la même ou est améliorée.

Hosseini et al. ont montré que l'incorporation d'additifs comme l'acrylonitrile-butadiène-styrène ou le polystyrène (PS) choc dans la formulation de la membrane [8], ou la distribution de nanoparticules d'argent sur la surface de la membrane [7], améliorent les propriétés électrochimiques des membranes hétérogènes. En outre, sous les mêmes conditions expérimentales, les membranes préparées présentent des propriétés électrochimiques améliorées comparés aux MEIs hétérogènes commerciales.

1.1.3.2. Membranes homogènes

Les membranes homogènes sont constituées exclusivement du matériau échangeur d'ions, formant une seule phase. Dans les membranes homogènes, les sites fonctionnels sont liés de façon covalente au squelette du polymère.

Les méthodes de fabrication de membranes échangeuses d'ions homogènes peuvent se classer en trois catégories différentes :

- L'introduction de groupements anioniques ou cationiques dans un film solide préformé [13-18].
- La polymérisation en chaîne ou la polycondensation de monomères ; au moins l'un d'eux doit comporter un groupement qui est ou qui peut devenir un groupe anionique ou cationique [19-22].
- L'introduction de groupements anioniques ou cationiques dans un polymère, suivie par dissolution et coulage [23, 24].

Le greffage induit par radiation est une autre méthode largement utilisé pour l'introduction de groupements anioniques ou cationiques dans un film solide préformé. Il est réalisé en utilisant des méthodes d'irradiation UV ou plasma.

Pour préparer des MECs des monomères acryliques, l'acide acrylique [16-18] et les acides méthacryliques [25, 26] sont greffés sur des films de polymère, puis le groupe époxy est converti en une fonction carboxylique. On peut aussi greffer du styrène sur des films de polymère suivi d'une sulfonation du PS [27, 28].

Le procédé couramment utilisé pour la préparation des MEAs est le greffage de monomères vinyliques comme le styrène, sur des films polymères, suivie par des modifications chimiques ultérieures, comme la chlorométhylation-amination au lieu de la sulfonation [29].

Néanmoins, le succès de ces membranes est limité. Lorsque le greffage induit par radiation est pratiqué à grande échelle, la quantité d'énergie électrique nécessaire à la production est d'une part très coûteuse et d'autre part physiquement impossible [30].

Si la membrane est préparée à partir de monomères, le styrène (St) et le divinylbenzène (DVB) sont les produits de départ neutres les plus couramment utilisés [31, 32].

Les membranes commercialisées par Tokuyama Soda Co. (Neosepta®) sont copolymerisées avec du St et du DVB, suivie par une sulfonation ou une amination pour former respectivement les membranes échangeuses de cations et d'anions. La sulfonation du polymère est réalisée à l'aide d'acide chlorosulfonique ou d'acide sulfurique concentré (Fig. 1-3). La membrane échangeuse d'anions est préparée par la chlorométhylation du polymère, suivie par une amination (Fig. 1-4).

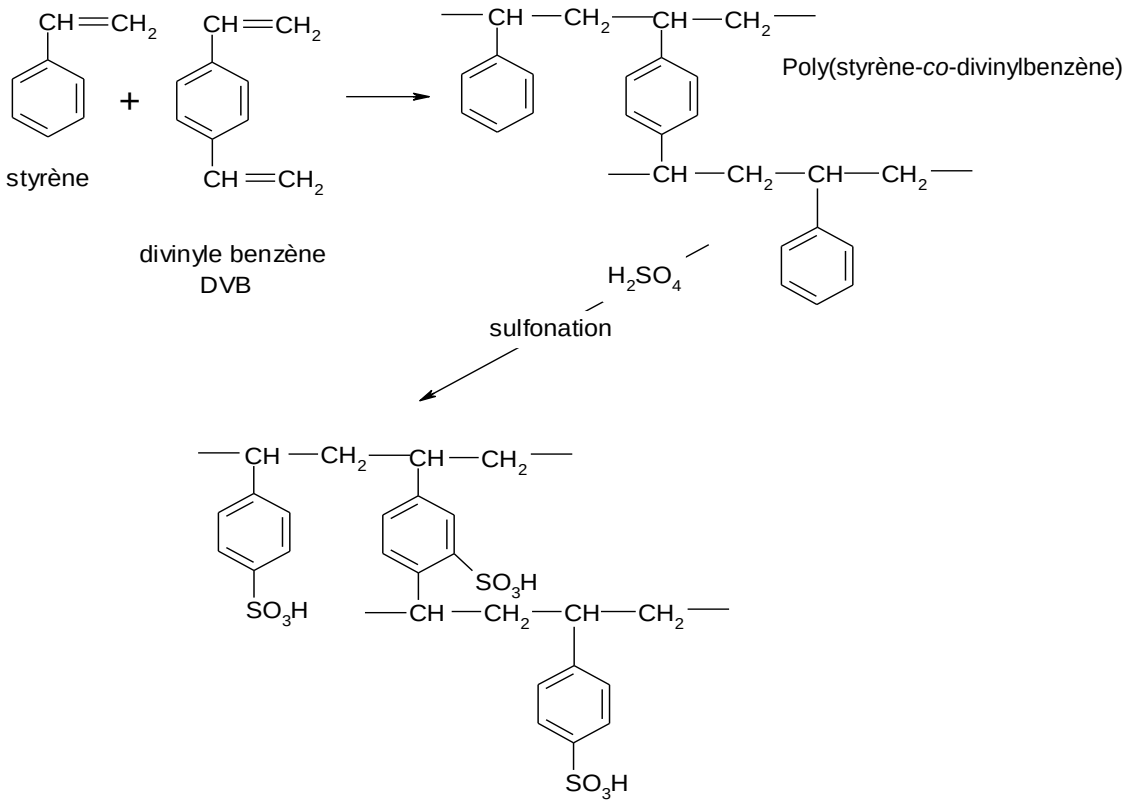

Fig. 1-3. Préparation d'une MEC homogène à partir des monomères St et DVB.

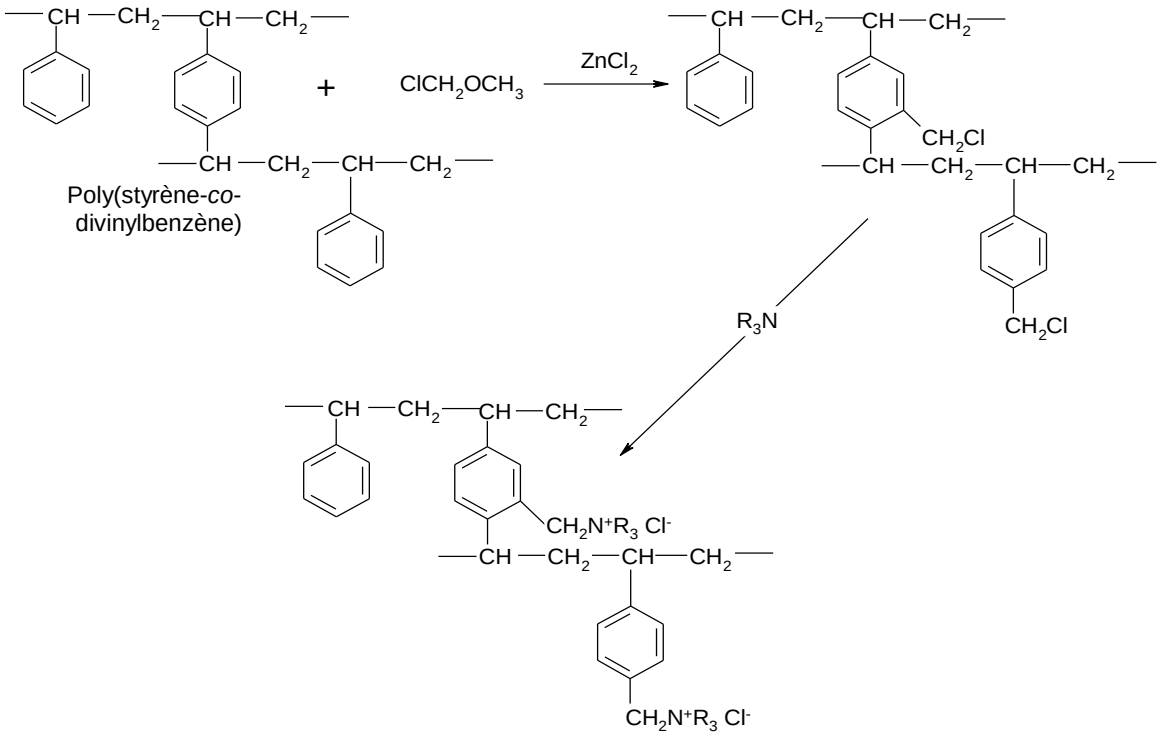

Fig. 1-4. Préparation d'une MEA homogène à partir des monomères St et DVB.

Dans cette étude, nous nous sommes intéressés à l'étude de ces membranes car elles sont largement utilisées dans les procédés d'électrodialyse à échelle industrielle. Le schéma de fabrication de ces membranes sur la base des travaux de Mizutani [31] et Xu [33] est illustré dans la Fig. 1-5.

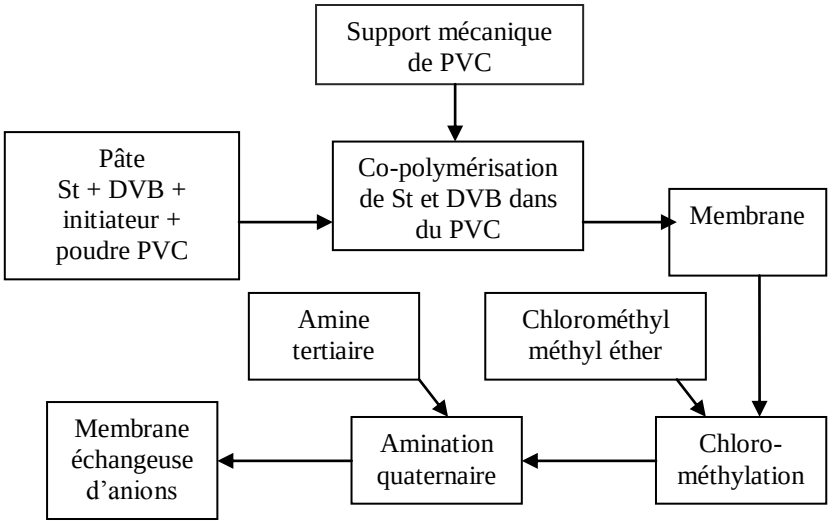

Fig. 1-5. Voie de fabrication d'une MEA hydrocarbonée [31, 33].

Les membranes perfluorés de type Nafion® sont des MEIs homogènes qui ont suscité l'intérêt de nombreux industriels et chercheurs par leurs exceptionnelles qualités chimiques et physiques. Elles sont largement utilisées dans le procédé chlore-soude et pour les piles à combustible mais pas pour l'électrodialyse du fait de leur coût. Ainsi, nous ne développons pas leurs méthodes de préparation.

En comparaison avec les MEIs hétérogènes décrites précédemment, les membranes homogènes sont connues pour leurs meilleures performances dans les applications électromembranaires, [1, 30, 33]. Ces membranes offrent une répartition de charges ionique fixes plus homogène sur toute la matrice polymère.

Les membranes hétérogènes montrent une meilleure stabilité dimensionnelle que celle des membranes homogènes. Dans le cas des membranes hétérogènes, la perte de solvant par évaporation entraîne la formation de macropores formés par les fissures entre les particules de résines et le liant inerte. Le volume des macropores est suffisant pour accueillir les molécules de solution qui viennent solvater des espèces ioniques dans la résine, de telle sorte que les dimensions de la membrane ne changent pas. Cette caractéristique des MEIs hétérogènes

pourrait être considérée comme une compensation de la faiblesse de leurs propriétés électrochimiques ce qui permet d'améliorer leur durabilité dans les applications industrielles.

1.1.4. Les modèles membranaires

La connaissance des relations qui relient la structure de la membrane avec les caractéristiques de transport est d'une importance fondamentale pour le développement des procédés membranaires. L'effet de la non-uniformité de la membrane sur les caractéristiques de transport des ions a été étudiée dans un certain nombre de documents [34-38]. Il a été montré par exemple que les propriétés de transport membranaire, telles que la conductivité électrique, la diffusion, la perméabilité hydraulique et la permsélectivité, y compris la concurrence entre les ions de même signe, sont déterminées par la morphologie interne de la membrane. La complexité de cette morphologie rend impossible l'étude exacte de toutes les interactions entre espèces mobiles (solvant, contre-ions, co-ions, solutés moléculaires,…) et le matériau. Il est donc nécessaire de concevoir des modèles membranaires, qui peuvent être définis comme étant des images théoriques, à paramètres calculables ou mesurables, inspirées de la réalité sans être forcément confondues avec elle, permettant de décrire le comportement d'une membrane dans des conditions physico-chimiques données. Un modèle est d'autant meilleur qu'il décrit correctement un plus grand nombre de comportements membranaires.

Nous distinguons deux grandes familles de modèles représentatifs d'une MEI : les modèles électriques appelés également électrochimiques [39-41] et les modèles physico-chimiques.

Les modèles électrochimiques décrivent le comportement d'une MEI sous l'effet d'un gradient de potentiel électrique. Toutefois, ils sont moins efficaces en présence d'autres forces motrices (gradient de concentration, gradient de pression, gradient de température,…). Il est donc nécessaire d'utiliser d'autres modèles basés sur la structure très fine des membranes et permettant d'interpréter les phénomènes de transport en présence d'une ou plusieurs forces motrices ; ce sont les modèles physico-chimiques.

1.1.4.1. Les modèles physicochimiques

Les MEIs sont des systèmes multiphasiques hébergeant des composants polaires et non-polaires dans une matrice polymère. Les échangeurs d'ions à l'état sec sont des diélectriques avec une conductivité de l'ordre de 10^{-5} S. m^{-1}. L'état conducteur d'une membrane est induit par une solution électrolytique qui entraîne une augmentation brusque de la conductivité du

matériau (ordres de grandeur de 2 à 3 fois) [42]. Cet effet indique la formation de « canaux de transport » d'ions et de l'eau dans la structure de la membrane influencée par le champ électrique et la force ionique de la solution externe. La distribution spatiale des molécules d'eau, des sites fonctionnels et des espèces ioniques, ainsi que leurs concentrations spécifiques au sein de la membrane, correspondent à une configuration donnée de l'ensemble du matériau membranaire et déterminent par conséquent leurs propriétés structurelles, mécaniques, thermiques et électrochimiques. Chaque famille de configuration est spécifique à un type de matériaux ou à un mode de transport.

Nous pouvons donc classer ces configurations, ou modèles, en deux catégories : les modèles descriptifs et les modèles quantitatifs permettant d'écrire des équations de transport. Dans les modèles quantitatifs nous allons décrire les modèles à répartition de phases.

1.1.4.1.a. Les modèles descriptifs

Des nombreuses études sur la structure des membranes chargées ont été effectuées sur des MEIs perfluorées de type Nafion®. La notion générale acceptée est celle basée sur des « clusters » de solution (4 à 5 nm de diamètre) reliés par des canaux étroits de 1 à 1,5 nm.

Selon le modèle de Gierke [43, 44], le cluster possède une forme sphérique (Fig. 1-6). Les ions fixes sont disposés à la périphérie du cluster, ce qui assure le minimum d'énergie superficielle et exclut tout contact du polymère hydrophobe avec de l'eau. Les contre-ions mobiles neutralisent la charge des ions fixes en formant avec eux une double couche électrique. Le volume intérieur du cluster est rempli avec une solution aqueuse. Bien que les canaux entre les clusters soient thermodynamiquement stables, la variation d'énergie lors de leur formation est faible (environ -11 $J.cm^{-3}$). Pour cette raison, Timashev [45] a émis l'hypothèse que les canaux apparaissent et disparaissent en permanence.

Plus tard, un nouveau modèle de canaux a été proposé [45, 46] et amélioré par Tovbin et Vasyutkin [47] pour expliquer des nouveaux résultats obtenus par diffraction de rayons X, spectroscopie Mössbauer et d'autres méthodes. D'après ce modèle à trois dimensions, la membrane perfluorée a une structure périodique « feuilletée » à deux types de canaux-pores. Les pores du premier type ont une forme de fente et portent les sites fonctionnels. Un pore de ce type représente un cluster hydraté. Les pores de deuxième type sont plutôt cylindriques et jouent un rôle analogue aux canaux du modèle de Gierke.

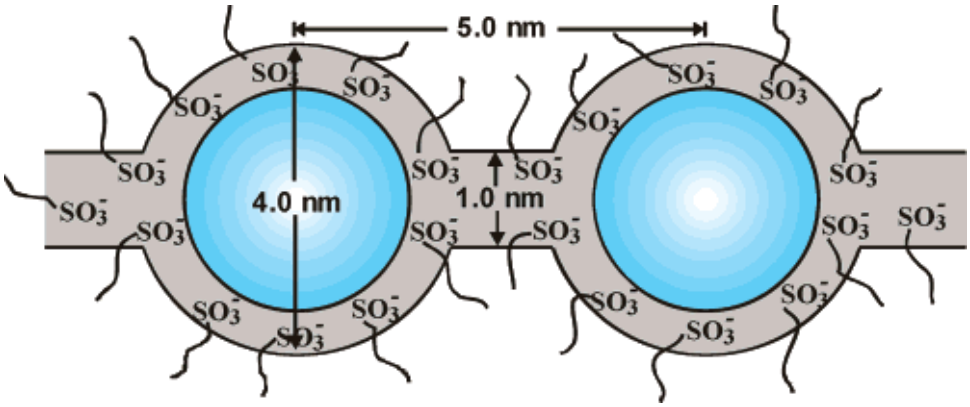

Fig. 1-6. Modèle de Gierke : notion de clusters et de canaux [44, 48].

Des études récentes proposent une interprétation des propriétés de percolation de la conductivité protonique en fonction de la teneur en eau à l'aide d'un « modèle du réseau aléatoire » [49] qui est une modification du modèle « clusters-canaux ». Ce modèle comporte une zone intermédiaire dans laquelle les chaînes latérales se terminant par des groupes acide sulfonique qui ont tendance à se grouper à l'intérieur de la structure globale formant ainsi des régions hydratées. Un schéma du réseau des clusters et du model du réseau aléatoire est représenté par la Fig. 1-7.

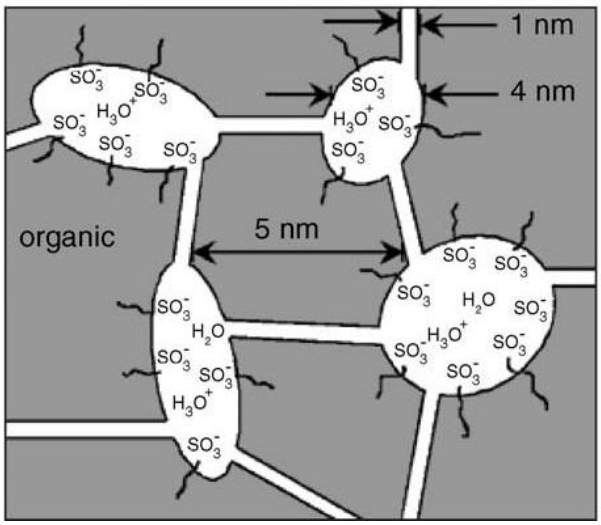

Fig. 1-7. Vue schématique du « modèle du réseau aléatoire » [49].

Contrairement au modèle « clusters-canaux », les régions hydratées sont réparties de manière aléatoire dans la matrice polymère, ce qui facilite le transport rapide d'ions lors de la rotation de ces chaînes latérales.

Une modèle représentant la microstructure de la membrane Nafion®117 a été présenté par Kreuer et al. [50-52] (Fig. 1-8) en utilisant les résultats de la diffraction des rayons-X aux petits angles et de la caractérisation physico-chimique de ces membranes.

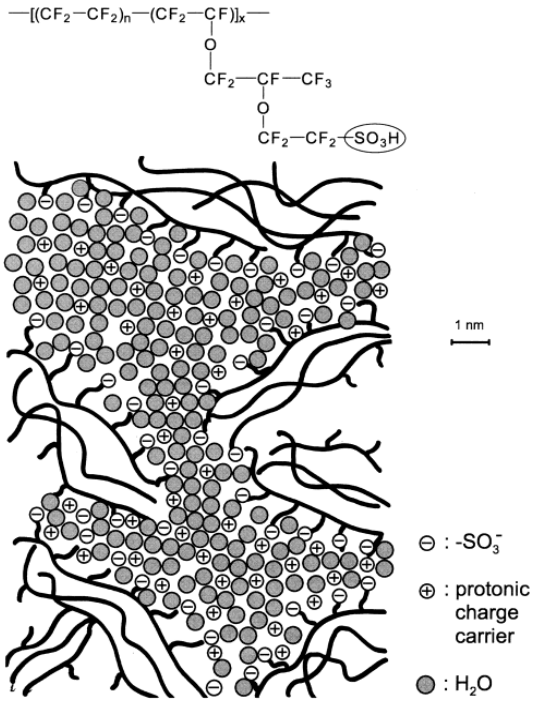

Fig. 1-8. Représentation schématique de la microstructure de la membrane Nafion® 117 selon Kreuer [51].

Pour ces auteurs, l'extrême hydrophobie des chaînes perfluorées de la membrane Nafion® et la très grande hydrophilie des sites fonctionnels sulfoniques engendre une nano-séparation des différentes phases. Les sites sulfoniques s'attirent pour former des domaines hydrophiles. Les chaînes hydrophobes assurent la stabilité de la membrane et évitent sa dissolution dans l'eau.

Ce modèle suppose que les clusters soient séparés par de petits canaux et que les dimensions des clusters et des canaux sont très proches de celles données par Gierke, Tovbin et Vasyutkin.

La structure est peu ramifiée ce qui est due à une différence d'hydrophobicité importante entre les deux phases. Selon ce modèle, il existe une bonne connectivité entre les différents

domaines hydrophiles (canaux et clusters) et une faible distance entre les sites fonctionnels – SO_3^- / $–SO_3^-$ qui facilite considérablement le passage des contre-ions d'un site à l'autre.

1.1.4.1.b. Le modèle à solution interstitielle homogène (1 phase)

C'est l'une des premières représentations utilisées pour modéliser le transfert de matière à travers des membranes échangeuses d'ions. Teorell, Meyer et Sievers [53] considéraient que l'ensemble de la membrane imprégnée de solution constituait une phase parfaitement homogène de sites fonctionnels, de contre-ions et de co-ions. Pour donner une représentation imagée du modèle, ils divisent le réseau macromoléculaire par le nombre de sites fixes ionisés ; cela revient à définir une espèce représentative du matériau, notée par exemple R^- dans le cas d'une MEC. Cette espèce comprend le site fonctionnel proprement dit et un fragment de la chaîne de polymère avoisinante, qui ensemble constituent le motif répétitif de la matrice. Il devient alors possible de représenter une MEI caractérisée par l'espèce R^- en équilibre avec une solution d'électrolyte M^+, A^- par une image du type suivant (Fig. 1-9).

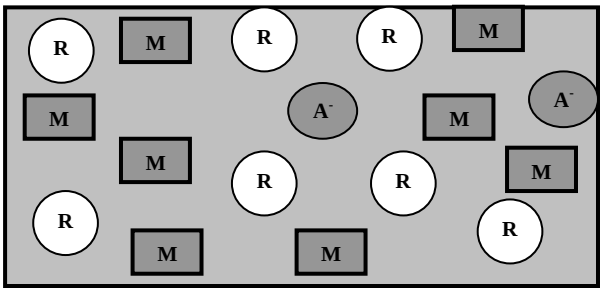

Fig. 1-9. Schéma représentatif du modèle à solution interstitielle homogène

Les concentrations des différentes espèces sont rapportées au volume total de l'échangeur et les flux sont calculés par rapport à toute la section en contact avec les solutions extérieures.

1.1.4.1.c. Le modèle microhétérogène (2 phases)

Le modèle microhétérogène permet de tenir compte à la fois de l'existence de différentes phases dans la MEI et de la disposition de ces phases les unes par rapport aux autres.

Considérons une MEI constituée de différentes zones électroneutres. Chacune de ces régions peut être caractérisée par un ensemble de paramètres physico-chimiques tels que la concentration des sites fixes et des ions mobiles, la conductivité en présence d'un contre-ion,

la perméabilité de diffusion. Ces zones sont également appelées « phases ». La notion de phase (microphase) est utilisée ici pour désigner un ensemble de petites zones caractérisées par les mêmes propriétés physico-chimiques. La membrane est supposée macrohomogène puisque les propriétés physico-chimiques de deux tranches fines coupées parallèlement aux interfaces et comprenant de nombreuses zones sont les mêmes.

Dans le cadre du modèle microhétérogène [38, 54, 55], la densité de flux normale à la surface membranaire est donnée par la relation :

$$J_i = -\frac{L_i^* d\tilde{\mu}_i}{dx} \tag{1.1}$$

Où $d\tilde{\mu}_i$ est la variation du potentiel électrochimique entre deux sections parallèles à la surface membranaire considérées aux distances *x* et *x*+*dx* de l'interface gauche.

Dans la Fig. 1-10 nous pouvons distinguer les deux phases de la membrane microhétérogène: (A) phase gel avec des groupes fonctionnels fixes; (B) phase inter-gel. La direction globale du courant est indiquée par une flèche. Deux plans équipotentiels, ainsi que les distances caractéristiques, macroscopiques (*dx*) et microscopiques (δ*x*), sont indiquées. Le transfert d'ions global à l'échelle macroscopique est déterminé par le gradient de potentiel électrochimique ($\tilde{\mu}_i$) sur la distance *dx*.

La phase gel est conformée par l'ensemble des chaînes macromoléculaires sur lesquelles sont greffés les sites fonctionnels équilibrés par les contre-ions et le solvant d'hydratation. La phase intergel est associée à la solution interne à la membrane qui est de même nature que la solution d'équilibrage.

Le coefficient effectif de conductance membranaire L_i^*, est une fonction des coefficients $L_i^{(k)}$ relatifs aux éléments de phase *k* (*k* =1, 2, …, N), des formes géométriques de ces éléments, leurs dispositions dans l'espace et leurs fractions volumiques :

$$L_i^* = \varphi\left(L_i^{(k)}, \Gamma\right) \tag{1.2}$$

où Γ est un ensemble de paramètres géométriques. Les éléments des différentes phases se trouvant dans une même tranche d'épaisseur *dx* sont supposés être en équilibre local entre

eux. Dans ce cas L_i^* est une fonction de la concentration locale des solutions électroneutres remplissant les zones centrales des pores situés entre les deux sections *x* et *x+dx* (Fig. 1-10).

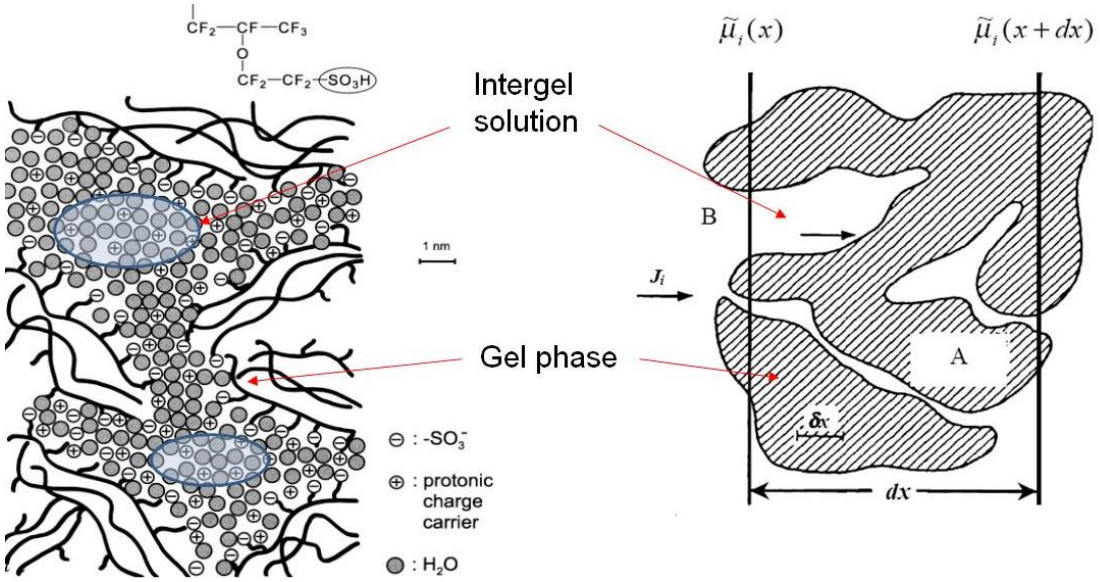

Fig. 1-10. A droite : Les deux phases de la membrane microhétérogène : (A) phase gel avec des groupes fonctionnels fixes ; (B) phase inter-gel. A gauche : les phases gel et inter-gel de la membrane Nafion® selon Kreuer [51].

Comme la distance *dx* est supposée petite, la variation de L_i^* dans cette tranche entre *x* et *x+dx* est négligeable. Ainsi, toutes les caractéristiques de cette tranche peuvent être reliées à l'abscisse x. Dans le cas d'une membrane microporeuse, qui ne contient pas de solution électroneutre, L_i^* peut être considéré comme fonction de la concentration de la solution virtuelle électroneutre en équilibre avec la tranche de membrane comprise entre *x* et *x+dx*.

Sous l'hypothèse d'un équilibre local, la relation :

$$\frac{d\tilde{\mu}_i}{dx} = \frac{[\tilde{\mu}_i(x+dx) - \tilde{\mu}_i(x)]}{dx} \tag{1.3}$$

peut être écrite pour n'importe quelle phase constituant la membrane :

$$\frac{d\tilde{\mu}_i}{dx} = RT\frac{d\ln a_i}{dx} + z_i F\frac{d\varphi}{dx} \tag{1.4}$$

où l'activité a_i et le potentiel φ sont reliés à la solution électroneutre (virtuelle) à l'abscisse x dans la membrane. R, T et F ont leurs significations habituelles. La substitution de l'équation (1.4) dans l'équation (1.1) donne l'équation de Nernst-Planck écrite avec un coefficient local de perméabilité de diffusion :

$$J_i = -L_i^*\left(RT\frac{d\ln a_i}{dx} + z_i F\frac{d\varphi}{dx}\right) \tag{1.5}$$

Après avoir considéré deux cas limites où les phases gel et intergel sont disposées en parallèle ou en série (Fig. 1-11), l'expression suivante est proposée pour les coefficients de conductance membranaires L_i^* comme fonction des quantités $\bar{L}_i$ et L_i dans la phase gel et solution, respectivement :

$$L_i^* = \left[f_1\bar{L}_i^{\alpha} + f_2 L_i^{\alpha}\right]^{1/\alpha} \tag{1.6}$$

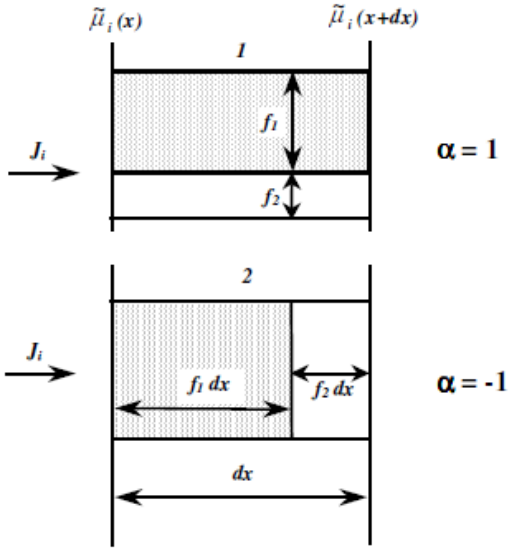

Fig. 1-11. Dispositions relatives des phases gel et intergel dans le cas du modèle microhétérogène.

Dans l'expresion 1.6, f_1 et f_2 sont les fractions volumiques des phases gel et intergel, respectivement ; α est le paramètre de structure caractérisant la disposition relative des phases : $\alpha = 1$ correspond à une disposition parallèle, $\alpha = -1$ au cas en série.

$\bar{L}_i$ et L_i peuvent être présentés comme fonction des coefficients de diffusion $\bar{D}_i$ et D_i , et des concentrations ioniques $\bar{c}_i$ et c_i dans les phases correspondantes :

$$L_i = \frac{D_i c_i}{RT}, \ \bar{L}_i = \frac{\bar{D}_i \bar{c}_i}{RT} \tag{1.7}$$

1.1.4.1.d. Modèle à solution interstitielle hétérogène (3 phases)

Le modèle à solution interstitielle hétérogène (SIH) a été développé par Auclair, Larchet et al. [56, 57]. Il suppose que la solution interstitielle remplissant l'espace entre les chaînes de polymères peut être séparée en deux zones :

- Une zone dite active qui contient l'ensemble des sites fonctionnels, les contre-ions les équilibrant et une partie de la masse du solvant qui a pénétré dans l'échangeur. La concentration des contre-ions étant très élevée dans cette zone, l'exclusion de l'électrolyte peut y être considérée comme pratiquement totale.
- Une zone dite inerte, par opposition à la précédente, qui ne contient aucun site actif et qui est caractérisée par une masse de solvant. L'exclusion de l'électrolyte est nulle et sa concentration y est égale à celle de la solution d'équilibrage.

La zone « inerte » est identique à la solution électroneutre remplissant les parties centrales des mésopores et des macropores. La zone « active » représente la zone chargée de la solution contenue dans les pores, donc elle représente la double couche électrique. Nous pouvons aussi interpréter la phase « gel » du modèle microhétérogène comme la somme des chaînes de polymères avec les sites fixes et de la zone « active ».

Le modèle SIH a permis d'interpréter correctement plusieurs phénomènes intervenant dans les MEI : la sorption d'électrolyte, la perméabilité hydraulique, la diffusion d'électrolyte.

Nous avons représenté sur la Fig. 1-12, la solution interstitielle comprise entre deux chaînes macromoléculaires greffées et reliées par un pont ne portant pas de sites fonctionnels.

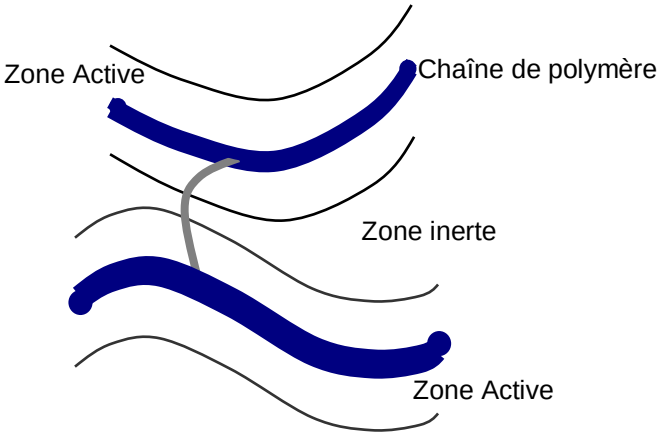

Fig. 1-12. Schéma du modèle à solution interstitielle hétérogène

Le modèle à solution interstitielle homogène est trop simpliste car il considère que la MEI n'est formée que d'une seule phase homogène, du même volume que la membrane et où toutes les espèces peuvent se déplacer à travers tout ce volume. Il n'exclut pas le volume des chaines de polymère et ne tient pas compte de l'organisation des parties hydrophiles et des parties hydrophobes.

Le modèle SIH apparaît plus détaillé, puisqu'il permet d'exclure le volume du polymère hydrophobe et sépare la phase hydrophile en deux parties différentes. Cependant, la caractérisation de chacune de ses trois phases est complexe ce qui a réduit considérablement son utilisation dans la modélisation des MEIs et des phénomènes de transport à travers ces matériaux.

Le modèle microhétérogène apparaît comme un bon compromis entre les modèles à solution interstitielle homogène et hétérogène, puisqu'il est caractérisé par deux phases. Ainsi, il est suffisamment détaillé pour tenir compte de la structure interne des MEIs et suffisamment simple pour ne pas avoir des calculs complexes à effectuer [58-60]. Par ailleurs, il reste un modèle bien développé dans la littérature [38, 42] avec de nombreuses études qui ont été effectuées sur sa validité [61, 62]. Nous avons choisi d'appliquer ce modèle pour exploiter nos résultats tout en apportant quelques améliorations.

1.1.5. Applications des membranes échangeuses d'ions

Selon leurs applications, les procédés utilisant des MEIs peuvent être classés en trois catégories principales [1] :

- Les procédés de séparation de masse tels que l'électrodialyse, la dialyse de diffusion, la dialyse de Donnan, l'électrodialyse avec des membranes bipolaires et l'électrodéionisation.
- Les procédés de synthèse chimique tel que le procédé chlore-soude et la production d'hydrogène et d'oxygène par électrolyse de l'eau.
- Les procédés de conversion et de stockage d'énergie tels que les piles à combustible et les batteries.

Nous nous sommes plus particulièrement intéressés aux procédés électromembranaires pour la séparation de masse que nous expliquerons avec plus de détails dans cette section.

1.1.5.1. La dialyse de diffusion

La dialyse de diffusion est un procédé de séparation qui utilise la diffusion ionique à travers d'une MEI, provoquée par un gradient de concentration.

Cette technique est appliquée aujourd'hui principalement dans la récupération d'acides ou de bases des effluents provenant de la production de l'acier et des métaux non-ferreux, du raffinage des métaux, de la galvanoplastie, de la régénération des résines échangeuses de cations et de la gravure d'aluminium [63, 64].

La Fig. 1-13 illustre d'une manière simplifiée le mécanisme de purification de l'acide chlorhydrique de ses sels métalliques. L'acide et le sel se trouvent dans la solution d'alimentation et tendent à diffuser à travers la membrane les séparant d'un deuxième compartiment alimenté en eau. En raison de la présence d'une MEA, les ions Cl^- (ou SO_4^{2-}, NO_3^-, PO_4^{3-}, etc.) sont autorisés au passage tandis que les métaux ($\mathbf{M^{n+}}$) dans la solution d'alimentation sont pratiquement arrêté.

Bien que les ions H^+ soient chargés positivement, en raison de leur petite taille ils ont une plus grande mobilité que les ions $\mathbf{M^{n+}}$. Par conséquent, ils peuvent diffuser avec les anions pour répondre à l'exigence de neutralité électrique [65]. Le transport des ions H^+ à travers de la MEA est un élément clé du processus demandant des propriétés appropriées spécifiques à ce

type de membranes, notamment une bonne stabilité en solution acide, une haute perméabilité aux ions H^+, un fort rejet pour les ions métalliques et une faible perméabilité à l'eau.

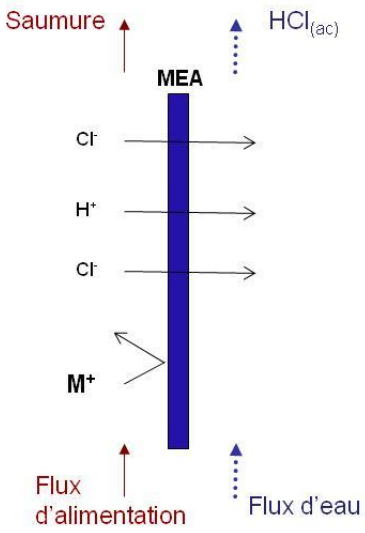

Fig. 1-13. Principe de la dialyse de diffusion pour la purification du HCl d'un mélange d'acide et du sel ($\mathbf{M}^{n+}$, nCl^-) avec une MEA.

L'avantage de la dialyse de diffusion réside dans son faible impact environnemental et sa faible consommation d'énergie. Parmi ses limitations nous trouverons sa faible capacité et le besoin d'une grande surface de membrane afin d'obtenir un débit convenable.

1.1.5.2. La dialyse ionique croisée ou dialyse de Donnan

La dialyse ionique croisée est un procédé de séparation membranaire dans lequel deux ou plusieurs ions sont échangés de part et d'autre de la membrane ionique sous la seule action de leur gradient de concentration [66].

Cette technique a reçu des applications très diverses dans le domaine industriel comme l'élimination des fluorures [67, 68], des nitrates [69-71] et d'arséniates [72, 73] des eaux usées. A l'heure actuelle, la dialyse de Donnan est une alternative pour le prétraitement des eaux avant le dessalement par électrodialyse [74-76].

Dans l'adoucissement des eaux (Fig. 1-14), les ions polyvalents tels que Ca^{2+}, sont enlevés d'un flux d'alimentation par échange avec des ions monovalents tels que Na^{+} à travers une MEC.

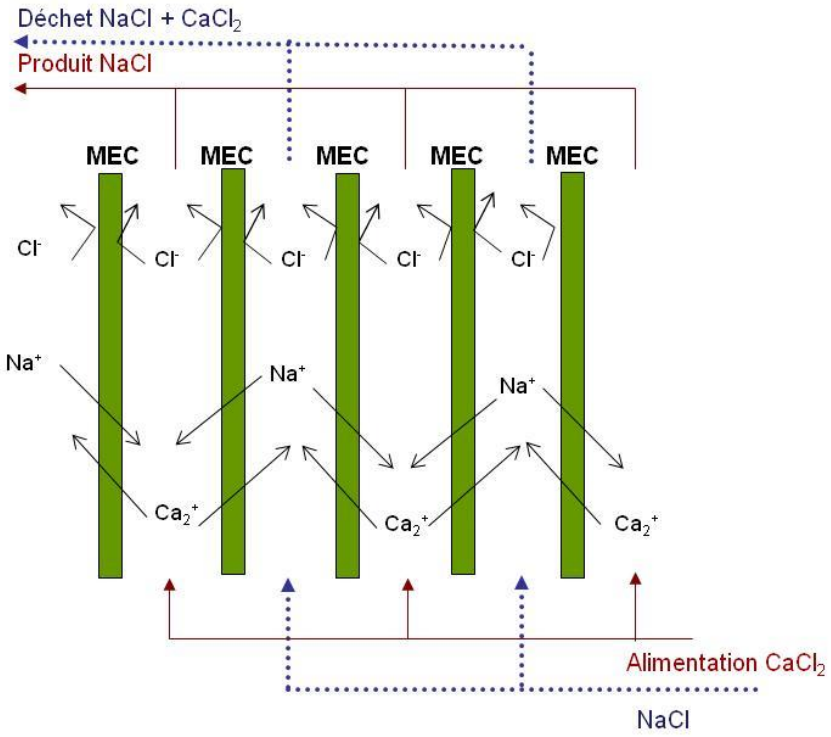

Fig. 1-14. Principe de la dialyse ionique croisée ou dialyse de Donnan dans un procédé d'adoucissement de l'eau par échange des ions Ca^{2+} contre Na^{+} dans un empilement avec des MECs.

Parmi les avantages de la dialyse de Donnan, nous pouvons mentionner les économies d'énergie comparativement aux procédés d'électrodialyse car on n'utilise pas de courant électrique. Par rapport à l'utilisation des résines échangeuses d'ions, la dialyse de Donnan n'a pas besoin de régénération et fonctionne en continu. Toutefois, le système n'est pas toujours avantageux car le gradient de concentration (et le gradient du potentiel résultant) est faible et il devient nécessaire d'utiliser une grande surface de membrane (ce qui représente des forts coûts d'investissement) afin d'obtenir un débit convenable.

1.1.5.3. L'électrodialyse

L'électrodialyse est un procédé électromembranaire qui utilise des MEIs soumises à l'action d'un champ électrique. Cette technique permet l'extraction ou la reconcentration d'espèces ionisées, dans le but, soit de dessaler un effluent, soit d'en récupérer des produits valorisables [32].

Il s'agit de placer sur le trajet des ions des séries alternées de membranes permsélectives aux anions et aux cations. La migration est limitée dans les compartiments formés par cette série de membranes, certains s'appauvrissent tandis que d'autres s'enrichissent en espèces ioniques.

Le schéma de la Fig. 1-15 permet d'illustrer l'agencement des membranes et les différents flux de transfert qui interviennent pendant l'électrodialyse d'une solution d'électrolyte M^+X^-.

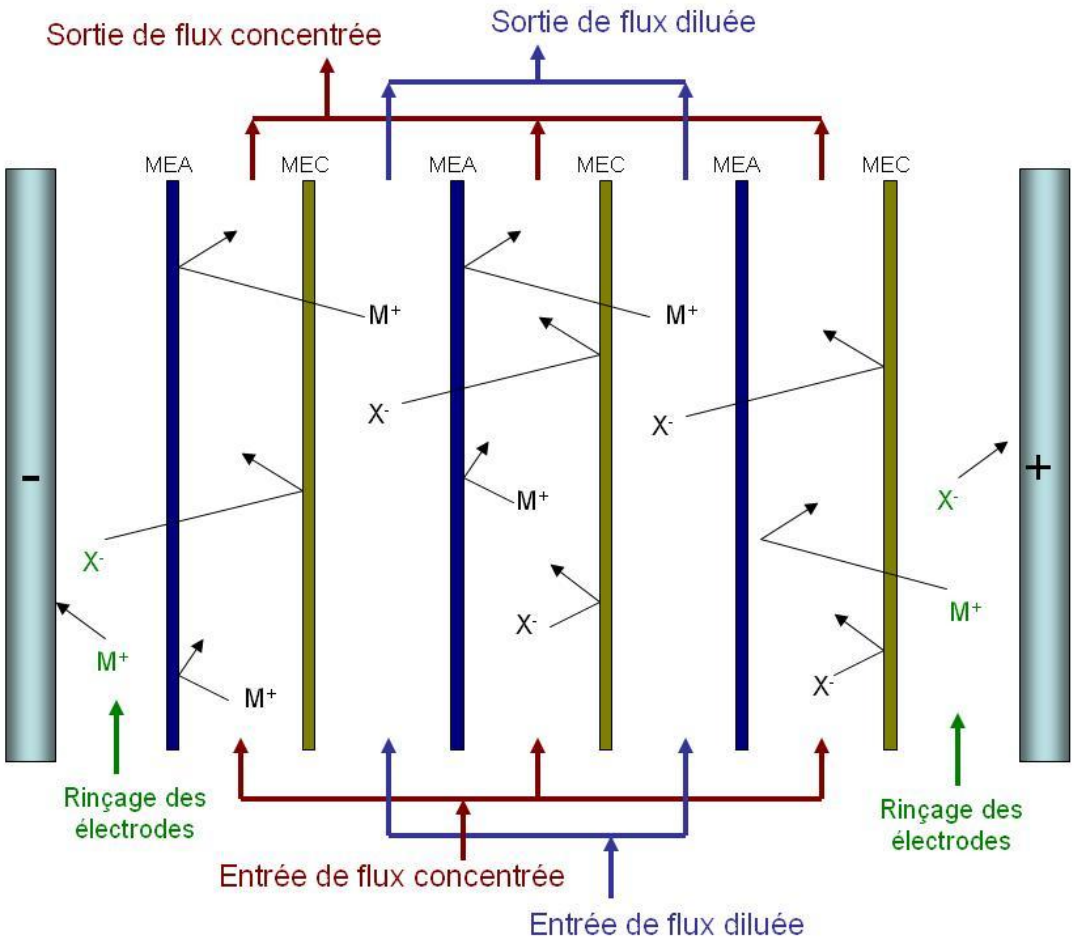

Fig. 1-15. Empilement d'électrodialyse avec des MECs et des MEAs alternées entre deux électrodes, pour le dessalement d'une solution d'électrolyte.

Les MEAs et MECs sont disposées alternativement entre deux électrodes situées aux extrémités du module. Une cellule élémentaire est constituée de deux compartiments, un dilué et un concentré. Lors du passage du courant électrique, les cations sont attirés par le pôle négatif : ils peuvent quitter le compartiment dilué en migrant à travers la MEC mais sont piégés dans le compartiment concentré à cause de la présence de la MEA. Les anions migrent en sens inverse. Ainsi, le compartiment dit dilué dans lequel arrive l'effluent brut s'appauvrit progressivement en espèces ioniques (la solution qui en résulte est appelée diluât) tandis que le compartiment dit concentré s'enrichit en ces mêmes ions (concentrât).

Les espèces neutres présentes dans l'alimentation ne sont pas concernées et se retrouvent dans le diluât. Les électrodes sont maintenues au contact de circuits indépendants isolés par des membranes et destinées seulement à assurer la conduction électrique et à éliminer les produits de réactions aux électrodes. Dans les installations industrielles, les empilements peuvent atteindre plusieurs centaines de cellules élémentaires dans des assemblages de type filtre-presse [77]. L'espace entre une paire de MEIs est occupé par des espaceurs en polymère qui, par leur géométrie et leur forme, fixent l'épaisseur du compartiment et le régime hydrodynamique. En effet, ces espaceurs créent des turbulences locales au niveau des interfaces membrane / solution qui permettent d'améliorer les échanges en réduisant l'effet des couches limites de diffusion [78].

1.1.5.4. Electrodialyse à membranes bipolaires

Une membrane bipolaire (MBP) est une membrane multicouche construite de telle sorte que l'une surface est une couche échangeuse de cations, tandis que la surface opposée est une couche échangeuse d'anions. L'électrodialyse à MBP permet de produire un acide et une base à partir d'un sel [79]. En outre, nous trouvons l'électrodialyse à membranes bipolaires intégrée dans des procédés, pour le contrôle du pH des jus de fruits ou dans des réacteurs de fermentation [80-82].

Dans ce processus, les MECs et les MEAs sont installées en alternance avec les MBP dans un empilement d'électrodialyse comme illustré à la Fig. 1-16.

Pour une électrodialyse à MBP à trois compartiments, une MEC, une MEA et une MBP forment une unité de répétition dans l'empilement entre deux électrodes. Ainsi, une unité de répétition est composée de trois flux d'écoulement distincts : le flux d'écoulement de la

solution d'alimentation contenant un sel et de deux flux d'écoulement de la solution sur les produits contenant respectivement un acide et une base.

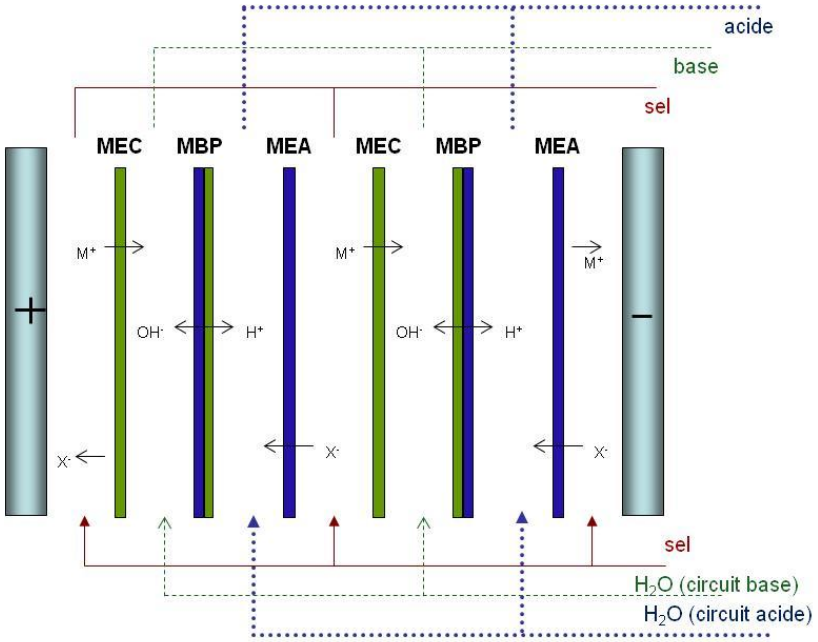

Fig. 1-16. Principe de la production des acides et des bases à partir de leurs sels correspondants par électrodialyse avec des membranes bipolaires à trois compartiments.

L'utilisation de l'ED avec une MBP est économiquement très attractive et a une multitude d'applications potentielles et intéressantes [83]. L'élément clé de ce processus est la membrane bipolaire. Sa fonction et les propriétés déterminent dans une large mesure l'efficacité globale du processus [84]. Un grand défi dans le développement de cette technologie réside dans à la réalisation d'une MBP avec une capacité de dissociation de l'eau, une faible résistance électrique, une haute perméabilité sélective et une longue durée de vie dans des conditions d'exploitation, ce qui signifie qu'elle doit être stable dans l'acide hautement concentré et dans les solutions alcalines.

1.1.5.5. L'électrodéionisation

L'électrodéionisation est un procédé qui consiste à éliminer, à l'aide d'un courant continu, les impuretés ionisées et ionisables d'une source d'eau d'alimentation. Cette technique est essentiellement un processus de désionisation intégré dans un système d'électrodialyse qui régénère en continu une résine échangeuse d'ions en utilisant de l'énergie électrique [1, 85].

La résine échangeuse d'ions est intégrée au compartiment dilué de l'empilement où les ions d'une solution d'alimentation migrent à travers de la résine et les MEIs au compartiment concentré grâce à un champ électrique appliqué (Fig. 1-17).

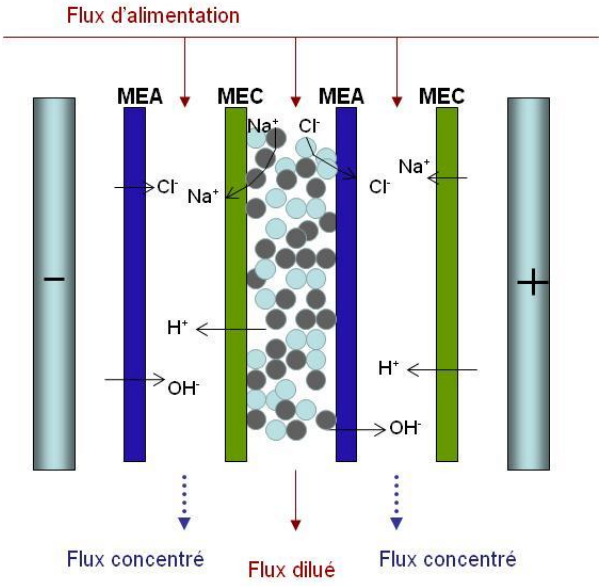

Fig. 1-17. Principe de fonctionnement de l'électrodéionisation pour la production d'eau ultra pure à partir d'une solution de NaCl.

Les MEAs et MECs sont disposées alternativement entre deux électrodes situées aux extrémités du module. Une cellule élémentaire est constituée de deux compartiments, un dilué et un concentré. Lors du passage du courant électrique, les cations sont attirés par le pôle négatif : ils peuvent quitter le compartiment dilué en migrant à travers la MEC mais sont piégés dans le compartiment concentré à cause de la présence de la MEA. Les anions migrent en sens inverse. Ainsi, le compartiment dit dilué dans lequel arrive l'effluent brut s'appauvrit progressivement en espèces ioniques (la solution qui en résulte est appelée diluât) tandis que le compartiment dit concentré s'enrichit en ces mêmes ions (concentrât).

Les espèces neutres présentes dans l'alimentation ne sont pas modifiées et se retrouvent dans le diluât. Les électrodes sont maintenues au contact de circuits indépendants isolés par des membranes et destinées seulement à assurer la conduction électrique et à éliminer les produits de réactions aux électrodes. Dans les installations industrielles, les empilements peuvent atteindre plusieurs centaines de cellules élémentaires dans des assemblages de type filtre-presse [77]. L'espace entre une paire de MEIs est occupé par des espaceurs en polymère qui,

par leur géométrie et leur forme, fixent l'épaisseur du compartiment et le régime hydrodynamique. En effet, ces espaceurs créent des turbulences locales au niveau des interfaces membrane / solution qui permettent d'améliorer les échanges en réduisant l'effet des couches limites de diffusion [78].

L'utilisation la plus courante de cette technique est la production d'eau ultra-pure pour l'industrie pharmaceutique, la fabrication de semi-conducteurs, la consommation dans des laboratoires académiques, cliniques, et industrie agroalimentaire et d'autres [86].

1.2. Applications de l'électrodialyse

De nos jours, l'électrodialyse (ED) est le procédé utilisant des MEIs le plus implanté dans l'industrie [1]. L'ED a est appliquée pour le dessalement des eaux saumâtres depuis plus de 50 ans. Néanmoins, dans le cadre de cette application précisément, l'ED a été mise ces dernières années en concurrence avec la nanofiltration et l'osmose inverse.

Bien que l'ED soit un procédé de séparation membranaire, elle diffère des approches telles que l'ultrafiltration, l'osmose inverse, la nanofiltration, car elle ne sépare pas en fonction de la taille des particules, mais par leurs charges électriques. Cela a favorisé le développement de nombreuses applications principalement dans l'industrie chimique et agroalimentaire [1, 87]. Par ailleurs, des applications prometteuses sont en cours de développement en ED avec l'utilisation de membranes bipolaires [83, 88] et dans le domaine de la « chimie verte » [89, 90].

Actuellement, des applications telles que la déminéralisation du lactosérum ou la désacidification des jus de fruit ont une place importante à l'échelle industrielle. Elles s'ajoutent à des applications liées au dessalement et à la purification de l'eau, bien implantées dans l'industrie depuis plusieurs décennies.

1.2.1. L'électrodialyse et l'eau

Le dessalement de l'eau saumâtre et la pré-concentration du NaCl provenant de l'eau de mer restent les applications à grande échelle les plus importantes de l'ED conventionnelle.

En 1995, la plus grande usine d'ED aux États-Unis a été installée dans le Comté de Sarasota, en Floride. En 2008, elle a produit 1900 m^3/h d'eau potable à partir d'eaux souterraines contenant 1300 ppm de sulfate de calcium. Selon Reahl [91] de la société GE Water, le nettoyage des membranes dans de telles installations se réalise en inversant le courant électrique pour éviter l'encrassement des membranes.

Parmi les unités de moyenne taille, on peut citer par exemple une unité de dessalement d'eau saumâtre en Biskra, Algérie, produisant 120 m^3/h d'eau potable. L'ED permet d'abattre de 80 % la teneur en TDS (« Total Dissolved Solids ») (de 2700 à 700 ppm) avec un taux de récupération d'eau de 80 %. La déminéralisation est obtenue en un seul étage, chaque empilement d'ED pouvant traiter 40 m^3/h [87].

L'ED est également appliquée pour produire de l'eau potable par dénitratation des eaux provenant des nappes phréatiques contaminées à cause de l'utilisation de fertilisants, [87, 92].

Enfin, si l'on considère les applications les plus répandues de l'ED liées à l'eau, nous devons également mentionner le traitement des eaux résiduelles et la pré-déminéralisation de l'eau d'alimentation de chaudière [32].

1.2.2. L'électrodialyse dans l'industrie agroalimentaire

Dans l'industrie agroalimentaire, l'ED permet de purifier, concentrer et déminéraliser des mélanges issus des produits laitiers, des jus de fruits, du sucre, du vin, etc. [93].

Sa faible consommation d'énergie, sa conception modulable, son efficacité et sa facilité d'utilisation, ainsi que la thermostabilité de nombreux produits alimentaires, sont les principaux arguments en faveur de cette technologie.

En 1998, l'autorisation par le Conseil de l'Europe d'utiliser l'ED pour la stabilisation tartrique du vin a permis d'accéder à un marché en pleine croissance [87]. Cette technologie permet d'extraire sélectivement le ditartrate de potassium et le tartrate de calcium et ainsi d'éviter des précipitations dans les bouteilles [94]. La stabilisation tartrique du vin peut être mise en place dans un empilement d'ED conventionnel opérant en mode batch. Les caractéristiques principales du vin (pH, acidité, teneur en sucre, dégrée d'alcool) ainsi que son goût, son arôme et sa couleur sont pratiquement inaltérées avec l'ED [93].

En 2006, la société EURODIA INDUSTRIE, S.A. a comptabilisé 90 unités d'ED, correspondant à plus de 200 réacteurs, principalement en France et Italie [87] ainsi que

plusieurs installations en service en Australie, Afrique du sud, Nouvelle-Zélande, États-Unis, Espagne, Allemagne et Portugal.

Parmi d'autres applications de l'ED dans l'industrie agroalimentaire nous pouvons mentionner la déminéralisation de la sauce soja [95], des mélasses [96], des acides aminés [97] du jus de cuisson des moules [98] ainsi que la désacification du jus de fruits [81].

Nous allons détailler un procédé sur lequel nous allons réaliser une partie de notre étude : la déminéralisation du lactosérum.

1.2.3. La déminéralisation du lactosérum par électrodialyse

Le lactosérum est un sous-produit de la fabrication du fromage. Avant sa réutilisation, il doit être déminéralisé pour devenir une solution valorisable dans une grande variété de produits. Outre l'eau, le lactosérum contient du lactose, de l'acide lactique, des protéines, de la matière grasse, et les sels suivants : NaCl, KCl, KH_2PO_4, $MgHPO_4$, $Ca(PO4)_2$, $NaCO_3$, K_2CO_3, $CaCl_2$, $Mg(H_2PO_4)_2$, $Na_3(C_6H_5O_7)$ et $K_3(C_6H_5O_7)$ [99]. En plus d'être économiquement pertinente, la réutilisation du lactosérum permet d'éviter de rejeter cette solution dans les eaux usées dans les égouts, en raison de sa forte demande biologique en oxygène (DBO). Le Tableau 1-1 montre la composition du lactosérum ainsi que le pH et le DBO.

pH	<6
DBO	31
Eau	93.6
Matières sèches	6.4
Lactose	4.9-5.0
Acide lactique	0.03-0.04
Protéines	0.84-1.10
Grasses	0.06-0.07
sels	0.49-0.56

Tableau 1-1. Données de pH, DBO et composition (en % en masse) du lactosérum doux [93].

Le lactosérum peut être déminéralisé soit par des résines échangeuses d'ions, soit par des procédés de séparation membranaires ou par combinaison de ces deux types de technologies. Parmi les procédés membranaires, l'ED ou la nanofiltration peuvent être appliquées. La nanofiltration est appropriée seulement pour la déminéralisation partielle, alors que l'ED et l'échange d'ions sont pratiques pour atteindre des niveaux plus élevés de déminéralisation.

L'ED présente plusieurs avantages par rapport à d'autres processus de déminéralisation, tels que le faible impact sur l'environnement et la qualité supérieure du produit. Etant donné que le temps de travail d'un empilement est normalement de 20 heures par jour, la productivité de l'ED est également élevée. La Fig. 1-18 montre un empilement d'ED industrielle pour la déminéralisation du lactosérum procuré par EURODIA INDUSTRIE S.A.

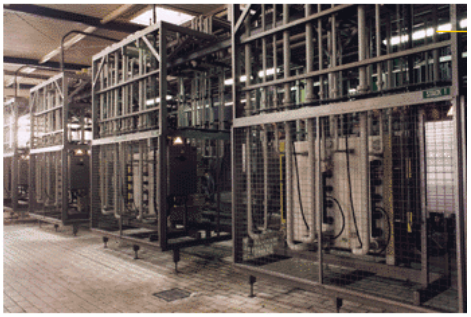

Fig. 1-18. Photographie montrant plusieurs empilements d'ED pour la déminéralisation du lactosérum (procuré par EURODIA INDUSTRIE S.A.).

Dans la déminéralisation du lactosérum par ED, des membranes échangeuses d'ions monopolaires sont placées dans l'empilement comme il est montré sur la Fig. 1-15. Au cours du procédé, les ions monovalents tels que K^+, Na^+ et Cl^- sont éliminés, suivis par des ions multivalents, Ca^{2+}, Mg^{2+}, PO_4^{3-} éliminant globalement 90% en masse de sels [93].

Généralement, le compartiment concentré est alimenté avec une solution de NaCl tandis que la solution idéale pour le rinçage des électrodes contient du Na_2SO_4 au lieu du NaCl pour éviter la formation de Cl_2 dans le compartiment anodique. Afin de diminuer la précipitation de sels, le compartiment concentré est légèrement acidifié avec du HNO_3 ou du HCl [100].

Pour les applications industrielles, il est plus favorable de concentrer le lactosérum à 20 TDS pour améliorer la performance faradique à haute densité de courant. La température optimale d'opération doit être entre 10 et 15 °C pour contrôler la croissance bactérienne et assurer la stabilité du lactosérum tout au long de la déminéralisation [101].

Dans le compartiment dilué, des grosses molécules organiques peuvent se déposer sur la surface des MEAs produisant du colmatage ou « fouling ». Cela entraîne une diminution de la surface active de la membrane et une baisse de l'efficacité de production. Dans le

compartiment concentré, des couches de sels ou « scaling » contenant Ca^{2+}, Mg^{2+}, PO_4^{3-}, SO_4^{2-} ou encore CO_3^{2-} apparaissent à la surface des MECs [102, 103].

De ce fait, le nettoyage des membranes dit « Cleaning-In-Place » (CIP) est nécessaire pour l'optimisation des performances de la membrane et pour la minimisation des coûts de traitement.

Le CIP est traditionnellement réalisé en alternant des lavages acide-base une fois par jour. Simová et al. [101] réalisent le CIP de la manière suivante :

- Rinçage à l'eau
- Rinçage acide
- Rinçage à l'eau
- Rinçage alcalin
- Rinçage à l'eau
- Rinçage acide
- Rinçage à l'eau

Le dernier rinçage acide permet de revenir au pH du travail. Outre le CIP, l'inversion de courant est couramment pratiquée pour eliminer le colmatage dans la surface des membranes.

Une autre possibilité qui a prouvé son efficacité pour la réduction du colmatage est l'application de champs électriques pulsés, comme présenté par Ruiz et Sistat [104, 105]. Cifuentes-Araya a montré que la fréquence des champs électriques pulsés doit être optimisée en ajustant les ratios pulse/pause appliqués en cours de traitements d'ED pour maximiser le contrôle du colmatage et pour améliorer la performance du procédé [106].

De nombreuses unités d'ED sont intégrées dans des procédés de déminéralisation de lactosérum en Europe et dans le monde. La société EURODIA INDUSTRIE S.A. a communiqué en 2009 que la surface de membranes Neosepta® installées pour cette application représente plus de 65000 m^2 en Europe [87].

1.3. Vieillissement des membranes échangeuses d'ions

L'efficacité des procédés d'ED dépend en grande partie des propriétés des MEIs utilisées. Les MEIs, tout comme les autres types de membranes, tendent à perdre de leurs propriétés physicochimiques et séparatives tout au long de leur utilisation. Il s'agit là du phénomène de vieillissement. Ce phénomène s'accompagne d'une diminution du rendement des opérations et de l'augmentation de leurs coûts : surconsommation d'énergie, et/ou remplacement plus fréquent des membranes et aussi des pertes d'exploitation. Ainsi, l'évaluation de la durée de vie d'une membrane à la sortie de sa chaîne de production, ou de son degré de vieillissement après une certaine durée d'utilisation, constitue un élément très important dans la sélection des matériaux, dans la maîtrise des coûts opérationnels (investissement et fonctionnement) et dans la réduction de volumes des polymères à recycler.

Récemment, le phénomène de vieillissement des MEIs en piles à combustible a fait l'objet d'enquêtes intéressantes [107-114] et même des revues ont été publiées [115, 116]. Cela contraste avec un nombre insuffisant d'études menées sur le vieillissement des MEIs appliquées en ED.

Etant donné que l'application d'ED la plus implantée dans l'industrie a toujours été le dessalement des eaux saumâtres, et vu que la durée des membranes dans cette application est de plusieurs années [1, 117], la recherche du vieillissement des MEIs en ED n'était pas apparue comme prioritaire. Cela a changé depuis la diversification des applications de l'ED. De nos jours, les nouvelles applications industrielles demandent des membranes plus résistantes à des environnements plus agressifs.

Le groupe de recherche Matériaux et Membranes de l'équipe Systèmes Polymères Complexes de l'ICMPE a lancé un axe de recherche portant sur le comportement à long terme des MEIs. Une première étude du phénomène de vieillissement a été effectuée sur la thèse doctorale de Mme. Rym Ghalloussi [118]. Son étude a été basée sur la comparaison de plusieurs caractéristiques physico-chimiques et structurales des échantillons neufs et usagés en ED pour l'industrie agroalimentaire. Elle a mis en évidence une perte de la capacité d'échange des MEIs et le colmatage sur leurs surfaces. Plusieurs changements structuraux dans une MEA on été constatés comme le montre la Fig. 1-19 [119].

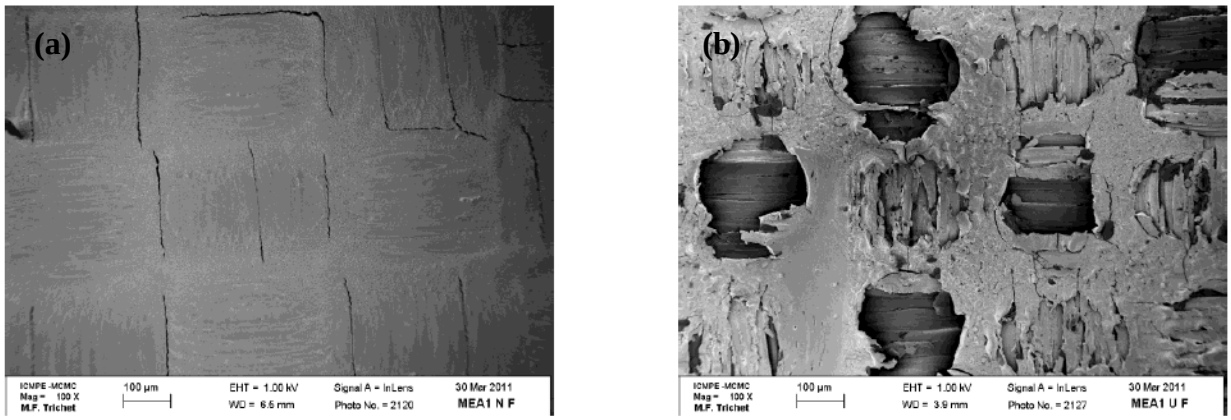

Fig. 1-19. Image MEB d'une MEA (a) avant et (b) après utilisation en ED pour l'industrie agroalimentaire [118].

Au cours de cette étude bibliographique, nous avons cherché à répertorier les travaux impliquant le comportement à long terme des MEIs en ED. Pour compléter cette étude et nous inspirer d'autres domaines, nous présentons également certains travaux réalisés sur des matériaux similaires aux MEIs et utilisés dans d'autres procédés membranaires.

1.3.1. La dégradation mécanique et thermique des membranes échangeuses d'ions

La dégradation mécanique des MEIs est souvent la cause du vieillissement précoce d'un empilement. Elle se manifeste par l'apparition de fissures, de déchirures, de perforations, etc. [115]. Les causes connues de la dégradation mécanique sont l'humidification insuffisante [120, 121], ce qui peut se produire pendant le stockage des MEIs ou pendant de longues périodes de pause dans l'ED sans remplir l'empilement avec une solution aqueuse. Le manque d'eau rend la membrane cassante et fragile. Une pression de contact non uniforme, une haute température et des changements brutaux de température sont d'autres causes de la dégradation mécanique des MEIs.

Afin de vérifier la tenue thermique des membranes, il est possible de suivre leur perte de masse en fonction de l'élévation de la température par analyse thermogravimétrique. La Fig. 1-20 présente le profil de dégradation en fonction de la température de la membrane Neosepta® AMX-SB (mode de préparation décrit dans la section 1.1.3.2).

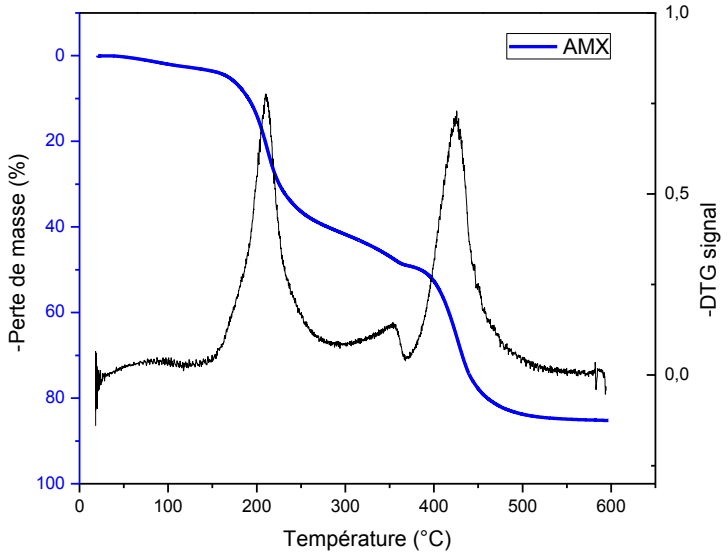

Fig. 1-20. Profil de dégradation thermique d'AMX-SB et sa dérivée.

De ces courbes nous déduisons l'existence de quatre étapes de dégradation. La première étape vers 100 °C correspond à l'élimination de l'eau liée aux sites fonctionnels. A partir de 150 °C les polymères commencent à se dégrader. La dégradation se déroule sur plusieurs étapes car la membrane est formée de plusieurs polymères avec des températures de dégradation distinctes.

D'autres études ont suggéré que des MEAs [122] et des MECs [123] commencent à se dégrader dès 150 °C. Les sites fonctionnels d'acide sulfonique dans les MECs sont connus pour se dégrader à environ 240 °C [124, 125]. Les sites ammonium quaternaire des MEAs se dégradent vers 250 °C [126, 127].

Cependant, cette technique ne reproduit pas les conditions réelles d'exploitation de l'ED puisque les échantillons membranaires sont chauffés sous atmosphère inerte, et ils ne sont maintenus à des températures élevées que pour des courtes périodes.

1.3.2. La dégradation chimique

Il existe plusieurs sources de dégradation chimique de la membrane. Les solutions d'alimentation dans l'industrie agroalimentaire sont des milieux hautement nutritifs qui peuvent entraîner la prolifération des micro-organismes. De plus, la matière colloïdale, les composés inorganiques ou les macromolécules peuvent former du colmatage à l'interface ou dans la membrane [102, 128, 129]. A cet égard, le CIP des membranes est essentiel pour

éviter le colmatage et la croissance des micro-organismes qui pourraient contaminer le produit à traiter [32]. Le CIP est nécessaire pour l'optimisation des performances de la membrane et pour la minimisation des coûts de traitement.

Les protocoles de CIP pourraient à court ou à long terme, endommager la membrane ou la rendre plus sensible à l'environnement, car ils sont traditionnellement réalisés en utilisant des acides et des bases. L'utilisation de produits puissants de nettoyage, comme les oxydants, devient parfois nécessaire pour obtenir un assainissement complet de l'empilement d'ED dans les applications de l'industrie agroalimentaire.

1.3.2.1.Vieillissement des membranes en milieu chloré

L'oxydation dégrade les groupements fonctionnels des protéines et de la matière organique pour produire des carboxyles, de la cétone et de l'aldéhyde, groupements plus sensibles à l'hydrolyse à pH élevé [130, 131]. Parmi les oxydants couramment utilisés dans les procédés membranaires, on peut citer l'acide péracétique (APA), le peroxyde d'hydrogène (H_2O_2) et l'hypochlorite de sodium (NaClO) [132]. Le NaClO est cependant l'oxydant le plus couramment utilisé dans l'osmose inverse, l'ultrafiltration, et les procédés membranaires de microfiltration [131, 133, 134]. Le contact avec le NaClO est soupçonné jouer un rôle important dans le vieillissement membranaire [135-146]. Dans ce contexte, les fournisseurs des MEIs conseillent de ne pas utiliser des agents oxydants forts car ils peuvent affecter la stabilité de la membrane.

Bien que le NaClO ne soit pas traditionnellement appliqué au CIP des MEIs, de grands besoins en matière de désinfection dans le traitement des solutions alimentaires pourraient conduire à son utilisation future. En effet, le NaClO est l'un des produits chimiques les plus efficaces en terme de nettoyage et de désinfection dans les procédés membranaires [136]. Ainsi, les conséquences de l'emploi du NaClO sur la dégradation des MEIs méritent d'être étudiées avant de passer à l'échelle industrielle.

Parmi les articles référencés, aucun ne s'attache à l'action du NaClO sur les polymères fonctionnalisés. Cependant, le vieillissement par le NaClO a déjà été étudié sur des membranes utilisées dans les procédés d'ultrafiltration, possédant une structure similaire à celle des MECs sulfonées : le polysulfone (PSf) et le polyéthersulfone (PES). Selon Gaudichet-Maurin et al. [138], l'exposition au NaClO produit la rupture de la chaîne macromoléculaire du PSf. Le mécanisme de dégradation repose sur l'oxydation radicalaire lorsque les radicaux hydroxyles •OH sont présents dans la solution [146]. Cela se produit

lorsque l'acide hypochloreux (HClO) et les ions hypochlorite (ClO^-) sont les espèces prédominantes en solution aqueuse [139] :

$$HClO + 3ClO^- \longrightarrow 3Cl^- + {}^{\bullet}ClO + O_2 + {}^{\bullet}OH \qquad (1.8)$$

Ces auteurs ont proposé le mécanisme suivant pour la dégradation du PSf par rupture de chaînes :

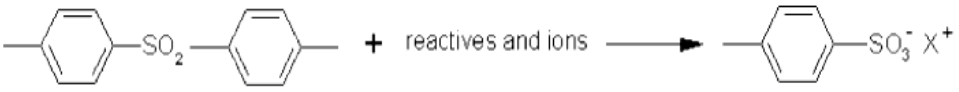

Fig. 1-21. Mécanisme de dégradation du PSf exposé à du NaClO [138].

Causserrand et al. [139] ont constaté que la dégradation des membranes de PSf est plus importante lorsque le pH varie de 8 à 10 que pour des valeurs de pH supérieures ou inférieures.

Arkhangelsky et al. [140] ont proposé que les membranes de PES souffrent d'une scission partielle de la liaison C-S du groupement sulfonyle, à pH 7,2 et en présence d'une quantité suffisante d'hypochlorite. Cette dégradation conduit à une augmentation de la taille des pores de la membrane.

Ils ont présenté un mécanisme de dégradation similaire au précédent, pour la dégradation du PES en contacte avec du NaClO:

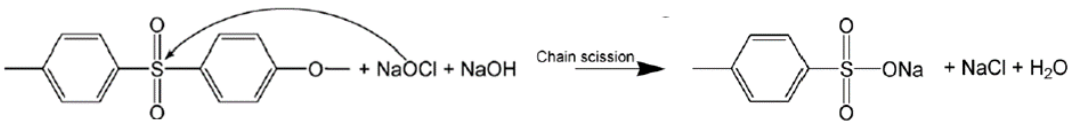

Fig. 1-22. Mécanisme de dégradation du PES exposé à du NaClO [140].

Yadav et al. [100] ont trouvé que les membranes de PES sont endommagées à pH 9 et 12. Cependant la dégradation a une plus grande ampleur à pH 9.

Dans une étude récente, Prulho et al. [101] ont critiqué le mécanisme de vieillissement proposé par Gaudichet-Maurin et Arkhangelsky après avoir étudié l'implication des produits d'oxydation radicalaire par mise en contact des matériaux avec les radicaux •OH produits par l'irradiation d'une suspension de dioxyde de titane. Ils ont estimé que le trempage des mélanges PES/PVP dans une solution d'hypochlorite à pH 8 provoque l'oxydation des cycles aromatiques dans des groupes phénoliques de la manière suivante :

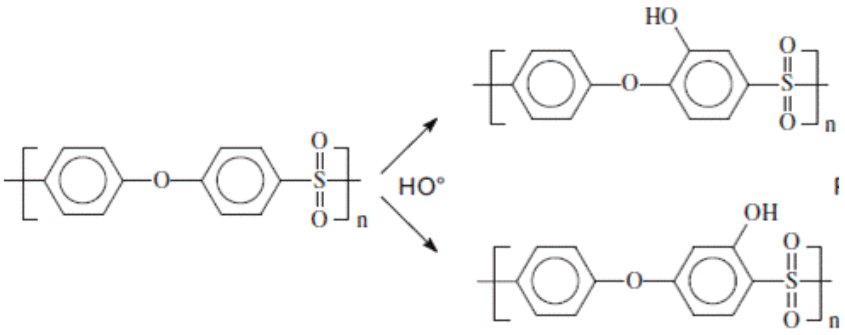

Fig. 1-23. Mécanisme de dégradation du PSf exposé au NaClO proposé par Prulho et al. [140].

Selon ces auteurs, l'oxydation du PSf dans le mélange implique l'oxydation préalable du PVP.

A partir de toutes ces études expérimentales, le NaClO semble être plus nuisible aux membranes de pH 7 à 9. Cela représente un problème dans des applications industrielles car l'eau potable ou les solutions alimentaires se trouvent généralement dans cette gamme de pH.

Dammak et al. [132] ont réalisé un vieillissement artificiel accéléré des MECs dans l'acide peracétique et de l'Oxonia Actif®, deux produits de nettoyage oxydants couramment utilisés dans les applications d'ED pour l'industrie agroalimentaire. Ils ont identifié une augmentation de la conductivité et la teneur en eau provenant de la modification de la structure du polymère sans être accompagnés de dégradation des groupements fonctionnels. Néanmoins, aucun mécanisme de dégradation n'a été proposé pour le vieillissement des MEIs exposées à des oxydants.

1.3.2.2. Vieillissement dans des conditions extrêmes du pH

Un défi majeur dans le développement des MEAs est leur stabilité à pH élevé [147]. Kneifel et Hattenbach [148], ainsi que Sata et al. [149], ont étudié l'évolution des MEIs en fonction du

temps d'exposition à différents produits chimiques : NaCl, HNO_3, ou NaOH. La dégradation (de la résistance, de la capacité d'échange et de la permsélectivité) la plus importante est celle provoquée par le NaOH. Sata et al. ont proposé comme hypothèse que le vieillissement dans des conditions alcalines était dû à la dégradation des polymères liants.

Les groupements fonctionnels des MEAs sont connus pour être facilement dégradés en milieu alcalin. Parmi les différentes espèces qui pourraient être utilisées en tant que sites d'échange d'anions, nous nous sommes intéressés à l'étude des sites ammonium quaternaire puisqu'ils sont les groupes échangeurs d'anions les plus utilisés dans les MEAs disponibles sur le marché. En outre, les groupements ammonium ont tendance à avoir la plus grande stabilité en milieu alcalin par rapport aux groupements phosphonium et sulfonium [150]. Ces groupes ont tendance à se dégrader dans des conditions aqueuses à pH élevé en raison de la présence des contre-ions hydroxyde, selon deux principales voies de dégradation lorsque la température augmente : les mécanismes d'élimination et de substitution nucléophile [151, 152]. La nature de l'amine détermine l'étendue de ces mécanismes de dégradation.

Le clivage de l'ammonium quaternaire par OH^- qui est suivie par son élimination est appelé dégradation de Hofmann ou élimination E2 [152]. Cela n'est possible que si le groupe partant est antipériplanaire par rapport à l'hydrogène β. Les groupements CN et C-Hβ doivent être situés dans un même plan. Les ions hydroxyles attaquent un bêta-hydrogène de l'ammonium. La dégradation conduit à la formation d'un alcène, d'une amine et d'une molécule d'eau (Fig. 1-24).

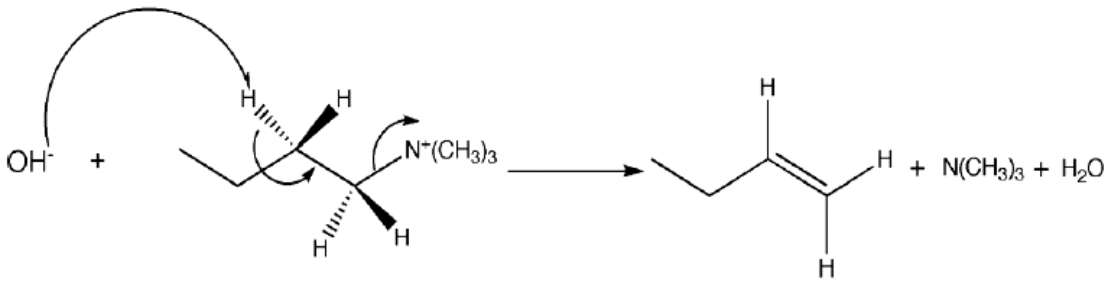

Fig. 1-24. Dégradation des groupements ammonium dans les milieux alcalins par la dégradation de Hoffman [152].

Un autre mécanisme appelé E1 se produit lorsque la molécule qui porte le groupement ammonium contient des atomes de carbone en α et β provoquant des encombrements stériques [152]. Ainsi, l'ion hydroxyde réagit avec un proton d'un groupement méthyle sur

l'ammonium. Par la suite, un réarrangement conduit à la formation d'un alcène et d'une amine (Fig. 1-25).

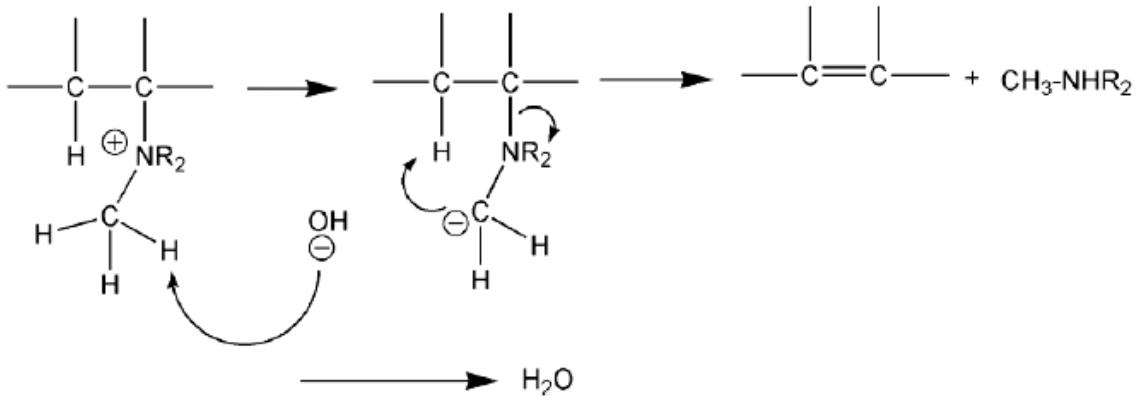

Fig. 1-25. Dégradation des groupements ammonium dans les milieux alcalins par élimination E1 [153].

La dégradation de l'ammonium par une substitution nucléophile correspond à deux réactions S_N2 entre un anion OH^- et un atome de carbone en position α du groupement d'ammonium. Deux produits sont alors générés : un alcool et une amine [154].

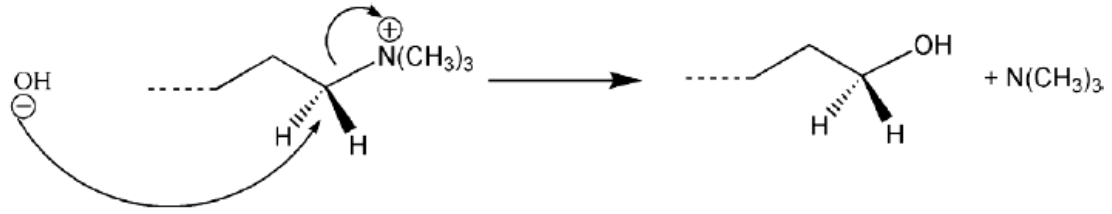

Fig. 1-26. La dégradation des groupements ammonium en milieu alcalin par substitution nucléophile [154].

Récemment, Chempath et al. [154, 155] se sont intéressés aux voies de dégradation des différents modèles d'hydroxydes de tétraalkylammonium : le trétraméthylammonium, éthyl-triméthylammonium et benzyltriméthylammonium.

Ils ont constaté que le cation (tétraméthyl ammonium par exemple), a subi une dégradation dans des conditions alcalines à partir de deux mécanismes différents. Dans le premier mécanisme, l'hydroxyle s'approche du groupement méthyle par le bas, effectue une attaque

S_N2 et forme directement le méthanol. Dans le deuxième mécanisme, l'approche s'effectue du côté de l'atome d'hydrogène du groupement méthyle, un ylure et une molécule d'eau sont formés par l'élimination d'un proton d'un groupement méthyle. L'ylure réagit ensuite avec la molécule d'eau pour former du méthanol.

En conséquence, les ylures jouent un rôle crucial dans la décomposition de l'hydroxyde de tétraméthylammonium.

Bien que la dégradation des sites fonctionnels des MEAs à pH élevé soit bien documentée dans la littérature, plusieurs questions relatives à la dégradation de la membrane restent floues. Notamment, la dégradation des polymères liants ou les conséquences de la dégradation de la matrice polymère dans les propriétés de transport des MEIs.

En outre, la dégradation due à des cycles de nettoyage acide-base (section 1.2.3) dans laquelle les membranes sont soumises à des changements dans la nature, le pH et la température de la solution d'équilibrage, n'ont pas été abordées.

1.4. Conclusions

Dans ce chapitre nous avons réalisé une synthèse bibliographique sur les MEIs et sur leurs principales applications.

Il existe de nombreuses méthodes de préparation et de caractérisation des membranes. Nous avons remarqué en particulier que les membranes homogènes possèdent d'excellentes propriétés physico-chimiques et séparatives et elles ont toujours été considérées comme plus performantes dans les procédés electromembranaires que les membranes hétérogènes. Néanmoins, ces dernières peuvent présenter des avantages, notamment leur faible coût et leur bonne stabilité mécanique.

La complexité de la morphologie des MEIs a conduit à la conception de nombreux modèles membranaires permettant de décrire le comportement de ces matériaux en relation avec leur microstructure. Le modèle microhétérogène permet de tenir compte de l'existence de différentes phases dans la MEI et de la disposition de ces phases les unes par rapport aux autres. Par ailleurs, il est suffisamment détaillé pour bien décrire la structure interne des MEIs et suffisamment simple pour ne pas nécessiter la détermination de nombreux paramètres.

Les MEIs sont largement utilisées dans les procédés industriels, surtout pour l'ED. Des applications comme la stabilisation tartrique du vin et le dessalement du lactosérum sont bien installées dans le paysage industriel mondial. Néanmoins, un des désavantages des applications dans cette industrie agroalimentaire est la courte durée de vie des membranes qui subissent différentes modifications en surface ou dans la masse. Cette dégradation entraîne des modifications dans leurs propriétés physico-chimiques, structurales et mécaniques accompagnées d'une diminution du rendement des opérations et de l'augmentation de coûts. Une des causes de dégradation des MEIs est le nettoyage réalisé avec des produits chimiques tels que les acides, les bases ou les produits oxydants.

Malgré l'intérêt théorique et pratique des phénomènes de vieillissement des MEIs en ED, nous avons pu constater que la littérature était jusqu'à là assez pauvre. Nous nous proposons d'explorer ces phénomènes.

Références

[1] H. Strathmann, Electrodialysis, a mature technology with a multitude of new applications, Desalination, 264 (2010) 268-288.

[2] G.E. Molau, Heterogeneous ion-exchange membranes, J. Membr. Sci., 8 (1981) 309-330.

[3] G.S. Gohil, V.K. Shahi, R. Rangarajan, Comparative studies on electrochemical characterization of homogeneous and heterogeneous type of ion-exchange membranes, J. Membr. Sci., 240 (2004) 211-219.

[4] P.V. Vyas, B.G. Shah, G.S. Trivedi, P. Ray, S.K. Adhikary, R. Rangarajan, Characterization of heterogeneous anion-exchange membrane, J. Membr. Sci., 187 (2001) 39-46.

[5] P.V. Vyas, B.G. Shah, G.S. Trivedi, P. Ray, S.K. Adhikary, R. Rangarajan, Studies on heterogeneous cation-exchange membranes, React. Funct. Polym., 44 (2000) 101-110.

[6] Y. Oren, V. Freger, C. Linder, Highly conductive ordered heterogeneous ion-exchange membranes, J. Membr. Sci., 239 (2004) 17-26.

[7] S.M. Hosseini, S.S. Madaeni, A. Zendehnam, A.R. Moghadassi, A.R. Khodabakhshi, H. Sanaeepur, Preparation and characterization of PVC based heterogeneous ion exchange membrane coated with Ag nanoparticles by (thermal-plasma) treatment assisted surface modification, J. Ind. Eng. Chem., 19 (2013) 854-862.

[8] S.M. Hosseini, S.S. Madaeni, A.R. Khodabakhshi, Preparation and characterization of ABS/HIPS heterogeneous anion exchange membrane filled with activated carbon, J. Appl. Polym. Sci., 118 (2010) 3371-3383.

[9] S.M. Hosseini, S.S. Madaeni, A.R. Khodabakhshi, Preparation and characterization of PC/SBR heterogeneous cation exchange membrane filled with carbon nano-tubes, J. Membr. Sci., 362 (2010) 550-559.

[10] M.Y. Kariduraganavar, R.K. Nagarale, A.A. Kittur, S.S. Kulkarni, Ion-exchange membranes: preparative methods for electrodialysis and fuel cell applications, Desalination, 197 (2006) 225-246.

[11] Y. Tanaka, Chapter 1 Preparation of Ion Exchange Membranes, in: T. Yoshinobu (Ed.) Membrane Science and Technology, Elsevier, 2007, pp. 3-16.

[12] R.K. Nagarale, G.S. Gohil, V.K. Shahi, Recent developments on ion-exchange membranes and electro-membrane processes, Adv. Colloid Interface Sci., 119 (2006) 97-130.

[13] B.L. Svarfvar, K.B. Ekman, M.J. Sundell, J.H. Näsman, Electron-beam graft-modified membranes with externally controlled flux, Polym. Adv. Technol., 7 (1996) 839-846.

[14] N. Tzanetakis, J.R. Varcoe, R.C.T. Slade, K. Scott, Radiation-grafted PVDF anion exchange membrane for salt splitting, Desalination, 174 (2005) 257-265.

[15] Y.-J. Choi, M.-S. Kang, J. Cho, S.-H. Moon, Preparation and characterization of LDPE/polyvinylbenzyl trimethyl ammonium salts anion-exchange membrane, J. Membr. Sci., 221 (2003) 219-231.

[16] S. Aouadj, A. Chapiro, Preparation of hydrophilic membranes by grafting acrylic acid onto pre-irradiated teflon-FEP films, Angew. Makromol. Chem., 235 (1996) 73-80.

[17] B.D. Gupta, A. Chapiro, Preparation of ion-exchange membranes by grafting acrylic acid into pre-irradiated polymer films—1. grafting into polyethylene, Eur. Polym. J., 25 (1989) 1137-1143.

[18] E.-S.A. Hegazy, I. Ishigaki, J. Okamoto, Radiation grafting of acrylic acid onto fluorine-containing polymers. I. Kinetic study of preirradiation grafting onto poly(tetrafluoroethylene), J. Appl. Polym. Sci., 26 (1981) 3117-3124.

[19] T. Sata, Studies on ion exchange membranes with permselectivity for specific ions in electrodialysis, J. Membr. Sci., 93 (1994) 117-135.

[20] T. Sata, Y. Yamane, K. Matsusaki, Preparation and properties of anion exchange membranes having pyridinium or pyridinium derivatives as anion exchange groups, J. Polym. Sci., Part A: Polym. Chem., 36 (1998) 49-58.

[21] M.S. Huda, R. Kiyono, M. Tasaka, T. Yamaguchi, T. Sata, Thermal membrane potential across anion-exchange membranes with different benzyltrialkylammonium groups, Sep. Purif. Technol., 14 (1998) 95-106.

[22] A.K. Pandey, A. Goswami, D. Sen, S. Mazumder, R.F. Childs, Formation and characterization of highly crosslinked anion-exchange membranes, J. Membr. Sci., 217 (2003) 117-130.

[23] T. Sata, Modification of properties of ion-exchange membranes. IV. Change of transport properties of cation-exchange membranes by various polyelectrolytes, J. Polym. Sci: Polym. Chem., 16 (1978) 1063-1080.

[24] R. Vinodh, A. Ilakkiya, S. Elamathi, D. Sangeetha, A novel anion exchange membrane from polystyrene (ethylene butylene) polystyrene: Synthesis and characterization, Mater. Sci. Eng., B, 167 (2010) 43-50.

[25] E.-S.A. Hegazy, N.H. Taher, A.R. Ebaid, Preparation and some properties of hydrophilic membranes obtained by radiation grafting of methacrylic acid onto fluorinated polymers, J. Appl. Polym. Sci., 41 (1990) 2637-2647.

[26] H. Omichi, D. Chundury, V.T. Stannett, Electrical and other properties of mutual radiation-induced methacrylic acid grafted polyethylene films, J. Appl. Polym. Sci., 32 (1986) 4827-4836.

[27] B. Gupta, F.N. Büchi, G.G. Scherer, A. Chapiró, Crosslinked ion exchange membranes by radiation grafting of styrene/divinylbenzene into FEP films, J. Membr. Sci., 118 (1996) 231-238.

[28] M. Mahmoud Nasef, H. Saidi, Preparation of crosslinked cation exchange membranes by radiation grafting of styrene/divinylbenzene mixtures onto PFA films, J. Membr. Sci., 216 (2003) 27-38.

[29] W. Lee, K. Saito, S. Furusaki, T. Sugo, K. Makuuchi, Design of urea-permeable anion-exchange membrane by radiation-induced graft polymerization, J. Membr. Sci., 81 (1993) 295-305.

[30] G. Merle, M. Wessling, K. Nijmeijer, Anion exchange membranes for alkaline fuel cells: A review, J. Membr. Sci., 377 (2011) 1-35.

[31] Y. Mizutani, Structure of Ion Exchange Membranes, J. Membr. Sci., 49 (1990) 121-144.

[32] H. Strathmann, in: Ion-exchange Membrane Separation Processes, Elsevier, 2004, pp. 287-328.

[33] T. Xu, Ion exchange membranes: State of their development and perspective, J. Membr. Sci., 263 (2005) 1-29.

[34] A.G. Guzmán-Garcia, P.N. Pintauro, M.W. Verbrugge, R.F. Hill, Development of a space-charge transport model for ion-exchange membranes, AIChE J., 36 (1990) 1061-1074.
[35] P. Ramírez, S. Mafé, A. Alcaraz, J. Cervera, Modeling of pH-Switchable Ion Transport and Selectivity in Nanopore Membranes with Fixed Charges, J. Phys. Chem. B, 107 (2003) 13178-13187.
[36] S. Koter, Transport of simple electrolyte solutions through ion-exchange membranes—the capillary model, J. Membr. Sci., 206 (2002) 201-215.
[37] S. Mafe, J.A. Manzanares, P. Ramirez, Modeling of surface vs. bulk ionic conductivity in fixed charge membranes, Phys. Chem. Chem. Phys., 5 (2003) 376-383.
[38] V.I. Zabolotsky, V.V. Nikonenko, Effect of structural membrane inhomogeneity on transport properties, J. Membr. Sci., 79 (1993) 181-198.
[39] K.S. Spiegler, Transport processes in ionic membranes, Transactions of the Faraday Society, 54 (1958) 1408-1428.
[40] R. Arnold, D. Koch, Electrical conductivity of cation-exchange membranes in the hydrogen ion form, Aust. J. Chem., 19 (1966) 1299-1313.
[41] G. Pourcelly, A. Oikonomou, C. Gavach, H.D. Hurwitz, Influence of the water content on the kinetics of counter-ion transport in perfluorosulphonic membranes, Journal of Electroanalytical Chemistry and Interfacial Electrochemistry, 287 (1990) 43-59.
[42] N.P. Berezina, N.A. Kononenko, O.A. Dyomina, N.P. Gnusin, Characterization of ion-exchange membrane materials: Properties vs structure, Adv. Colloid Interface Sci., 139 (2008) 3-28.
[43] T.D. Gierke, G.E. Munn, F.C. Wilson, The morphology in nafion perfluorinated membrane products, as determined by wide- and small-angle x-ray studies, J. Polym. Sci.: Polym. Phys., 19 (1981) 1687-1704.
[44] W.Y. Hsu, T.D. Gierke, Ion transport and clustering in nafion perfluorinated membranes, J. Membr. Sci., 13 (1983) 307-326.
[45] S. Timashev, T. Kemp, Physical chemistry of membrane processes, Ellis Horwood, London, 1991.
[46] A.N. Orezin, A.V. Rebrov, A.N. Yakunin, L.P. Bogotseva, N.F. Bakeyev, Structural changes in perfluorinated membranes in the processes of saponification and orientation stretching, Polym. Sci. U.S.S.R., 28 (1986) 275-282.
[47] Y.K. Tovbin, Vasyutkin, To the theory of migration of cations in Nafion membranes, Russ. J. Phys. Chem. A, 67 (1993) 524-527.

[48] K.A. Mauritz, R.B. Moore, State of Understanding of Nafion, Chem. Rev., 104 (2004) 4535-4586.

[49] M. Eikerling, A.A. Kornyshev, U. Stimming, Electrophysical Properties of Polymer Electrolyte Membranes: A Random Network Model, J. Phys. Chem. B, 101 (1997) 10807-10820.

[50] K.D. Kreuer, On the development of proton conducting materials for technological applications, Solid State Ionics, 97 (1997) 1-15.

[51] K.D. Kreuer, On the development of proton conducting polymer membranes for hydrogen and methanol fuel cells, J. Membr. Sci., 185 (2001) 29-39.

[52] K.-D. Kreuer, S.J. Paddison, E. Spohr, M. Schuster, Transport in Proton Conductors for Fuel-Cell Applications: Simulations, Elementary Reactions, and Phenomenology, Chem. Rev., 104 (2004) 4637-4678.

[53] K.H. Meyer, J.F. Sievers, La perméabilité des membranes. IV. Analyse de la structure de membranes végétales et animales, Helv. Chim. Acta, 19 (1936) 987-995.

[54] N.P. Gnusin, V.I. Zabolotsky, V. Nikonenko, Meshechkov, Development of the generalized conductance principle to the description of transfer phenomena in disperse systems under the acting of different forces, Zh. Fiz. Khimii (Rus. J. Phys. Chem.), 54 (1980) 1518–1522

[55] N.P. Gnusin, N.P. Berezina, N.A. Kononenko, O.A. Dyomina, Transport structural parameters to characterize ion exchange membranes, J. Membr. Sci., 243 (2004) 301-310.

[56] N.N. Belaid, B. Ngom, L. Dammak, C. Larchet, B. Auclair, Conductivité membranaire: interprétation et exploitation selon le modèle à solution interstitielle hétérogène, Eur. Polym. J., 35 (1999) 879-897.

[57] H. Ellouze, B. Ngom, B. Auclair, Interpretation de la perméabilite hydraulique d'une membrane échangeuse de cations à l'aide du modèle à solution interstitielle hétérogene, Eur. Polym. J., 25 (1989) 395-403.

[58] X.T. Le, Contribution to the study of properties of Selemion AMV anion exchange membranes in acidic media, Electrochim. Acta.

[59] X.T. Le, T.H. Bui, P. Viel, T. Berthelot, S. Palacin, On the structure–properties relationship of the AMV anion exchange membrane, J. Membr. Sci., 340 (2009) 133-140.

[60] L.X. Tuan, C. Buess-Herman, Study of water content and microheterogeneity of CMS cation exchange membrane, Chem. Phys. Lett., 434 (2007) 49-55.

[61] N. Pismenskaya, E. Laktionov, V. Nikonenko, A. El Attar, B. Auclair, G. Pourcelly, Dependence of composition of anion-exchange membranes and their electrical conductivity

on concentration of sodium salts of carbonic and phosphoric acids, J. Membr. Sci., 181 (2001) 185-197.

[62] X.T. Le, Permselectivity and microstructure of anion exchange membranes, J. Colloid Interface Sci., 325 (2008) 215-222.

[63] J. Luo, C. Wu, T. Xu, Y. Wu, Diffusion dialysis-concept, principle and applications, J. Membr. Sci., 366 (2011) 1-16.

[64] Y. Tanaka, Chapter 6 Diffusion Dialysis, in: T. Yoshinobu (Ed.) Membrane Science and Technology, Elsevier, 2007, pp. 487-494.

[65] A. Agrawal, K.K. Sahu, An overview of the recovery of acid from spent acidic solutions from steel and electroplating industries, J. Hazard. Mater., 171 (2009) 61-75.

[66] Y. Tanaka, Chapter 7 Donnan Dialysis, in: T. Yoshinobu (Ed.) Membrane Science and Technology, Elsevier, 2007, pp. 495-503.

[67] A. Dieye, C. Larchet, B. Auclair, C. Mar-Diop, Elimination des fluorures par la dialyse ionique croisée, Eur. Polym. J., 34 (1998) 67-75.

[68] F. Durmaz, H. Kara, Y. Cengeloglu, M. Ersoz, Fluoride removal by donnan dialysis with anion exchange membranes, Desalination, 177 (2005) 51-57.

[69] G. Wiśniewska, T. Winnicki, Removal of nitrate ions acidic wastewater by donnan dialysis involving tabular exchange membranes, Desalination, 56 (1985) 161-173.

[70] O. Altintas, A. Tor, Y. Cengeloglu, M. Ersoz, Removal of nitrate from the aqueous phase by Donnan dialysis, Desalination, 239 (2009) 276-282.

[71] S. Ben Hamouda, K. Touati, M. Ben Amor, Donnan dialysis as membrane process for nitrate removal from drinking water: Membrane structure effect, Arab. J. Chem.

[72] S. Velizarov, Transport of arsenate through anion-exchange membranes in Donnan dialysis, J. Membr. Sci., 425–426 (2013) 243-250.

[73] B. Zhao, H. Zhao, S. Dockko, J. Ni, Arsenate removal from simulated groundwater with a Donnan dialyzer, J. Hazard. Mater., 215–216 (2012) 159-165.

[74] J. Wiśniewski, A. Różańska, Donnan dialysis for hardness removal from water before electrodialytic desalination, Desalination, 212 (2007) 251-260.

[75] A. Rózańska, J. Wiśniewski, Modification of brackish water composition by means of Donnan dialysis as pretreatment before desalination, Desalination, 240 (2009) 326-332.

[76] J. Wiśniewski, A. Różańska, Donnan dialysis with anion-exchange membranes as a pretreatment step before electrodialytic desalination, Desalination, 191 (2006) 210-218.

[77] Y. Tanaka, Chapter 1 Electrodialysis, in: T. Yoshinobu (Ed.) Membrane Science and Technology, Elsevier, 2007, pp. 321-381.

[78] Y. Tanaka, Water dissociation in ion-exchange membrane electrodialysis, J. Membr. Sci., 203 (2002) 227-244.

[79] G. Pourcelly, Chapter 2: Bipolar membrane applications, in: A.J.B. Kemperman (Ed.) Handbook on Bipolar Membrane Technology, Twente University Press, Enschede, The Netherlands, 2000.

[80] E. Vera, J. Sandeaux, F. Persin, G. Pourcelly, M. Dornier, J. Ruales, Deacidification of passion fruit juice by electrodialysis with bipolar membrane after different pretreatments, J. Food Eng., 90 (2009) 67-73.

[81] E. Vera, J. Sandeaux, F. Persin, G. Pourcelly, M. Dornier, J. Ruales, Deacidification of clarified tropical fruit juices by electrodialysis. Part I. Influence of operating conditions on the process performances, J. Food Eng., 78 (2007) 1427-1438.

[82] P. Pinacci, M. Radaelli, Recovery of citric acid from fermentation broths by electrodialysis with bipolar membranes, Desalination, 148 (2002) 177-179.

[83] M. Bailly, Production of organic acids by bipolar electrodialysis: realizations and perspectives, Desalination, 144 (2002) 157-162.

[84] F.G. Wilhelm, Bipolar Membrane Electrodialysis, membrane development ans transport characteristics, in: Membrane Science & Technology, University of Twente, Enschede, The Netherlands, 2001.

[85] Y. Tanaka, Chapter 4 Electro-deionization, in: T. Yoshinobu (Ed.) Membrane Science and Technology, Elsevier, 2007, pp. 437-460.

[86] J. Wood, J. Gifford, J. Arba, M. Shaw, Production of ultrapure water by continuous electrodeionization, Desalination, 250 (2010) 973-976.

[87] F. Lutin, L'electrodialyse et ses nombreuses applications, L'Actualité Chimique, 327 (2009) 59-72.

[88] O.M. Kattan Readi, H.J. Kuenen, H.J. Zwijnenberg, K. Nijmeijer, Novel membrane concept for internal pH control in electrodialysis of amino acids using a segmented bipolar membrane (sBPM), J. Membr. Sci., 443 (2013) 219-226.

[89] O.M. Kattan Readi, M. Gironès, K. Nijmeijer, Separation of complex mixtures of amino acids for biorefinery applications using electrodialysis, J. Membr. Sci., 429 (2013) 338-348.

[90] C. Abels, F. Carstensen, M. Wessling, Membrane processes in biorefinery applications, J. Membr. Sci., 444 (2013) 285-317.

[91] E. Reahl, Half A Century of Desalination with Electrodialysis, in: G.E. Water (Ed.), http://www.gewater.com/pdf/Technical%20Papers_Cust/Americas/English/TP1038EN.pdf, 2008.

[92] K. Kesore, F. Janowski, V.A. Shaposhnik, Highly effective electrodialysis for selective elimination of nitrates from drinking water, J. Membr. Sci., 127 (1997) 17-24.

[93] M. Fidaleo, M. Moresi, Electrodialysis Applications in The Food Industry, Adv. Food Nutr. Res, 51 (2006) 265-360.

[94] F. Gonçalves, C. Fernandes, P. Cameira dos Santos, M.N. de Pinho, Wine tartaric stabilization by electrodialysis and its assessment by the saturation temperature, J. Food Eng., 59 (2003) 229-235.

[95] M. Fidaleo, M. Moresi, A. Cammaroto, N. Ladrange, R. Nardi, Soy sauce desalting by electrodialysis, J. Food Eng., 110 (2012) 175-181.

[96] A. Elmidaoui, L. Chay, M. Tahaikt, M.A.M. Sahli, M. Taky, F. Tiyal, A. Khalidi, M.R. Alaoui Hafidi, Demineralisation of beet sugar syrup, juice and molasses using an electrodialysis pilot plant to reduce melassigenic ions, Desalination, 165 (2004) 435.

[97] T.V. Elisseeva, V.A. Shaposhnik, I.G. Luschik, Demineralization and separation of amino acids by electrodialysis with ion-exchange membranes, Desalination, 149 (2002) 405-409.

[98] S. Cros, B. Lignot, P. Bourseau, P. Jaouen, C. Prost, Desalination of mussel cooking juices by electrodialysis: effect on the aroma profile, J. Food Eng., 69 (2005) 425-436.

[99] M. Bleha, G. Tishchenko, V. Šumberová, V. Kůdela, Characteristic of the critical state of membranes in ED-desalination of milk whey, Desalination, 86 (1992) 173-186.

[100] L. Diblíková, L. Čurda, J. Kinčl, The effect of dry matter and salt addition on cheese whey demineralisation, International Dairy Journal, 31 (2013) 29-33.

[101] H. Šímová, V. Kysela, A. Černín, Demineralization of natural sweet whey by electrodialysis at pilot-plant scale, Desalin. Water Treat., 14 (2010) 170-173.

[102] E. Ayala-Bribiesca, G. Pourcelly, L. Bazinet, Nature identification and morphology characterization of cation-exchange membrane fouling during conventional electrodialysis, J. Colloid Interface Sci., 300 (2006) 663-672.

[103] E. Ayala-Bribiesca, G. Pourcelly, L. Bazinet, Nature identification and morphology characterization of anion-exchange membrane fouling during conventional electrodialysis, J. Colloid Interface Sci., 308 (2007) 182-190.

[104] B. Ruiz, P. Sistat, P. Huguet, G. Pourcelly, M. Araya-Farias, L. Bazinet, Application of relaxation periods during electrodialysis of a casein solution: Impact on anion-exchange membrane fouling, J. Membr. Sci., 287 (2007) 41-50.

[105] B. Ruiz, P. Sistat, P. Huguet, G. Pourcelly, M. Araya-Farias, L. Bazinet, Effect of pulsed electric field on anion-exchange membrane fouling during electrodialysis of a casein solution, Desalination, 200 (2006) 208-209.

[106] N. Cifuentes-Araya, Etude de la formation de colmatages minéraux sur les membranes échangeuses d'ions en cours d'électrodialyse de solutions salines modèles : mécanismes de formation et contrôle par des ratios de champs électriques pulsés oprimisés, in: Departement des Sciences des Aliments et de Nutrition, Université Laval, Quebec, 2012.

[107] S.-i. Sawada, T. Yamaki, S. Kawahito, M. Asano, A. Suzuki, T. Terai, Y. Maekawa, Thermal stability of proton exchange fuel-cell membranes based on crosslinked-polytetrafluoroethylene for membrane-electrode assembly preparation, Polym. Degrad. Stab., 94 (2009) 344-349.

[108] Y. Akiyama, H. Sodaye, Y. Shibahara, Y. Honda, S. Tagawa, S. Nishijima, Study on degradation process of polymer electrolyte by solution analysis, J. Power Sources, 195 (2010) 5915-5921.

[109] Y. Iwai, A. Hiroki, M. Tamada, K. Isobe, T. Yamanishi, Radiation deterioration of ion-exchange Nafion N117CS membranes, Radiation Physics and Chemistry, 79 (2010) 46-51.

[110] T. Sugawara, N. Kawashima, T.N. Murakami, Kinetic study of Nafion degradation by Fenton reaction, J. Power Sources, 196 (2011) 2615-2620.

[111] F.M. Collette, C. Lorentz, G. Gebel, F. Thominette, Hygrothermal aging of Nafion®, J. Membr. Sci., 330 (2009) 21-29.

[112] F. Wang, H. Tang, M. Pan, D. Li, Ex situ investigation of the proton exchange membrane chemical decomposition, Int. J. Hydrogen Energy, 33 (2008) 2283-2288.

[113] G. Meyer, G. Gebel, L. Gonon, P. Capron, D. Marscaq, C. Marestin, R. Mercier, Degradation of sulfonated polyimide membranes in fuel cell conditions, J. Power Sources, 157 (2006) 293-301.

[114] H. Tang, S. Peikang, S.P. Jiang, F. Wang, M. Pan, A degradation study of Nafion proton exchange membrane of PEM fuel cells, J. Power Sources, 170 (2007) 85-92.

[115] A. Collier, H. Wang, X. Ziyuan, J. Zhang, D. Wilkinson, Degradation of polymer electrolyte membranes, Int. J. Hydrogen Energy, 31 (2006) 1838-1854.

[116] S. Zhang, X. Yuan, H. Wang, W. Merida, H. Zhu, J. Shen, S. Wu, J. Zhang, A review of accelerated stress tests of MEA durability in PEM fuel cells, Int. J. Hydrogen Energy, 34 (2009) 388-404.

[117] Y. Tanaka, Chapter 14 Membrane Deterioration, in: T. Yoshinobu (Ed.) Membrane Science and Technology, Elsevier, 2007, pp. 293-317.

[118] R. Ghalloussi, Contribution à l'étude du vieillissement de membranes échangeuses d'ions utilisées dans un procédé d'électrodialyse pour l'industrie agroalimentaire, in, Université Paris-Est, Thiais, France, 2012.

[119] R. Ghalloussi, W. Garcia-Vasquez, N. Bellakhal, C. Larchet, L. Dammak, P. Huguet, D. Grande, Ageing of ion-exchange membranes used in electrodialysis: Investigation of static parameters, electrolyte permeability and tensile strength, Sep. Purif. Technol., 80 (2011) 270-275.

[120] J. Healy, C. Hayden, T. Xie, K. Olson, R. Waldo, M. Brundage, H. Gasteiger, J. Abbott, Aspects of the Chemical Degradation of PFSA Ionomers used in PEM Fuel Cells, Fuel Cells, 5 (2005) 302-308.

[121] S.D. Knights, K.M. Colbow, J. St-Pierre, D.P. Wilkinson, Aging mechanisms and lifetime of PEFC and DMFC, J. Power Sources, 127 (2004) 127-134.

[122] A.K. Pandey, A. Goswami, D. Sen, S. Mazumder, R.F. Childs, Formation and characterization of highly crosslinked anion-exchange membranes, J. Membr. Sci., 217 (2003) 117-130.

[123] C.A. Wilkie, J.R. Thomsen, M.L. Mittleman, Interaction of poly(methyl methacrylate) and nafions, J. Appl. Polym. Sci., 42 (1991) 901-909.

[124] B. Bauer, D. Jones, J. Rozière, L. Tchicaya, G. Alberti, M. Casciola, L. Massinelli, A. Peraio, S. Besse, E. Ramunni, Electrochemical characterisation of sulfonated polyetherketone membranes, J. New Mater. Electrochem. Syst., 3 (2000) 93-98.

[125] A.B. LaConti, M. Hamdan, R.C. McDonald, Mechanisms of membrane degradation, in: Handbook of Fuel Cells, John Wiley & Sons, Ltd, 2010.

[126] H. Xu, J. Fang, M. Guo, X. Lu, X. Wei, S. Tu, Novel anion exchange membrane based on copolymer of methyl methacrylate, vinylbenzyl chloride and ethyl acrylate for alkaline fuel cells, J. Membr. Sci., 354 (2010) 206-211.

[127] H. Zarrin, J. Wu, M. Fowler, Z. Chen, High durable PEEK-based anion exchange membrane for elevated temperature alkaline fuel cells, J. Membr. Sci., 394–395 (2012) 193-201.

[128] A. Bukhovets, T. Eliseeva, Y. Oren, Fouling of anion-exchange membranes in electrodialysis of aromatic amino acid solution, J. Membr. Sci., 364 (2010) 339-343.

[129] N. Tanaka, M. Nagase, M. Higa, Organic fouling behavior of commercially available hydrocarbon-based anion-exchange membranes by various organic-fouling substances, Desalination, 296 (2012) 81-86.

[130] L. Paugam, D. Delaunay, M. Rabiller-Baudry, Cleaning efficiency and impact on production fluxes of oxidizing disinfectants on a PES ultrafiltration membrane fouled with proteins, Food Bioprod. Process., 88 (2010) 425-429.

[131] N. Porcelli, S. Judd, Chemical cleaning of potable water membranes: A review, Sep. Purif. Technol., 71 (2010) 137-143.

[132] L. Dammak, C. Larchet, D. Grande, Ageing of ion-exchange membranes in oxidant solutions, Sep. Purif. Technol., 69 (2009) 43-47.

[133] X. Tang, S.H. Flint, R.J. Bennett, J.D. Brooks, The efficacy of different cleaners and sanitisers in cleaning biofilms on UF membranes used in the dairy industry, J. Membr. Sci., 352 (2010) 71-75.

[134] L. Paugam, D. Delaunay, M. Rabiller-Baudry, Cleaning efficiency and impact on production fluxes of oxidising disinfectants on a PES ultrafiltration membrane fouled with proteins, Food Bioprod. Process., 88 (2010) 425-429.

[135] M.E. Mansour, A. Ettori, S. Luque, J.R. Álvarez, C. Causserand, P. Aimar, Accelerated Ageing of Crosslinked Polyamide Membranes, Procedia Eng., 44 (2012) 789.

[136] C. Regula, E. Carretier, Y. Wyart, M. Sergent, G. Gésan-Guiziou, D. Ferry, A. Vincent, D. Boudot, P. Moulin, Ageing of ultrafiltration membranes in contact with sodium hypochlorite and commercial oxidant: Experimental designs as a new ageing protocol, Sep. Purif. Technol., 103 (2013) 119-138.

[137] A. Ettori, E. Gaudichet-Maurin, J.-C. Schrotter, P. Aimar, C. Causserand, Permeability and chemical analysis of aromatic polyamide based membranes exposed to sodium hypochlorite, J. Membr. Sci., 375 (2011) 220-230.

[138] E. Gaudichet-Maurin, F. Thominette, Ageing of polysulfone ultrafiltration membranes in contact with bleach solutions, J. Membr. Sci., 282 (2006) 198-204.

[139] C. Causserand, S. Rouaix, J.-P. Lafaille, P. Aimar, Ageing of polysulfone membranes in contact with bleach solution: Role of radical oxidation and of some dissolved metal ions, Chemical Engineering and Processing: Process Intensification, 47 (2008) 48-56.

[140] E. Arkhangelsky, D. Kuzmenko, V. Gitis, Impact of chemical cleaning on properties and functioning of polyethersulfone membranes, J. Membr. Sci., 305 (2007) 176-184.

[141] E. Arkhangelsky, D. Kuzmenko, N.V. Gitis, M. Vinogradov, S. Kuiry, V. Gitis, Hypochlorite Cleaning Causes Degradation of Polymer Membranes, Tribology Lett., 28 (2007) 109-116.

[142] Y.-N. Kwon, J.O. Leckie, Hypochlorite degradation of crosslinked polyamide membranes, J. Membr. Sci., 283 (2006) 21-26.

[143] K. Yadav, K. Morison, M.P. Staiger, Effects of hypochlorite treatment on the surface morphology and mechanical properties of polyethersulfone ultrafiltration membranes, Polym. Degrad. Stab., 94 (2009) 1955-1961.

[144] R. Prulho, S. Therias, A. Rivaton, J.-L. Gardette, Ageing of polyethersulfone/polyvinylpyrrolidone blends in contact with bleach water, Polym. Degrad. Stab., 98 (2013) 1164-1172.

[145] S. Rouaix, C. Causserand, P. Aimar, Experimental study of the effects of hypochlorite on polysulfone membrane properties, J. Membr. Sci., 277 (2006) 137-147.

[146] C. Causserand, S. Rouaix, J.-P. Lafaille, P. Aimar, Degradation of polysulfone membranes due to contact with bleaching solution, Desalination, 199 (2006) 70-72.

[147] J.A. Vega, C. Chartier, W.E. Mustain, Effect of hydroxide and carbonate alkaline media on anion exchange membranes, J. Power Sources, 195 (2010) 7176-7180.

[148] K. Kneifel, K. Hattenbach, Properties and long-term behavior of ion exchange membranes, Desalination, 34 (1980) 77-95.

[149] T. Sata, M. Tsujimoto, T. Yamaguchi, K. Matsusaki, Change of anion exchange membranes in an aqueous sodium hydroxide solution at high temperature, J. Membr. Sci., 112 (1996) 161-170.

[150] B. Bauer, H. Strathmann, F. Effenberger, Anion-exchange membranes with improved alkaline stability, Desalination, 79 (1990) 125-144.

[151] G. Couture, A. Alaaeddine, F. Boschet, B. Ameduri, Polymeric materials as anion-exchange membranes for alkaline fuel cells, Prog. Polym. Sci., 36 (2011) 1521-1557.

[152] A.C. Cope, A.S. Mehta, Mechanism of the Hofmann Elimination Reaction: An Ylide Intermediate in the Pyrolysis of a Highly Branched Quaternary Hydroxide, J. Am. Chem. Soc., 85 (1963) 1949-1952.

[153] A.C. Cope, E.R. Trumbull, Olefins from Amines: The Hofmann Elimination Reaction and Amine Oxide Pyrolysis, in: Organic Reactions, John Wiley & Sons, Inc., 2004.

[154] S. Chempath, B.R. Einsla, L.R. Pratt, C.S. Macomber, J.M. Boncella, J.A. Rau, B.S. Pivovar, Mechanism of Tetraalkylammonium Headgroup Degradation in Alkaline Fuel Cell Membranes, J. Phys. Chem. C, 112 (2008) 3179-3182.

[155] S. Chempath, J.M. Boncella, L.R. Pratt, N. Henson, B.S. Pivovar, Density Functional Theory Study of Degradation of Tetraalkylammonium Hydroxides, J. Phys. Chem. C, 114 (2010) 11977-11983.

Chapitre 2

Vieillissement des membranes échangeuses d'ions utilisées en électrodialyse : Etude structurale et physico-chimique

Présentation de l'article

Dans le chapitre précédent, nous avons présenté les généralités sur les membranes échangeuses d'ions et les principaux procédés les utilisant. Il a été montré que les études systématiques portant sur le comportement à long terme des membranes échangeuses d'ions en électrodialyse sont rares et insuffisantes.

En partenariat avec EURODIA INDUSTRIE S.A., nous avons lancé une première étude scientifique portant sur les mécanismes de dégradation de ces matériaux en électrodialyse conventionnelle.

Une étude comparative des caractéristiques physico-chimiques et structurales a été menée sur quatre paires de membranes, deux échangeuses de cations et deux échangeuses d'anions. Chaque paire est formée d'un échantillon neuf et d'un autre retiré d'une unité d'électrodialyse après deux ans de service dans la purification d'un acide organique dans l'industrie agroalimentaire. Pour des raisons de confidentialité, nous ne dévoilons pas dans ce chapitre la nature exacte de cette application et des membranes utilisées.

L'objectif essentiel était d'évaluer les principales modifications subies par les membranes et de conclure sur leurs causes de dégradation.

Pour cela, nous avons testé de nombreuses méthodes de caractérisation des membranes échangeuses d'ions et identifié les méthodes les plus appropriées pour l'étude du vieillissement. Nous nous sommes basés sur le modèle microhétérogène afin d'expliquer les variations des propriétés statiques et dynamiques des membranes échangeuses d'ions.

Cette étude nous a permis de conclure que les mécanismes de dégradation des membranes échangeuses de cations sont différents de ceux subis par les membranes échangeuses d'anions.

Pour la membrane échangeuse de cations on constate une perte d'hydrophilie causée par la perte des sites fixes, tandis que pour la membrane échangeuse d'anions on remarque une augmentation de son hydrophobie. Ce phénomène a été attribué au colmatage organique par des molécules hydrophiles. Les conséquences du colmatage sont l'augmentation du taux de gonflement et la formation de macro-défauts dans la membrane.

D'une manière générale, les membranes échangeuses d'anions sont plus sensibles au vieillissement que les membranes échangeuses de cations.

Ageing of ion-exchange membranes in electrodialysis: A structural and physicochemical investigation

Journal of Membrane Science (436) **2013** 68-78

R. GHALLOUSSI[1], W. GARCIA-VASQUEZ[1], L. CHAABANE[1], L. DAMMAK[1], C. LARCHET[1], S. V. DEABATE[2], E. NEVAKSHENOVA[3], V. NIKONENKO[3], D. GRANDE[1]

[1] *Institut de Chimie et des Matériaux Paris-Est, UMR 7182 CNRS – Université Paris-Est Créteil. 2 rue Henri Dunant, 94320 Thiais, France.*

[2] *Institut Européen des Membranes, UMR 5635 Université Montpellier 2-ENSCM-CNRS, CC047, place Eugène Bataillon, 34095 Montpellier Cedex 5, France.*

[3] *Kuban State University, 149 Stavropolskaya st., 350040 Krasnodar, Russia.*

Abstract

Understanding the ageing mechanisms of Ion-Exchange Membranes (IEMs) used in electrodialysis (ED) for food industry applications constitutes a major challenge. In this regard, four used membranes (two cationic ones and two anionic ones) were analyzed at the end of their useful life (2 years of ED operation) and compared with their respective fresh new samples to assess the evolution of their structural and physicochemical characteristics, and explore their deterioration. The conductivity, ion-exchange capacity, water content, contact angle and counterion transport number were determined for each new and used membrane. Scanning electron microscopy (SEM), energy dispersive X-ray (EDX), and FTIR analyses were also performed.

The used cation-exchange membranes (CEMs) suffered significant degradation; nonetheless, they were generally more robust and resistant than the anion-exchange counterparts, which were more unstable. A significant degradation in the polymer matrix of both membrane types was found. Both used CEMs and anion-exchange membranes (AEMs) lost a part of ion-exchange sites, and their specific electrical conductivity decreased. However, the CEMs became denser with lower water content and higher surface hydrophobicity, while the water content and the thickness of the AEMs increased in about two times. The permselectivity of used CEMs decreased, while that of AEM analogues was not modified. A physicochemical model schematically describing the time evolution of membrane structure and properties was built on the basis of the microheterogeneous model and the experimental data. The main idea was to present colloid aggregates adsorbed by the membrane as nanoparticles occupying a part of membrane pores. This model was used to explain the variation of the totality of equilibrium and transport properties, and in particular, the apparent contradiction between the loss of ion-exchange capacity and the increase in permselectivity of the used AEMs.

2.1. Introduction

Ion-Exchange Membranes (IEMs) are successfully and widely used for the desalination of seawater and brackish water as well as for the treatment of industrial effluents [1]. IEMs are efficient materials for the concentration and separation of ionic species in food and pharmaceutical industrial processes as well as in the chemical industry. The use of this type of membranes makes the processes cleaner and less energy-consuming. Electrodialysis (ED) is one of the most important IEM based separation processes [1]. It presents several advantages compared to other membrane processes, such as high water recovery and long useful life of the membranes at temperatures up to 50 °C.

Moreover, new applications of ED in water and waste treatment [2], in food [3] and chemical industries have been identified, as well as in dairy [4], fruit juice [5], sugar [6], and wine production [7]. Nevertheless, even if ED is already present in some of these commercial applications, it is still considered as a state-of-the-art process as IEMs do not always show the same advantages as they do for brackish water desalination. Strathmann [1, 8] has identified the limitations and key problems in ED for waste treatment and desalination of food products, thus highlighting the need for membranes with higher permselectivity, lower electrical resistance, and better chemical and thermal stability at lower costs. In this regard, the understanding of ageing processes occurring in IEMs used in ED for food industry applications, and the investigation of their long-term behaviour are necessary to enhance the progress of this advantageous technology.

In addition, the evaluation of the IEM lifetime is a very important element in the control of the ED operations, as the loss of their physico-chemical and separative properties is usually accompanied by lower yields and increased costs, due to the replacement of IEMs and the growth of energy consumption. Generally, the main causes associated with the deterioration of membrane properties and discussed in the literature are membrane fouling and poisoning [9, 10]. IEMs are fouled by ionic species of medium molecular mass, such as surface active agents having the charge opposite to that of fixed site of the membranes. The poisoning is produced by multiply charged big counter-ions, such as ferrocyanide ions, i.e. $Fe(CN)_6^{4-}$ [11], due to their high selective adsorption and low mobility in the membrane. In addition, concentration polarization of membranes results in deposition of particles of poorly soluble salts on the membrane surface and in their pores. This phenomenon is known as membrane scaling [12]. In all three cases, the electrical resistance of the membrane increases with time;

generally, the ion-exchange capacity and permselectivity are deteriorated. It is noteworthy that these three mechanisms of membrane deterioration are rather common for all types of membrane processes.

In the case of ED, there are a number of particular studies. Kneifel and Hattenbach [11] and later Sata et al. [12] have evaluated the membrane property changes with elapsed time under the effect of several chemical agents, such as NaCl, HNO_3, NaOH and an oxidizing agent (0.1 N K_2CrO_4 + 1 N HCl + 1 N NaCl). The strongest deterioration of membrane properties (resistivity, ion-exchange capacity and permselectivity) was observed in the case of the NaOH solution and the oxidizing agent. Sata et al. [12] have established that the alkaline deterioration of anion-exchange membranes (AEMs) was caused by the decomposition of backing polymers and anion-exchange groups. Quaternary ammonium groups decompose in the concentrated alkaline solution by the Hofmann degradation reaction. High attention was paid by Japanese researchers to study the performance change of ion-exchange membranes in long-term seawater ED [10, 13]. In this case, a very important effect is exerted by the precipitation of $CaCO_3$ and $CaSO_4$ on the membrane surfaces, which finally results in the membrane destruction [14]. Moreover, surface fouling produced by microorganisms and organic components present in seawater makes a high effect on ED operation parameters [15]. Grossman and Sonin [16] studied the mechanism of surface biofouling and showed that the deposition of a film by suspended matters on the membrane surface leads to increasing concentration polarization. This study permitted a theoretical explanation of experimental results obtained during ED of seawater and brackish water, in particular that of Korngold et al. [17], concerning the influence of current density on fouling. It is noteworthy that the deposition of a film of colloids on the membrane surface may be interpreted as an increase in effective thickness of the boundary diffusion layer [17]. It was also shown [18] that AEMs are more sensitive to the organic fouling than cation-exchange membranes (CEMs) because organic compounds are often composed of a large anion, while the size of cations is smaller. The charged organic molecules are larger than simple ions and can be trapped within the double electrical layer at the external and internal surface of AEMs where they partly neutralize the fixed charge of the membranes. As a result, the effective fixed charge density of the pore walls decreases. This causes an increased ohmic resistance [17-21] and a reduced permselectivity [18, 22] of the membrane. The rate of membrane deterioration generally increases with increasing current density/concentration polarization.

Similar results were obtained when studying fouling and scaling in reverse electrodialysis (RED), where an electrical potential difference is generated when two solutions of different salinity are flowed on either side of a membrane. However, unlike conventional ED or electrodialysis reversal (EDR), in the case of RED, the intermembrane distance is essentially lower and there is no current density imposed. As a result, the concentration polarization is lower and membrane fouling and especially scaling are less strong [23]. Post et al. [23, 24] and Vermaas et al. [25, 26] have found that in RED, similarly as in reverse osmosis, fouling is mostly concentrated on the feed water spacers. This resulted in an increasing pressure drop over the RED compartment, under the same flow rate. Spacerless stacks made using profiled membranes showed essentially lower rate of fouling [26]: the pressure drop through the stacks with profiled membranes were lower, the stack electrical resistance increased less and the loss in permselectivity was less important. Vermaas et al. [25, 26] have remarked that the charge of the membranes had a strong influence on the rate and the type of fouling. For the AEMs, remnants of diatoms, clay minerals and organic fouling were observed. While for the CEMs, the main deterioration was caused by scaling of calcium phosphate. At the same time, plastic sheets of non-conductive PE use instead of membranes in an additional stack were least sensitive to fouling.

Another field of membrane applications where the membrane degradation presents one of the main obstacles is fuel cells, because the lifetime of the PEM fuel cell is highly dependent on the lifetime of the ion-exchange membrane [27, 28]. There are several known modes of perfluorosulfonic acid (PFSA) membranes degradation during fuel cell operation. They involve mechanical [29], thermal, and electrochemical processes [28]. It is admitted that the most important cause of PFSA membrane failure is a chemical degradation initiated by free-radical attack on reactive end groups [28, 29].

The issue of degradation of AEMs is largely presented in an excellent review by Merle et al.[30] on the use of these membranes in alkaline fuel cells. Several mechanisms of degradation of the ammonium ion-exchange groups in alkaline media are described, the most important being the Hofmann elimination and the nucleophilic substitution.

However, published information on IEM ageing is scarce, and especially for the membranes used in ED for food industry applications. Some studies concerning the characterization of membranes at the end of their lifetime in ED and the effect of cleaning agents or stress conditions have been carried out [12, 31-35]. Dammak et al. [31] have performed an artificial ageing of two membranes (a homogeneous one (MX) and a heterogeneous one (MK-40))

under oxidizing conditions, *i.e*. in peracetic acid, and in P3 Active Oxania® solutions, cleaning agents commonly used in industrial ED for food industry applications. It was established an increase in conductivity and swelling rate, resulting from the modification of the polymer chain structure, without a significant deterioration of the functional groups, since the ion-exchange capacity remained almost constant.

In another recent work, Ghalloussi et al. [32] have compared the electrolyte permeability and tensile strength of two IEM pairs. Each pair was composed of a new sample and a used one extracted from an electrodialyzer after two years of operation. The authors observed a sevenfold decrease in the permeability of membranes after their use in a food industrial application, and a significant decrease in the tensile strength, which was more important for the AEMs (eightfold) than for the CEMs (1.5 times). They also observed inhibition and disappearance of a large part of membrane functional sites, as well as polymer degradation and fouling by organic species present in the solution.

In the present paper, four pairs of IEMs are compared, namely two pairs of CEMs and two others of AEMs. Each pair is constituted of a new sample and a sample used for two years in an ED process for food industry. This investigation focuses on the comparison of structural, equilibrium and transport properties in order to identify the origin of the differences in the behaviour of the studied CEMs and AEMs, and to propose a model explaining the evolution of membrane properties.

2.2. Experimental

2.2.1. Ion-exchange membranes

Eight Neosepta® IEM specimens were provided in pairs by Eurodia Industry SA.

Each pair consisted of a sample of a new membrane and another one retired from an ED module after two years of operation in a food industry process.

For confidentiality reasons, the exact references of the tested membranes were not disclosed. Therefore, we use the following notation: IEMxy where IEM was CEM or AEM, x referred to the membrane (x = 1 or 2), and y to the membrane state (y = N for new samples and y = U for used samples).

Neosepta® membranes were prepared [36], using a mixture of poly(vinyl chloride) (PVC) fine powder and mainly two comonomers, *i.e.* styrene (St) and divinylbenzene (DVB). This mixture was coated on a polymer cloth and heated to polymerize the comonomers. Ion-exchange groups were introduced at the end of the process. CEMs contained sulfonated sites, while AEMs had quaternary ammonium groups. Fig. 2-1 shows the milestones of Neosepta® CEM and AEM syntheses.

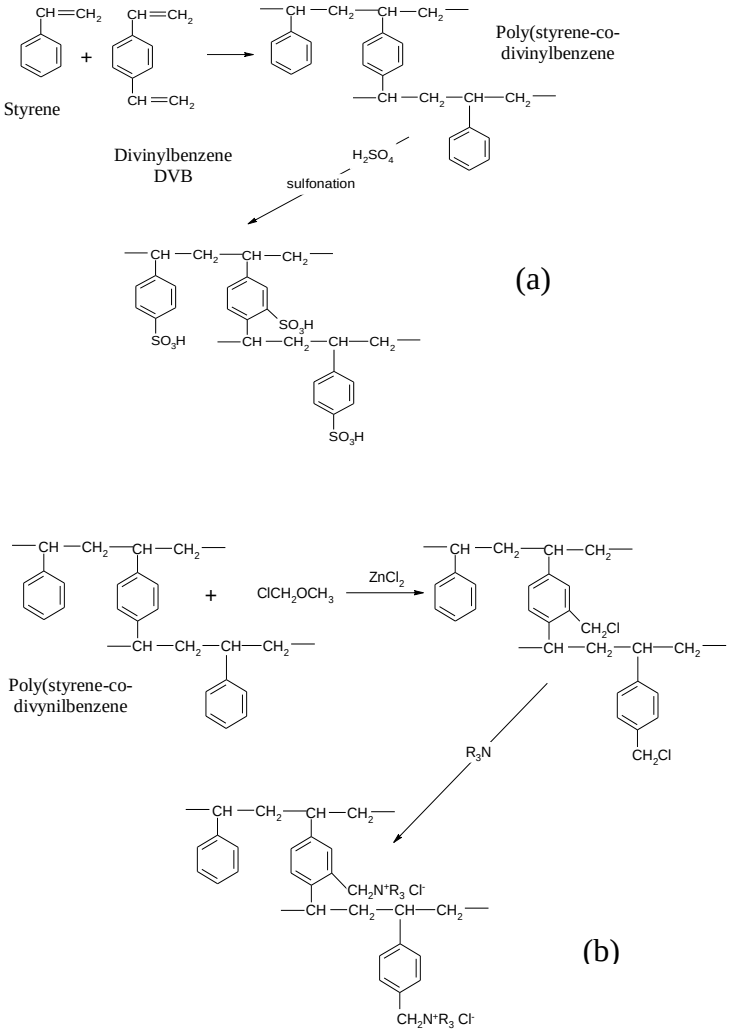

Fig. 2-1. Reaction schemes of Neosepta® CEM (a) and AEM (b) syntheses.

The SEM image in Fig. 2-2 displays the general appearance of a cross-section of the membranes. We distinguished the polymer cloth from the functionalized polystyrene polymer cross-linked with DVB and the added PVC.

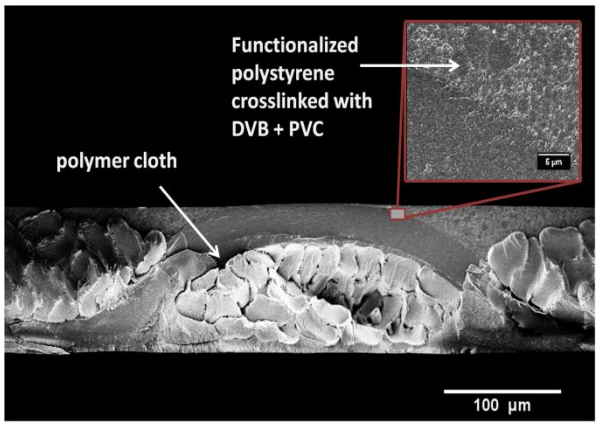

Fig. 2-2. SEM micrograph of the cross-section of a Neosepta® membrane.

Prior to any measurement, we conditioned the new samples in order to stabilize their physico-chemical properties and remove impurities that may come from their manufacturing process. The French standard NF X 45-200 was followed to realise this treatment [37]. The same stabilization treatment was applied to t<he aged membranes.

2.1.1. Ion-exchange capacity

The CEM samples were placed in a 1 M HCl solution (250 mL per 10 cm²). The samples were then abundantly washed with water; they were converted into the Na^+ form by soaking them in a solution obtained from mixing 230.0 mL of a 0.1 M NaCl and 20.0 mL of a 0.1 M NaOH solutions, during 2 h at 25 °C. The ion-exchange capacities (E_C) were determined by titration of the remaining OH^- ions and expressed as the amount of adsorbed H^+ ($meq.g^{-1}$ dry).

The AEM samples were placed in a 0.1 M HCl solution. The samples were also abundantly washed with water; they were immersed in a 1.0 M HNO_3 solution during 12 h at 25 °C. The ion-exchange capacity was determined by the chloride content in the equilibrium solution.

2.1.2. Water content

The membranes were soaked during 24 h at 25 °C in an electrolyte solution (0.1 M NaCl for the CEMs and 0.1 M HCl for the AEMs). The wet mass W_a was measured after slightly wiping the membrane surface with filter paper. The dry mass W_b was obtained by drying the samples at 60 °C for 24 h. The water content was then found as follows:

$$\%W = \frac{W_a - W_b}{W_b} \times 100 \tag{2.1}$$

2.1.3. Membrane thickness

Samples were taken directly from their equilibrating solution and the membrane thicknes (T_m) values were measured in the wet state using a Käfer Thicknes Dial Gauge specially devised for plastic film thickness measurements, with a resolution of 1 μm. These values were averaged from 10 measurements at different locations on the effective surface region of the membrane.

2.1.4. Contact angle

The measurements of the contact angle values were performed using a FM40 EasyDrop device from Krüss. The images of a water drop at the surface of the membrane were captured by a high resolution camera, and they were then processed by the Wingoutte software to determine the contact angle value using interpolation methods.

The measurements were repeated 5 times at different spots of the dry membrane at room temperature (just the bound water was remaining). The contact angle was determined as an average value of 5 measurements.

2.1.5. Alternating current conductivity

The experimental assembly used consisted of a clip-type cell to measure the membrane conductivity, a conductivity meter and a water bath at 25 ± 1 °C [38].

The determination of membrane conductance G_m needed two measurements, one without the membrane (G_1) and another one with the membrane (G_2), to deduce the value:

$$G_m = \frac{G_1 G_2}{G_1 - G_2} \tag{2.2}$$

Using the value of the membrane thickness (T_m) value and the electrodes section area (A = 1 cm²), the membrane conductivity was calculated as:

$$\kappa_m = G_m \times \frac{T_m}{A} \tag{2.3}$$

The conductivity of the four pairs of membranes was measured in NaCl solutions at different concentrations ranging from 10^{-2} to 0.5 mol.L^{-1}.

2.1.6. Counter-ion transport number

The method of concentration cell [39, 40], giving an apparent counterion transport number, was used. The potential difference (ΔU) between two compartments separated by an IEM was measured. Applying Ag/AgCl electrodes, the apparent counterion transport number was calculated by Eq. (2.1) for CEMs and by Eq. (2.2) for AEMs [39, 40]:

$$t_{counterion} = t_+ = \frac{\Delta U - \Delta U^\circ}{2\,E^\circ} \tag{2.4}$$

$$t_{counterion} = t_- = \frac{2\,E^\circ - (\Delta U - \Delta U^\circ)}{2\,E^\circ} \tag{2.5}$$

where ΔU^0 was the asymmetric potential of electrodes and:

$$E^0 = \frac{RT}{F} \ln\left(\frac{a_{\pm 1}}{a_{\pm 2}}\right) \tag{2.6}$$

the Nernst potential, $a_{\pm 1}$ and $a_{\pm 2}$ the mean ionic activities of electrolyte in compartments 1 (containing a more diluted NaCl solution) and 2 (containing a more concentrated NaCl solution), respectively. The mean activity values were considered to be equal to the concentrations since they were lower than 10^{-1} mol.L^{-1}. The method gave apparent transport numbers, which depended on water transfer through the membrane in the conditions of potential difference measurements [39]. However, it was possible to find the "real" transport number by applying the Scatchard equation [39] or by using the values of specific conductivity and diffusion permeability [41].

The membrane sample conditioned in a chosen ionic form was inserted into the cell already described by Dammak et al. [42]. The surface of the IEM was rather small and equal to 0.5 cm² in order to reduce the flux of NaCl crossing the membrane and polluting the solution in the diluted compartment. This cell was assembled using threaded rods and then placed in a holder immersed into the water bath that automatically centered the cell between two blocks of agitation. The different series of measurements were made according to the following cycle:

- The membrane was fixed in the cell and deionised water began to circulate in both compartments at a rate of 1300 $mL.h^{-1}$ for 15 min to remove any residue of electrolyte contained in the membrane. The stirring speed was set at the maximum value ω_{max} = 950 rpm.
- The water was removed from the cell, then the two solutions of NaCl and the two electrodes were introduced (the flow rate and the stirring speed values were kept constant).
- The value of ΔU was read after the establishment of a steady state (around 10-15 min) when the potential difference became constant.

2.1.7. Scanning electron microscopy and EDX analyses

SEM images were obtained from a Pt/Pd coated sample with an accelerating tension of 3 kV using a LEO 1530 microscope. The surface elemental composition of the samples was also determined by energy-dispersive X-ray (EDX) spectroscopy with a 10 mm² germanium diode as an X-ray detector (lmix, Princeton Gamma-Tech) attached to the SEM equipment.

2.1.8. Infrared spectroscopy

Fourier-transform infrared (FTIR) transmittance measurements were carried out on a Nicolet ‘‘Nexus’’ spectrometer equipped with a Globar source and a DTGS detector between 550 and 4000 cm^{-1}. The spectral resolution was 2 cm^{-1} and 32 scans were realized for each spectrum. Samples were pellets made of a ground mixture of dried KBr and 1 wt% of powdered membrane. $K_3[Fe(CN)_6]$ was also added to the mixture (2 mg for each pellet) as an internal standard in order to permit quantitative comparison between fresh and used materials. All spectra were normalized according to the ν(C≡N) band at 2095 cm^{-1}.

2.2. Results

2.2.1. Morphological, equilibrium and transport characteristics

SEM microphotographs of fresh and used membranes are shown in Fig. 2-3. As it can be seen, the surface of a fresh Neosepta® membrane is smooth and homogeneous, at least at the scale of the order of several micrometers. The surface of the corresponding used CEM presents some "scales". They are due to the fact that the membrane becomes fragile: the surface of a used swollen membrane is smooth, but when the membrane is drying, the scales appear. The surface of a used AEM shows important structural defects.

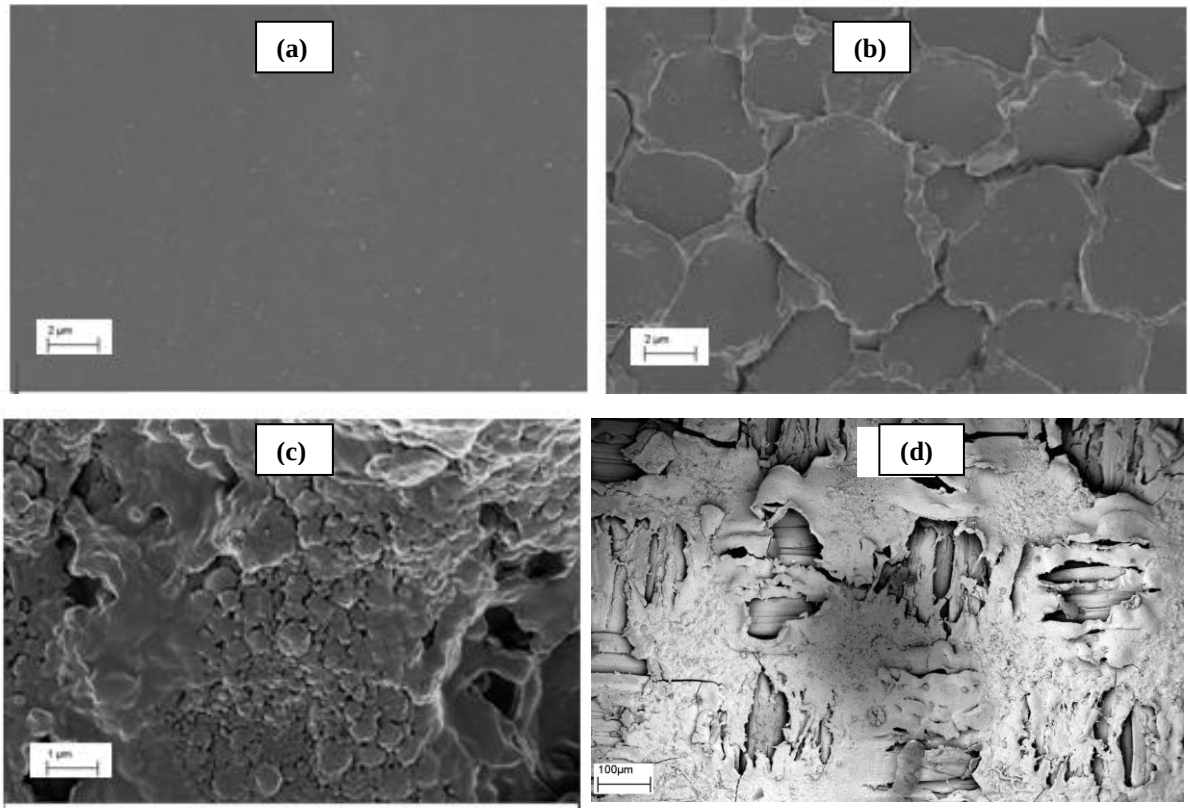

Fig. 2-3. SEM micrographs of Neosepta® membranes. New CEM (a), used CEM (b) and used AEM (c,d).

The cavities seen on the surface of the AEM2U, which was less deteriorated than the AEM1U, are quite similar to those observed by Pismenskaya et al. [43] on the surface of a CMX (Neosepta®) membrane exposed to an overlimiting current (Fig. 2-4). The cavities on

the surface of the AEM1U are so large that the reinforcing cloth is exposed, while it is normally located at about ten micrometers from the surface.

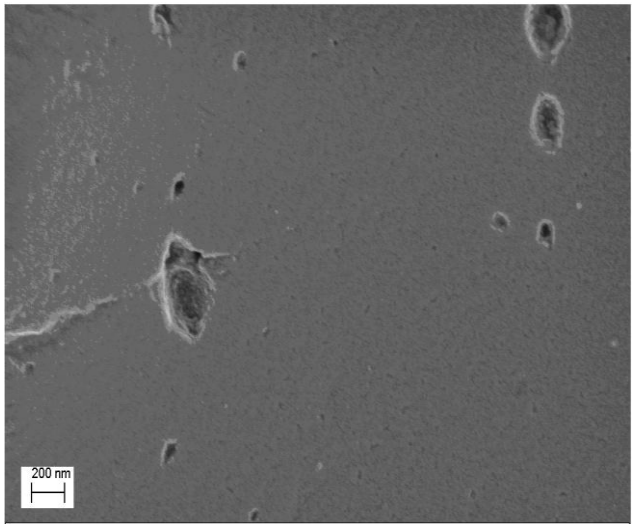

Fig. 2-4. SEM micrograph of the surface of a used AEM.

Obviously enough, such strong deteriorations of membrane structure should be accompanied with significant changes in membrane properties. The main equilibrium and transport characteristics of the IEMs under study are listed in Table 2-1.

The ion-exchange capacities of nearly all membranes drop significantly after two years of use in ED treatment of solutions containing weak organic acids, in a food industry application. The CEM2 sample seems to be an exception: it is stable and very little affected. The CEM1 specimen shows a dramatic variation in its contact angle (+108 %), ion-exchange capacity (-71 %), and Na^+ transport number (-38 %), but it displays a moderate decrease in its water content (-16 %) and thickness (-9 %).

The AEM1 appears to be the most affected membrane by the decrease in ion-exchange capacity (-84 %) and contact angle (-25 %), accompanied by a large increase in water content (+40 %) and thickness (+130 %). The AEM2 has exactly the same behaviour as that of AEM1 (except for water content) but in more moderate proportions.

The contact angle of CEM1 increases significantly after ED operation, thus showing that the membrane becomes less hydrophilic. This is consistent with the decrease in the water content.

Membranes	CEM				AEM			
	CEM1N	CEM1U	CEM2N	CEM2U	AEM1N	AEM1U	AEM2N	AEM2U
E_C (meq.g^{-1} of dry IEM)	2.66	0.77	1.11	1.08	1.45	0.23	1.94	1.40
%W	28.2	23.7	21.1	28.4	28.7	40.3	24.90	23.10
T_m (µm)	176	160	170	175	148	344	160	170
θ (°)	38 ± 2	79 ± 2	43 ± 2	48 ± 2	69 ± 2	52 ± 2	67 ± 2	62 ± 2
κ_m (mS cm^{-1})	6.1	2.3	5.1	4.8	5.6	2.9	7.9	5.0
f_2	0.12	0.10	0.11	0.07	0.11	0.39	0.12	0.30
$t_{counterion}$	0.97	0.60	0.92	0.91	0.99*	0.99*	0.92*	0.95*

Table 2-1. Static characteristics of the studied membranes: ion-exchange capacity (E_C), water content (%W), thickness (T_m), contact angle (θ°), electric conductivity in 0.1 M NaCl (κ_m), volume fraction of inter-gel solution (f_2), and apparent counterion transport number ($t_{counterion}$).

The loss of water and the increase in surface hydrophobicity apparently arise from the reduction in the concentration of active functional sites resulting from their detachment. The contact angle for CEM2 increases as well, but to lower extent. In contrast, the decrease in the contact angles of both used AEMs show that the membranes become more hydrophilic. For the AEM1 membrane, the decrease is more significant. This is confirmed by an important increase in the water content and in the membrane thickness. Taking into account that the ion-exchange capacity decreases, this effect might be due to the sorption of highly hydrophilic substances, which could be organic acids with hydrophilic groups such as carboxyl and hydroxyl ones. For AEM2, the changes of parameters occur in similar way, but they are less significant.

2.2.2. Spectroscopic investigation

The variations of water content and contact angle associated with the studied membranes correlate well with the evolution of their infrared spectra shown for the CEM1 and AEM1 membranes in Figs. 2-5a-d.

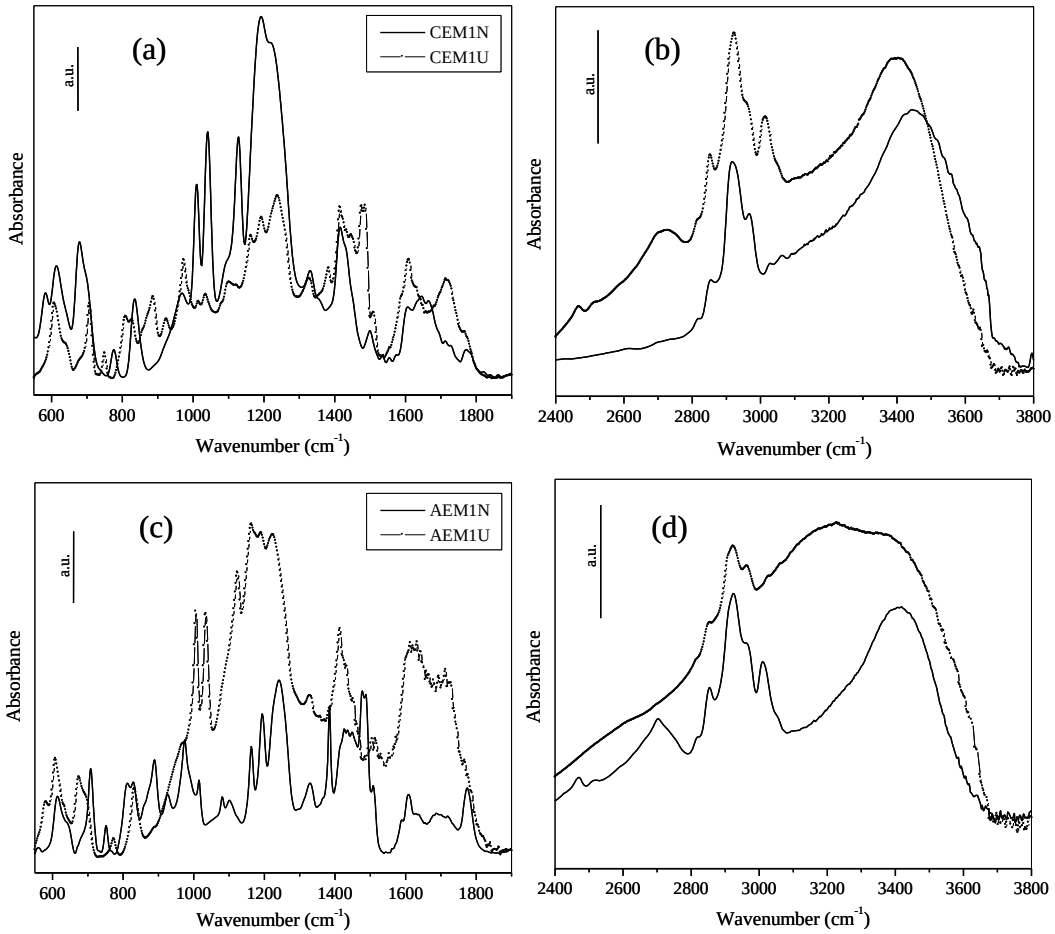

Fig. 2-5. Comparison of FTIR spectra for the CEM1 (a,b) and AEM1 (c,d) membranes before and after use: low (a,c) and high (b,d) frequency spectral regions.

Both materials exhibit significant modifications of their spectral profile after use, especially in the low frequency region (Figs. 2-5a-c), in which stretching and bending vibrations of the polymer skeleton and functional groups appear. For the CEM1U, the decrease in the initially strong and sharp bands located at 1010, 1040, 1130, 1190 and 1235 cm^{-1} is particularly evident (Fig. 2-5a). Most of these bands have been previously observed in the IR spectra of aromatic sulfonic acid salts [44, 45], sulfonated polysulfone membranes [46], as well as other polymer materials for fuel cells applications, *i.e.* sulfonated poly(arylene ether sulfone) [47,48] and sulfonated poly(ether ether ketone) [49]. They have been attributed to the $–SO_3^-$ functional group: one S-phenyl and three ν(S-O) modes. Therefore, the absorbance decrease in the low frequency IR bands for the CEM1U spectrum strongly suggests the loss of sulfonic functional groups within this membrane during its use in ED.

In the high frequency region (Fig. 2-5b), the CEM1U spectrum displays a low amount of residual organic moieties through a relatively broad band around 2700 cm^{-1}, that appears regularly in carboxyl dimers and is usually attributed to overtones and combinations of the ~1300 and ~1420 cm^{-1} modes due to interacting ν(C-O) and σ(O-H) vibrations [44].

In the case of AEMs, there is an absorbance increase larger than that for CEM (Fig. 2-5c), observed in the 1400 – 1800 cm^{-1} range where ν(C=O), ν(C=C), ν(C=N), ν(N=O) and ν((C-)NO_2) vibrations usually appear, along with some σ(C-O-C) and σ(C-H) modes from aliphatic as well as aromatic compounds [44,45]. This is related to the appearance of new bands between 900 and 1500 cm^{-1} which suggests a fouling of AEMs more pronounced than that of CEMs with organic acids. As mentioned above, bands in the same region present a lower absorbance in CEM spectra. Moreover, the obvious increase in the ν(O-H) mode (broad band dominating the high frequency domain and extending from 2400 to 3700 cm^{-1}) (Fig 2-5d) strongly corroborates macroscopic measurements, and definitively attests the higher water content of AEM1U compared to the fresh material.

The results of EDX analyses for CEM1 and CEM2 membranes are displayed in Fig. 2-6, and those for AEM1 and AEM2 in Fig. 2-7 a-d. For each IEM, an area of 1 μm^2 of functional polymer is considered (the membrane cloth was avoided): both the surface (Figs. 2-6 a,c ; Figs. 2-7 a,c) and the cross-section (Figs. 2-6 b,d ; Figs. 2-7 b,d) are analyzed.

The analyzed elements are oxygen, sodium, magnesium, sulfur, chlorine and calcium.

Figs. 2-6 a,b show a significant decrease in the intensity of the peaks corresponding to sulfur and sodium in the used membranes. This confirms that some of the sulfonic functional sites of CEM1U (here in balance with sodium: $SO_3^-Na^+$) are completely removed from the membrane: the loss is seen both in the surface and in the cross-section. The magnitude of this decrease is comparable to that of E_C (see Table 2-1).

For CEM2U, the same trends as those for CEM1U are observed, however in lower proportions, which is correlated with the slight decrease in the E_C and all the other parameters listed in Table 2-1.

It is important that the Cl content decreases with membrane ageing for both CEMs and AEMs. This should result from a decrease in the PVC content, whose segments detach from the membrane due to erosion of the ion-exchange polymer [43] forming a continuous phase in Neosepta® membranes and weakening junctions between interpenetrating ion-exchange and PVC polymers. While the content of S decreases in CEMs, testifying the loss of ion-exchange

capacity, its content increases in AEMs due to the presence of this element in solutions under treatment.

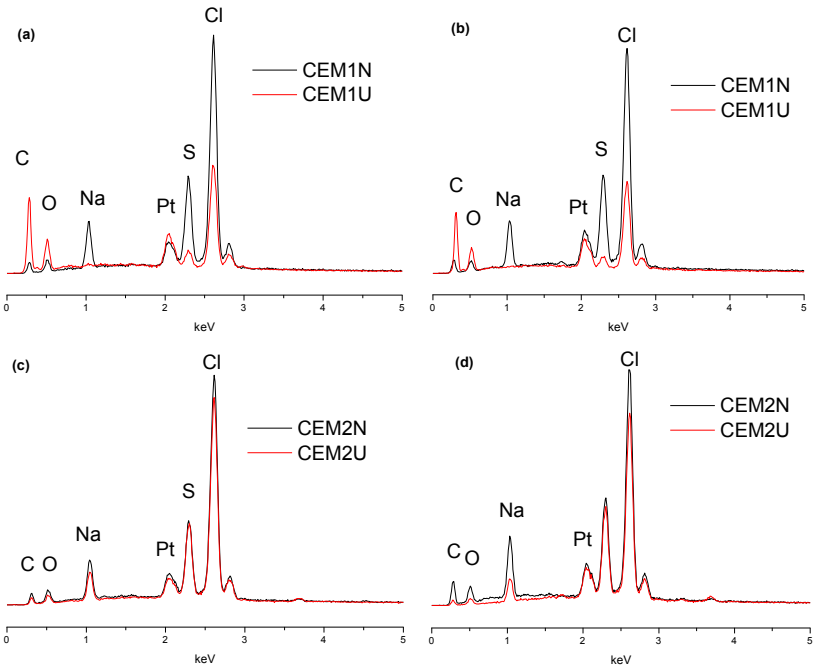

Fig. 2-6. EDX analysis of the membrane surface (a,c) and cross-section (b,d): CEM1N and CEM1U (a,b); CEM2N and CEM2U (c,d).

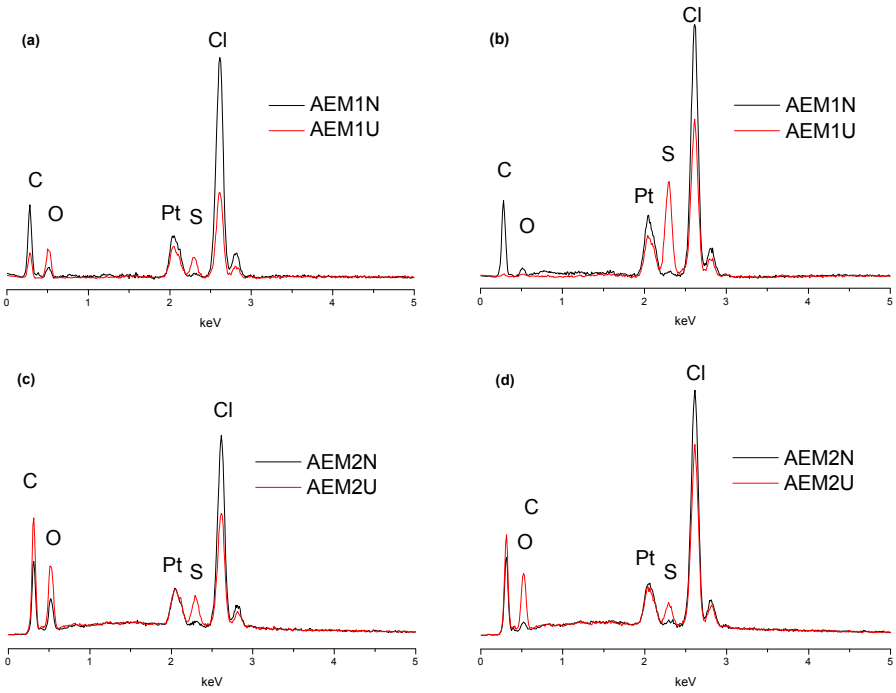

Fig. 2-7. EDX analysis of the membrane surface (a,c) and cross-section (b,d): AEM1N and AEM1U (a,b); AEM2N and AEM2U (c,d).

2.2.3. Electrical conductivity: data treatment using the microheterogeneous model

Electrical conductivity of membranes is an important parameter that control power consumption in ED processes. The values of the membrane conductivity in 0.1 M NaCl for the 4 pairs of IEMs investigated are shown in Table 2-1. In all cases, we observe a decrease in the conductivity between the new and used samples, which may generally be explained by the loss of ion-exchange capacity. In the case of CEMs, the decrease in the values of ion-exchange capacity and conductivity occur to a similar extent. However, in the case of the AEM1 membrane, an important loss in ion-exchange capacity does not lead to a comparable decrease in conductivity.

Apparently this should be due to the difference in microstructure changes of CEMs and AEMs during their use in ED. In order to try to identify these changes in both cases, we applied the well-established microheterogeneous model [50,51]. According to this model, two phases in an IEM can be distinguished: the gel phase and the interstitial neutral solution, with volume fractions f_1 and f_2, respectively ($f_1 + f_2 = 1$). A schematic representation of this model is given in Fig. 2-8.

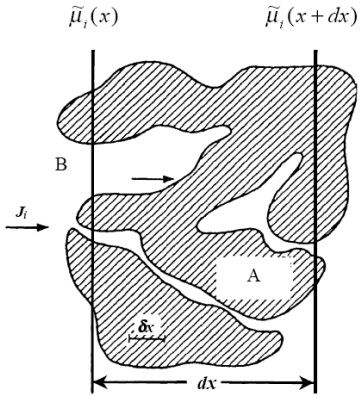

Fig. 2-8. Scheme of two-phase microheterogeneous membrane: (A) gel phase with fixed functional groups; (B) inter-gel solution phase. The global direction of the current is indicated by an arrow. Two equipotential planes, as well as macroscopic (dx) and microscopic (δx) characteristic distances are shown. The global ion transfer at the macroscopic scale is determined by the gradient of electrochemical potential ($\tilde{\mu}_i$) over distance dx [25].

The gel phase is a nanoporous medium, globally electroneutral, which contains functional sites, mobile ions, the polymer matrix, and water. The interstitial electroneutral solution,

which is assumed to be identical to the outer equilibrium solution, fills the inner parts of meso- and macro-pores as well as fissures and cavities (= intergel spaces). Thus, both cations and anions contribute here to the conduction. On the contrary, in the gel phase, almost exclusively the mobile counterions assure the conduction. The co-ions are present there in a very low amount, which increases with increasing bulk concentration, but remains negligible in the case of dilute solutions (up to 1 M) and relatively high ion-exchange capacity values as in the case of Neosepta® membranes used in this work (except for the AEM1U sample). Besides, with increasing solution concentration, the water uptake decreases, which can result in a decrease in the counterion mobility. For these reasons, the specific conductivity of the gel phase varies only slightly with the external solution concentration; hence, it can be considered as constant. In the range of concentrations from 0.1 c_{iso} to 10 c_{iso} (c_{iso} is the isoconductance concentration at which the specific conductivity of the membrane and that of the external solution are the same), the variation of the membrane conductivity κ_m with the external solution concentration may be approximately described by Eq. (2-7) [50]:

$$\log \kappa_m = f_1 \log \kappa_g + f_2 \log \kappa_s \tag{7}$$

where κ_g and κ_s are the conductivities of the gel phase and the external solution, respectively.

The slopes of the linear variation associated with $\log \kappa_m$ vs. $\log \kappa_s$ dependence give the f_2 values for different IEMs. These values for fresh and used samples are given in Table 2-1.

The values of f_2 obtained for the new membranes are consistent with those published for homogeneous membranes by other authors (see Table 2-2): the value of f_2 for homogeneous IEMs are in the range of 0.05 to 0.13, while in the case of heterogeneous IEMs this parameter is rather close to 0.2 [50-52].

Both CEMs show a decrease in the f_2 value. It may be explained by a lower swelling of the membranes after their use in ED. On the contrary, the f_2 value for AEMs increases after their use. This trend is in good agreement with the variations of water content and thickness of these membranes.

Membranes	f_2	Ref.
CM2 (Neosepta®)-NaCl	0.07	[53]
CM2 (Neosepta®)-LiCl	0.05	[54,55]
CMS (Neosepta®)-NaCl	0.13	[56]
CMV (Neosepta®)-NaCl	0.10	[57]
Nafion® 117-NaCl	0.05	[58]
MA-100 (Shchekinoazot, Russia)-NaCl	0.11	[50]
AMX (Neocepta®)-NaCl	0.11	[52]

Table 2-2. Values of f_2 obtained by different authors for homogeneous IEMs in aqueous solutions.

2.3. Discussion

In both cases of CEMs and AEMs, their use in ED treatment of food industry solutions containing organic acids results in the loss of ion-exchange capacity and the decrease in electrical conductivity. Such a decrease leads to increasing power consumption and a deterioration of economic efficiency of the ED process. However, the mechanism of cation-exchange and anion-exchange membrane ageing is different.

In the case of CEMs, FTIR and EDX analyse show a significant loss of sulfonic functional sites, which are strongly hydrophilic. This loss leads to a decrease in the water content and the membrane thickness. It also leads to an increase in the contact angle values. Hence, the membranes become denser, their pores narrower, that is manifested by a decrease in the volume fraction of inter-gel solution, f_2. Lower ion-exchange capacity and narrower pores result in a decrease in the concentration and mobility of counterions, and therefore, in a loss of the specific conductivity, κ_m. However, even though the ion-exchange capacity of CEM1U decreases in about 3.5 times, κ_m decreases only in 2.7 times. The simultaneous deterioration of permselectivity expressed by decreasing apparent transport number, $t_{counterion}$ may account for this variation. A lower ion-exchange capacity leads to increasing sorption of co-ions, which contribute to higher conductivity, but cause a loss in permselectivity.

The ageing of AEMs occurs in a different way. While the used CEMs only contains a small quantity of adsorbed organic matter, the content of organic substances in AEMs increases essentially after electrodialysis, as it is shown by FTIR and EDX. Besides, the water content and the membrane thickness increase significantly, which may be caused by the presence of hydrophilic fragments in the organic compounds fouling the membranes. Indeed, this higher hydrophilicity is evidenced by a decrease in contact angle values. The volume fraction of the inter-gel solution (f_2) increases as well. At the same time there is a loss in ion-exchange capacity and electrical conductivity. However, the simultaneous increase in the fraction of inter-gel solution and the permselectivity does not apparently agree with the loss in ion-exchange capacity. Following the classical ideas about the behaviour of homogeneous IEMs [59], a decrease in ion-exchange capacity leads to an increase in co-ion concentration, and therefore, to a loss in selectivity. To explain this apparent contradiction, let us consider schematic presentation of IEM structure evolution in the course of membrane fouling (Figs. 2-9 a,b). In accordance to the microheterogeneous model, two phases are shown. The gel phase is presented as a uniform media in micrometer scale, containing nanoscale pores shown in the enclosure. The inter-gel macropores filled with electroneutral solution are shown as "lakes" on the ground of the gel phase. High (more than twofold) swelling of AEMs after there exposure to ED leads to increasing the size of macropores, but also to formation of new structure defects, such as fissures, cavities and caverns (Fig. 2-3d, Fig. 2-4), hence, to increasing f_2. The solution filling these defects does not exhibit any permselectivity, but it contributes to increasing electrical conductivity, κ_m. (if the external concentration is so that the electrical conductivity of solution is higher than that of the gel phase). However, the other part of the structure, the gel phase, shows different, rather opposite behaviour. First, its conductivity decreases, mainly due to the loss of the exchange capacity. Second, nanopores could provide a rather high permselectivity to the membrane, even higher than that of unused membranes. Really, it is highly probable that the molecules of organic foulants (such as amino acids) form colloid associates located within the nanopores [9]. Such an associate occupies the central part of a nanopore pushing out the electroneutral solution. As a result, the volume fraction of the charged solution counterbalancing the charge of the pore walls increases that leads to increasing permselectivity. In fact, the concentration of mobile counterions in the charged solution forming the interfacial double electrical layer (DEL) is much higher than that of co-ions. In some cases, the DELs formed at the pore wall and at the colloid particle surface may overlap providing highly selective transport of counterions.

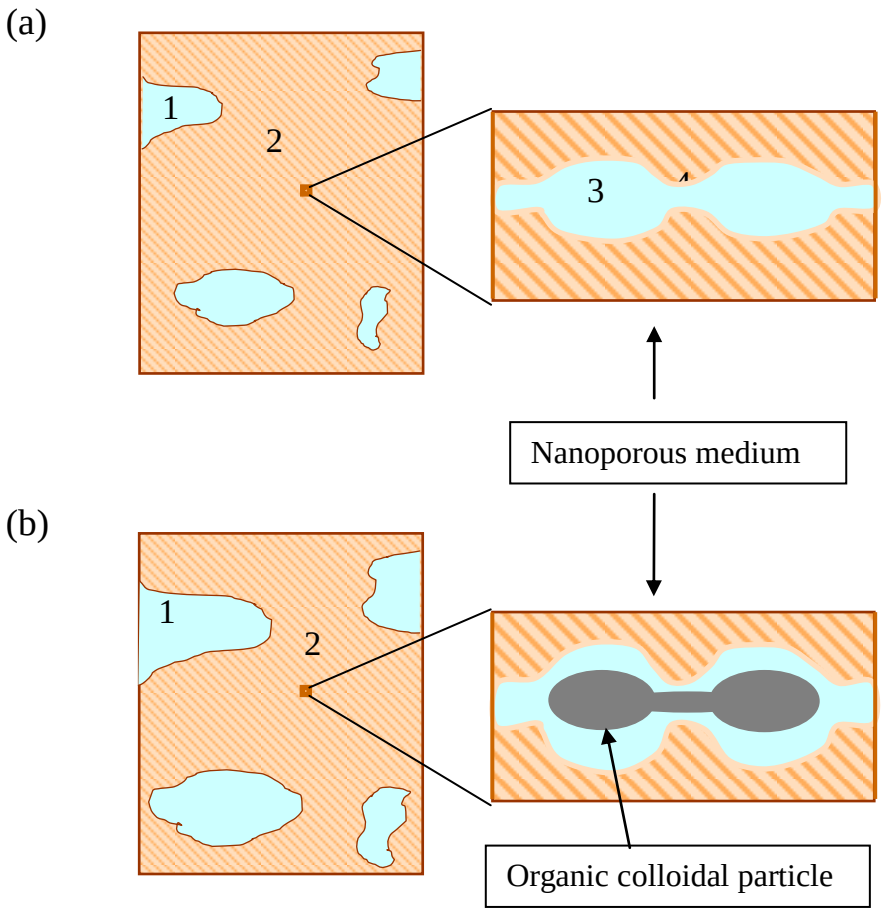

Fig. 2-9. Possible structure of an AEM: (a) before and (b) after its use in electrodialysis of organic acid containing solutions; 1: macro-defects of structure, 2: nanoporous medium, 3: nanopore filled with a charged solution, 4: hydrophobic matrix.

On the other hand, the presence of hydrophilic colloid nanoparticles within a pore leads to increasing the internal osmotic pressure, π_{mb}. It is due to a decrease in molar fraction of free water, N_w, in the internal solution. Free water molecules are expulsed from the pore together with the electroneutral solution. According to the Gregor model [60], π_{mb} increases with decreasing N_w [59]:

$$\pi_{mb} = -\frac{RT}{\bar{V}_w} \ln N_w \tag{2-8}$$

where $\bar{V}_w$ is the water molar volume, R and T have their usual meanings.

The increase in osmotic pressure results in higher membrane swelling and might be one of the main reasons of polymer chains rupture, leading to a strong increase in membrane thickness, the appearance of structure defects and the loss of ion-exchange sites. It is known that increasing swelling of ion-exchange membranes leads to a faster membrane deterioration. For example, Iwai and Yamanishi [61] report that when Nafion is exchanged for cations with a larger ionic radius (hence, lower hydration number), the membrane attains superior thermal stability.

It should be noted that a similar nanoporous structure with nanoparticles immobilised within membrane pores and leading to increased permselectivity was recently described by Berezina et al. [50, 62] (the case of polyaniline in Nafion® membranes) and by Yaroslavtsev et al. [63, 64] (the case of SiO_2, ZrO_2 and other nanoparticles in Nafion-type membranes).

The chain of main events conducting to membrane deterioration is schematically shown in Fig. 2-10. It should be also noted that in the course of ED operation, the stacks are periodically cleaned using some oxidizing and other agents. This cleaning contributes essentially to the membrane deterioration as shown in Refs. [9, 11, 31].

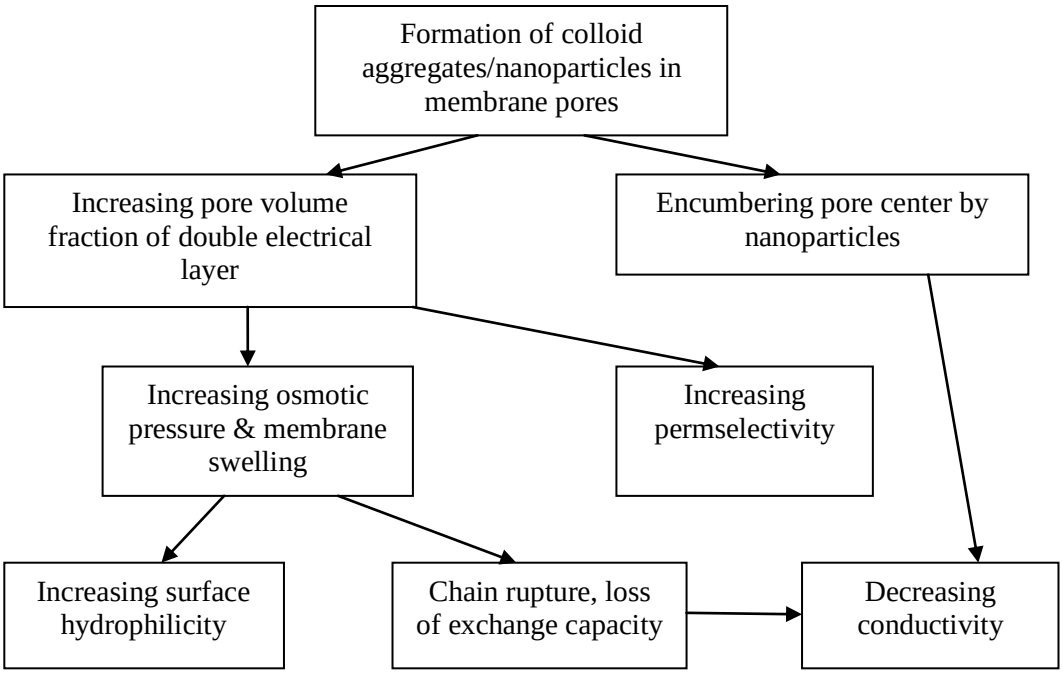

Fig. 2-10. Schematic presentation of events occurring in the course of IEM operation in ED treatment of solutions containing organic acids

2.4. Conclusions

This report gives an insight into the understanding of long-term behaviour of both CEMs and AEMs in ED operation of food industry solutions containing organic acids. Both types of membranes lose a part of ion-exchange sites; their specific electrical conductivity decreases. However, the CEMs are generally more robust and resistant than the anion-exchange counterparts. The structure and properties of CEMs and AEMs vary in different ways. The CEMs become denser, their water content and thickness decrease, and the surface becomes more hydrophobic. Apparently, it is due to the loss of hydrophilic ion-exchange sites. Organic and inorganic compounds found in the used CEMs in excess as compared with the fresh ones are present there in too small amounts to contribute noticeably to the water content and swelling. The loss of ion-exchange sites leads to an increasing concentration of co-ions in CEMs and a deterioration of their permselectivity.

In contrast to CEMs, the water content in AEMs and their thickness increase essentially in the course of ED. Consequently, the surface hydrophilicity increases. This behaviour is explained by sorption of organic colloidal particles within membrane nanopores. As these particles are generally hydrophilic, they attract water which leads to higher swelling. At the same time, these particles replace electroneutral solution in the pore centre. As a result, the effective radius of ion conducting channels decreases, and the double electrical layers occupy a more important volume fraction of the pore solution that favours permselectivity. However, the higher swelling of AEMs leads to rupture of some bonds and polymer chains. As a result, structure macro-defects (fissures, cavities, caverns) filled with external solution appear in the membranes. In the long-term run, these defects may form through unselective passages leading to fully unfit membranes.

2.5. Acknowledgements

This investigation was realized within French-Russian laboratory "Ion-exchange membranes and related processes". The authors are grateful to CNRS, France, and to RFBR, Russia (grants 11-08-93107_CNRSL, 12-08-00188_CNRSL, 13- 8-96508r_yug), as well as to FP7 Marie Curie Actions "CoTraPhen" project PIRSES-GA-2010-269135 for financial support.

References

[1] H. Strathmann, Electrodialysis, a mature technology with a multitude of new applications, Desalination 264 (2010) 268-288.

[2] R.K. Nagarale, G.S. Gohil, V.K. Shahi, Recent developments on ion-exchange membranes and electro-membrane processes, Adv. Colloid Interface Sci. 119 (2006) 97–130.

[3] M. Fidaleo, M. Moresi, Electrodialysis Applications in the Food Industry, Adv., Food Nutrition Res. 51 (2006) 265–360.

[4] L.J. Andrés, F.A. Riera, R. Alvarez, Skimmed milk demineralization by electrodialysis: Conventional versus selective membranes, J. Food Eng. 26 (1995) 57–66.

[5] E. Vera, J. Sandeaux, F. Persin, G. Pourcelly, M. Dornier, J. Ruales, Modeling of clarified tropical fruit juice deacidification by electrodialysis, J. Membr. Sci. 326 (2009) 472–483.

[6] A. Elmidaoui. F. Lutin. L. Chay. M. Taky. M. Tahaikt, My R. Alaoui Hafid, Removal of melassigenic ions for beet sugar syrups by electrodialysis using a new anion-exchange membrane, Desalination 148 (2002) 143- 148.

[7] F. Goncalves, C. Fernandes, P.C. Dos Santos, M. Norberta de Pinho, Wine tartaric stabilization by electrodialysis and its assessment by the saturation temperature, J. Food Eng. 59 (2003) 229-235.

[8] H. Strathmann, Ion-exchange membrane separation processes, Membr. Sci. Techno. Series, 9 (2004).

[9] T. Sata, Ion Exchange Membranes: Preparation, Characterization, Modification and Application, Roy. Soc. Chem., (2004), pp 314.

[10] Y. Tanaka, Ion Exchange Membranes: Fundamentals and Applications, Chapter 14 Membrane Deterioration, Membr. Sci. Technol., 12, (2007) 293–317.

[11] K. Kneifel, K. Hattenbach, Properties and long-term behavior of ion exchange membranes, Desalination 34 (1980) 77–95.

[12] T. Sata, M. Tsujimoto, T. Yamaguchi, K. Matsusaki, Change of anion exchange membranes in an aqueous sodium hydroxide solution at high temperatures J. Membr. Sci. 112 (1996) 161-170.

[13] L.K. Wang, Membrane and Desalination Technologies, Handbook of environmental Engineering 13, Springer (2010) 525-556.

[14] N. Hanzawa, T. Yuyama, K. Suzuki, M. Nakayama, Studies on durability of ion exchange membrane (IV): Long term electrodialytic concentration test, Scientific Papers of

the Odawara Salt Experiment Station, Japan Monopoly Corporation, Odawara, Japan, 11 (1966) 1–13

[15] K. Ohwada, U. Shimizu, N. Taga, Microorganism and organic matter deposited on the ion exchange membrane, Bull. Sea Water Sci. Jpn., 34 (1981) 367–372.

[16] G. Grossman, A.A. Sonin, Membrane fouling in electrodialysis: A model and experiments, Desalination 12 (1973) 107–125.

[17] E. Korngold, F.D.E. Korosy, R. Rahav, M.F. Taboch, Fouling of anionselective membranes in electrodialysis, Desalination 8 (1970) 195–220.

[18] V.D. Grebenyuk, R.D. Chebotareva, S. Peters, V. Linkov, Surface modification of anion-exchange electrodialysis membranes to enhance anti-fouling characteristics. Desalination 115 (1998) 313-329.

[19] V.D. Grebenyuk, O.V. Grebenyuk, Electrodialysis: From an Idea to Realization. Russ. J. Electrochem. 38 (2002) 806-809.

[20] V. Lindstrand, A.-S. Jönsson, G. Sundström, Organic fouling of electrodialysis membranes with and without applied voltage. Desalination 130 (2000) 73-84.

[21] V. Lindstrand, G. Sundström, A.-S. Jönsson, Fouling of electrodialysis membranes by organic substances. Desalination 128 (2000) 91-102.

[22] P.E. Długołęcki, K. Nijmeijer, S.J. Metz, M. Wessling, Current status of ion exchange membranes for power generation from salinity gradients, J. Membr. Sci. 319 (2008) 214-222.

[23] J.W. Post, J. Veerman, H.V.M. Hamelers, G.J.W. Euverink, S.J. Metz, K. Nijmeijer, C.J.N. Buisman, Salinity-gradient power: Evaluation of pressure-retarded osmosis and reverse electrodialysis, , J. Membr. Sci. 288 (2007) 218-230.

[24] J.W. Post, Blue Energy: electricity production from salinity gradients by reverse electrodialysis. PhD thesis, Wageningen University, (2009).

[25] D.A. Vermaas, M. Saakes, K. Nijmeijer, Power generation using profiled membranes in reverse electrodialysis, J. Membr. Sci. 385-386 (2011) 234-242.

[26] D.A. Vermaas, D. Kunteng, M. Saakes, K. Nijmeijer, Fouling in reverse electrodialysis under natural conditions, Water Research, in press (2013) http://dx.doi.org/10.1016/j.watres.2012.11.053.

[27] J. Rozière, D.J. Jones, Non-fluorinated polymer materials for proton exchange membrane fuel cells, Annu. Rev. Mater. Res. 33 (2003) 503-555.

[28] A.A. Shah, T.R. Ralph, F.C. Walsh, Modeling and Simulation of the Degradation of Perfluorinated Ion-Exchange Membranes in PEM Fuel Cells, J. Electrochem. Soc. 156 (2009) B465-B484

[29] A. Collier, H. Wang, X. Yuan, J. Zhang, D. Wilkinson, Int. J. Hydrogen Energy 31 (2006) 1838-1854.

[30] G. Merle, M. Wessling, K. Nijmeijer, Anion exchange membranes for alkaline fuel cells: A review, J. Membr. Sci. 377 (2011) 1– 35.

[31] L. Dammak, C. Larchet, D. Grande, Ageing of ion-exchange membranes in oxidant solutions, Sep. Purif. Technol. 69 (2009) 43-47.

[32] R. Ghalloussi, W. Garcia-Vasquez, N. Bellakhal, C. Larchet, L. Dammak, P. Huguet, D. Grande, Ageing of ion-exchange membranes used in electrodialysis: Investigation of static parameters, electrolyte permeability and tensile strength, Sep. Purif. Technol. 80 (2011) 270–275.

[33] U.S. Hwang, J.H. Choi, Changes in the electrochemical characteristics of a bipolar membrane immersed in high concentration of alkaline solutions, Sep. Purif. Technol. 48 (2006) 16–23.

[34] J.A. Vega, C. Chartier, W.E. Mustain, Effect of hydroxide and carbonate alkaline media on anion exchange membranes, J. Power Sources 195 (2010) 7176–7180.

[35] J.H. Choi, S.H. Moon, Structural change of ion-exchange membrane surfaces under high electric fields and its effects on membrane properties J. Colloid Interface Sci. 265 (2003) 93–100.

[36] Y. Mizutani, Structure of ion exchange membranes, J. Membr. Sci. 49 (1990) 121-144.

[37] Norme Française NF X 45-200. AFNOR, (Décembre 1995).

[38] R. Lteif, L. Dammak, C. Larchet, B. Auclair, Conductivité électrique membranaire: étude de l'effet de la concentration, de la nature de l'électrolyte et de la structure membranaire, Europ. Polym. J. 35 (1999) 1187-1195.

[39] N. Lakshminarayanaiah, Transport Phenomena in Membranes, Academic Press, New York, 1969.

[40] R. Lteif, L. Dammak, C. Larchet, B. Auclair, Détermination du nombre de transport d'un contre-ion dans une membrane échangeuse d'ions en utilisant la méthode de la pile de concentration, Europ. Polym. J. 37 (2001) 627-639.

[41] B. Auclair, V. Nikonenko, C. Larchet, M. Métayer, L. Dammak, Correlation between transport parameters of ion-exchange membranes, J. Membr. Sci. 195 (2002) 89-102.

[42] L. Dammak, C. Larchet, B. Auclair, V.V. Nikonenko, V.I. Zabolotsky, From the multi-ionic to the bi-ionic potential, Europ. Polym. J. 32 (1996) 1199.

[43] N.D. Pismenskaya, V.V. Nikonenko, N.A. Melnik, K.A. Shevtsova, E.I. Belova, G. Pourcelly, D. Cot, L. Dammak, C. Larchet, Evolution with Time of Hydrophobicity and

Microrelief of a Cation-Exchange Membrane Surface and its Impact on Overlimiting Mass Transfer, J. Phys. Chem. B 116 (2012) 2145–2161.

[44] N.B. Colthup, L.H Daly, S.E. Wiberley, Introduction to Infrared and Raman Spectroscopy, Academic Press, London 1990.

[45] B. Schrader, Infrared and Raman Spectroscopy, VCH, New York 1995.

[46] R. Chennamsetty, I. Escobar, X. Xu, Polymer evolution of a sulfonated polysulfone membrane as a function of ion beam irradiation fluence, J. Membr. Sci. 280 (2006) 253-260.

[47] D. Xing, J. Kerres, Improvement of synthesis procedure and characterization of sulfonated poly(arylene ether sulfone) for proton exchange membranes, J. New Mater. Electrochem. Syst. 9 (2006) 51-60.

[48] R.T.S. Muthu Lakshmi, J. Meier-Haack, K. Schlenstedt, H. Komber, V. Choudhary, I.K. Varma, Synthesis, characterisation and membrane properties of sulphonated poly(aryl ether sulphone) copolymers, React. Funct. Polym. 66 (2006) 634-544.

[49] L. Grosmaire, S. Castagnoni, P. Huguet, P. Sistat, M. Boucher, P. Bouchard, P. Bébin, S. Deabate, Probing proton dissociation in ionic polymers by means of in-situ ATR-FTIR spectroscopy, Phys. Chem. Chem. Phys. 10 (2008) 1577-1583.

[50] N.P. Berezina, N.A. Kononenko, O.A. Dyomina, N.P. Gnusin, Characterization of ion-exchange membrane materials: properties vs structure, Adv. Colloid Interface Sci. 139 (2008) 3-28.

[51] V.I. Zabolotsky, V.V. Nikonenko, Effect of structural membrane inhomogeneity on transport properties, J. Membr. Sci. 79 (1993) 181-198.

[52] E. Volodina, N. Pismenskaya, V. Nikonenko, C. Larchet, G. Pourcelly, Ion transfer across ion-exchange membranes with homogeneous and heterogeneous surfaces, J. Colloid Interfacial Sci., 285 (2005) 247-258.

[53] F. Helfferich, Ion Exchange, McGraw Hill, New York (1962).

[54] H. P. Gregor, J. Am. Chem. Soc. 70 (1948) 1293-1299; 73 (1951) 642-651.

[55] Y. Iwai, T. Yamanishi, Thermal stability of ion-exchange Nafion N117CS membranes, Polym. Degrad. Stab. 94 (2009) 679–687.

[56] N.P. Berezina, S.V. Timofeev, A.L. Rollet, N.V. Fedorovich, S. Durand-Vidal, Transport-structural parameters of perfluorinated membranes Nafion-117 and MF-4SK, Russ. J. Electrochem. 38 (2002) 903-908.

[57] S. A. Novikova, E. Y. Safronova, A. A. Lysova, A. B. Yaroslavtsev, Mendeleev Commun. 20 (2010) 156-157.

[58] V. Nikonenko, A.B. Yaroslavtsev, G. Pourcelly, Ion transfer in and through charged membranes, Structure, properties, theory. Chapter 9 in Ionic Interactions in Natural and Synthetic Macromolecules, edited by A. Ciferri and A. Perico, John Wiley & Sons, Inc., (2012) 267-336.

Chapitre 3

Evolution des propriétés d'une membrane échangeuse d'anions dans un empilement d'électrodialyse industrielle

Présentation de l'article

Après avoir étudié les changements survenus en fin de vie des deux MEIs, des questions sur l'évolution de la dégradation de ces membranes restent encore sans réponse. Par exemple, nous ne pouvons pas encore confirmer avec certitude les étapes de dégradation des membranes échangeuses d'ions, ou encore la manière avec laquelle les transformations ont eu lieu. De même, les mécanismes de vieillissement restent toujours méconnus.

Dans ce chapitre nous nous sommes intéressés à l'étude d'échantillons à différents moments de leur utilisation dans un empilement d'électrodialyse à échelle industrielle. Nous avons comparé les propriétés d'une membrane neuve avec des échantillons prélevés à 45, 70 et 100% de sa durée de vie totale.

Il est à noter que dans ce chapitre nous avons présenté uniquement les résultats concernant la membrane échangeuse d'anions. En effet, selon le chapitre précédent, celles-ci sont plus sensibles au vieillissement que les membranes échangeuses de cations, ce qui est confirmé lors du remplacement de membranes dans notre empilement industriel puisque nous remarquons que les membranes cationiques étaient toujours convenables alors que les anioniques perdaient de leur efficacité.

Dans cette deuxième étape du projet, nous avons décidé de nous concentrer sur une application particulière de l'ED : la déminéralisation du lactosérum. Dans l'industrie agroalimentaire, celle-ci est l'application la plus répandue. Par ailleurs, le lactosérum est une solution « simple » et chimiquement non-agressive. Par conséquent on pourra supposer que le vieillissement n'est pas lié à la solution traitée mais aux conditions et aux paramètres de fonctionnement du système, tels que la température, le pH, le nettoyage chimique, etc.

Lors de ce travail on a suivi les propriétés physico-chimiques, structurales et mécaniques d'une membrane échangeuse d'anions homogène. Cette étude a révélé des faits importants concernant les propriétés des membranes échangeuses d'anions et leur comportement à long terme.

Nous avons etabli que la variation des propriétés des membranes échangeuses d'ions lors de leur utilisation est fortement liée aux variations de leur microstructure.

A l'issue de ce travail, nous avons identifié trois étapes de dégradation des membranes échangeuses d'anions : colmatage, formation d'interstices et défaillance mécanique. Le PVC présent dans ces membranes joue un rôle très important dans leur vieillissement.

Ce mécanisme est très dépendant de la nature de l'application mise en ouvre car les conditions et paramètres du système peuvent changer d'un procédé à l'autre.

Evolution of anion-exchange membrane properties in a full scale electrodialysis stack

Journal of Membrane Science (446) **2013** 255-265

W. GARCIA-VASQUEZ[1], L. DAMMAK[1], C. LARCHET[1], V. NIKONENKO[2], N. PISMENSKAYA[2], D. GRANDE[1]

[1] Institut de Chimie et des Matériaux Paris-Est (ICMPE) UMR 7182 CNRS – Université Paris-Est, 2 Rue Henri Dunant, 94320 Thiais, France.

[2] Kuban State University, 149 Stavropolskaya st., 350040 Krasnodar, Russia.

Abstract

In this paper, the physicochemical, structural and mechanical properties of an anion-exchange membrane were investigated, during its lifetime in industrial electrodialysis for whey demineralization. Several analytical techniques permitted to disclose the membrane structure and to describe the evolution with time of the membrane properties. The homogeneous anion-exchange membrane, AMX-SB, is constituted of a semi-interpenetrating polymer network of poly(vinyl chloride) and functional poly(styrene-*co*-divinylbenzene). No significant loss of the ion-exchange capacity or degradation of the functional poly(styrene-*co*-divinylbenzene) chains were detected. However, fouling caused a decrease in the counter-ion mobility within the membrane, which produced a reduction of the electrical conductivity. A progressive loss of poly(vinyl chloride), which was degraded or washed out from the membrane during the cleaning-in-place process, was clearly evidenced. This led to the formation of non-charged pores available for electroneutral electrolyte solution and large molecules, such as lactose and proteins. The occurrence of such pores resulted in an increase in electrolyte permeability through the membrane and a rebound of the conductivity at the last stage of electrodialysis. The microheterogeneous model was applied to well account for these changes. By means of tensile strength tests, it was possible to investigate the mechanical properties of the membrane, which turned gradually from a rigid and tough material, to a rigid and brittle one, due to the loss of poly(vinyl chloride), leading to the end of the membrane lifetime.

3.1. Introduction

For many years, electrodialysis (ED) has been used on a large industrial scale for water desalination, wastewater treatment and a large number of applications in biotechnology as well as food and beverage industry. In the dairy industry, ED is used to reduce the salt content in whey [1-3]. Whey is the major by-product of cheese making. Before its re-utilization, it has to be desalted to become a valuable solution used in a variety of products. Besides water, whey contents lactose, lactic acid, raw protein, fat and salts. During whey demineralization by ED, monovalent ions such as K^+, Na^+ and Cl^- are removed, followed by multivalent ions Ca^{2+}, Mg^{2+}, PO_4^{3-} eliminating globally 90 wt % of salts [4]. In addition of being economically wise, whey re-utilization is necessary as this solution cannot be discharged as wastewater into sewage, due to its high biological oxygen demand. ED presents several advantages over other demineralization processes, such as low environmental impact and higher product quality [5, 6].

It is known that the efficiency of ED processes depends in a large part on the properties of the ion exchange membranes (IEMs) used. The evaluation of IEM lifetime is an important aspect in the control of the operation, as membranes tend to lose their physico-chemical and separative properties during ED, which is accompanied by lower yields and increasing costs due to the replacement of IEMs and the growth of energy consumption.

In this context, the understanding of ageing processes occurring in IEMs used in ED for food industry applications, and the investigation of their long-term behavior are necessary to enhance the progress of this advantageous technology.

The deterioration of IEMs is intimately related to the modification of two parts of the membrane, namely the polymer matrix and the nature and concentration of the functional sites. In this paper, we will focus on the evolution of physico-chemical, structural and mechanical properties of IEMs after their use in a full scale ED stack.

Mechanical degradation of IEMs is often the cause of early life failures. It occurs in many forms, including cracks, tears, punctures or pinhole blisters [7]. The known causes of mechanical degradation are inadequate humidification [8, 9], which may occur during IEM storage or during long periods of pause in ED without taking appropriate precautions. This is detrimental to the membrane, as lack of water makes the membrane brittle and fragile. Non-uniform contact pressure [10], high temperature and temperature changes are causes of IEM

degradation as well. Studies on anion-exchange membranes (AEMs) [11] and different perfluorocarbon cation-exchange membranes (CEMs) [12] using thermogravimetric analysis suggest that temperature may reach 150 °C before the membranes start to be affected. Sulfonic acid sites in CEMs are known to be lost around 240 °C [10, 13]. However, this technique does not reproduce the real conditions of ED operations as membrane samples are heated under an inert atmosphere, and they are kept at high temperatures only for a few minutes.

Mechanical failure can be aggravated by chemical degradation [14] and probably, by fouling as well. In a recent study, Ghalloussi et al. [15] have discovered that fouled membranes used in a food industry ED application after 2 years of operation lost 93 % of their rigidity and that the breaking strength decreased of 87% for a fouled AEM compared to a 37% decrease for a CEM of the same polymer backbone that was not obstructed. Nevertheless, degradation caused by fouling of membranes in food industry is still largely unknown in ED technologies. Fouling of IEMs in ED is mostly a reversible process that might be repaired by reversing the current and/or performing a chemical cleaning-in-place (CIP). This CIP might damage the membrane or make it more susceptible to the environment in a short or in a long term, as it is carried out using oxidizing, acidic and/or basic solutions.

Kneifel and Hattenbach [16], and later Sata et al. [17], have evaluated the evolution of membrane changes with elapsed time under the effect of several chemical agents, such as NaCl, HNO_3, NaOH and an oxidizing agent (0.1 N K_2CrO_4 + 1 N HCl + 1 N NaCl). The strongest deterioration of membrane properties (resistivity, ion-exchange capacity and permselectivity) was observed in the case of the NaOH solution and the oxidizing agent. Sata et al. established that the alkaline deterioration of AEMs was caused by the decomposition of both backing polymers and anion-exchange groups. These results have been corroborated and enriched by other authors through the investigation of the deterioration of membranes in contact with high pH solutions [18, 19]. Quaternary ammonium groups in AEMs decompose in concentrated alkaline solutions by nucleophilic substitution or elimination (Hofmann degradation reaction) [20, 21].

Dammak et al. [22] have performed an artificial ageing of IEMs under oxidizing conditions, *i.e*. in peracetic acid, and in P3 Active Oxania® solutions, which are cleaning agents commonly used in industrial ED for food industry applications. It was established an increase in conductivity and swelling rate, resulting from the modification of the polymer chain

structure, without a significant deterioration of the functional groups, since the ion-exchange capacity remained almost constant.

Accordingly, published information on IEM ageing remains scarce, especially for membranes used in food industry ED applications. This work lies within the scope of a research project aiming to explore the effects, causes and mechanisms of IEM ageing in ED for food industry applications [15, 22-24]. In our previous work [24], it was seen that CEMs suffered significant degradation; nonetheless, they were generally more robust and resistant than the AEM counterparts which were more unstable.

In this paper, physico-chemical, structural and mechanical properties of AEMs are investigated throughout their lifetime in a full scale ED stack used for whey demineralization, in order to get a deeper insight into the understanding of AEM degradation. This fundamental investigation reveals significant issues concerning AEM properties and their long-term behavior. The approach is based upon the interpretation of the membrane characterization by means of a systematic analysis of new samples and samples used at different times in actual ED for whey demineralization.

3.2. Experimental

3.2.1. Membrane preparation and sampling

Whey demineralization was carried out using AMX-SB membrane produced by Astom (Japan). This kind of membranes are supposed to be homogeneous, and they are prepared by the so-called "Paste Method" [25], which consists in preparing a base membrane with a functional group appropriate for the insertion of an ion-exchange group.

According to the literature, a fine powder of poly(vinyl chloride) (PVC), styrene (S) and divinyl benzene (DVB) are mixed to prepare the paste. This is coated to a reinforcing PVC cloth rolled up in a film and then heated at high pressure to 100-120 °C during 30 min, then to 60-70 °C during 16 h [26]. As a result, the PVC powder melts and allows S and DVB to copolymerize within the PVC matrix so as to form an entwined structure [27]. The positively charged quaternary amonium groups are introduced by a chloromethylation procedure, followed by an amination with a tertiary amine. This type of AEM has been selected as it is widely used in ED for food industry applications [28, 29].

Samples of AMX-SB membranes were taken from an industrial ED stack at 45%, 70% and 100% of their lifetime in whey demineralization (several thousands of h). They were named A1, A2 and A3, respectively. To take out every sample, it was necessary to stop the production and disassembly the ED stack; ED was performed under standard conditions of whey demineralization in industry. The details of the process are not disclosed for confidentiality reasons; however, similar conditions have been previously described in several papers and books [4, 30-32]. A fresh sample called A0 was also studied to compare a new membrane with the used ones and to establish the evolution of membrane characteristics with time.

Before characterization, membranes were conditioned following the French standard NF X 45-200 [33] in order to stabilize their physico-chemical properties, remove any impurities that may come from their manufacturing process and achieve reproducible initial conditions for all membranes.

This procedure consisted in immersing the samples in solutions of different natures starting with 0.1 M HNO_3. Membranes were then rinsed with water and carefully dried with filter paper, then immersed for 1 h in 0.1 M HCl and rinsed by immersing in 0.1 M NaCl. The procedure was repeated twice and finally, the membrane was conserved in 0.1 M HCl.

3.2.2. Characterization

3.2.2.1. Ion-exchange capacity

This parameter, which is the number of functional sites per gram of dry membrane, was also determined following the NF X 45-200. The counter-ions were forced to transfer to a determined solution with the purpose of titrating them. Samples of 10 cm^2 were immersed into 0.1 M HCl (the counter-ion is Cl^-) for 2 h, then rinsed in ultrapure water and immersed in 1 M HNO_3 for at least 12 h. The chloride content was determined immediately after this time. Samples were eventually vacuum dried at 40 °C for 24 h to determine the dry mass.

3.2.2.2. Water uptake

Samples were separated from the stabilization solution and the excess of external liquid was removed by placing them between two foils of filter paper and pressing slightly. The membranes were immediately placed in a HB43-S Mettler-Toledo moisture thermobalance in

which they were heated to 140°C until their mass did not change in 0.001 g for ten minutes. The water uptake (W) was calculated by the mass differences between hydrated (W_b) and dried (W_a) samples as follows:

$$W = \frac{W_a - W_b}{W_b} \times 100 \tag{3.1}$$

3.2.2.3. Thickness

The membrane thickness (T_m) was measured using a Käfer Thickness Dial Gauge specially devised for plastic film thickness measurements with a resolution of 1 μm. The membrane thickness value was averaged from measurements at 10 different locations on the effective surface region of the membrane.

3.2.2.4. Contact angle

The measurements of the contact angle values were performed using a FM40 EasyDrop goniometer from Krüss. The images of a water drop at the surface of AEM samples in the chloride form were captured by a high resolution camera, and they were then processed by the Wingoutte software to determine the contact angle value using interpolation methods. The membrane samples were in the swollen state, pre-equilibrated with a 0.1 M NaCl solution as it was described by Pismenskaya et al. [34] to keep similar conditions to those found in electrodialysis cell. The experiment was repeated in no less than 10 different spots of each sample, and the average value was reported.

3.2.2.5. Alternating current conductivity

The experimental assembly used consisted of a clip-type cell to measure the membrane conductivity, a conductivity meter CDM92 (RADIOMETER-TACUSSEL) and a water bath at 25 ± 1 °C [35].

The determination of membrane conductance G_m needed two measurements, one without the membrane (G_1) and another one with the membrane (G_2), to deduce:

$$G_m = \frac{G_1 G_2}{G_1 - G_2} \tag{3.2}$$

Using the value of T_m and the electrodes section area (A = 1 cm²), the membrane conductivity (κ_m) was calculated as:

$$\kappa_m = G_m \times \frac{T_m}{A} \quad (3.3)$$

Measurements were conducted in 0.1 M NaCl to compare the changes in membrane conductivity since NaCl solutions are commonly used as reference media of membrane conductivity and resistance. Moreover, membrane electrical conductivity was measured in NaCl solutions at different concentrations ranging from 10^{-2} to 1M, to apply the microheterogeneous model.

3.2.2.6. Electrolyte permeability

The membranes were disposed in a two-compartment cell as described by Dammak et al. [36]. It consisted of a horizontal diffusion cell, where 0.1 NaCl and water were placed into the donor and the receiver compartments respectively, stirred and maintained at room temperature. The NaCl concentration in the receiving compartment was determined as a function of time by measuring the conductivity of the solution, as previously explained by Ghalloussi et al. [15].

3.2.2.7. Scanning electron microscopy

SEM images were obtained from Pt/Pd coated samples with an accelerating tension of 3 kV and a 5 mm working distance, using a LEO 1530 microscope.

3.2.2.8. Infrared Spectroscopy

Samples were vacuum-dried at 40 °C for 24 h and then cryo-ground as powders using a freezer miller with liquid nitrogen. This step is important for this kind of samples as there are several materials forming the membrane and simple surface Fourier-transform infrared in attenuated total reflectance mode (FTIR-ATR) measurements would not be representative of all the inner materials. FTIR transmittance measurements were carried out on a Nicolet ‘‘Nexus’’ spectrometer equipped with a Globar source and a DTGS detector between 550 and 4000 cm^{-1}. The spectral resolution was 2 cm^{-1} and 32 scans were realized for each spectrum. Samples were pellets made of a ground mixture of dried KBr and 1 wt% of powdered membrane. $K_3Fe(CN)_6$ was also added to the mixture (0.5 mg for each pellet) as an internal

standard in order to permit quantitative comparison between fresh and used materials. All spectra were normalized according to the ν(C≡N) band at 2095 cm^{-1}.

3.2.2.9. Nitrogen sorption porosimetry

Nitrogen sorption measurements were carried out at 77 K with a Quantachrome Autosorb iQ analyzer. All the samples were degassed at 140 °C for 8 h prior to analysis. The specific surface area values for the investigated membranes were quantified using the BET method at relative pressure (P/P_0) values ranging from 0.05 to 0.3, while the pore size distribution profiles and pore volume values were determined by the BJH method using the adsorption portion of the isotherms.

3.2.2.10. Tensile strength measurements

Stress-strain curves were obtained in an INSTRON 5965 testing machine. A dumbbell of 12x3mm^2 of active area was fixed into two grips and stretched at 1mm.min^{-1} rate. The samples were in the humid state and in the Cl^- form. Each test was carried out twice.

Besides the membrane samples, tensile strength measurements were performed on poly(styrene-*co*-DVB) (PS-DVB) and PVC films to inquire about the mechanical behavior of the two main polymeric components of the membranes. A PS-DVB specimen was prepared by free-radical copolymerization of styrene (95 mol %) with DVB (5 mol %) initiated by azobisisobutyronitrile (AIBN, 2 mol% of [C=C] vinylic groups). The comonomer mixture was poured into a rubber mold between two glass plates, and then placed in an oven for 2 h at 60 °C, followed by a 2 h curing at 110 °C. Films of approximately 500 mm were obtained.

A PVC film was obtained by solvent evaporation in a 2 x 2 cm^2 Teflon® mold. Films of approximately 500 mm were obtained as well.

3.2.2.11. Soxhlet extraction

This procedure was performed with the aim to better identify the structural changes of the samples. Approximately 0.5 g of dried membrane was placed in a cellulose thimble, and loaded in a Soxhlet apparatus. The extraction was carried out with 200 mL of tetrahydrofurane (THF) for 48 h at 90 °C. The extractable fraction was concentrated to 10 mg/mL by using a rotary evaporator, and it was analyzed by size exclusion chromatography

(SEC). Membrane was treated as well in 200 mL of ethanol for 24 h at 70°C. The solid residue and the extractable fraction were identified using FTIR-ATR spectroscopy as well.

3.3. Results

3.3.1. Physicochemical properties

Macroscopic changes have occurred from A0 to A3 samples. With increasing time of operation, the membranes became darker and more fragile, particularly A3 was brittle and easily torn. In the dry state, A3 broke almost instantly with a sudden movement.

After sampling out from the industrial ED stack, AEMs were conditioned and then characterized. In this study, some physico-chemical properties providing essential information about the membrane performance were determined. ED processes require IEMs to fulfill some features in permeability, electrical conductivity and ion-exchange capacity, which are directly correlated to other properties, such as thickness, water uptake and contact angle characterizing surface hydrophilicity.

The ion-exchange capacity values were equal to 2.20, 2.18, 1.80 and 1.78 meq/g of dry membrane for A0, A1, A2 and A3, respectively. As it could be noticed, anion-exchange capacity did not decrease in more than 20% even when the membrane was used for several thousands of hours (A3 specimen). It must be taken into account that uncertainty in the ion-exchange capacity measurements is estimated to be equal to 5%. Furthermore, from the view point of available functional sites, 1.78 meq/g of dry membrane would be theoretically enough for the demineralization of a whey solution. Hence, the loss of anion-exchange sites was not the reason for the removal and replacement of the membranes in the stack.

Fig. 3-1 describes the evolution of some physico-chemical characteristics associated with AEMs.

From A0 to A1, water uptake remained almost constant and thickness decreased only in 2%, i.e. within the experimental error. However, a decrease of about 20% in membrane conductivity was observed, which should be caused by internal and external fouling resulting in lower counterion mobility in the membrane. The fouling might be due to sorption of organic species present in whey.

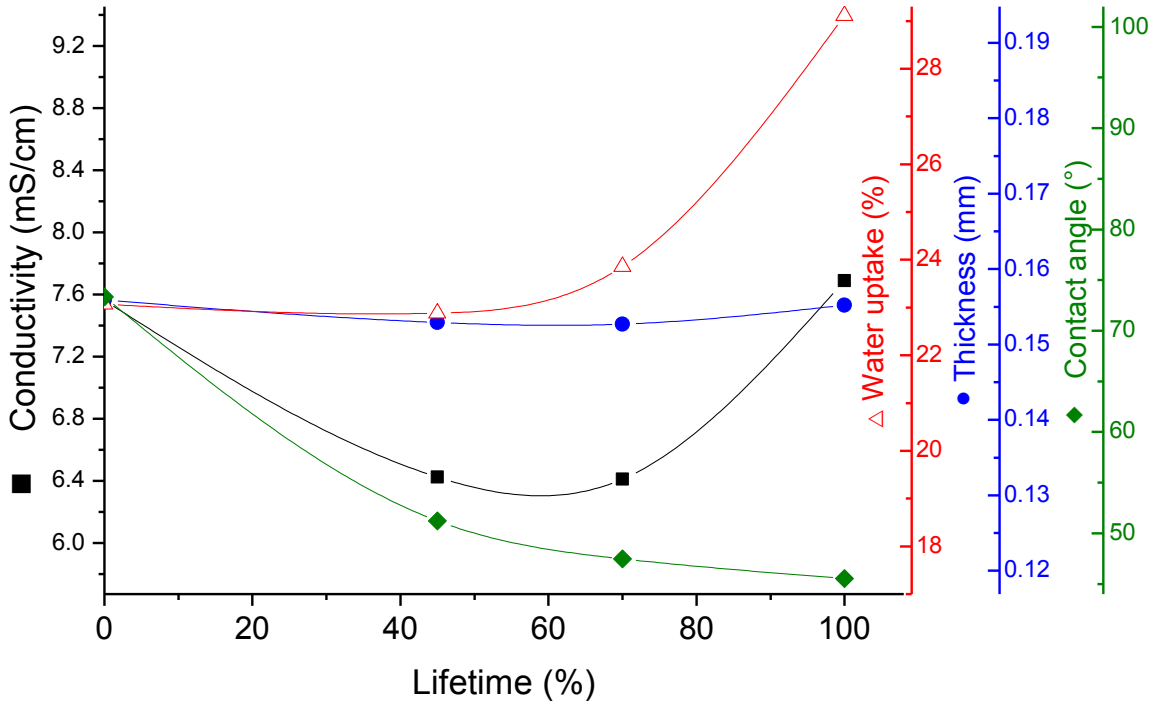

Fig. 3-1. Physico-chemical properties of AEM samples: conductivity, thickness, water content, contact angle.

Fig. 3-2 shows that NaCl permeability increased, as a function of AEM lifetime. This might be explained by increase in the size of existing pores or by the appearance of new ones, thus forming channels for non-selective electrolyte transfer.

The increase in the size of existing pores was not expected at this stage of ageing, since the membrane did not swell additionally, as shown by constant water uptake and membrane thickness. However, a possible degradation of the polymer binder (PVC) during the ED operation could result in formation of new non-selective pores.

Evidently, decreasing membrane conductivity (κ_m) and increasing electrolyte permeability (P^*) implies a loss of permselectivity, as suggests the following equation relating these parameters to the co-ion transport number (t_2^*) [37]:

$$t_2^* = \frac{F^2 P^* c}{2RT\kappa_m t_{1app}^* g} \quad (3.4)$$

where t_{1app}^{*} is the apparent counterion transport number, c is the concentration of the electrolyte solution in equilibrium with the membrane, and g is the activity factor [37, 38]. Since κ_m decreases (by about 20%) and P^{*} increases by nearly 10 times, while t_{1app}^{*} and g remain close to 1, we can expect that during ED operation, t_2^{*} would increase more than 10 times.

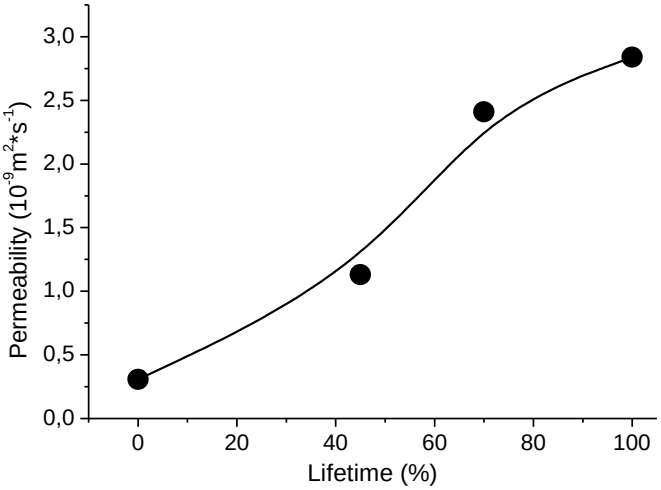

Fig. 3-2. Evolution of 0.1M NaCl diffusion permeability through the AEM samples as a function of lifetime in ED stack.

In the next stages of AEM lifetime, the water uptake continued to increase until reaching +30% of the initial value, which was accompanied only by a slight increase in membrane thickness. The increase in water uptake could be correlated not only with large hydration numbers of organic species sorbed by the existing charged pores of nanometer size, but also with the new non-charged pores caused by the degradation or loss of PVC. These new pores contributed not only to increase electrolyte permeability, but also to enhance conductivity. The latter resulted from substitution of non-conductive regions occupied by PVC for pores filled with electrolyte solution apparently containing also organic components of whey. The fact that higher water uptake did not result in a large increase in membrane thickness suggested that water absorption by new pores was the main mechanism involved, at least in stages A0-A1 and A1-A2. Further uptake seemed to be accompanied by a deterioration of the polymer chains giving rise to increasing membrane thickness.

The contact angle values decreased throughout the ED operation, thus showing that the membrane gradually became more hydrophilic. This was consistent with the increase in water uptake and with the hypothesis of the PVC degradation, i.e. a hydrophobic component of the membrane.

3.3.2. Structural properties

Fig. 3-3 shows SEM micrographs of AEM samples. In the first row, it could be seen that A0 had a flat and fairly homogeneous surface, even at the nanoscopic length scale (magnification x30 000 in the right column). A1 and A2 images elucidate the existence of some micrometric heterogeneity on the surface.

Concerning A3, the low magnification image revealed some cracks formed in the membrane. We might suppose that these cracks existed before drying the sample or they were formed as a consequence of it. To clarify this fact, images of a sample in the humid state were taken at the same magnification with an optical microscope (not shown here), and we were able to distinguish the cracks as well.

A3 also displayed cavities from several tens to several hundreds of nanometers, as shown in the image with higher magnification.

To further quantify the extent of porosity in the used membranes, the BET specific surface area (S_p) was measured (Table 3-1). For the new membrane A0, the S_p value of the material was equal to 0 m^2/g, which indicated no detectable porosity. The S_p value increased to 32 and 212 m^2/g for A1 and A2 respectively, which were typical values for a nanofiltration membrane.

Two main reasons may permit to explain the surface area decrease from A2 to A3. The first reason could be related to organic fouling blocking cavities and pores, thus reducing the gas adsorption area. This is supported by the decrease in pore volume (V_p) (Table 3-1). The second reason could be the formation of large cracks and tears, as illustrated by SEM (Fig. 3-3). It is well known that the larger the pore size, the lower the S_p value, for a given sample.

Further analysis was performed to unveil the polymer structure of this kind of membrane, to comprehend the changes suffered during ageing, and to identify the origin of the new cavities.

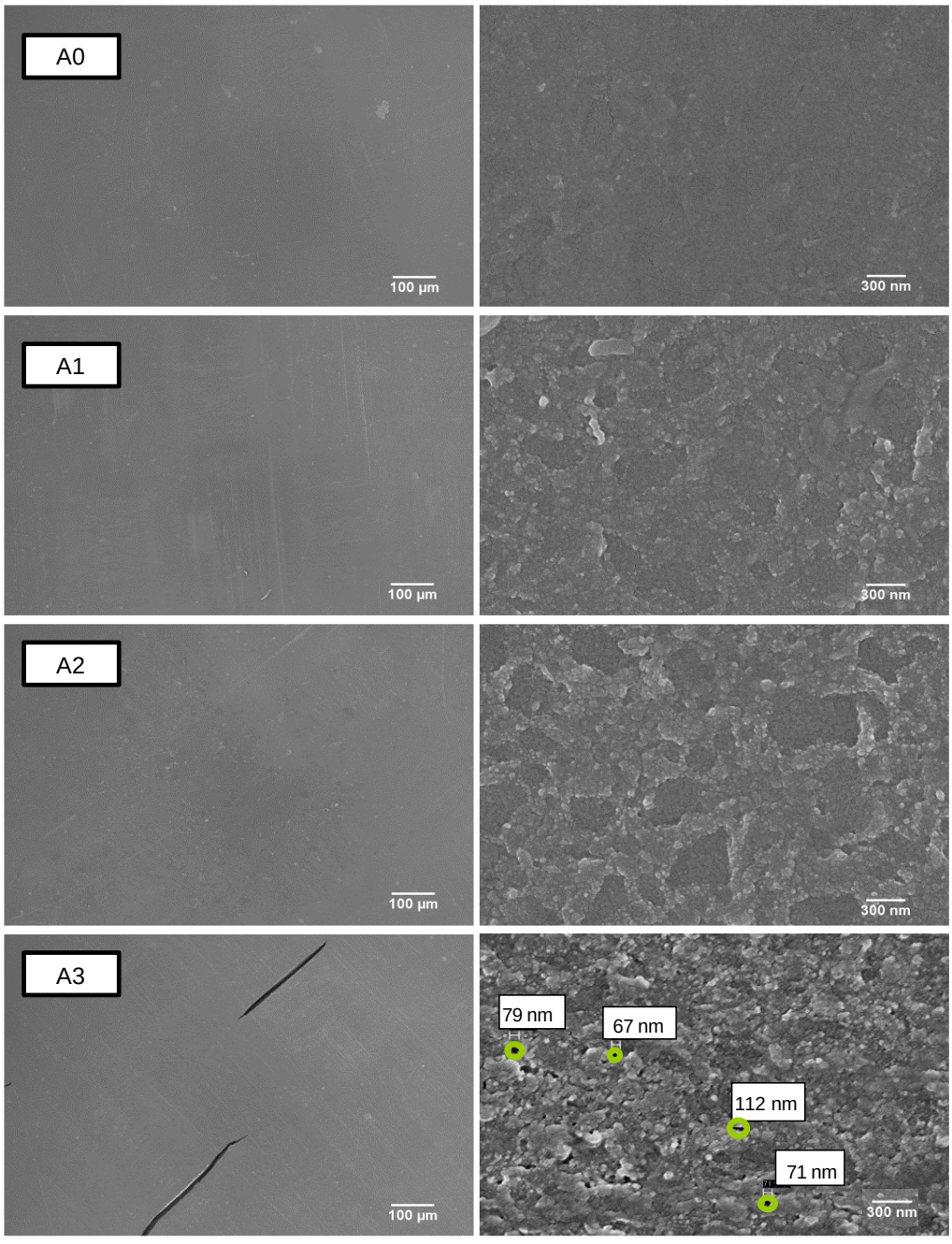

Fig. 3-3. SEM images of the AEM surface as a function of lifetime in ED stack. A0: new membrane, A1: 45%, A2: 70% and A3: 100% of lifetime.

	Sp (m^2/g)	Vp (cm^3/g)
A0	0	0
A1	32	0.012
A2	212	0.058
A3	60	0.018

Table 3-1. BET specific surface area (Sp) and pore volume (Vp) values of AEM samples. A0: new membrane, A1: 45%, A2: 70% and A3: 100% of lifetime.

Fig. 3-4 shows the comparison of characteristic FTIR spectra split into two parts: the high (a) and the low (b) frequency regions. Even though samples were vacuum-dried before FTIR analysis, water was still present in the membrane, as evidenced by the broad ν(O-H) band extending from 3100 to 3700 cm^{-1}. Water molecules were linked to the functional sites and probably to the hydrophilic parts of the membrane. Fig. 3-5 also displays the typical absorption bands associated with the ion-exchange polymer, namely ν(C-H) between 2500-3100 cm^{-1} (above 3000 cm^{-1} from aromatic rings and those between 2815-2900 cm^{-1} with just single bonds from methylene and methine stretching of PS and PVC) [39].

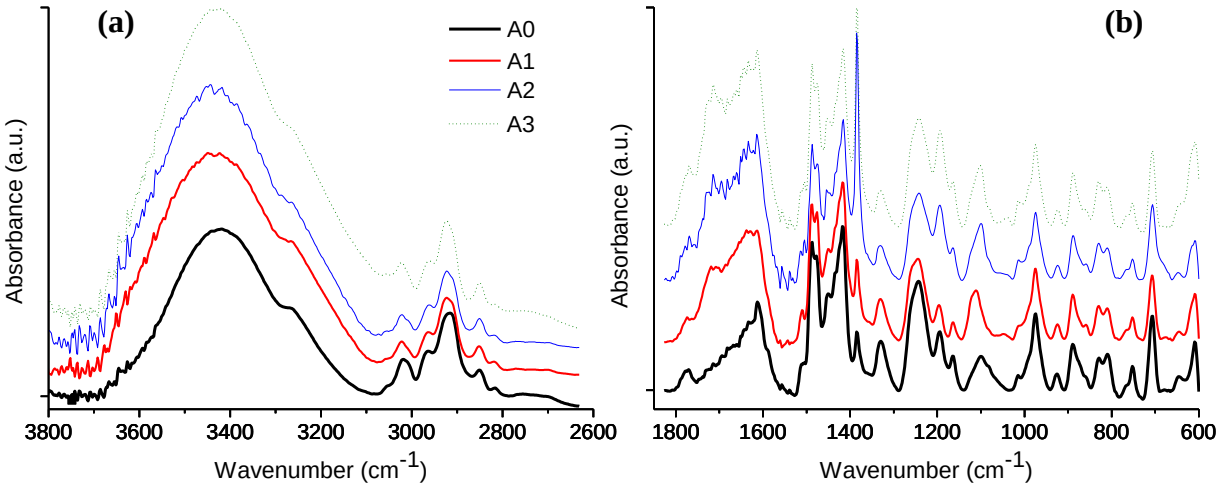

Fig. 3-4. FTIR spectra of AEM samples: high (a) and low (b) frequency spectral regions. A0: new membrane, A1: 45%, A2: 70% and A3: 100% of lifetime.

No significant changes in the 600-1500 cm^{-1} region were observed, as previously reported by Ghalloussi et al. [24] when they studied AEMs used for the treatment of an organic acid

solution in ED. Nonetheless, an increase in absorbance intensity of peaks around 1200 and 1400 cm^{-1}, and a large increase in the 1600-1800 cm^{-1} range in which ν(C=O), ν(C=C), ν(C=N) and ν(N=O) absorption bands appeared, which might result from fouling. Identifying all the elements of the membrane would be a hard task as the spectra were complex with many of the vibrational bands overlapping. Therefore, attempts to extract meaningful information from the spectra may appear futile. This is the reason why we chose to extract the different parts of AEM samples using two different solvents, i.e. ethanol and THF.

None of the membrane constituents were really soluble in ethanol. When soaking was performed on A0, no soluble material was present in the flask. However, around 2% of the A1, A2 and A3 total mass was recovered from the flask in each soaking. When the solvent was evaporated from the flask, a paste was obtained. Fig. 3-5 shows the FTIR-ATR spectra of the paste in the 1000-1800 cm^{-1} region (it was identical for all samples). The 1040 and 1075 cm^{-1} bands were assigned to ν(C-O) in an ether bond (C-O-C) from lactose [40]. Bands extending from 1200 to 1400 cm^{-1} could belong to hydroxyl deformations from lactose, as well. It was also possible to detect the 1710 and 1650 cm^{-1} signals that could be assigned to ν(C=O) and δ(N=H) from proteins, respectively [41]. Therefore, whey was remaining in A1, A2 and A3. In addition, the augmentation of the band intensity at 1200, 1400 and in the 1600-1800 cm^{-1} range in Fig. 3-4 could be attributed to the presence of whey in the samples.

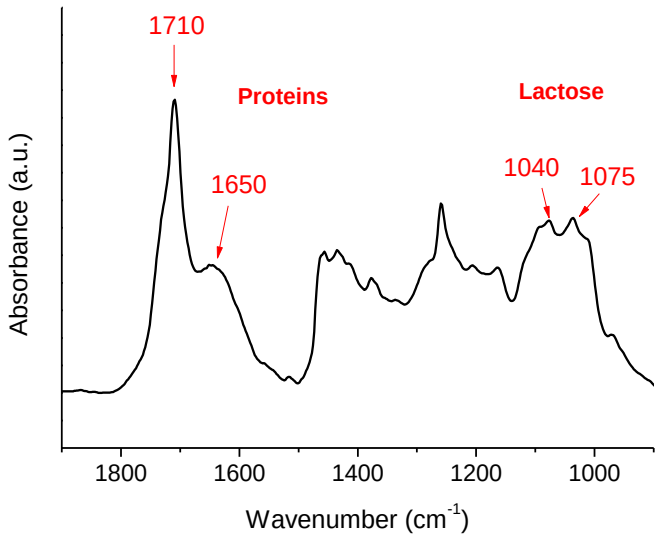

Fig. 3-5. FTIR spectra (1000 to 1800 cm^{-1} region) of the extractables after Soxhlet extraction with ethanol of AEM samples.

Even though copolymerization S and DVB yielded a cross-linked structure that was insoluble in THF, 44% of the new membrane was soluble (Table 3-2). The amount of extractables decreased gradually for the used samples up to 11 % for A3.

	Extractable content wt%	**M_n (g/mol)**
A0	44	21 920
A1	27	17 510
A2	23	18 780
A3	11	17 950

Table 3-2. Extractable contents after THF extraction of AEM samples and their respective number-average molar mass values (M_n). A0: new membrane, A1: 45%, A2: 70% and A3: 100%.

The extractables and the residues were analyzed by FTIR-ATR and typical spectra are presented in Fig. 3-6 (a) and (b), respectively.

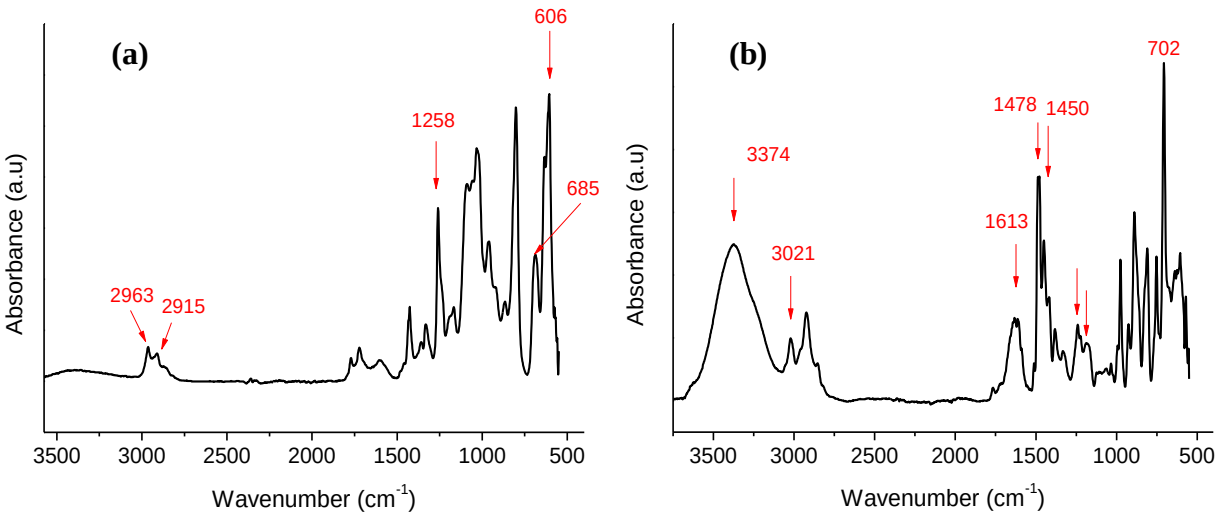

Fig. 3-6. FTIR spectra (400 to 4000 cm^{-1} region) of the extractables (a) and residue (b) after Soxhlet extraction with THF of AEM samples.

In Fig. 3-6a, it was possible to identify ν(C-Cl) stretching bands at 606 and 685 cm^{-1}, a strong band with a maximum at 1258 cm^{-1}, due to δ(CH_2) wagging when the adjacent C atom has a

chlorine atom attached, as well as the methylene asymmetric stretching band at 2915 cm^{-1}, and a methine ν(C-H) stretching bands at 2963 cm^{-1}. In conclusion, the extractables mainly consisted of PVC.

In Fig. 3-6b the aromatic ring breathing modes appeared at 1613, 1478 and 1452 cm^{-1}. The out-of-plan δ(C-H) band of the aromatic ring was intense at 702 cm^{-1}. The band at 3024 cm^{-1} corresponded to the absorption due to the aromatic ν(C-H) stretching. In this case, it was possible to conclude that the residues from the Soxhlet extraction with THF were constituted of the functional PS-based ion-exchange crosslinked polymer. The bands around 1200-1250 cm^{-1} could correspond to the ν(N-C) stretching from the quaternary ammonium functional sites. Moreover, it was possible to identify the ν(O-H) mode associated with bound water to the anion-exchange groups at 3374 cm^{-1}.
It is noteworthy that a SEM image of the cross-section gave evidence of presence of the PVC cloth in the residue; however, the FTIR-ATR technique did not enable us to identify it as this technique only takes into account the surface of the sample. In other words, the extracted PVC was the binder in the AEM samples, while the PVC used to build the reinforcement cloth had a much higher molar mass and it was not soluble in THF.

Fig. 3-7a shows a typical SEM image of the residue. It could be observed the network formed by the functionalized PS-DVB and the cavities left by the extracted PVC.

The soluble PVC binder was analyzed by SEC and it was possible to monitor its apparent molar mass (Table 3-2). A value around 20000 g/mol was determined, regardless of the membrane lifetime.

Finally, to get a conclusive insight into the membrane structure, an attack with a 0.1% hypochlorite solution was performed during 300 h, to oxidize the functional polymer and study the remaining PVC from the polymer binder. Fig. 3-7b shows the SEM image of the treated membrane surface. The spaces left by the disappeared PS-DVB and the remaining PVC from the semi-interpenetrating polymer network, are clearly seen.

The AEM became darker after use in ED for whey demineralization. The darkening of the membrane may be explained by the action of OH^- ions contained in the solutions used for the CIP process or generated in the water splitting. OH^- ions can produce dehydrochlorination of PVC with formation of polyenes [17]. It is noteworthy that cation-exchange membrane CMX, which is manufactured from the same styrene-DVB polymer and containing PVC as a filler

[42] does not darken when used in electrodialysis [33]. Hence, there is no apparent PVC degradation in this case, due to the absence of OH^- ions in a cation-exchange membrane.

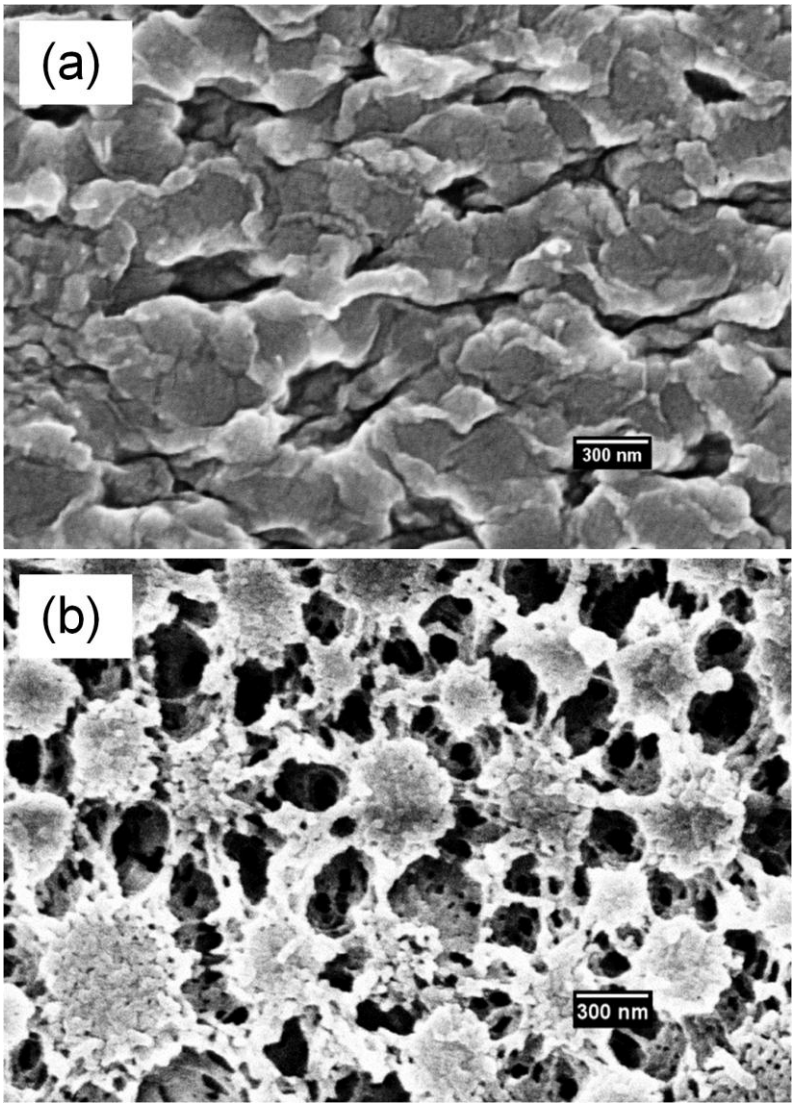

Fig. 3-7. SEM images of the polymers forming the semi-interpenetrated network: (a) functionalized PS-DVB isolated by a THF Soxhlet extraction, (b) PVC binder isolated by a treatment with an oxidizing agent.

3.3.3. Mechanical properties

The stress-strain curves of AEM samples are presented in Fig. 3-8 and the information of the mechanical behavior of the membranes obtained from these curves is displayed in Fig. 3-9.

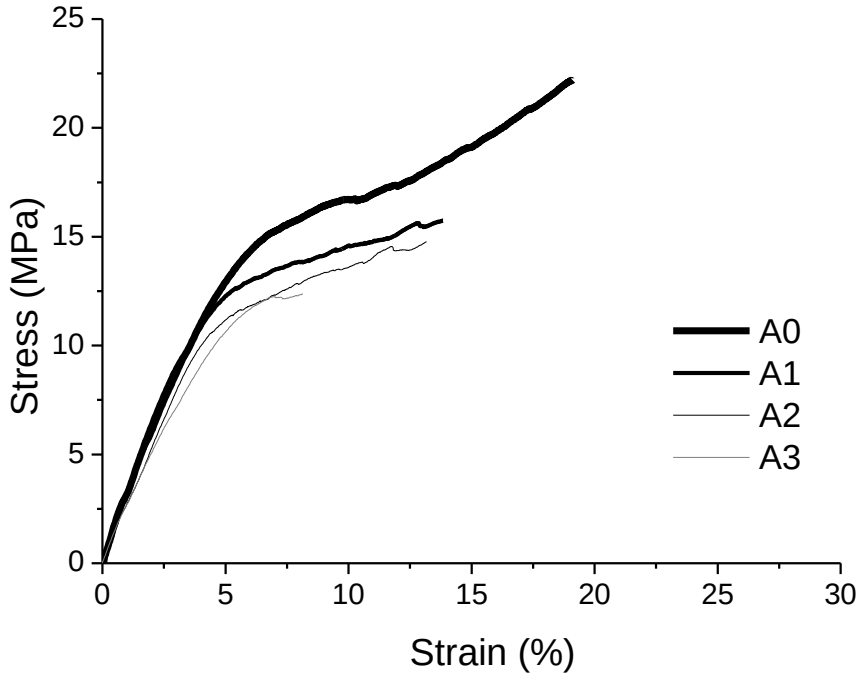

Fig. 3-8. Stress-strain curves of samples: A0 new membrane, A1 45%, A2 70% and A3 100%

.

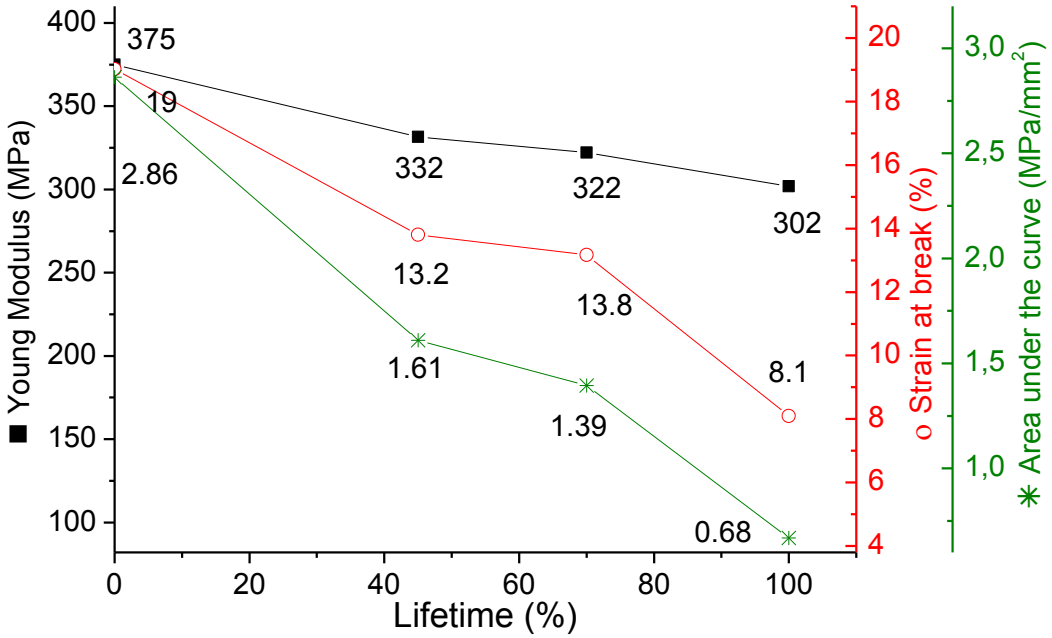

Fig. 3-9. Evolution of mechanical properties of AEM samples as a function of lifetime in ED stack.

The mechanical degradation of samples was evident, as illustrated by a decrease not only in the stress at the breaking point but also in the elongation at the breaking point (which was even more flagrant).The mechanical behavior of a new AEM should be influenced by its three main components, *i.e*. the functionalized ion-exchange polymer, the PVC binder and the PVC cloth.

For this particular membrane, the stress-strain curve changed according to the polymer cloth orientation, which means that the influence of the cloth is important. The curves shown in Fig. 3-8 were performed by pulling the samples in the direction parallel to the cloth. Nonetheless, a similar behavior was found when samples were pulled perpendicularly to the cloth; the difference being smaller values of stress and strain.

It is also noteworthy that curves where different if the samples were in the humid state or not, which means that the influence of the functional polymer and the solution solvating the functional sites and swelling the membrane was also significant and we were not just pulling the polymer cloth.

Since the mechanical properties of the membrane were conditioned by the functional PS based polymer and probably by the PVC as well, we decided to study and compare the behavior of these two single polymers via tensile strength measurements. Fig. 3-10a shows the stress-strain curve of a PS-DVB sample which is characterized by a high modulus of rigidity and a low elongation at the breaking point, thus indicating that this material was brittle, as expected for a crosslinked polymer as PS-DVB. The area under the curve was small and there was low elongation to break which means that this material was brittle, as it was expected for a crosslinked polymer like this.

In the case of PVC (Fig. 3-10b), the Young modulus and tensile strength were medium while the elongation at break was high. This material was obviously softer and tougher than PS-DVB.

Obviously enough, stress-strain curves of A0 in Fig. 3-8 showed that the AEM did not exhibit the mechanical properties of sole PS-DVB. Nonetheless, it presented a combination of the mechanical properties associated with the two polymeric components, *i.e*. the rigidity of PS-DVB and the toughness of PVC.

Fig. 3-9 shows that the Young modulus, which can be related to the rigidity of a material, decreased by 20% from A0 to A3. The breaking strength, which represents the membrane plasticity, decreased by 45%, and the area under the stress-strain curve decreased of almost 80%, which strongly indicated a loss of the material toughness.

Accordingly, the AEM gradually converted from a rigid and tough material to a rigid and brittle one.

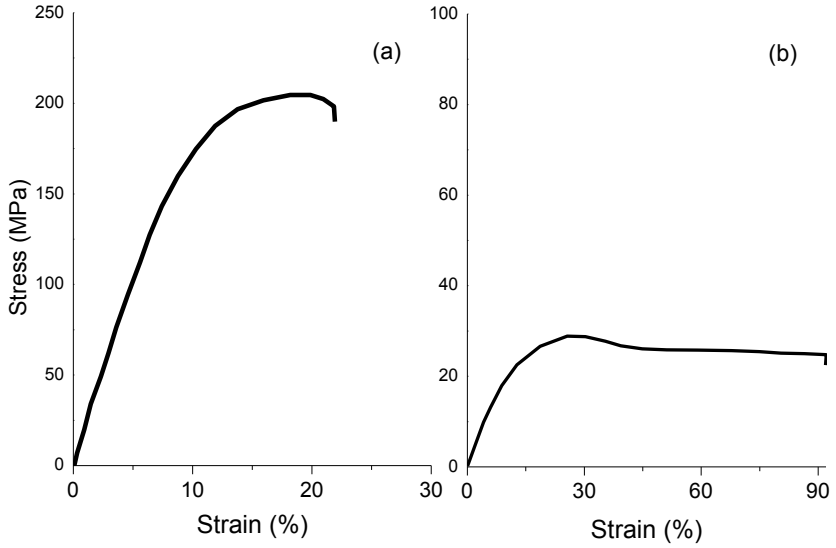

Fig. 3-10. Stress-strain curves for PS-DVB (a) and PVC (b).

3.3.4. Concentration dependence of conductivity: application of microheterogeneous model

The microheterogeneous model [43, 44] correlates membrane physico-chemical properties with its kinetic and structural parameters. Namely, a simple equation linking the membrane conductivity κ_m to the external electrolyte conductivity, κ_s, allows for the determination of the volume fractions f_1 and f_2 of the membrane gel phase and the electrically neutral solution filling the intergel spaces, respectively ($f_1 + f_2 = 1$). As in our previous paper [24], let us write this equation in the logarithmic form:

$$\log \kappa_m = f_1 \log \kappa_g + f_2 \log \kappa_s \qquad (3.5)$$

where κ_g is the conductivity of the gel phase.

According to this model, two phases in an IEM can be distinguished. The gel phase is a nanoporous medium, globally electroneutral, which contains functional sites, mobile ions, the

polymer matrix, and water. The interstitial electroneutral solution, which is assumed to be identical to the outer equilibrium solution, fills the inner parts of meso- and macro-pores as well as fissures and cavities (= intergel spaces). Eq. (3.5) holds in the range of concentrations from 0.1 c_{iso} to 10 c_{iso} [44] (c_{iso} is the isoconductance concentration at which the specific conductivity of the membrane and that of the external solution are the same).

The slope of the log κ_m vs. log κ_s curve gives the f_2 value. Fig. 3-11 presents the experimental dependence of log κ_m on log κ_s found for the fresh and the used AEMs equilibrated with NaCl solutions of different concentrations. As it could be deduced from these curves, f_2 increased progressively from 0.118 (A0) to 0.162 (A3), while the membrane conductivity in dilute solutions (e.g. 0.05 M) decreased from about 3.6 to 2.6 mS/cm. At the same time, there was an inversion of the range of membrane conductivity in concentrated solution (1.0 M): the conductivity of A3 was higher than that of A2.

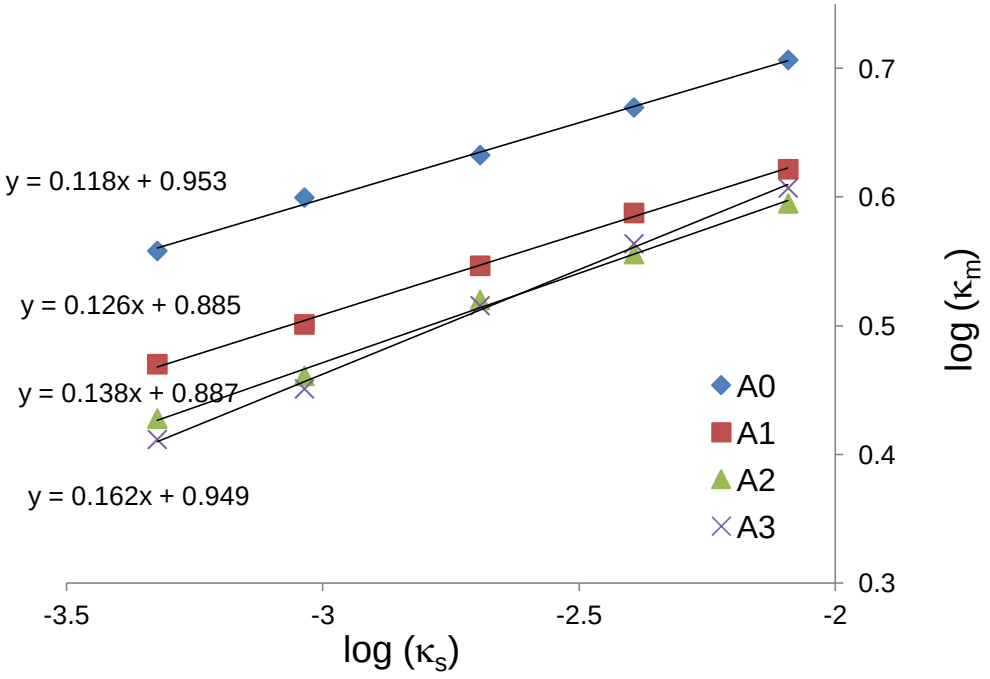

Fig. 3-11. Log κ_m on Log κ_s. A0: new membrane, A1: 45%, A2: 70% and A3: 100% of lifetime.

These results were in good agreement with the other experimental data, and they could well be explained by the microheterogeneous model. The increase in f_2 with the time of operation in electrodialysis resulted from the degradation and/or loss of PVC and formation of

uncharged pores filled with electrically neutral solution and eventually fouled with big bio-molecules. In dilute solutions; the conductivity of these pores was low, like that of the membrane as a whole: with increasing time of operation, f_2 increased and κ_m decreased. In concentrated solutions, the conductivity of the uncharged pores was rather high; they contributed to the increase in κ_m.

3.4. Discussion

In this paper, the studied samples are known as "homogeneous membranes", since the functional sites are part of the polymer matrix. Even so, the AEMs under study have a microheterogeneous structure formed by hydrophilic (functionalized PS-DVB) and hydrophobic (PVC) parts, forming an entwined framework supported in a PVC cloth. The overall properties of this kind of membrane depend on all the constitutive parts. The PVC occupies a considerable portion of the total membrane volume and it is added to improve its mechanical strength, flexibility and dimensional stability. The variation of ion-exchange properties during ED operation is closely linked to variations occurring with the membrane microstructure. These variations are in strong dependence on the application and on the membrane type. In our previous paper [24], we have reported on ageing of CEMs and AEMs in a food industrial ED application. Both types of membranes lost a part of ion-exchange sites and their specific electrical conductivity decreased. However, CEMs were less concerned than the anion-exchange counterparts. There was an elevated loss of ion-exchange capacity and conductivity in comparison with the present study. The water uptake and the membrane thickness increased much higher as well. However, contrary to the present case, we have found that the electrolyte permeability decreased, while the permselectivity did not change. This behavior of AEMs was explained [24] by the formation of organic colloidal dense particles within membrane nanopores. These highly hydrated nanoparticles attracted water resulting in higher membrane swelling, in spite of the loss of exchange sites. At the same time, these particles replace electroneutral solution in the pore centre. As a result, the effective radius of ion conducting channels decreased, and the double electrical layers occupied a more important volume fraction of the pore solution that favored permselectivity. However, the higher swelling of AEMs led to the formation of structural macro-defects (tears, cavities) filled with external solution. The presence of these macropores was detected by the evolution

of conductivity vs. concentration with the assistance of the microheterogeneous model [44]. In the long-term run, these defects form unselective flow through passages leading to full loss of permselectivity.

In the present study, the electrolyte permeability of AEMs used in ED of whey increases while the permselectivity decreases. This behavior can be explained by the loss of PVC, which constitutes a part of the membrane matrix along with the functionalized PS-DVB polymer chains. These two polymers are interpenetrated, and when PVC is removed from the matrix, uncharged pores and cavities/voids are formed. The network of these pores form channels for electrolyte passage through the membrane. These pores also serve as a refuge for whey big organic molecules, e.g. lactose and proteins.

The lactose molecular mass is 342 g mol^{-1}, its hydrodynamic (Stokesian) radius is reported to be between 0.44 nm [45] and 0.49 nm [46]. Its binary mutual (with water) diffusion coefficient at 25°C is 0.57 10^{-9} m^2 s^{-1} [45]. Whey proteins are constituted of more than one hundred amino acids, their molecular mass range is from 10 000 to up to 70 000 g mol^{-1}. The properties of water molecules near the surface of a bio-molecule were the subject of numerous experimental and theoretical studies, with some of them suggesting the existence of rather rigid water structures around lactose and proteins [47].

The hydration layer around a carbohydrate (lactose) is determined to extend to 5.13 ± 0.24 Å from the surface corresponding to ≈123 water molecules beyond the first solvation shell [48]. Thus, we can expect that lactose molecule can fairly easily penetrate inside the functional nanopores and foul them, while it is much less probable for the proteins. The latter would rather occupy larger uncharged spaces abandoned by the washed PVC.

When soaking in ethanol, about 2% of the membrane total mass was extracted in the cases of A1, A2 and A3 membranes. The FTIR-ATR analysis showed that the paste, which was obtained after evaporation of ethanol, contained mainly lactose and proteins. The fact that the amount of extracted products did not increase with the time of membrane exploitation seemed, at a first glance, in contradiction with the increasing loss of PVC and the expected increase in membrane porosity. However, we can explain this constant extracted mass if we assume that the constituents of whey (lactose, proteins) form a sort of gel within membrane pores. When ethanol penetrated in the pores, it caused precipitation of water soluble lactose. This resulted in destruction of gel structure and elution of whey constituents from the membrane. However, these constituents were extracted only from the near-surface pore layer, they remained blocked in deeper pore layer. On the other hand the pore fouling begun by the

near-surface layer. Hence, in all cases approximately, a same near-surface layer is involved, which is fouled even at the first stage of ageing.

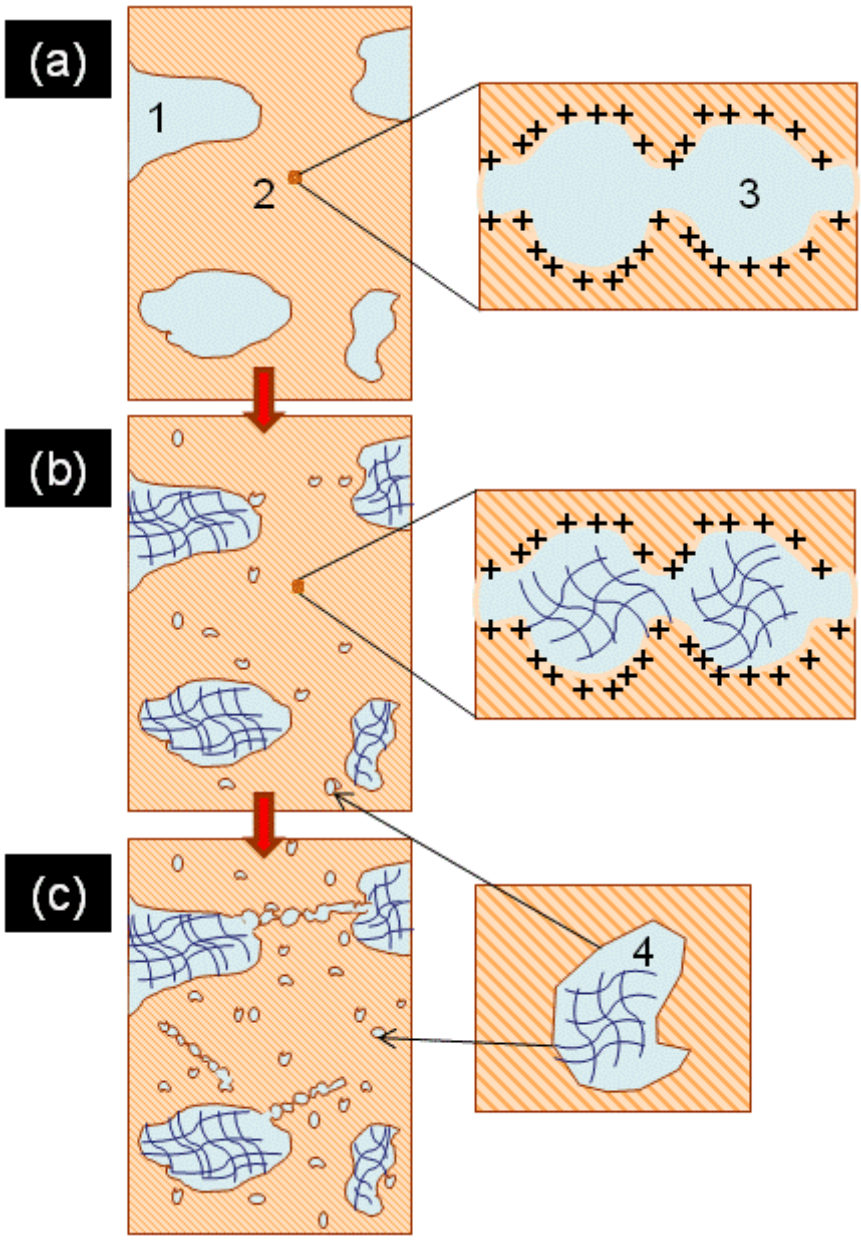

Fig. 3-12. Possible structure of AEM: (a) before ED, (b) during ED and (c) at the end of its lifetime in ED for whey demineralization. 1: macro-defects of structure, 2: nanoporous medium, 3: nanopore filled with the charged solution, 4: non-selective cavities left by the lost PVC.

The apparent scenario of changes in structure of an AEM during its operation in ED of whey is shown in Fig. 3-12. A fresh membrane contains a small amount of macropores and a nanoporous medium providing selective transport to the membrane. The major part of solution within nanopores is charged, while its central part is electrically neutral. This solution together with the solution in macropores forms the "intergel" solution with volume fraction f_2. During ED operation, lactose can foul nanopores thus reducing the mobility of ions there. Under the attack of OH^- ions, a degradation of PVC occurs leading to appearing uncharged pores with a size of the order of 100 nm. These pores may be fouled by lactose and proteins; they form a network allowing for higher electrolyte permeability through the membrane. Due to these pores, the parameter f_2 increases with the time of operation, while the membrane electrical conductivity in dilute solutions decreases, but increases in concentrated ones.

3.5. Conclusions

This report has discussed for the first time the experimental results of a comprehensive study on AEM deterioration during the use in ED of whey demineralization. We have found that there are several events accompanying the process of membrane ageing. Membrane fouling occurs from the beginning of the operation when small-size constituents of whey, such as amino acids, are accumulated within charged nanopores. Such a fouling leads to a decrease in counterion mobility within these pores and to a lowering of electrical conductivity. No significant loss in anion-exchange capacity and variation in membrane swelling are observed in this phase. The following phases of membrane deterioration are apparently due to the loss of the PVC binder within the membrane matrix (not including the reinforcing cloth) caused by the attack of OH^- ions during the CIP process. This loss results in the formation of non-charged pores (voids) within the membrane matrix, which are available for electroneutral electrolyte solution and for large molecules such as lactose and proteins. As a consequence, the membrane conductivity does not continue to decrease, but there is even a tendency to its increase. Likewise, these non-selective pores form a network for increasing electrolyte permeability through the membrane. The water uptake increases first slightly and then, dramatically in the last phase. There is also deterioration of the membrane toughness evidently caused by the elimination of PVC from the semi-interpenetrating polymer network

which leads to the formation of cracks and tears. This is the reason of membrane final failure in the ED stack. Further research will be implemented to get a deeper insight into the ageing mechanisms by the action of hydroxide ions in this kind of membranes.

3.6. Acknowledgements

This investigation was realized within French-Russian laboratory "Ion-exchange membranes and related processes". The authors are grateful to CNRS, France, and to RFBR, Russia (grants 11-08-93107_CNRSL, 12-08-00188_CNRSL, 13- 8-96508r_yug), as well as to FP7 Marie Curie Actions "CoTraPhen" project PIRSES-GA-2010-269135 for financial support.

References

[1] Wyeth Uses Electrodialysis to Desalt Whey, Chem. Eng. News Archive, 40 (1962) 45-46.
[2] W.A. McRae, Process for treating whey, in: U.S. Patent (Ed.) USPTO, IONICS US, 1979.
[3] L.J. Andrés, F.A. Riera, R. Alvarez, Skimmed Milk Demineralization by Electrodialysis Conventional Versus Selective Membranes, J. Food Eng., 26 (1995) 57-66.
[4] M. Fidaleo, M. Moresi, Electrodialysis Applications in The Food Industry, Adv. Food Nutr. Res, Volume 51 (2006) 265-360.
[5] T. Xu, Ion exchange membranes: State of their development and perspective, J. Membr. Sci., 263 (2005) 1-29.
[6] R.K. Nagarale, G.S. Gohil, V.K. Shahi, Recent developments on ion-exchange membranes and electro-membrane processes, Adv. Colloid Interface Sci., 119 (2006) 97-130.
[7] A. Collier, H. Wang, X. Ziyuan, J. Zhang, D. Wilkinson, Degradation of polymer electrolyte membranes, Int. J. Hydrogen Energy, 31 (2006) 1838-1854.
[8] J. Healy, C. Hayden, T. Xie, K. Olson, R. Waldo, M. Brundage, H. Gasteiger, J. Abbott, Aspects of the Chemical Degradation of PFSA Ionomers used in PEM Fuel Cells, Fuel Cells, 5 (2005) 302-308.
[9] S.D. Knights, K.M. Colbow, J. St-Pierre, D.P. Wilkinson, Aging mechanisms and lifetime of PEFC and DMFC, J. Power Sources, 127 (2004) 127-134.

[10] A.B. LaConti, M. Hamdan, R.C. McDonald, Mechanisms of membrane degradation, in: Handbook of Fuel Cells, John Wiley & Sons, Ltd, 2010.

[11] A.K. Pandey, A. Goswami, D. Sen, S. Mazumder, R.F. Childs, Formation and characterization of highly crosslinked anion-exchange membranes, J. Membr. Sci., 217 (2003) 117-130.

[12] C.A. Wilkie, J.R. Thomsen, M.L. Mittleman, Interaction of poly(methyl methacrylate) and nafions, J. Appl. Polym. Sci., 42 (1991) 901-909.

[13] B. Bauer, D. Jones, J. Rozière, L. Tchicaya, G. Alberti, M. Casciola, L. Massinelli, A. Peraio, S. Besse, E. Ramunni, Electrochemical characterisation of sulfonated polyetherketone membranes, J. New Mater. Electrochem. Syst., 3 (2000) 93-98.

[14] F.A. de Bruijn, V.A.T. Dam, G.J.M. Janssen, Review: Durability and Degradation Issues of PEM Fuel Cell Components, Fuel Cells, 8 (2008) 3-22.

[15] R. Ghalloussi, W. Garcia-Vasquez, N. Bellakhal, C. Larchet, L. Dammak, P. Huguet, D. Grande, Ageing of ion-exchange membranes used in electrodialysis: Investigation of static parameters, electrolyte permeability and tensile strength, Sep. Purif. Technol., 80 (2011) 270-275.

[16] K. Kneifel, K. Hattenbach, Properties and long-term behavior of ion exchange membranes, Desalination, 34 (1980) 77-95.

[17] T. Sata, M. Tsujimoto, T. Yamaguchi, K. Matsusaki, Change of anion exchange membranes in an aqueous sodium hydroxide solution at high temperature, J. Membr. Sci., 112 (1996) 161-170.

[18] J.-H. Choi, S.-H. Moon, Structural change of ion-exchange membrane surfaces under high electric fields and its effects on membrane properties, J. Colloid Interface Sci., 265 (2003) 93-100.

[19] J.A. Vega, C. Chartier, W.E. Mustain, Effect of hydroxide and carbonate alkaline media on anion exchange membranes, J. Power Sources, 195 (2010) 7176-7180.

[20] S. Chempath, B.R. Einsla, L.R. Pratt, C.S. Macomber, J.M. Boncella, J.A. Rau, B.S. Pivovar, Mechanism of Tetraalkylammonium Headgroup Degradation in Alkaline Fuel Cell Membranes, J. Phys. Chem. C, 112 (2008) 3179-3182.

[21] G. Merle, M. Wessling, K. Nijmeijer, Anion exchange membranes for alkaline fuel cells: A review, J. Membr. Sci., 377 (2011) 1-35.

[22] L. Dammak, C. Larchet, D. Grande, Ageing of ion-exchange membranes in oxidant solutions, Sep. Purif. Technol., 69 (2009) 43-47.

[23] R. Ghalloussi, W. Garcia-Vasquez, L. Chaabane, L. Dammak, C. Larchet, N. Bellakhal, Decline of ion-exchange membranes after utilization in electrodialysis for food applications, Phys. Chem. News, 65 (2012) 66-72.

[24] R. Ghalloussi, W. Garcia-Vasquez, L. Chaabane, L. Dammak, C. Larchet, S.V. Deabate, E. Nevakshenova, V. Nikonenko, D. Grande, Ageing of ion-exchange membranes in electrodialysis: A structural and physicochemical investigation, J. Membr. Sci., 436 (2013) 68-78.

[25] Y. Mizutani, R. Yamane, H. Ihara, H. Motura, Studies of Ion Exchange Membranes. XVI. The preparation of Ion Exchange Membranes by the "Paste Method", Bull. Chem. Soc. Jpn., 36 (1963) 361-366.

[26] Y. Mizutani, R. Yamane, H. Motomura, Studies of Ion Exchange Membranes. XXII. Semicontinuous Preparation of Ion Exchange Membranes by the “Paste Method", Bull. Chem. Soc. Jpn., 38 (1965) 689-694.

[27] Y. Mizutani, Studies of Ion Exchange Membranes. XXX. The tetrahydrofuran Extraction of the Ion-exchange Membrane and its Base Membrane Prepared by the "Paste Method", Bull. Chem. Soc. Jpn., 42 (1969) 2459-2463

[28] M. Fidaleo, M. Moresi, A. Cammaroto, N. Ladrange, R. Nardi, Soy sauce desalting by electrodialysis, J. Food Eng., 110 (2012) 175-181.

[29] L. Bazinet, S. Brianceau, P. Dubé, Y. Desjardins, Evolution of cranberry juice physico-chemical parameters during phenolic antioxidant enrichment by electrodialysis with filtration membrane, Sep. Purif. Technol., 87 (2012) 31-39.

[30] H. Strathmann, in: Ion-exchange Membrane Separation Processes, Elsevier, 2004, pp. 287-328.

[31] G. Gernigon, P. Schuck, R. Jeantet, H. Burling, Whey Processing | Demineralization, in: W.F. Editor-in-Chief: John (Ed.) Encyclopedia of Dairy Sciences (Second Edition), Academic Press, San Diego, 2011, pp. 738-743.

[32] H. Simova, V. Kysela, A. Cernin, Demineralization of natural sweet whey by electrodialysis at pilot-plant scale, Desalin. Water Treat., 14 (2010) 170-173.

[33] AFNOR, Norme Française NF X 45-200, in, 1995.

[34] N.D. Pismenskaya, V.V. Nikonenko, N.A. Melnik, K.A. Shevtsova, E.I. Belova, G. Pourcelly, D. Cot, L. Dammak, C. Larchet, Evolution with time of hydrophobicity and microrelief of a cation-exchange membrane surface and its impact on overlimiting mass transfer, J. Phys. Chem. B, 116 (2012) 2145-2161.

[35] R. Lteif, L. Dammak, C. Larchet, B. Auclair, Conductivité électrique membranaire: étude de l'effet de la concentration, de la nature de l'électrolyte et de la structure membranaire, Eur. Polym. J., 35 (1999) 1187-1195.

[36] L. Dammak, C. Larchet, B. Auclair, V.V. Nikonenko, V.I. Zabolotsky, From the multi-ionic to the bi-ionic potential, Eur. Polym. J., 32 (1996) 1199-1205.

[37] B. Auclair, V. Nikonenko, C. Larchet, M. Métayer, L. Dammak, Correlation between transport parameters of ion-exchange membranes, J. Membr. Sci., 195 (2002) 89-102.

[38] R.A. Robinson, R.H. Stokes, Electrolyte solutions; the measurement and interpretation of conductance, chemical potential and diffusion in solutions of simple electrolytes, 2nd ed., Butterworths Scientific Publications, London, 1959.

[39] C. Knill, Handbook of Fourier Transform Raman and Infrared Spectra of Polymers A.H. Kuptsov and G.N. Zhizhin, Bioseparation, 9 (2000) 55-55.

[40] M. Solís-Oba, O. Teniza-García, M. Rojas-López, R. Delgado-Macuil, J. Díaz-Reyes, R. Ruiz, Application of Infrared Spectroscopy to the Monitoring of Lactose and Protein from Whey after Ultra and Nano Filtration Process, J. Mex. Chem. Soc., 55 (2011) 190-193.

[41] L. Bégoin, M. Rabiller-Baudry, B. Chaufer, C. Faille, P. Blanpain-Avet, T. Bénézech, T. Doneva, Methodology of analysis of a spiral-wound module. Application to PES membrane for ultrafiltration of skimmed milk, Desalination, 192 (2006) 40-53.

[42] J.J. Krol, M. Wessling, H. Strathmann, Chronopotentiometry and overlimiting ion transport through monopolar ion exchange membranes, J. Membr. Sci., 162 (1999) 155-164.

[43] N.P. Gnusin, V.I. Zabolotsky, V. Nikonenko, Meshechkov, Development of the generalized conductance principle to the description of transfer phenomena in disperse systems under the acting of different forces, Zh. Fiz. Khimii (Rus. J. Phys. Chem.), 54 (1980) 1518–1522

[44] V.I. Zabolotsky, V.V. Nikonenko, Effect of structural membrane inhomogeneity on transport properties, J. Membr. Sci., 79 (1993) 181-198.

[45] A.C.F. Ribeiro, O. Ortona, S.M.N. Simões, C.I.A.V. Santos, P.M.R.A. Prazeres, A.J.M. Valente, V.M.M. Lobo, H.D. Burrows, Binary Mutual Diffusion Coefficients of Aqueous Solutions of Sucrose, Lactose, Glucose, and Fructose in the Temperature Range from (298.15 to 328.15) K, J. Chem. Eng. Data, 51 (2006) 1836-1840.

[46] S. Schultz, A. Solomon, Determination of the Effective Hydrodynamic Radii of Small Molecules by Viscometry J. Gen. Physiol., 44 (1961) 1189-1199.

[47] S.K. Pal, J. Peon, B. Bagchi, A.H. Zewail, Biological Water: Femtosecond Dynamics of Macromolecular Hydration, J. Phys. Chem. B, 106 (2002) 12376-12395.

[48] U. Heugen, G. Schwaab, E. Bründermann, M. Heyden, X. Yu, D.M. Leitner, M. Havenith, Solute-induced retardation of water dynamics probed directly by terahertz spectroscopy, Proc. Natl. Acad. Sci. U. S. A., 103 (2006) 12301-12306.

Chapitre 4

Vieillissement des membranes échangeuses d'anions induit par le nettoyage acide-base

Présentation de l'article

Grâce à l'étude physico-chimique, structurale et mécanique des membranes échangeuses d'anions faite lors du chapitre précédent, nous avons pu identifier les différentes étapes de leur vieillissement en électrodialyse.

Le PVC utilisé comme polymère liant de la membrane échangeuse d'anions homogène s'est dégradé ; il en a résulté une formation de pores non chargés dans la matrice de la membrane. L'élimination du PVC a entraîné une diminution de la tenue du matériau et une formation conséquente de fissures et fractures. Ceci a été la raison principale de la fin de vie de la membrane dans l'empilement d'électrodialyse.

Nous nous sommes intéressés par la suite à la détermination des causes et des mécanismes de vieillissement de ces membranes. Les principales causes qui pourraient engendrer la dégradation de la membrane sont les conditions ou paramètres de fonctionnement du système, tels que la température, le pH, le nettoyage chimique, etc. Habituellement, la déminéralisation du lactosérum est effectuée à basse température et à pH légèrement acide pour éviter le pourrissement du produit et la précipitation des sels des ions divalents sur la surface de la membrane, respectivement. Par ailleurs, le nettoyage chimique des membranes après une certaine période de fonctionnement est réalisé selon des cycles de lavage alternant des solutions acides et d'autres basiques (voir section 1.2.3).

Vu que le procédé est réalisé à basse température, nous estimons que le vieillissement des membranes en électrodialyse ne peut pas être engendré par une dégradation thermique du polymère. Nous suspectons alors que la principale source de la dégradation du matériau membranaire est l'utilisation de solutions à pH acide (fonctionnement normal et nettoyage) ou basique (nettoyage).

Dans ce contexte, nous avons mis en place des procédés de vieillissement artificiel, accéléré et contrôlé (vieillissement *ex-situ*) dans lesquels une membrane est exposée au contact prolongé de l'acide chlorhydrique concentrée, de l'hydroxyde de sodium concentré ainsi qu'à des cycles acide-base simulant les conditions d'un nettoyage classique en électrodialyse.

Par ailleurs, nous avons réalisé le vieillissement *ex-situ* sur des membranes possédant des structures distinctes : homogènes et hétérogènes. Cela nous a permis de faire une comparaison entre leurs mécanismes de vieillissement et de conclure sur la stabilité de chacune dans les solutions acides et basiques.

Nous nous sommes aperçus que la stabilité des polymères liants joue un rôle essentiel dans le comportement à long terme des membranes échangeuses d'ions. Leur vieillissement entraine principalement des défaillances mécaniques réduisant par la même occasion la sélectivité des membranes (présence de porosités, fissures,…).

Les membranes échangeuses d'anions aussi bien homogènes qu'hétérogènes vieillissent principalement par le processus de nettoyage chimique acide-base. La dégradation entraînée par les cycles de vieillissement semble être beaucoup plus nuisible que la seule exposition au NaOH ou HCl.

Aussi, nous avons constaté que les modifications physico-chimiques, mécaniques et structurelles de la membrane homogène, résultant de l'exposition aux cycles de nettoyage, sont similaires à celles identifiées dans le chapitre précédent pour une membrane échangeuse d'anions retirée d'un module d'électrodialyse pour la déminéralisation du lactosérum.

Tous ces éléments nous ont permis de conclure que la dégradation de ce type de membranes échangeuses d'anions utilisées en électrodialyse conventionnelle pour la déminéralisation du lactosérum est une conséquence du nettoyage chimique traditionnel effectué par des cycles alternant des solutions acides et d'autres basiques

Degradation of anion-exchange membranes induced by acid-base cleaning

Submitted to Journal of Membrane Science

W. GARCIA-VASQUEZ[1], A. BALDETTI[2], L. DAMMAK[1], V. NIKONENKO[3], D. GRANDE[1]

[1] Institut de Chimie et des Matériaux Paris-Est, ICMPE, UMR 7182 CNRS – Université Paris-Est, 2 Rue Henri Dunant, 94320 Thiais, France.

[2] Universidad de San Carlos de Guatemala, Ciudad Universitaria zona 12, Guatemala City, Guatemala

[3] Kuban State University, 149 Stavropolskaya st., 350040 Krasnodar, Russia.

Abstract

In electrodialysis (ED), cleaning-in-place (CIP) protocols are traditionally performed using acids and bases. Several ED applications take place in strong basic and/or strong acidic environments. Nevertheless, the role of the acids and bases, and more generally the role of the cleaning protocols on the ion-exchange membrane ageing during ED are still unclear. The aim of this paper is to thoroughly assess the consequences of traditional chemical CIP used in ED on the structure and properties of anion-exchange membranes (AEMs), in order to get further insight into the possible causes and mechanisms of AEM ageing. For this purpose, homogeneous AMX-SB and heterogeneous MA-41 membranes were soaked in parallel in 2 M NaOH and 2 M HCl from 50 to 700 h at room temperature. Moreover, both types of AEMs were subjected to cleaning cycles in which they were soaked alternatively in 0.1 M HCl and 0.1 M NaOH (30 min each) from 100 to 400 h to simulate cleaning conditions commonly used in industrial practice. Exposure to 2 M NaOH resulted in degradation of the quaternary ammonium sites of both AMX-SB and MA-41 probably by E1 or E2 elimination reactions. Strong alkaline conditions resulted in dehydrochlorination of the PVC binder of homogeneous AMX-SB. In contrast, PE binder of heterogeneous MA-41 was resistant to the contact with the 2 M NaOH solution. Exposure to 2 M HCl did not result in severe changes of the physico-chemical properties of both membranes or in damage of the PVC binder structure of AMX-SB. On the other hand, mechanical properties of PE binder of MA-41 severely declined. The damage caused by the cleaning cycles played an important role on membrane degradation and seemed to be even more severe than the damage induced by sole NaOH. The ageing cycles caused an increase in the macropores ratio of MA-41, and severe changes in the mechanical properties. For AMX-SB, a formation of pores in the inner matrix left by PVC resulted in deterioration of the membrane toughness and a further formation of fractures.

This investigation permits to correlate the degradation of AMX-SB resulting from the HCl-NaOH ageing cycles, and that suffered after conventional ED for food applications where traditional CIP is performed in acid-base sequences.

4.1 Introduction

Conventional electrodialysis (ED) with ion-exchange membranes (IEMs) is applied for demineralization, purification and concentration of electrolyte solutions. Over the past years, several ED applications have been developed, mainly in the food and in the chemical industry [1, 2]. In the food industry, ED is used for the concentration, purification or demineralization of dairy products, fruit juice, sugar and wine [2, 3], among others. Such solutions are highly nutritious media where microorganisms may cause spoilage or where colloidal matter, inorganic compounds or macromolecules form fouling at the interface or inside the membrane [4-6].

Cleaning-in-place (CIP) is crucial to avoid fouling and growth of microorganisms that could contaminate the product [7]. CIP protocols are traditionally performed using acids and bases. Acidic cleaning aims to remove multivalent cationic species, such as in hardness salts and metal hydroxides (the mineral scaling) [8], while bases encourages dissolution of weakly acidic organic matter and promotes the cleavage of polysaccharides and proteins into smaller sugars and amides [9, 10]. Commonly, the cleaning protocols in industrial ED stacks are made in a sequence of acid-base or acid-base-acid, according to the pH of the feed solution.

Besides, during the CIP procedure, IEMs might be exposed to extreme pH or pH changes due to water splitting in bipolar ED stacks [11, 12] (where monopolar IEMs are used as well), or beyond the limiting current density [13], because of the formation of H^+ and OH^- ions. Furthermore, several ED applications take place in strong basic [14] and strong acidic [15-18] environments for the chemical and the food industry.

For these reasons, the contact with acids and bases may be crucial factor on the chemical degradation of IEMs in ED.

Nevertheless, the role of the acids and bases, and more generally the role of the cleaning protocols on the IEM ageing during ED, is still unclear. Investigating the effect of such chemical agents will help to develop better extreme pH resistant membranes, to adjust optimized operating conditions and to predict membrane lifetime.

To the best of our knowledge, no published information on the degradation of IEMs in acidic environments is available. Concerning alkaline environments, there is more available documentation as the degradation of polymer materials at high pH has always been of major concern.

The deterioration of IEMs is intimately related to the modification of two parts of the membrane, namely the polymer matrix and the functional sites.

After studying the degradation at high pH of different types of commercially available IEMs, Sata et al. [19] established that anion-exchange membranes (AEMs) deteriorated from three parts: the backing fabric (mechanical support), the polymer matrix and the anion-exchange groups attached to it.

Anion-exchange groups are known to be unstable at high pH [20, 21]. Among the different species that can be used as anion-exchange sites, we are interested in quaternary ammonium groups as they are the most commonly used in the commercially available AEMs. These groups tend to degrade under aqueous conditions at high pH, following two main degradation pathways: elimination and/or nucleophilic substitution [22, 23]. The nature of the alkyl groups of ammonium sites determines the extent of these degradation mechanisms.

The nucleophilic attack of the polymer backbone by OH^-, along with the elimination of the quaternary ammonium group is called Hofmann degradation or E2 elimination [23]. This is only possible if the leaving group is antiperiplanar compared to the β hydrogen. C-N and C-Hβ groups have to be located in the same plane. The hydroxide ions attack a β hydrogen of the ammonium groups. Their simultaneous elimination leads to the formation of an alkene, an amine and a water molecule (Fig. 4-1a).

Another mechanism called E1 elimination occurs when the molecule that bears the ammonium group has α and β sterically hindered carbon atoms [23, 24]. Thus, the hydroxide ions react with a proton of methyl groups from the ammonium sites. Subsequently, a rearrangement leads to an alkene and an amine (Fig. 4-1b).

The degradation of the ammonium sites by a nucleophilic substitution (Fig. 4-1c) corresponds to an S_N2 reaction involving an OH^- anion and a carbon atom in α position of the ammonium groups. Two products are then generated: an alcohol and an amine [25].

Even though anion-exchange site degradation at high pH is quite well documented in literature, several issues on membrane degradation remain unclear, including the degradation of the polymer binder or the consequences of the polymer matrix degradation in the transport properties.

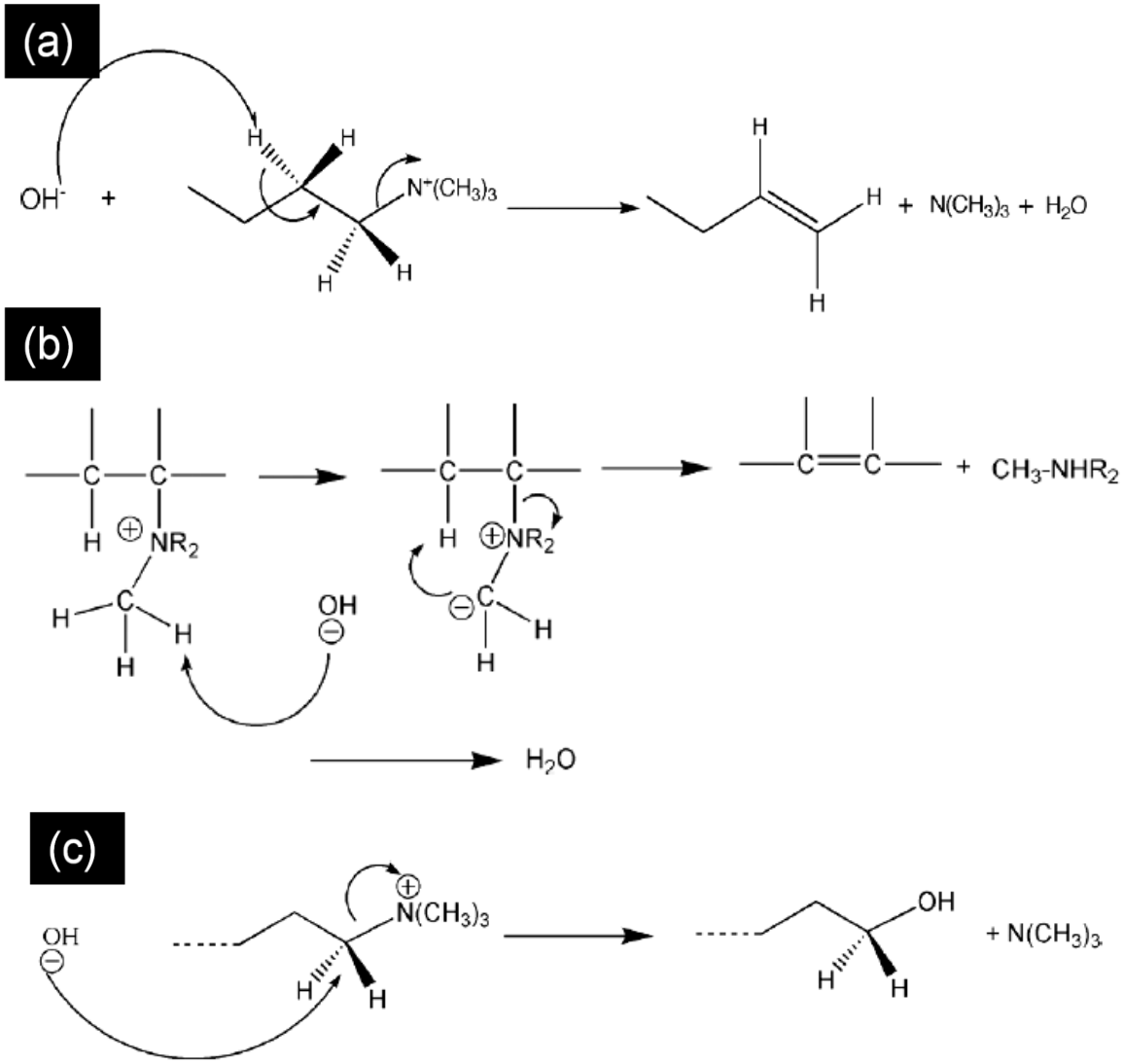

Fig. 4-1. Degradation of the quaternary ammonium groups in alkali media by: (a) the Hofmann or E2 elimination [23], (b) E1 elimination [24], (c) nucleophilic substitution S_N2 [25].

Moreover, the degradation due to acid-base cleaning cycles, in which membranes are subjected to changes in the nature, pH and temperature of the equilibrating solution, has not been addressed so far.

This work lies within the scope of a research project aiming to investigate the effects, causes and mechanisms of IEM ageing in ED for food industry applications [26-30]. In our most recent report [30], the degradation of an AEM after industrial ED for whey demineralization was studied. A progressive loss of poly(vinyl chloride) (PVC) led to the formation of non-charged pores and consequently an increase in electrolyte conductivity along with

permeability through the membrane. The PVC loss caused changes in the mechanical properties of the membrane, and resulted in the formation of cracks and tears, which led to the end of the membrane lifetime. In this context, the aim of this paper is to thoroughly assess the consequences of traditional chemical CIP used in ED on the structure and properties of AEMs in order to get the possible causes and mechanisms of AEM ageing.

As the membrane lifetime is accounted for several thousands of hours, real-time experimentation is impossible, and ageing protocols must be developed to shorten experimental time. The strategy herein adopted consisted in immersing membranes in ageing solutions constituted of concentrated HCl and NaOH, and afterwards simulating a cleaning protocol by immersing membranes consecutively in solutions of different natures and under different conditions. The physico-chemical, structural and mechanical properties of AEMs are then investigated by means of several analytical techniques. This fundamental investigation reveals significant issues concerning AEM long-term behavior. The approach is based upon the interpretation of the membrane characterization through a systematic analysis of new samples and aged ones.

4.2 Experimental

4.2.1 Membranes

For the degradation experiments, a homogeneous AMX-SB membrane from Tokuyama Soda and a heterogeneous MA-41 specimen from Shchekinoazot were used. According to the literature, AMX-SB is made of a fine powder of poly(vinyl chloride) (PVC), styrene (S) and divinyl benzene (DVB), mixed together to prepare a paste. This is coated on a reinforcing PVC cloth rolled up in a film and then heated at high pressure [31].
As a result, the PVC powder melts and allows S and DVB to form poly(styrene-*co*-divynilbenzene) (PS-DVB) within the PVC matrix so as to form an entwined structure [32]. The positively charged quaternary amonium groups are introduced by a chloromethylation procedure, followed by an amination with a tertiary amine.

Heterogeneous MA-41 consists of fine polymer particles of ion-exchange resin anchored to a polyethylene (PE) matrix and reinforced by fitted fabrics [33]. The ion-exchange resin also consists of functionalized polystyrene crosslinked with DVB. This AEM possesses

quaternary ammonium fixed sites as well. The main characteristics of the AEMs used in this study are summarized in Table 4-1.

Membrane	Type	Mechanical support	Structure/binder	Ion-exchange resin	Ion-exchange group
AMX-SB [31]	Homogeneous	PVC	Semi-IPN/PVC	PS-DVB	$- N^+ (CH_3)_3$
MA-41 [33]	Heterogeneous	Caprone fabric	Resin particles/ polyethylene	PS-DVB	$- N^+ (CH_3)_3$

Table 4-1. Main characteristics of AEMs used in this study.

As a starting point, MA-41 was specifically treated according to the manufacturer. Each sample was wiped with tetrachloromethane and then immersed in ethanol for 6 h to draw the impurities. Finally, it was immersed in several NaCl solutions (2 M, 1 M, 0.5 M and 0.1 M) for 24 h in each one.

Then, both homogeneous and heterogeneous membranes were conditioned following the French standard NF45-200 [34] in order to stabilize their physico-chemical properties, to remove any impurities that may come from their manufacturing process and to achieve a reproducible initial condition for all membranes.

This procedure consisted in immersing the samples in solutions of different natures starting with 0.1 M HNO_3. Membranes were then rinsed with water and carefully dried with filter paper, then immersed for 1 h in 0.1 M HCl and rinsed by immersing in 0.1 M NaCl. The procedure was repeated twice and finally, the membranes were conserved in 0.1 M NaCl.

4.2.2 Ageing protocol

After the conditioning process, membranes were soaked in parallel in a 2 M NaOH and 2 M HCl solutions for 50, 100, 200, 300 and 700 h, to acknowledge the time effects of strong alkaline and acidic conditions. This accelerated ageing was performed at room temperature.

Another test was carried out to simulate cleaning conditions in ED. Membranes underwent the following cycle:

1. 30 minutes in 0.1M HCl at 40°C under stirring

2. Rinsing with deionized water at room temperature
3. 30 minutes in 0.1M NaOH at 40°C under stirring
4. Rinsing with deionized water at room temperature before restarting the cycle

This cycle was repeated at least 8 times per day until membranes spent 100, 200 and 400 h in the ageing cycle; membranes were kept in 0.1 M NaCl at room temperature overnight. A 100 h cycle is equivalent to a daily cleaning of 1 h during 2500 h in an ED process. Thus, equivalent times to 2500, 5000 and 10 000 h in actual ED were simulated.

The purpose of this procedure was to reproduce cleaning conditions commonly used in industrial practice, and to elucidate the consequences of changing periodically the nature, pH and temperature of the solution equilibrating the IEM.

When the ageing time was completed, every sample was removed from the ageing solution, it was washed with deionized water and immersed successively in 1 M NaCl, 0.5 M NaCl and 0.1 M NaCl (24 h in each solution) in order to turn it into Cl^- form and to remove any remaining of H^+ or OH^- within the membrane or in the functional sites. AEMs were kept in 0.1 M NaCl, prior to characterization.

4.2.3 Characterization

4.2.3.1 Ion-exchange capacity

Ion-exchange capacity (E_c), which is the number of functional sites per gram of dry membrane, was determined following the French standard NF X 45-200. The counter-ions were forced to transfer to a determined solution with the purpose of titrating them. Samples were immersed in 0.1 M HCl (the counter-ion was Cl^-) for 2 h, then rinsed in ultrapure water and immersed in 1 M HNO_3 for at least 12 h. The chloride content was determined immediately after this time. Samples were eventually vacuum dried at 40 °C for 24 h to determine the dry mass.

4.2.3.2 Water uptake

Samples were separated from the stabilization solution and the excess of external liquid was removed by placing them between two foils of filter paper and pressing slightly. The membranes were immediately placed in a HB43-S Mettler-Toledo moisture thermobalance in which they were heated to 140°C until their mass did not change in 0.001 g for ten minutes.

The water uptake (W) was calculated by the mass differences between hydrated (W_b) and dried (W_a) samples as follows:

$$W = \frac{W_b - W_a}{W_b} \times 100 \tag{4.1}$$

4.2.3.3 Thickness

The membrane thickness (T_m) was measured using a Käfer Thickness Dial Gauge specially devised for plastic film thickness measurements with a resolution of 1 μm. The membrane thickness value was averaged from measurements at 10 different locations on the effective surface region of the membrane.

4.2.3.4 Contact angle

The measurements of the contact angle values were performed using a FM40 EasyDrop goniometer from Krüss. The images of a water drop at the surface of AEM samples in the chloride form were captured by a high resolution camera, and they were then processed by the Wingoutte software to determine the contact angle value using interpolation methods. The membrane samples were in the swollen state, pre-equilibrated with a 0.1 M NaCl solution as it was described by Pismenskaya et al. [13] to keep similar conditions to those found in ED cell. The experiment was repeated in no less than 10 different spots of each sample, and the average value was reported.

4.2.3.5 Alternating current conductivity

The experimental assembly used consisted of a clip-type cell to measure the membrane conductivity, a conductimeter CDM92 (RADIOMETER-TACUSSEL) and a water bath at 25 ± 1 °C [35]. The determination of membrane conductance (G_m) needed two measurements, one without the membrane (G_1) and another one with the membrane (G_2), to deduce:

$$G_{\mathrm{m}} = \frac{G_1 G_2}{G_1 - G_2} \tag{4.2}$$

Using the value of T_m and the electrodes section area (A = 1 cm²), the membrane conductivity (κ_m) was calculated as follows:

$$\kappa_m = G_m \times \frac{T_m}{A} \tag{4.3}$$

Measurements were conducted in 0.1 M NaCl to compare the changes in membrane conductivity since NaCl solutions are commonly used as reference media of membrane conductivity and resistance. In addition, electrical conductivity of samples subjected to the HCl-NaOH ageing cycles was measured in NaCl solutions at different concentrations ranging from 10^{-2} to 1 M, to apply the microheterogeneous model [36].

4.2.3.6 Electrolyte permeability

The membranes were disposed in a two compartment cell as described by Dammak et al. [37]. It consisted of a horizontal diffusion cell, in which 0.1 NaCl and water were placed into the donor and the receiver compartments respectively, stirred and maintained at room temperature. The NaCl concentration in the receiving compartment was determined as a function of time by measuring the conductivity of the solution, as previously explained by Ghalloussi et al. [26].

4.2.3.7 Porosity measurements

For AMX-SB samples, nitrogen sorption measurements were carried out at 77 K with a Quantachrome Autosorb iQ analyzer. All the samples were degassed at 150 °C for 8 h prior to analysis. The specific surface area values for the investigated membranes were quantified using the BET method at relative pressure (P/P_0) values ranging from 0.05 to 0.3.

Porosity percentage and average pore diameter of MA-41 samples were measured using a mercury intrusion porosimeter Autopore IV 9500 (Micromeritics Instruments). The determination of porosity features was based on the relationship between the applied pressure (from 1.03 to 206.8 MPa) and the pore diameter into which mercury intrudes (Washburn's equation).

4.2.3.8 Structural investigation by SEM and ATR-FTIR

Samples used for the structural investigation were vacuum dried overnight at 40 °C prior to analyses. Scanning electron microscopy (SEM) images were obtained from Pt/Pd coated samples with an accelerating tension of 3 kV using a LEO 1530 microscope.

Attenuated total reflectance-Fourier transform infrared (ATR-FTIR) spectra were carried out on a Nicolet ‘‘Nexus’’ spectrometer equipped with a Globar source and a DTGS detector between 550 and 4000 cm^{-1}. The spectral resolution was 2 cm^{-1} and 32 scans were realized for each spectrum. ATR-FTIR was performed at least three times for each sample.

4.2.3.9 Soxhlet extraction

This procedure was performed with the aim to better identify the structural changes of the AMX-SB samples. Approximately 0.5 g of dried membrane was placed in a cellulose thimble, and loaded in a Soxhlet apparatus. The extraction was carried out with 200 mL of tetrahydrofurane (THF) for 48 h at 90 °C.

4.2.3.10 Tensile strength measurements

Stress-strain curves were obtained in an INSTRON 5965 testing machine. A dumbbell of 12 ×3 mm^2 of active area was fixed into two grips and stretched at a 1mm.min^{-1} rate. The samples were in the humid state and in the Cl^- form. Each test was carried out at least twice.

4.3 Results and discussion

4.3.1 Ageing in NaOH

At the outset, some physico-chemical properties were determined to inquire about the membrane performance after contact with concentrated sodium hydroxide solutions. ED processes require IEMs to fulfill some features in electrical conductivity and ion-exchange capacity, which are directly correlated to other properties, such as thickness and water uptake. Fig. 4-2 shows the evolution of the physicochemical properties associated with AEMs as a function of time in a 2 M NaOH solution.

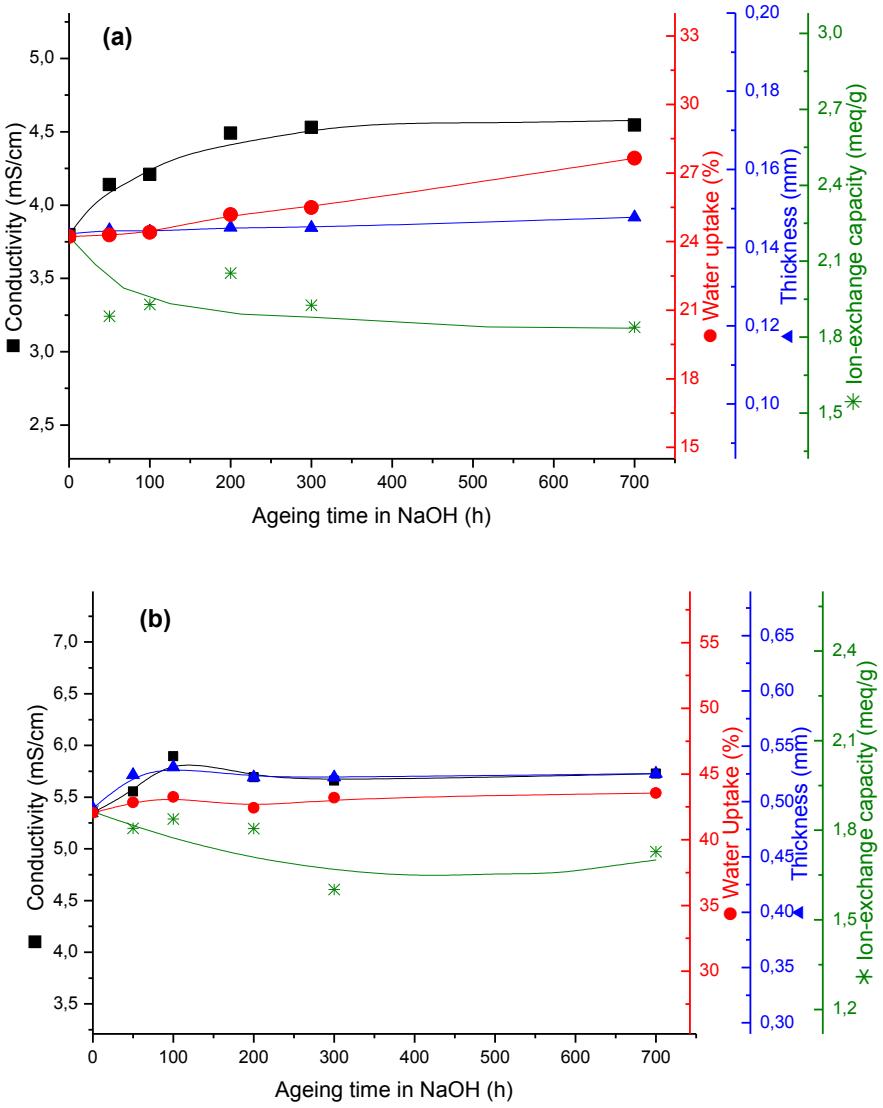

Fig. 4-2. Evolution of physico-chemical properties of AEMs as a function of time in 2 M NaOH solution: (a) AMX-SB, (b) MA-41.

The concentration or nature of the AMX-SB functional sites decreased as shown in Fig. 4-2a; there was an ion-exchange capacity loss of 15 % from 50 h of exposure to NaOH. Meanwhile, conductivity increased up to 20 %. A decrease in concentration of functional sites is generally related to a decrease in conductivity. However, in a previous study it was observed, that the conductivity of IEMs with degraded ion-exchange sites increased as the polymer matrix suffered damage [30].

In Fig. 4-2, it was observed as well, that water uptake increased gradually up to 15 % while membrane thickness slightly increased.

On the other hand, the concentration of ion-exchange sites in MA-41 started to decrease after 300 h in the 2 M NaOH solution as the ion-exchange capacity decreased by 15 %. Conductivity, thickness and water uptake slightly increased by no more than 10%.

For both membranes, a decrease in ion-exchange capacity was observed. There was an increase in the swelling and water uptake accompanied by an increase in conductivity. These alterations were more severe for homogeneous AMX-SB than for heterogeneous MA-41.

Fig. 4-3 shows the FTIR spectra of AMX-SB samples. The changes suffered in the membrane structure were evidenced by using the sample with the highest degree of degradation, the one exposed during 700 h to 2 M NaOH, since the changes were easier to distinguish.

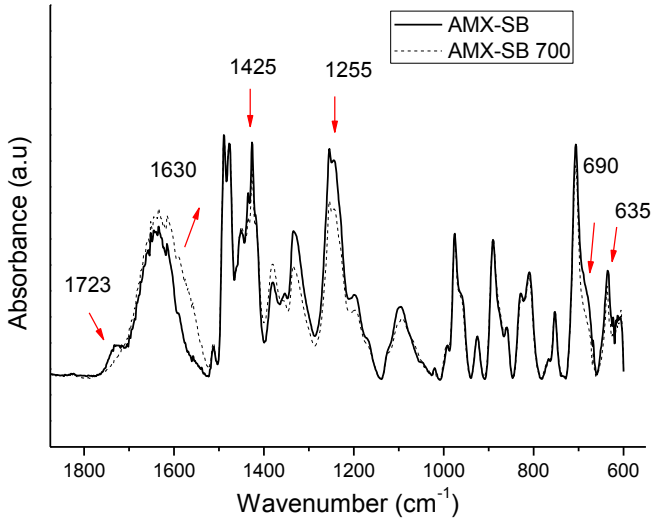

Fig. 4-3. FTIR spectra (1800-600 cm^{-1} region) of new AMX-SB sample and aged sample (AMX-SB 700) in 2 M NaOH for 700 h.

Table 4-2 presents the assignments of the more relevant FTIR bands. We distinguished bands belonging to the two different parts of the membrane, *i.e.* the functional PS-DVB and the PVC binder. The aromatic ring breathing modes of PS-DVB appeared at 1630, 1490 and 1475 cm^{-1}. The out-of-plan δ(C-H) band of the aromatic ring was recognized at 704 cm^{-1}. Bands belonging to the quaternary ammonium groups were not recognized, as the ν(N-C) stretching bands had low absorbance intensity, and a band belonging to PVC at 1255 cm^{-1}

overlapped the 1200-1250 cm^{-1} region, where they were supposed to appear. The absorbance intensity of bands belonging to the aromatic rings (at 704, 1490 and 1475 cm^{-1}) did not seem to be changed. However, the intensity of the broad band from 1500 to 1650 cm^{-1} belonging to ν(C=C) vibrations increased significantly.

Concerning the other bands present in the FTIR spectra, those at 635 and 690 cm^{-1} corresponded to ν(C-Cl) stretching bands from PVC. The band at 1255 cm^{-1} belonged to the δ(CH_2) wagging when the adjacent C atom had a chlorine atom attached, and bands at 1425 & 1435 cm^{-1} were associated with the methylene scissors deformation from PVC, as well.

It is noteworthy that all bands assigned to PVC suffered a decrease in the absorbance intensity, suggesting that there was some damage in the PVC structure.

Polymer	IR band (cm^{-1})	Assignment
PS-DVB	704	δ(C-H) out-of-plan deformation from aromatic rings
	1475 & 1490	ν(C-C) breathing modes from aromatic ring
	1630	ν(C=C) breathing modes from aromatic ring
PVC	635	ν(C-Cl)
	690	ν(C-Cl)
	1255	δ(CH_2) wagging from CH_2Cl
	1425 &1435	δ(CH_2) scissors deformation
Other	1723	ν(C=O belonging probably to a PVC plasticizer or stabilizer

Table 4-2. Assignments of the relevant FTIR bands of AMX-SB in the spectral region of 1800-600 cm^{-1}.

To better inquire about the membrane structural changes, we chose to extract the different parts of AMX-SB samples by means of a Soxhlet extraction using THF. The extractables and the residues were previously analyzed by FTIR-ATR [30]. The extractables mainly consisted of the PVC binder, and the residues were constituted of PS-DVB and the PVC cloth. The PVC binder and PS-DVB formed a semi-interpenetrating polymer network (semi-IPN) whose morphology was shown by SEM images in our previous paper [30].

44 wt % of new AMX-SB were soluble in THF. However, only 2% wt. of the sample exposed to NaOH during 700 h were recovered as extractables, thus confirming that a degradation of the PVC structure did occur in NaOH solutions.

The BET specific surface area (S_p) values were measured to evaluate the porosity in the membranes. For both, new and aged samples, the S_p values were equal to 0 m^2/g, which indicated no detectable porosity. This was confirmed by SEM images (not shown) were there were no macroscopic cracks or nanoscopic cavities, as found for industrially aged membranes in our previous papers [28, 30].

When analyzing the FTIR spectra of MA-41, we realized that it was only possible to distinguish the methylene stretching and bending bands from the PE binder. Still, no modification was detected in the PE chemical structure after NaOH ageing. Therefore, the utilization of this technique did not provide further information on the structure changes after hydroxide exposure for this kind of heterogeneous membrane.

Mechanical properties of both types membranes were studied by means of tensile tests to determine changes or damage in the polymer structure.

First, to detect any anisotropy in the mechanical properties, membranes were cut and tested along two orthogonal directions, namely the tensile test axes parallel to the length and width of the AEM. For AMX-SB, the sample tested with the main axis along its length exhibited higher stiffness associated with both an increase in the yield stress and a decrease in the strain at break. This provided evidence for mechanical anisotropy that came from the membrane cloth arrangement. In the rest of the article, the mechanical properties of AMX-SB were discussed with respect to samples whose main axis strength was parallel to the length. This fact was not observed for MA-41 for which the direction of the sample in the tensile test did not change the results, as the cloth was isotropic.

Fig. 4-4a shows the stress-strain curves of new and aged AMX-SB samples. The mechanical degradation of samples was obvious, as illustrated by a decrease in the Young modulus, the stress at break and the strain at break. After 700 h of NaOH exposure, the Young modulus decreased gradually from 290 to 245 MPa, the stress at break did it from 24 to 13.5 MPa, and the strain at break did it as well from 25 to 16 %. Therefore, aged AMX-SB became more brittle, due to PVC degradation.

Stress-strain curves of MA-41 samples are shown in Fig. 4-4b.

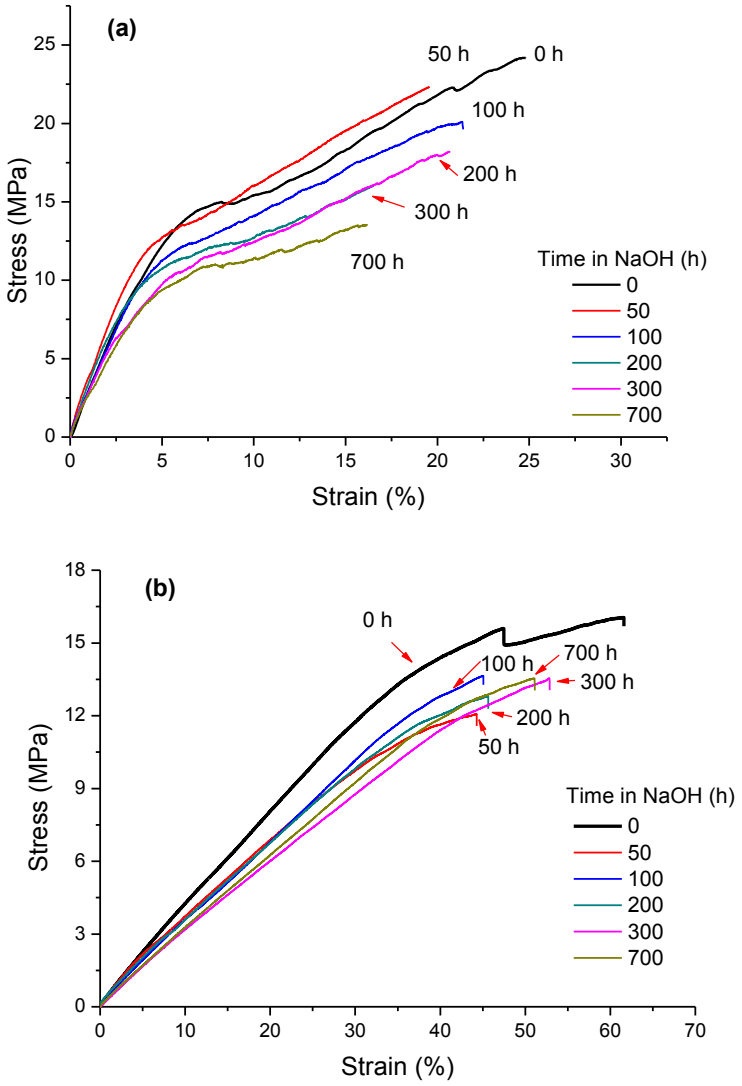

Fig. 4-4. Stress-strain curves of new and aged AEMs in 2 M NaOH: (a) AMX-SB, (b) MA-41.

MA-41 is actually a composite made from rigid particles of PS-DVB casted in a ductile PE matrix. According to Nefedova, this material possesses around 38 wt % of high density PE as a binder [33], therefore a great part of MA-41 mechanical properties should be determined by the PE binder.

For MA-41, with increasing ageing time, the Young modulus tended to decrease. However, the ultimate stress and ultimate strain did not suffer severe changes. It is possible that exposure to 2 M NaOH gave place to degradation of the PS-DVB resin, without alteration of

PE. In this case, the damage of PS-DVB caused a decrease in the composite reinforcement, and consequently a loss of rigidity, although ductility was not severely injured.

Based on the results of the physico-chemical, structural and mechanical investigation of AMX-SB samples, we suggest the occurrence of two degradation events in the membrane after exposure to 2M NaOH:

- Some part of PVC was degraded by the NaOH solution and the degradation product was an alkene.
- Quaternary ammonium sites were degraded by E1 or E2 elimination, resulting in the formation of alkenes.

The occurrence of the first event was supported by the changes in the mechanical properties and by the increase in the absorbance intensity associated with ν(C=C) stretching bands in the FTIR spectra. Dehydrochlorination of PVC might be carried out by hydroxides in the presence of quaternary ammonium salts [38] and results in the formation of polyene sequences, as it follows:

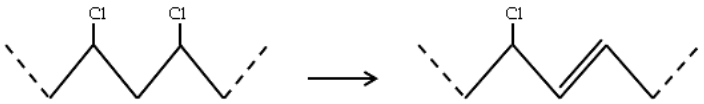

(4.4)

This polyene structure was not soluble in THF and did not cause any appearance of cavities, as shown by the BET method and SEM.

It is worth mentioning the existence of a band at 1723 cm^{-1} in the FTIR spectra that did not seem to belong to PS-DVB or PVC. However, PVC is often plasticized with poly(carboxylic acids) or stabilized with fatty acid salts. This might explain the occurrence of such a band assigned to the ν(C=O). Furthermore, it could be seen that the absorbance intensity of this band decreased, which might suggest degradation of the plasticizer and/or stabilizer, after soaking in the 2 M NaOH solution (Fig.4-3).

Stabilizers slow down the dehydrochlorination reaction and absorption of the evolved hydrogen chloride. If the stabilizer degrades, PVC is prone to a lowering of its chemical resistance and a decline of its mechanical properties.

Plasticizers usually break interchain dipole interactions, providing PVC with mobility and flexibility. According to our results, both phenomena –loss of stabilizer or loss of plasticizer-

were likely to happen in a certain extent, as chemical and mechanical degradation of PVC occurred after ageing in 2 M NaOH.

The increase in the absorbance intensity associated with ν(C=C) stretching bands in the FTIR spectra of aged AMX-SB samples may also indicate a degradation of the quaternary ammonium sites by E1 or E2 elimination, explaining the decrease of ion-exchange capacity.

In contrast, MA-41 only suffered degradation in the PS-DVB structure, according to changes identified in the physic-chemical properties and the stress-strain curves. A portion of the functional sites was eliminated by E1 or E2 elimination (as they possess the same ion-exchange groups as those of AMX-SB). Nonetheless, PE serving as polymer binder for the MA-41 membrane was more resistant to the contact with concentrated hydroxide solutions, than PVC serving as polymer binder for AMX-SB. No degradation was indeed detected in the PE structure after exposure to 2 M NaOH.

4.3.2 Ageing in HCl

Fig. 4-5 shows the physic-chemical properties of AMX-SB and MA-41 as a function of the ageing time in a 2 M HCl solution. It is noteworthy that changes are less flagrant for both membranes than those suffered after ageing in the alkaline solution.

For the AMX-SB membrane, conductivity and membrane thickness did not change however there was a decrease in the water uptake and in the ion-exchange capacity. For MA-41, there was a decrease in ion-exchange capacity after ageing in 2 M HCl.

No significant changes were found in the FTIR spectra of new and aged AMX-SB samples, except an increase in the absorvance intensity of the broad band at 1623 cm^{-1} assigned to ν(C=C) bonds (Fig. 4-6).

When performing a Soxhlet extraction using THF to the AMX-SB sample exposed to 2 M HCl during 700 h, 44 wt % were recovered as extractables. This was the same ammount as in the new membrane, thus suggesting that there was no degradation of the PVC structure. Furthermore, no porosity was detected for the same sample by the BET method or SEM.

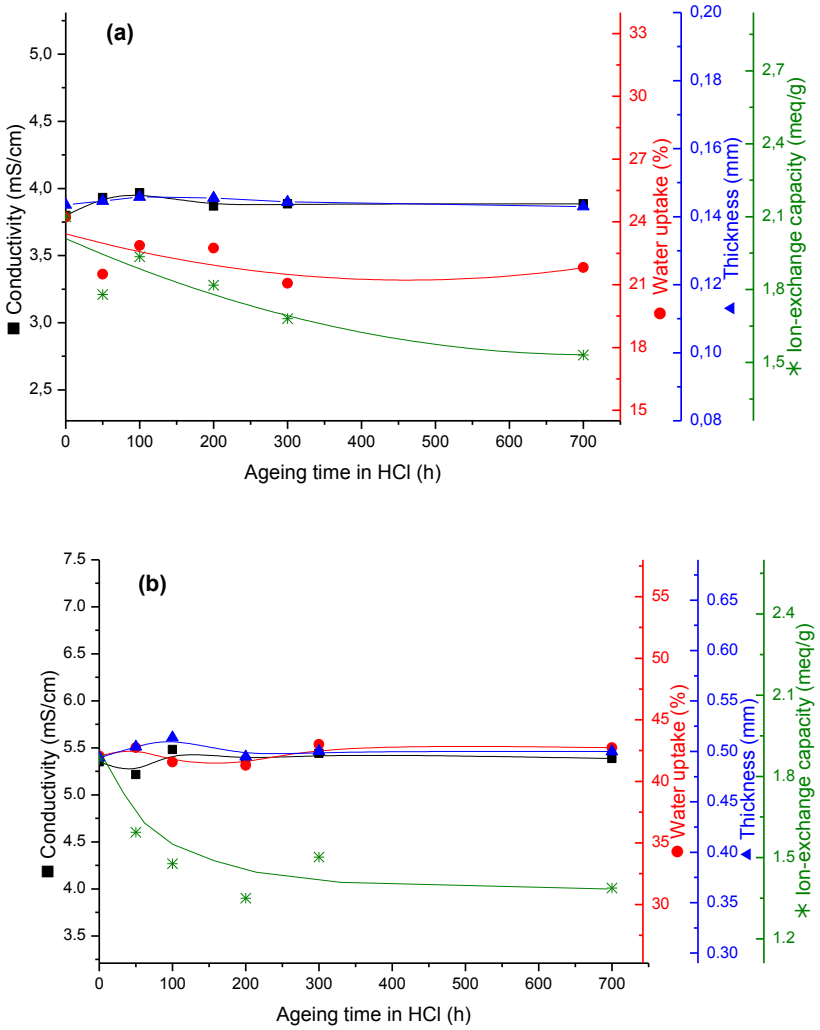

Fig. 4-5. Evolution of physico-chemical properties of AEM samples as a function of time in 2 M HCl solution: (a) AMX-SB, (b) MA-41.

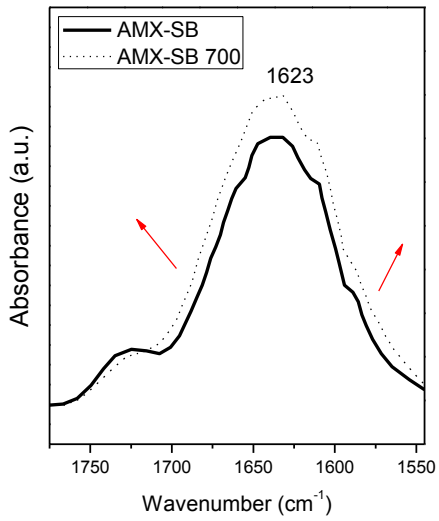

Fig.4- 6. FTIR spectra (1800-1550 cm^{-1} region) of new AMX-SB sample and aged sample (AMX-SB 700) in 2 M HCl for 700 h.

There were some changes in the mechanical properties as shown by the stress-strain curves in Fig. 4-7. The tensile strength of AMX-SB samples subjected to ageing in 2 M HCl increased as shown in Fig. 4-7a, while the strain at break remained almost constant.

These evolutions confirmed that, there were no changes in the PVC structure of AMX-SB membrane. However, degradation probably took place in the ion-exchange resin structure which led to an increase in the membrane rigidity (caused by an augmentation of the cross-linking degree) and a loss of the ion-exchange capacity.

For MA-41 samples, the Young modulus and strain at break decreased after 700 h of HCl exposure (Fig. 4-7b). The sharp decrease in tensile strength and strain at break strongly suggested a degradation of the PE binder.

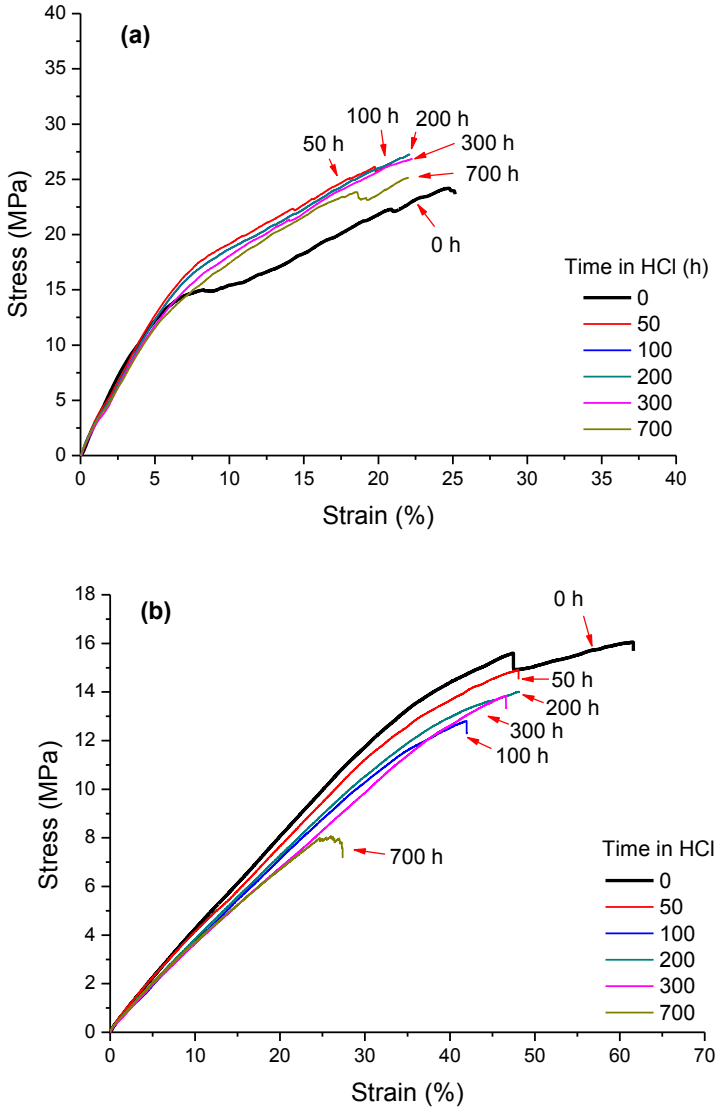

Fig. 4-7. Stress-strain curves of new and aged samples in 2 M HCl: (a) AMX-SB, (b) MA-41.

4.3.3 Ageing in the HCl-NaOH cleaning cycles

Table 4-3 presents the ion-exchange capacity values for AMX-SB and MA-41 at different exposure times to the ageing cycles. As it could be noticed, anion-exchange capacity was not degraded for AMX-SB but it did decrease by 10 % for MA-41 after exposure to the ageing cycles for 400 h. It must be taken into account that uncertainty in the ion-exchange capacity measurements was estimated to be equal to 5%.

Time (h)	AMX-SB E_c (meq/g)	MA-41 E_c (meq/g)
0	1.62	1.86
100	1.58	1.77
200	1.60	1.77
400	1.61	1.70

Table 4-3. Ion-exchange capacity of AEM samples as a function of time in the HCl-NaOH ageing cycles.

Fig. 4-8 describes the evolution of the main physico-chemical characteristics of AEMs: conductivity, thickness, water uptake, and contact angle characteristic of surface hydrophilicity.

For both membranes, the hydrophilicity increased as shown by the reduction of contact angle and the augmentation of water uptake. This was accompanied by an increase in membrane conductivity, which means higher counter-ion mobility and/or concentration in the membrane.

For MA-41, there was more solution absorbed into the membranes, as shown by the membrane thickness measurements, which facilitated the counter-ion passage. The hydrophilicity of the surface increased, probably as particles of PS-DVB resin were more exposed to the membrane surface (as the resin is the hydrophilic component of the membrane), thus amplifying the contact between the external solution and the ion-exchange resin.

The electrical conductivity of AMX-SB increased up to 30% after 400 h of exposure to the ageing cycles. Since the ion-exchange capacity did not decrease, we might suppose that changes in the physic-chemical properties came from a possible degradation of the polymer binder during the cleaning operations. Actually, a degradation of the functionalized PS-DVB would be accompanied by a loss of the functional sites, which means a decline of the ion-exchange capacity.

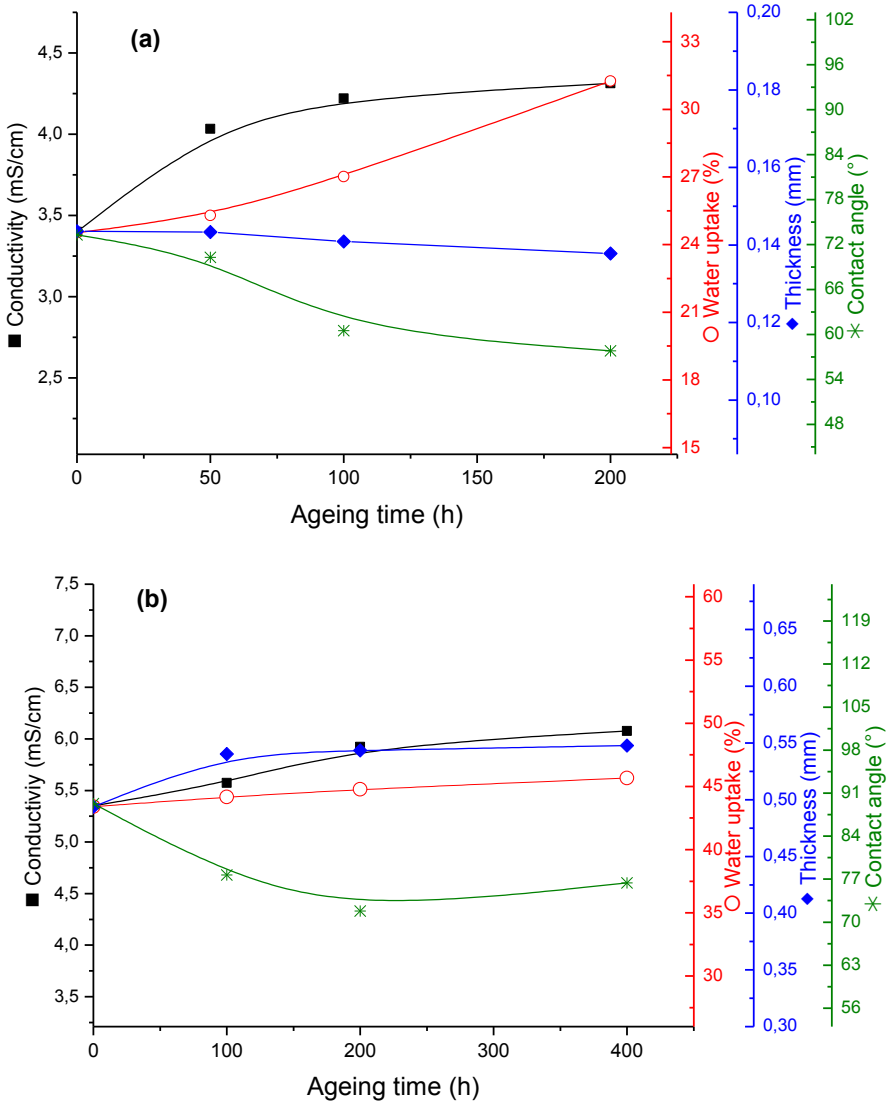

Fig. 4-8. Evolution of physico-chemical properties of AEMs as a function of time in the HCl-NaOH cleaning cycles: (a) AMX-SB, (b) MA-41.

The degradation of the polymer binder was indeed identified by means of a FTIR investigation of the new sample and that exposed for 400 h to the ageing cycles (Fig. 4-9). AMX-SB exhibited some modifications of its spectral profile, especially in the 1800-1200 cm^{-1} region. Changes were predominantly noticed for stretching and bending vibrations of PVC, *i.e.* at 635, 690, 1255 and 1425 cm^{-1} (see Table 4-2). The absorbance decrease of these bands suggests degradation of the PVC structure. Once again, bands assigned to PS-DVB did not seem to have suffered absorbance variations, excluding the broad band at 1619 cm^{-1} belonging to ν(C=C) stretching, which was slightly modified.

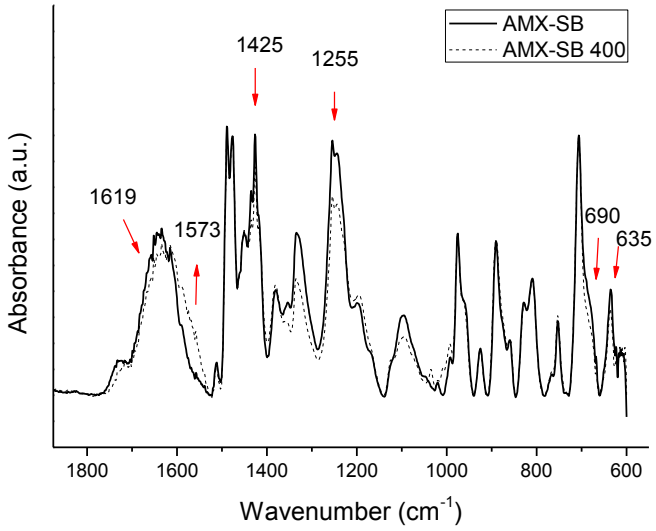

Fig. 4-9. FTIR spectra (1800-600 cm^{-1} region) of new AMX-SB sample and aged sample (AMX-SB 400) exposed to the HCl-NaOH cleaning cycle for 400 h.

To further inquire about the membrane structure, the different parts of AMX-SB samples were extracted with a Soxhlet assembly using THF. The amount of extractables of each sample subjected to the ageing cycles is shown in Table 4-4. It is noteworthy that the extractable contents declined gradually from 44 wt % for the new sample to 17 wt % for the sample exposed during 400 h to the ageing cycles, thus indicating loss or damage of the PVC binder.

Ageing time (h)	**Extractables contents (wt %)**	**Residue contents (wt %)**
0	44	56
100	21	79
200	20	80
400	17	83

Table 4-4. Extractable contents and residue contents after THF extraction of AMX-SB samples subjected to the HCl-NaOH ageing cycles.

The S_p values were employed to evaluate the porosity in the membrane. As explained before, no porosity was detected in the new AMX-SB sample by the BET method, as the S_p value was equal to 0 m^2/g. The S_p value of the sample subjected to the ageing cycle during 400 h increased to 108 m^2/g indicating a formation of new pores or cavities in the aged samples

Stress-strain curves of AMX-SB samples are displayed in Fig. 4-10. The mechanical degradation of samples was evident, as illustrated by a dramatic decrease not only in the stress at the breaking point but also in the elongation at the breaking point (which was even more flagrant). The decrease in the Young modulus and ultimate stress and strain was much more pronounced than that suffered after ageing in NaOH or HCl.

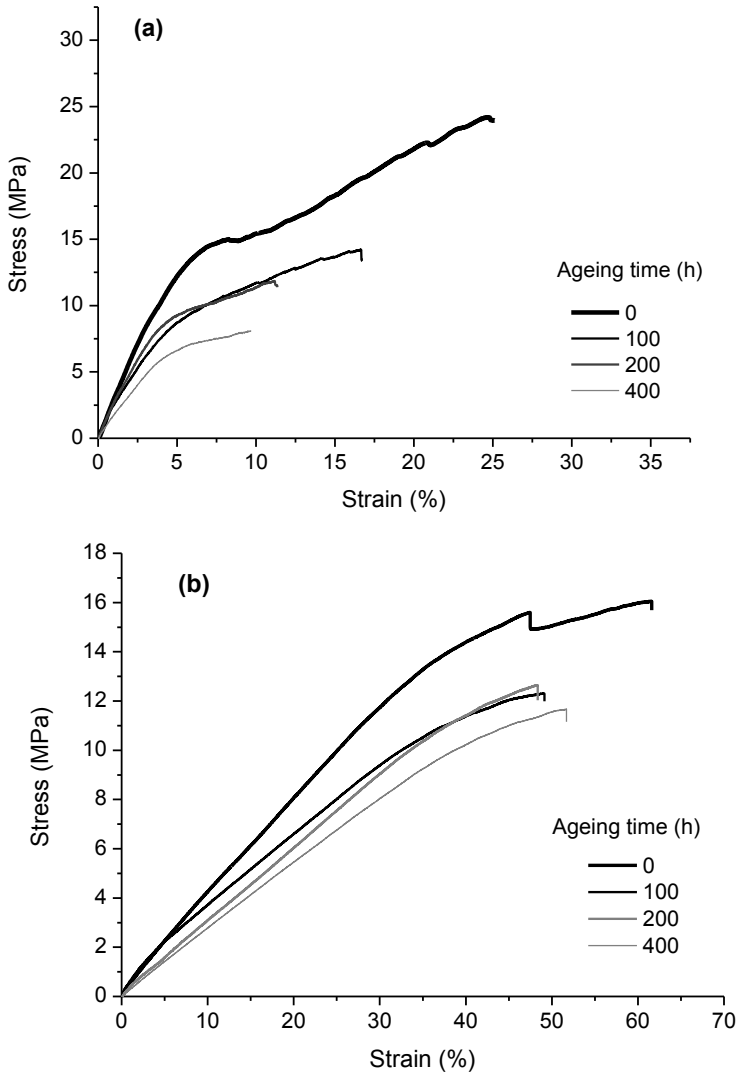

Fig. 4-10. Stress-strain curves of new and aged AEMs exposed to the HCl-NaOH cleaning cycles: (a) AMX-SB, (b) MA-41.

As explained in our previous report [30], the mechanical behavior of a new AMX-SB was influenced by its three main components, *i.e*. the functionalized PS-DVB, the PVC binder and the PVC cloth.

PS-DVB is characterized by a high modulus of rigidity and a low elongation at break, thus indicating that this material is brittle, which is expected for a crosslinked polymer. On the other hand, Young modulus and tensile strength of PVC are medium, while the elongation at break is high. This material is softer and tougher than PS-DVB. Thus, adding PVC to the membrane formulation helps to improve the mechanical strength, softness and dimensional stability.

Obviously enough, stress-strain curves showed that AMX-SB exhibited a combination of the mechanical properties associated with these two polymeric components, *i.e*. the rigidity of PS-DVB and the toughness of PVC.

Fig. 4-10 shows that the Young modulus, which can be related to the rigidity of a material, decreased from 274 to 222 MPa after 400 h in the ageing cycles. The breaking strength, which represents the membrane ductility, decreased from 25 to 9 %, and the area under the stress-strain curve decreased from 3.9 to 0.6 MPa/mm^2, which strongly indicated a loss of the material toughness.

Accordingly, the AEM gradually converted from a rigid and tough material into a brittle one.

From the results explained above, we acknowledged the following modifications in AMX-SB membrane after exposure to the ageing cycles:

- Increase in the material hydrophilicity.
- Enhancement of the membrane electrical conductivity.
- Formation of pores or cavities in the membrane surface and/or inner matrix.
- Severe changes in mechanical properties (loss of toughness and flexibility).
- The PVC binder was degraded.

Interestingly, the membrane modifications were similar to those reported in our previous study on AMX-SB after ED for whey demineralization [30]. Table 4-5 presents a comparison between some of the physico-chemical parameters of a new AMX-SB sample, that exposed to the ageing cycles for 400 h, and that at the end of its lifetime in ED for whey demineralization [30].

Sample	P^* (10^{-9} m^2/s)	f_2 (%)	S_p (m^2/g)	Extractable contents (wt %)
New AMX-SB	0.30	11.8	0	44
AMX-SB after 400 h in cleaning cycles	2.97	18.8	108	17
AMX-SB at the end of lifetime in ED	2.84	16.2	60	11

Table 4-5. Physico-chemical properties of new AMX-SB sample, sample exposed to the HCl-NaOH ageing cycles for 400 h, and sample at the end of lifetime in ED [30]: permeability (P^*), volume fraction of inter-gel solution (f_2), BET specific surface area (S_p) and extractable contents after THF extraction.

In our previous research [30] we proposed that the last steps of membrane deterioration in ED were due to the loss or degradation of the PVC binder within the membrane matrix. The hypothesis underlying the removal or degradation of the PVC binder was the attack by OH^- ions during the CIP process [30]. We will discuss this hypothesis based on the results of the present investigation.

Extractable contents of samples exposed to the ageing cycle gradually decreased as shown in Table 4-4. Similar results were found for samples after real use in ED (Table 4-5). This decline may be a consequence of PVC dehydrochlorination, due to NaOH exposure, as shown in section 3.1; this was supported by the changes on the shape of ν(C=C) band in FTIR spectra (Fig. 4-9). Nevertheless, two events were different from the case of the previous section: first, the band at 1723 cm^{-1} in AMX-SB spectra (Fig. 4-9) did not disappear after the ageing cycles as it did after ageing in 2 M NaOH (Fig. 4-3) and second, the S_p values revealed the occurrence of pores.

If the band at 1723 cm^{-1} corresponds to ν(C=O) vibrations from a PVC stabilizer, the dehydrochlorination reaction would have been slowed by it. In this case, PVC degradation might not be completed, and that was the reason why 40 % of the total PVC binder was still present in aged AEM and was recovered by Soxhlet extraction with THF. Furthermore, there was another modification in the membrane namely the formation of cavities and/or pores of some tens of nanometers, as suggested by S_p values and evidenced on SEM images (Fig. 4-11). These nanopores were probably left behind by PVC that was leached out from the

membrane, due to changes in the entanglement of the semi-IPN during the ageing cycles. Pores resulted from the constant changes of pH, temperature or nature of the solution.

Cavities were noticed in the high magnification images (second row) for both the sample aged in ED and that aged during the cleaning cycles. SEM analysis also illustrated the formation of cracks and fissures in the low magnification images (first row). Such fractures might result from the deterioration of the membrane toughness caused by the elimination of PVC from the semi-IPN.

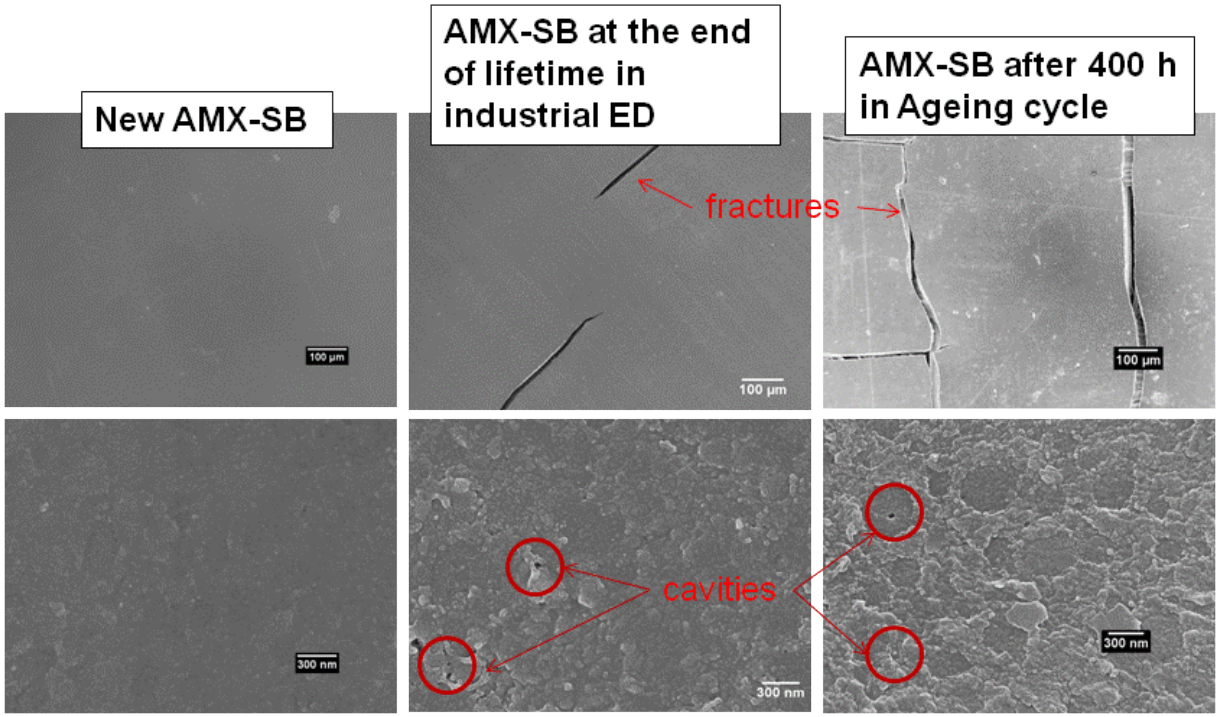

Fig. 4-11. SEM images of AMX-SB: new sample (first column), aged sample in industrial ED for whey demineralization [30] (second column), and sample after the HCl-NaOH cleaning cycle performed in this study (third column)

It was previously stated that functional PS-DVB is prone to be attacked by OH^-, especially at the quaternary ammonium sites by elimination or nucleophilic substitution [23-25]. However, there was no other evidence of damage in the PS-DVB structure after the ageing cycles. Furthermore, damage in the PS-DVB structure would have been accompanied by a severe loss of the ion-exchange capacity and changes in the breathing modes of the aromatic rings of PS-DVB in FTIR spectra. Degradation of functional sites did not occur as the concentration and temperature of exposition to HCl or NaOH were not high enough to promote the ion-exchange sites degradation.

Therefore, we may state that the PVC binder of the AMX-SB membrane suffered two kinds of modifications after the ageing cycles: dehydrochlorination (due to the contact with NaOH during cycles) and loss of entanglement (due to multiple changes of environment during cycles) which created pores or voids in the inner matrix of the AEM.

The new non-charged pores created by the PVC degradation allowed for the increase in water uptake and the enhancement of conductivity. The fact that higher water uptake did not result in a large increase in membrane thickness suggested that water absorption by new pores was the main mechanism involved.

Furthermore, Table 4-5 shows that electrolyte permeability increased from 0.3 for the new sample to 2.97 $10^{-9}m^2/s$ for the sample exposed for 400 h to the ageing cycles, as the appearance of new pores formed channels for non-selective electrolyte transfer.

The microheterogeneous model [36] correlates membrane physico-chemical properties with its kinetic and structural parameters. It was used in our previous investigation for the determination of the volume fractions f_1 and f_2 of the membrane gel phase and the electrically neutral solution filling the intergel spaces, respectively ($f_1 + f_2 = 1$) ([30]). The increase in f_2 for AMX-SB after exposure to the ageing cycles (Table 4-5) resulted from the degradation and loss of PVC and the formation of uncharged pores filled with electrically neutral solution.

A comparison between mechanical behaviour of AMX-SB samples, obtained from the stress-strain curves, is shown in Fig 4-12. The decrease in Young modulus, breaking strain and area under the curve when samples were exposed to industrial ED is equivalent to that suffered after exposure to the artificial ageing cycles for 400 h.

Therefore, the action of OH^- was not the only reason for AMX-SB membrane degradation in ED. The damage caused by the ageing cycles, which simulated conditions during the CIP process, played an important role on membrane degradation and seemed to be even more severe than the damage caused by sole NaOH, as studied in section 3.1.

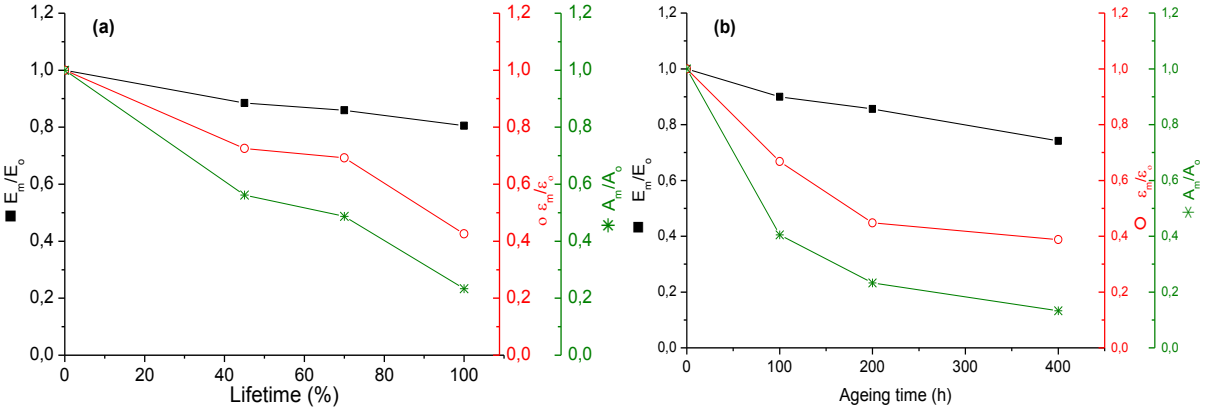

Fig. 4-12. Evolution of normalized Young modulus (E_m/E_o), strain at break ($\varepsilon_m/\varepsilon_o$), and area under the curve (A_m/A_o) of AMX-SB as a function of (a) lifetime in industrial ED [30], (b) time in the HCl-NaOH cleaning cycles performed in this study.

Concerning MA-41 results, Fig. 4-10b shows the stress-strain curves of samples subjected to the ageing cycles. It is observed a severe loss in Young modulus, breaking strain and breaking stress. Significant changes in mechanical properties are a strong argument to state that degradation was not only a surface reaction, but bulk properties of the membrane also changed significantly.

Based on the results of the physic-chemical and mechanical study of MA-41, we acknowledge the following modifications:

- Decrease in ion-exchange capacity decreased.
- Increase in the material hydrophilicity.
- Enhancement of membrane electrical conductivity.
- Severe changes in mechanical properties.

Table 4-6 shows that the electrolyte permeability displayed a fourfold increase, and the fraction of the membrane intergel fraction, f_2, also increased, in more than 30 %. Changes in the pH, temperature or nature of the solution may have affected adhesion between the resin particles and the PE binder, thus creating additional porosity.

Sample	P^* (10^{-8} m^2/s)	f_2 (%)	Porosity (%)	Pore diameter (µm)
New MA-41	1.2	21.2	5.9	1.01
MA-41 after 400 h in cleaning cycle	4.5	28.7	26.1	2.44

Table 4-6. Physico-chemical properties of new MA-41 sample and that exposed to the HCl-NaOH ageing cycles for 400 h: permeability (P^*), volume fraction of inter-gel solution (f_2), porosity ratio and pore diameter.

Unfortunately, structural investigation of MA-41 is more challenging as ATR-FTIR did not provide information on the functional polymer. In addition the membrane components were not or hardly soluble (due to the cross-linking of resin and crystallinity of PE), which did not permit to decompose the membrane parts and study each one separately.

Nevertheless, it was clear that the degradation suffered after the ageing cycles was more severe than that suffered after exposure to concentrated NaOH or HCl.

Heterogeneous AEM seemed to be prone to degradation due to the CIP procedure, as well as homogeneous AEM. More broadly, there was a possible damage of the PS-DVB structure of MA-41; the ion-exchange capacity decrease may indicate that there was some degradation at the functional sites during the ageing cycles, because of the contact with NaOH.

4.3.4 Ageing of homogeneous and heterogeneous AEMs

Modifications of MA-41 and AMX-SB properties after being subjected to the ageing protocols were not of the same extent. Table 4-7 shows the decrease or increase percentage in membranes properties after the longest time of exposure (700 h in NaOH, 700 in HCl and 400 in the ageing cyclse) compared to the new samples.

In all cases, decrease in Young modulus was more severe for MA-41 than for AMX-SB probably as modification of the rigid ion-exchange resin particles of MA-41 highly affected this parameter. Decline of strain at break was more flagrant for AMX-SB subjected to ageing in NaOH and the cleaning cycles as ductility in AMX-SB was mostly given by its thermoplastic component, the PVC binder, and the latter suffered degradation in both cases. On the other hand, strain at break did not change in a great extent after ageing in HCl for

AMX-SB, as PVC was not degraded; however, it changed significantly for MA-41 as for this composite material, the ductility and softness is given by PE binder, which was probably degraded.

		NaOH	HCl	Cycle
Young modulus	AMX-SB	-15%	+17%	-25%
	MA-41	-23%	-9%	-34%
Strain at break	AMX-SB	-45%	-10%	-61%
	MA-41	-17%	-51%	-28%
Ion-exchange capacity	AMX-SB	-17%	-17%	0
	MA-41	-10%	-25%	-10%
Permeability	AMX-SB	---	---	+9 times
	MA-41	---	---	+3 times
Water uptake	AMX-SB	+14%	-10%	+27%
	MA-41	+4%	0	+5%
Conductivity	AMX-SB	+20%	0	+27%
	MA-41	+6%	0	+13

Table 4-7. Percentage of increase or decrease in the mechanical and physic-chemical properties of AEM samples after exposure to 2 M NaOH for 700 h, 2 M HCl for 700 h and the HCl-NaOH ageing cycle for 400 h, compared to the new samples.

It is noteworthy that modifications in the physic-chemical properties seemed to be smaller for MA-41 than those suffered by AMX-SB. Nevertheless it is important to note that thickness of the former membrane is at least 4 times larger than that of the latter one, which means that mechanical or structural changes occurring in MA-41 may have lower consequences on its physico-chemical properties.

4.4 Conclusions

Heterogeneous and homogeneous AEMs have been investigated in conditions simulating the CIP process used in ED, namely concentrated NaOH and HCl solutions, as well as HCl-NaOH cleaning cycles.

After exposure to 2 M NaOH, quaternary ammonium sites of both AMX-SB and MA-41 were degraded to some extent, probably following an E1 or E2 elimination reaction. Strong alkaline conditions resulted in dehydrochlorination of the PVC binder of homogeneous AMX-SB. The latter was enhanced or propagated by the presence of quaternary ammonium salts, by the loss of a stabilizer, by the loss of a plasticizer or by a combination of these events. In contrast, PE binder of heterogeneous MA-41 was resistant to the contact with the 2 M NaOH solution.

Exposure to concentrated HCl did not result in severe changes of the physico-chemical properties of both membranes or in damage of the PVC binder structure of AMX-SB. On the other hand, PE binder of MA-41 was less resistant to the acidic environment as shown by the decline of the membrane mechanical properties.

Heterogeneous and homogeneous AEMs are prone to degradation due to the CIP process, as shown by changes suffered after exposure to the HCl-NaOH cleaning cycles.

For AMX-SB, the PVC binder underwent a certain degree of dehydrochlorination resulting from the contact with NaOH during the cleaning cycles. In addition, there was a loss of entanglement of PVC from the semi-IPN due to multiple changes in nature, pH and temperature of the solution. The latter resulted in pores or voids in the inner matrix of the AEM. The elimination of PVC from the semi-IPN resulted in a deterioration of the membrane toughness and a further formation of fractures.

The cleaning cycles caused an increase in the ratio of MA-41 macropores, and severe changes in the mechanical properties.

The damage caused by the cleaning cycles which closely simulated conditions during the CIP process played an important role on membrane degradation and seemed to be even more severe than the damage caused by sole NaOH.

It is noteworthy that physico-chemical, structural and mechanical modifications of AMX-SB resulting from the exposure to the ageing cycles are similar to those previously identified on membranes used in real-time ED for whey demineralization [30].

For AMX-SB used in ED, degradation of PVC resulted in the formation of non-charged pores (voids) within the membrane matrix, available for electroneutral electrolyte solution and for large molecules such as lactose and proteins. There was also a deterioration of the membrane toughness caused by the elimination of PVC from the semi-IPN, which led to the formation of cracks and tears. This was the reason of membrane final failure in the ED stack.

Accordingly, the degradation of this kind of membrane used in conventional ED for food applications is likely to be a consequence of the traditional CIP performed in acid-base sequences.

4.5 Acknowledgements

This investigation was realized within the French-Russian laboratory on "Ion-exchange membranes and related processes". The authors are grateful to CNRS, France, and to RFBR, Russia (grants 11-08-93107_CNRSL, 12-08-00188_CNRSL, 13- 8-96508r_yug), as well as to FP7 Marie Curie Actions "CoTraPhen" project PIRSES-GA-2010-269135 for financial support.

References

[1] H. Strathmann, Electrodialysis, a mature technology with a multitude of new applications, Desalination, 264 (2010) 268-288.

[2] F. Lutin, L'electrodialyse et ses nombreuses applications, L'Actualité Chimique, 327 (2009) 59-72.

[3] M. Fidaleo, M. Moresi, Electrodialysis Applications in The Food Industry, Adv. Food Nutr. Res, 51 (2006) 265-360.

[4] A. Bukhovets, T. Eliseeva, Y. Oren, Fouling of anion-exchange membranes in electrodialysis of aromatic amino acid solution, J. Membr. Sci., 364 (2010) 339-343.

[5] N. Tanaka, M. Nagase, M. Higa, Organic fouling behavior of commercially available hydrocarbon-based anion-exchange membranes by various organic-fouling substances, Desalination, 296 (2012) 81-86.

[6] E. Ayala-Bribiesca, G. Pourcelly, L. Bazinet, Nature identification and morphology characterization of cation-exchange membrane fouling during conventional electrodialysis, J. Colloid Interface Sci., 300 (2006) 663-672.

[7] H. Strathmann, in: Ion-exchange Membrane Separation Processes, Elsevier, 2004, pp. 287-328.

[8] G. Trägårdh, Membrane cleaning, Desalination, 71 (1989) 325-335.

[9] A. Al-Amoudi, R.W. Lovitt, Fouling strategies and the cleaning system of NF membranes and factors affecting cleaning efficiency, J. Membr. Sci., 303 (2007) 4-28.

[10] H. Lee, G. Amy, J. Cho, Y. Yoon, S.-H. Moon, I.S. Kim, Cleaning strategies for flux recovery of an ultrafiltration membrane fouled by natural organic matter, Water Research, 35 (2001) 3301-3308.

[11] U.-S. Hwang, J.-H. Choi, Changes in the electrochemical characteristics of a bipolar membrane immersed in high concentration of alkaline solutions, Sep. Purif. Technol., 48 (2006) 16-23.

[12] K. Richau, Bipolar membrane characterization. , in: A.J.B. Kemperman (Ed.) Handbook Bipolar Membrane Technology Twente University Press, Enschede, 2000.

[13] N.D. Pismenskaya, V.V. Nikonenko, N.A. Melnik, K.A. Shevtsova, E.I. Belova, G. Pourcelly, D. Cot, L. Dammak, C. Larchet, Evolution with time of hydrophobicity and microrelief of a cation-exchange membrane surface and its impact on overlimiting mass transfer, J. Phys. Chem. B, 116 (2012) 2145-2161.

[14] D.J. Hutchison, The Chlor-Alkali Business, in: Modern Chlor-Alkali Technology, Blackwell Science Ltd, 2007, pp. 1-18.

[15] R. Audinos, A. Nassr-Allah, J.R. Alvarez, J.L. Andres, R. Alvarez, Electrodialysis in the separation of dilute aqueous solutions of sulfuric and nitric acids, J. Membr. Sci., 76 (1993) 147-156.

[16] P.V. Vyas, B.G. Shah, G.S. Trivedi, P.M. Gaur, P. Ray, S.K. Adhikary, Separation of inorganic and organic acids from glyoxal by electrodialysis, Desalination, 140 (2001) 47-54.

[17] S. Koter, Separation of weak and strong acids by electro-electrodialysis—Experiment and theory, Sep. Purif. Technol., 60 (2008) 251-258.

[18] T.V. Eliseeva, E.V. Krisilova, V.P. Vasilevsky, E.G. Novitsky, Electrodialysis of solutions of tartaric acid and its salts, Pet. Chem., 52 (2012) 609-613.

[19] T. Sata, M. Tsujimoto, T. Yamaguchi, K. Matsusaki, Change of anion exchange membranes in an aqueous sodium hydroxide solution at high temperature, J. Membr. Sci., 112 (1996) 161-170.

[20] J.A. Vega, C. Chartier, W.E. Mustain, Effect of hydroxide and carbonate alkaline media on anion exchange membranes, J. Power Sources, 195 (2010) 7176-7180.

[21] G. Merle, M. Wessling, K. Nijmeijer, Anion exchange membranes for alkaline fuel cells: A review, J. Membr. Sci., 377 (2011) 1-35.

[22] G. Couture, A. Alaaeddine, F. Boschet, B. Ameduri, Polymeric materials as anion-exchange membranes for alkaline fuel cells, Progress in Polymer Science, 36 (2011) 1521-1557.

[23] A.C. Cope, A.S. Mehta, Mechanism of the Hofmann Elimination Reaction: An Ylide Intermediate in the Pyrolysis of a Highly Branched Quaternary Hydroxide, J. Am. Chem. Soc., 85 (1963) 1949-1952.

[24] A.C. Cope, E.R. Trumbull, Olefins from Amines: The Hofmann Elimination Reaction and Amine Oxide Pyrolysis, in: Organic Reactions, John Wiley & Sons, Inc., 2004.

[25] S. Chempath, B.R. Einsla, L.R. Pratt, C.S. Macomber, J.M. Boncella, J.A. Rau, B.S. Pivovar, Mechanism of Tetraalkylammonium Headgroup Degradation in Alkaline Fuel Cell Membranes, J. Phys. Chem. C, 112 (2008) 3179-3182.

[26] R. Ghalloussi, W. Garcia-Vasquez, N. Bellakhal, C. Larchet, L. Dammak, P. Huguet, D. Grande, Ageing of ion-exchange membranes used in electrodialysis: Investigation of static parameters, electrolyte permeability and tensile strength, Sep. Purif. Technol., 80 (2011) 270-275.

[27] R. Ghalloussi, W. Garcia-Vasquez, L. Chaabane, L. Dammak, C. Larchet, N. Bellakhal, Decline of ion-exchange membranes after utilization in electrodialysis for food applications, Phys. Chem. News, 65 (2012) 66-72.

[28] R. Ghalloussi, W. Garcia-Vasquez, L. Chaabane, L. Dammak, C. Larchet, S.V. Deabate, E. Nevakshenova, V. Nikonenko, D. Grande, Ageing of ion-exchange membranes in electrodialysis: A structural and physicochemical investigation, J. Membr. Sci., 436 (2013) 68-78.

[29] L. Dammak, C. Larchet, D. Grande, Ageing of ion-exchange membranes in oxidant solutions, Sep. Purif. Technol., 69 (2009) 43-47.

[30] W. Garcia-Vasquez, L. Dammak, C. Larchet, V. Nikonenko, N. Pismenskaya, D. Grande, Evolution of anion-exchange membrane properties in a full scale electrodialysis stack, J. Membr. Sci., (2013).

[31] Y. Mizutani, Structure of Ion Exchange Membranes, J. Membr. Sci., 49 (1990) 121-144.

[32] Y. Mizutani, Studies of Ion Exchange Membranes. XXX. The tetrahydrofuran Extraction of the Ion-exchange Membrane and its Base Membrane Prepared by the "Paste Method", Bull. Chem. Soc. Jpn., 42 (1969) 2459-2463

[33] G.Z. Nefedova, Z.G. Klimova, G.S. Sapozhnikova, Granules and Powders, in: Pashkov (Ed.) Ion-Exchange Membranes, NIITEKhim, Moscow, 1977.

[34] AFNOR, French standar NF X 45-200, in, 1995.

[35] R. Lteif, L. Dammak, C. Larchet, B. Auclair, Conductivité électrique membranaire: étude de l'effet de la concentration, de la nature de l'électrolyte et de la structure membranaire, Eur. Polym. J., 35 (1999) 1187-1195.

[36] V.I. Zabolotsky, V.V. Nikonenko, Effect of structural membrane inhomogeneity on transport properties, J. Membr. Sci., 79 (1993) 181-198.

[37] L. Dammak, C. Larchet, B. Auclair, V.V. Nikonenko, V.I. Zabolotsky, From the multi-ionic to the bi-ionic potential, Eur. Polym. J., 32 (1996) 1199-1205.

[38] Y. Fu, D. Xie, R. Wang, W. C., Z. X., W. Q., Dehydrochlorination of Poly vinyl chloride Catalyzed by Quarternary Ammonium Salts in Solid Phase, Chem. Res. Chin. Univ., 8 (1992) 53-58.

Chapitre 5

Structure et propriétés des membranes échangeuses d'ions hétérogènes et homogènes soumises au vieillissement dans l'hypochlorite de sodium

Présentation de l'article

Dans ce chapitre, nous présentons la suite des protocoles de vieillissement *ex-situ*. Nous nous sommes intéressés à l'effet des produits oxydants sur le vieillissement des membranes échangeuses d'ions.

Dans d'autres procédés membranaires, tels que l'ultrafiltration et l'osmose inverse, le NaClO (eau de Javel) est l'oxydant le plus utilisé grâce à son efficacité pour le nettoyage et désinfection des membranes exposées à la matière organique. Tel est le cas des solutions traitées dans l'industrie agroalimentaire où les flux d'alimentation sont très riches en protéines, polysaccarides ou autres. Un nettoyage chimique efficace est nécessaire car ces grosses molécules peuvent encrasser les membranes et les microorganismes qui s'y développent peuvent altérer l'innocuité de la solution.

Nous avons un double intérêt en réalisant cette étude. Tout d'abord, nous voulons identifier les conséquences de l'utilisation du NaClO sur la stabilité des membranes échangeuses d'ions. Ceci pour savoir si ce produit chimique est convenable ou pas pour le nettoyage des membranes échangeuses d'ions en électrodialyse (à la place des cycles acide-base étudiés lors du chapitre précédent). Ensuite, à partir de cette étude nous allons distinguer les principales caractéristiques des membranes ayant été mises en contact avec du NaClO ce qui sera un outil pour la recherche des causes de dégradation des membranes échangeuses d'ions dans les futures études *in-situ*.

De nouveau, nous avons réalisé le vieillissement *ex-situ* sur des membranes homogènes et hétérogènes, aussi bien échangeuses d'anions ainsi qu'échangeuses de cations.

Les résultats ont montré que les mécanismes de vieillissement dans du NaClO sont différents entre les membranes échangeuses d'anions et les membranes échangeuses de cations. Cependant, les mécanismes de vieillissement sont les mêmes entre les membranes homogènes et hétérogènes.

Suite à l'utilisation du NaClO les groupements ammonium quaternaire des membranes échangeuses d'anions sont dégradés. Des chaînes du poly(styrène-*co*-divinylebenzene) sont rompues pour les deux types de membranes anioniques et cationiques.

L'utilisation du NaClO en fortes concentrations s'est révélée non convenable pour le nettoyage chimique des membranes échangeuses d'ions en électrodialyse.

Structure and properties of heterogeneous and homogeneous ion-exchange membranes subjected to ageing in sodium hypochlorite

Journal of Membrane Science (452) **2014** 104-116

W. GARCIA-VASQUEZ[1], R. GHALLOUSSI[1], L. DAMMAK[1], C. LARCHET[1], V. NIKONENKO[2], D. GRANDE[1]

[1] Institut de Chimie et des Matériaux Paris-Est, ICMPE, UMR 7182 CNRS – Université Paris-Est, 2 Rue Henri Dunant, 94320 Thiais, France.

[2] Kuban State University, 149 Stavropolskaya st., 350040 Krasnodar, Russia.

Abstract

The effects of sodium hypochlorite (NaClO) on ion-exchange membranes were carefully investigated and discussed with the aim to assess one of their possible causes of ageing. A thorough comparison was carried out for the degradation of ion-exchange membranes with different structures, *i.e.* homogeneous and heterogeneous ones, as well as with different functional groups, *i.e* anionic (bearing $-CH_2N^+R_3$ groups) and cationic (bearing $-SO_3^-$ groups) ones. An artificial ageing protocol was implemented, which consisted in immersing four types of membranes, homogeneous AMX-SB and CMX-SB as well as heterogeneous, MA-41 and MK-40 in aqueous NaClO solutions at constant pH and concentration for different times over a 700 h period. The physico-chemical, structural, and mechanical properties of each sample were investigated, before and after ageing, by means of complementary analytical techniques, namely conductivity, ion-exchange capacity, water uptake, and thickness measurements, as well as SEM, ATR-FTIR, TGA, and tensile strength tests.

The results demonstrated that ageing mechanisms were different for anion-exchange membranes and cation-exchange membranes; however, ageing was similar among homogeneous and heterogeneous membranes of the same type (anionic or cationic). Sodium hypochlorite provoked a degradation of the quaternary ammonium sites of anion-exchange membranes and chain scission of the poly(styrene-*co*-divinylbenzene) backbone from anion and cation-exchange membranes through chain radical oxidation. No significant degradation was found for the polymer binder of membranes investigated in this paper.

5.1. Introduction

Conventional electrodialysis (ED) with ion-exchange membranes (IEMs) is applied for demineralization, purification, and concentration of electrolyte solutions. During the past years, several ED applications have been developed, mainly in the food and drug industry, in the chemical process industry as well as in waste water treatment and production of high quality water [1-4]. In the food industry, ED is used in dairy products, fruit juice, sugar, wine, among others [2, 5]. Such solutions are highly nutritious media in which microorganisms may cause spoilage or colloidal matter, inorganic compounds or macromolecules form fouling at the interface or into the membrane [6-9]. In this regard, the effective cleaning-in-place (CIP) of membranes is crucial to prevent fouling and growth of microorganisms that could contaminate the product to be analyzed [10]. CIP is necessary to optimize the membrane performance and minimize the process costs.

CIP protocols are traditionally performed using acids and bases; sometimes however, the employment of stronger cleaning agents, like oxidants, might be necessary to achieve a complete cleaning in ED for food industry applications. Oxidation degrades the functional groups of proteins, which makes them more sensitive to hydrolysis at high pH [11, 12]. Sodium hypochlorite (NaClO) is the most common oxidant used in reverse osmosis, ultrafiltration, and microfiltration membrane processes at alkaline pH and 200 ppm [12-14]. Nevertheless, contact with NaClO is suspected to play an important role in membrane ageing [15-26].

The chemistry of aqueous NaClO solutions is complex and pH dependent. Free available chlorine is the sum of aqueous $Cl_{2(aq)}$, HClO, and ClO^- concentrations and is a measure of the amount of chlorine species that can oxidize organic or inorganic compounds. NaClO dissociates in water according to the following equilibrium equations:

$$\text{Free available chlorine} = [HClO] + [ClO^-] + [Cl_2] \quad (5.1)$$

$$Cl_2 + 2H_2O \longrightarrow HClO + Cl^- + H_3O^+ \qquad pKa < 2 \text{ at } 25\ °C \quad (5.2)$$

$$HClO + H_2O \longrightarrow ClO^- + H_3O^+ \qquad pKa = 7.5 \text{ at } 25\ °C \quad (5.3)$$

The ageing due to NaClO has been previously addressed for membranes based on polysulfone (PSf) and PSf modified with poly(vinylpyrrolidone) (PVP). According to Gaudichet-Maurin [18], exposure to NaClO produces chain breaking of the PSf macromolecules. The mechanism of degradation relies on radical oxidation when hydroxyl radicals $^{\bullet}OH$ are present in the solution [26], which occurs when hypochlorous acid (HClO) and hypochlorite ions (ClO^-) are the predominant species [19]:

$$HClO + 3ClO^- \longrightarrow 3Cl^- + {}^{\bullet}ClO + O_2 + {}^{\bullet}OH \quad (5.4)$$

Causserrand et al. [19] have then found that degradation of PSf membranes is greater when pH ranged from 8 to 10 than for higher or lower pH values. Arkhangelsky et al. [20] have proposed that polyethersulfone (PES) membranes suffer partial scission of the sulfonyl C-S bond with the formation of phenyl sulfonate, at pH 7.2 and in the presence of sufficient hypochlorite, which leads to enlarged pore sizes and increase in the membrane charge. Yadav et al. [23] have found that PES membranes suffer damage at both pH 9 and 12, however the damage is greater at pH 9.

In a recent study, Prulho et al. [24] have stated that the soaking of PES/PVP blends in hypochlorite solution at pH 8 provokes the oxidation of the aromatic rings into phenol groups. The oxidation of PES in the blend involves the primary oxidation of PVP, and it is accompanied by chain scission and cross-linking reaction.

From these experimental investigations, NaClO seems to be more harmful at pH 7 or 8. This represents a problem in practical applications as potable water or food solutions generally lie within the same pH range.

In this regard, IEM suppliers advise not to use strong oxidizing agents as they could affect the membrane stability. Even though NaClO is not traditionally applied to the IEM CIP, great needs for sanitization in the ED treatment of food solutions might lead to the use of NaClO since it is one of the most efficient chemicals in terms of membrane cleaning and disinfection [16]. Therefore, the consequences of NaClO employment on IEM degradation are worth being investigated.

This work lies within the scope of a research project aiming to explore the effects, causes, and mechanisms of IEM ageing in ED for food industry applications [27-31]. In our more recent papers, ageing of cation-exchange membranes (CEMs) [30] and anion-exchange membranes

(AEMs) [30, 31] was investigated in two different applications of industrial ED. Membranes suffered a significant decrease in the ion-exchange capacity and an important damage in the functional polymer chains, when performing ED for the treatment of organic acids [30], in which diluted oxidizing solutions might be used to clean and sanitize the ED stack. On the other hand, no significant loss of the ion-exchange capacity or degradation of the functional polymer chains was detected on membranes used for whey demineralization [31]; ageing comes from a progressive loss of the polymer binder, thus leading to the formation of non-charged pores that change the permselectivity and the mechanical properties of the membranes. In this case, CIP is performed with acidic and alkaline solutions. The aim of the current study is to assess the possible causes of IEM ageing in the presence of NaClO.

Depending on their structure, IEMs may be classified into homogeneous membranes and heterogeneous ones. Homogeneous membranes are prepared by introducing an ion-exchange moiety directly into the structure of the constitutive polymer. This leads to a relatively even distribution of the charged groups over the entire membrane matrix. Heterogeneous membranes are prepared by mixing a fine ion-exchange resin powder with a polymer binder. This results in a structure where the ion-exchange groups are clustered and very unevenly distributed in the membrane matrix. Most heterogeneous membranes have relatively low production costs but they have a higher electrical resistance, due to the longer pathway of the mobile ion in the heterogeneous structure [1]. To the best of our knowledge, thorough studies on the differences or similarities in the stability and durability of both kinds of membranes remain scarce.

This paper constitutes a fundamental investigation of the effects of hypochlorite on heterogeneous and homogeneous IEM properties. As the membrane lifetime is accounted for several thousands of hours, real-time experimentation is impossible, and ageing protocols must be developed to shorten experimental time. Herein, the artificial ageing protocol consists in immersing each membrane in NaClO at constant pH and concentration for different times. Physico-chemical, structural and mechanical properties of each sample are then investigated by means of complementary analytical techniques. This experimental investigation reveals significant issues concerning IEM structure and long-term behavior. The approach is based upon the interpretation of the membrane characterization through a systematic analysis of new samples and aged ones.

5.2. Experimental

5.2.1. Membranes

For the ageing experiments, well-known and frequently used IEMs were investigated. Neosepta® CMX-SB and AMX-SB from Tokuyama Soda (Japan) are homogeneous CEMs and AEMs, respectively. They are made of functionalized polystyrene (PS) crosslinked with divinylbenzene (DVB) and mixed with finely powdered poly(vinyl chloride) (PVC), which are coated on a PVC cloth used as a reinforcing material [32].

Cationic MK-40 and anionic MA-41 from the Shchekinoazot (Russia) were used as heterogeneous IEMs. They consist in fine polymer particles of ion-exchange resin anchored to a polyethylene matrix and reinforced by caprone fitted fabrics [33]. The ion-exchange resin also consists in functionalized PS crosslinked with DVB. Both types of CEMs possess sulfonate fixed sites, and both types of AEMs possess quaternary ammonium fixed sites.

As a starting point, heterogeneous MA-40 and MA-41 were specifically treated according to the manufacturer. Each sample was wiped with tetrachloromethane and then, immersed during 6 h in ethanol to eliminate the impurities. Afterwards, samples were successively immersed in several NaCl solutions, *i.e.* 2 M, 1 M, 0.5 M, and 0.1 M, for 24 h in each case.

Then, all samples were conditioned following the French standard NF 45-200 [34] in order to stabilize their physico-chemical properties, to remove any impurities that may come from their manufacturing process and to achieve a reproducible initial condition for all membranes before characterization.

This procedure consisted in immersing the samples in solutions of different natures. AEMs were first treated 1 h with 0.1 M HNO_3, rinsed with water, and carefully dried with filter paper. Then, they were immersed for 1 h in 0.1 M HCl, and rinsed by immersing in 0.1 M NaCl. The procedure was repeated twice, and finally the membrane was stored in 0.1 M NaCl.

CEMs were immersed in 0.1 M HCl, rinsed with water, and dried with filter paper. Then, they were immersed in 0.1 M NaOH, and rinsed by immersing them in 0.1 M NaCl. The procedure was repeated twice as well, and the membrane was kept in 0.1 M NaCl, before the ageing treatment.

5.2.2. Ageing protocol

Membrane samples of 40 cm^2 were soaked in 400 mL of the ageing solution during 20, 60, 100, 200, 300, and 700 h.

Ageing solutions were prepared with sodium hypochlorite (VWR) with 16% of active chlorine at filling. The precise concentration of hypochlorite (ClO^-) was determined by performing an iodometric titration. The commercial bleach solution was diluted with ultrapure water to 0.1% of total free chlorine, and the pH (initially around 11) was adjusted to 8 using 37% wt. HCl (Fischer Scientific).

The ClO^- concentration was monitored during the accelerated ageing through an iodometric titration to ensure a constant chlorine concentration in the ageing solutions. Furthermore, ageing solutions were replenished every two days to avoid concentration changes due to the natural ClO^- decomposition to Cl^- and O_2 [35]. The solutions were kept away from natural light.

After removing samples from the ageing solution, they were rapidly rinsed with ultrapure water and immersed in 1 M NaCl, 0.5 M NaCl, and 0.1 M NaCl, for 24 h in each solution, in order to wash membranes and turn them into the Cl^- and Na^+ forms, and to remove any remaining of H^+ or ClO^- within the membranes or in the functional sites. In this manner, the presence of remaining NaClO was avoided and no further ageing took place after the respective exposure time for each sample. The samples were kept in 0.1 M NaCl, prior to characterization.

5.2.3. Analytical techniques

5.2.3.1. Alternating current conductivity

The experimental assembly used was constituted of a clip-type cell to measure the membrane conductivity, a conductimeter CDM92 (RADIOMETER-TACUSSEL), and a water bath at 25 ± 1 °C [36].

The determination of membrane conductance G_m needed two measurements, one without the membrane (G_1) and another one with the membrane (G_2), to deduce the following equation:

$$G_m = \frac{G_1 G_2}{G_1 - G_2} \tag{5.5}$$

Using the membrane thickness value (L_m) and the electrodes section area (A = 1 cm²), the membrane conductivity was calculated as follows:

$$\kappa_m = G_m \times \frac{T_m}{A} \tag{5.6}$$

Measurements were conducted in 0.1 M NaCl to compare the changes in membrane conductivity since NaCl solutions are commonly used as reference media of membrane conductivity and resistance.

5.2.3.2. Ion-exchange capacity

This parameter, which is the number of functional sites per gram of dry membrane, was determined following the French standard NF X 45-200. The counter-ions were forced to transfer to a determined solution with the purpose to titrate them. AEM samples were immersed into 0.1 M HCl (the counter-ion was Cl^-) for 2 h, then rinsed in ultrapure water, and immersed in 1 M HNO_3 for at least 12 h. The chloride content was determined immediately after this time. To finish, samples were vacuum dried at 40 °C for 24 h to determine the dry mass.

CEM samples were immersed into 1 M HCl (the counter-ion was H^+) for 2 h, then immersed (three times) into deionised water for 30 min, and finally 2 h in a mixture of NaOH and NaCl for 2 h. The NaOH remaining was titrated. Finally, samples were vacuum dried at 40 °C for 24 h to determine the dry mass. It must be taken into account that uncertainty in the ion-exchange capacity measurements was estimated to be equal to 5%.

5.2.3.3. Water uptake

Samples were separated from the stabilization solution and the excess of external liquid was removed by placing them between two foils of filter paper and pressing slightly. The membranes were immediately placed in a HB43-S Mettler-Toledo moisture thermobalance in which they were heated to 140°C until their mass did not change in 0.001 g for ten minutes.

The water uptake (W) was calculated by the mass differences between hydrated (W_a) and dried (W_b) samples as follows:

$$W = \frac{W_a - W_b}{W_a} \times 100 \tag{5.7}$$

According to Belaid et al. [37] the inaccuracy of water uptake measurements is of 8% in diluted solutions and less than 2% in concentrated solutions (>1 M).

5.2.3.4. Thickness

The membrane thickness (L_m) was measured using a Käfer Thickness Dial Gauge specially devised for plastic film thickness measurements with a resolution of 1 μm. The membrane thickness value was averaged from measurements at 10 different locations on the effective surface region of the membrane.

5.2.3.5. Structural investigation by SEM, ATR-FTIR, and TGA

Samples used for the structural investigation were vacuum dried overnight at 40 °C, before analysis. Scanning electron microscopy (SEM) images were obtained from Pt/Pd coated samples with an accelerating tension of 3 kV using a LEO 1530 microscope.

Attenuated total reflection-Fourier transform infrared (ATR-FTIR) spectra were carried out on a Nicolet ‘‘Nexus’’ spectrometer equipped with a Globar source and a DTGS detector between 550 and 4000 cm^{-1}. The spectral resolution was 2 cm^{-1} and 32 scans were realized for each spectrum. ATR-FTIR was performed at least three times for each sample.

For thermogravimetric analysis (TGA), a 10 mg sample was placed into a Pt pan and loaded into a Setsys thermobalance from Setaram. It was heated from 20 to 600 °C at 10 °C.min^{-1} under argon atmosphere.

5.2.3.6. Tensile strength measurements

Stress-strain curves were obtained with an Instron 5965 testing machine. A dumbbell of 12 ×3 mm^2 of active area was fixed into two grips and stretched at a 1 mm.min^{-1} rate. The samples were in the humid state and in the Cl^- form. Each test was carried out twice.

5.3. Results and discussion

To assess the ageing effect of NaClO, the analysis of aged membranes was conducted and compared to that of new samples. Firstly, the membranes transport (conductivity) and equilibrium (ion-exchange capacity, thickness and water uptake) properties were investigated. Secondly, the changes in morphology and structure were evaluated by SEM, FTIR, and TGA. Finally, the mechanical properties were studied by means of tensile strength tests.

Fig. 5-1 shows the normalized conductivity of AMX-SB, MA-41, CMX-SB and MK-40 as a function of ageing time. Normalized conductivity was defined as conductivity of samples (κ_m) divided by conductivity of the virgin sample (κ_o) under comparable conditions. Tendencies in the evolution of normalized conductivity in function of exposure time to NaClO were different for AEMs and CEMs. The physicochemical, structural and mechanical properties of AEMs samples are presented in section 5.3.1 and those of CEMs in section 5.3.2.

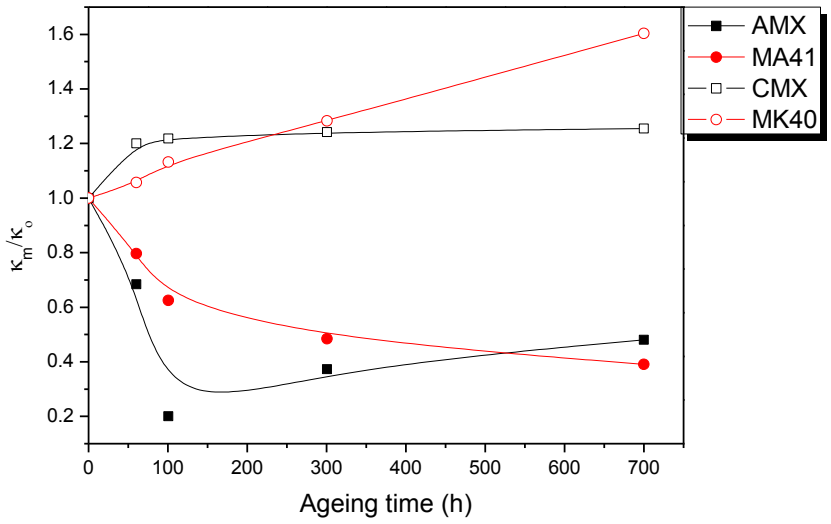

Fig. 5-1. Evolution of normalized electrical conductivity (κ_m/κ_o) of AMX-SB, MA-41, CMX-SB and MK-40 as a function of time in the ageing solution.

5.3.1. Anion-exchange membranes

Changes of membrane conductivity entail reductions of the ED process performance, as the major part of the resistance in an ED stack is owed to the IEMs.

Both membranes suffered severe changes, as shown by Fig. 5-1. There was a gradual drop of MA-41 electrical conductivity. After 700 h of chlorine exposition, a decrease by about 60 % was observed. Meanwhile, AMX-SB electrical conductivity dropped more than 80 % after 100 h of exposition; however, a rebound from 100 to 700 h was observed.

A reduction of electrical conductivity might be associated to damage in other physico-chemical properties of the membranes. The equilibrium properties, *i.e.* ion-exchange capacity, thickness, and water uptake, are shown in Fig. 5-2.

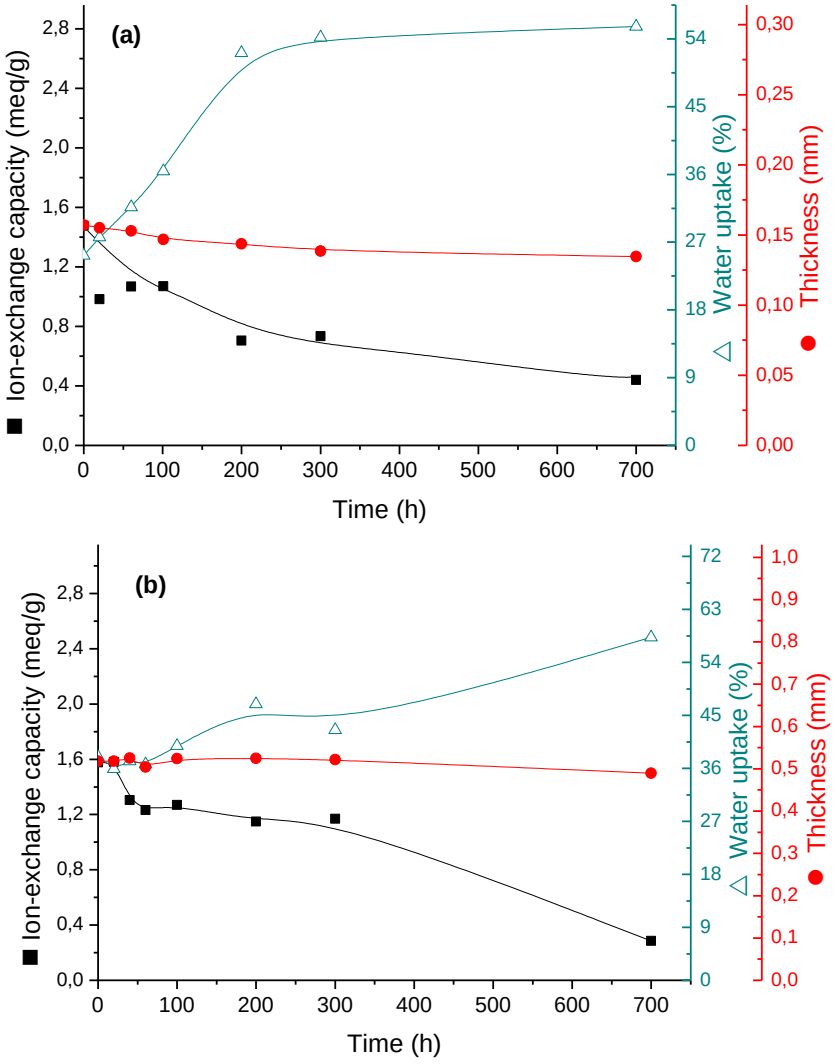

Fig. 5-2. Evolution of AEM equilibrium properties as a function of time in the ageing solution. AMX-SB (a) and MA-41 (b).

Fig. 5-2a shows that AMX-SB progressively lost up to 70 % of its ion-exchange capacity after 700 h of ageing. Meanwhile, MA-41 (Fig. 5-2b) seemed to be affected to a minor extent compared to AMX-SB. After 300 h of exposition, MA-41 ion-exchange capacity decreased by 25 %. A dramatic drop of conductivity occurred between 300 and 700 h.

The decrease in electrical conductivity apparently arose from the reduction of the concentration of active functional sites resulting from their degradation, as observed before by Komkova et al. [38] in AEMs exposed to concentrated alkaline conditions. However, it was observed a conductivity rebound for AMX-SB after 100 h along with a sharp increase in the water uptake. The membrane did not swell additionally, as shown by the slight reduction of membrane thickness. A possible degradation of the polymer structure could result in the formation of holes or cavities that became larger or more numerous after 100 h of exposure. These holes and cavities were filled with the electrically neutral solution identical to the external one. As the specific conductivity of this solution, κ_s (the measurements were conducted in 0.1 M NaCl, accordingly κ_s = 10.6 mS cm^{-1}) was higher than that of the membrane gel phase, κ_g, an increase in the membrane porosity led to increasing κ_m. The approximate relation between κ_m, κ_s and κ_g is given by the microheterogeneous model reported by Zabolotsky and Nikonenko [39]:

$$\kappa_m = \kappa_g^{f_1} \kappa_s^{f_2} \tag{5.8}$$

where f_1 and f_2 ($f_1 + f_2 = 1$) are the volume fractions of the gel and the inter-gel solution phases, respectively.

For our samples, the κ_g values were equal to 3.3 mS.cm^{-1} and 4.8 mS.cm^{-1}, while the f_2 values were equal to 0.11 and 0.22, for new AMX-SB and MA-41, respectively. The shape of the κ_m vs. time curve (Fig. 5-1) finally depended on two factors: the decrease in κ_g was dominant for short times, and the increase in f_2 seemed progressively to increase with time.

The dynamics of degradation was not the same for both membranes: the initial loss in ion-exchange capacity (hence, in κ_g) was higher for AMX-SB that led to a higher loss in κ_m. However, at t > 300 h, the rate in the ion-exchange capacity loss became higher for MA-41, hence κ_g decreased more rapidly, thus resulting in a progressive decrease in κ_m. Nevertheless, as Fig. 5-2 shows, the water uptake increase of MA-41 was not as high as that of AMX-SB. Hence, the MA-41 porosity and the f_2 value did not increase as strongly as these parameters

did for AMX-SB. As a result, the factor of increase in f_2 was less important in the case of MA-41; therefore, we did not observe the increase in κ_m of this membrane, even at the end of the ageing period.

The appearance of holes and cavities may be confirmed through SEM micrographs of AMX-SB samples (Fig. 5-3). In the first row, it is possible to see that new AMX-SB had a flat and fairly homogeneous surface, even at the nanoscopic length scale.

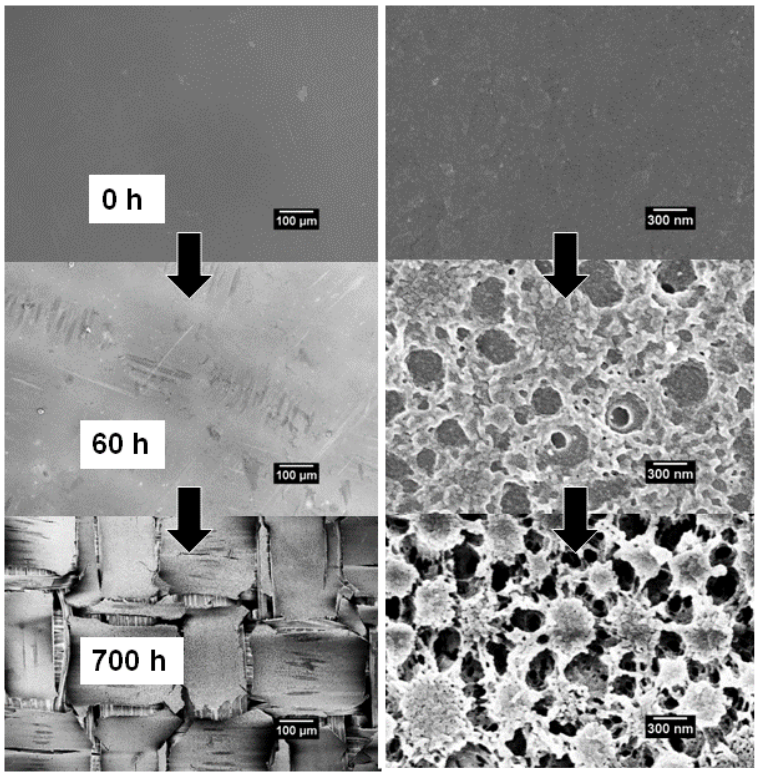

Fig. 5-3. SEM images of AMX-SB surface after 0, 60, and 700 h in the ageing solution.

After 60 h, there were no great changes in the low magnification image; however when zooming, it was possible to observe some microheterogeneity formed on the membrane surface. In the last row, images of the membrane after 700 h of exposition are shown. From the first column, the destruction was already evident; it was even possible to recognize the PVC cloth. Nevertheless, there was still some remaining polymer above the cloth, as observed in the high magnification image in the last column. A network formed of particles of 50 to 200 nm of diameter was displayed.

Typically, AMX-type membranes are known as homogeneous IEMs; however, they are apparently constituted of an interpenetrating polymer network structure, and one of the components of the network was degraded and lost.

The method to prepare these membranes was called by the suppliers the "Paste Method" [40]. It consisted in mixing a fine powder of PVC and a monomer mixture of styrene and DVB to prepare the paste. This paste was coated on a reinforcing PVC material rolled up in a film, and then heated at high pressure to 100-120 °C for 30 min, then to 60-70 °C for 16 h [41]. At this temperature, the PVC powder melted and allowed styrene and DVB to copolymerize in the presence of PVC [42], thus forming a semi-interpenetrating polymer network. In spite of being known as homogeneous, they possessed a microheterogeneous structure.

The changes suffered in the membrane structure will be explained using the sample with the highest degree of degradation, *i.e.* that exposed during 700 h to NaClO, since the polymer degradation changes is easier to distinguish. Fig. 5-4 shows the comparison of characteristic FTIR spectra of AMX-SB split into two parts: the high (a) and the low (b) frequency regions for new and aged samples. Water was still present in the new sample, linked to the functional sites, as evidenced by a broad ν(O-H) band around 3380 cm^{-1}. In the new sample, Fig. 5-4b shows that the aromatic ring breathing modes of PS-DVB appeared at 1630, 1490 and 1475 cm^{-1}. The out-of-plan δ(C-H) band of the aromatic rings was intense at 704 cm^{-1}. The absorption band at 3023 cm^{-1} corresponded to the aromatic ν(C-H) stretching, and that at 2853 cm^{-1} to the aliphatic ν(C-H) from PS.

Bands around 1200-1250 cm^{-1} corresponding to ν(N-C) stretching vibrations from the quaternary ammonium functional sites were identified in a previous work [31]. However, in this case, the spectra presented many of the vibrational bands overlapping, especially the strong band with a maximum at 1255 cm^{-1}, due to δ(CH_2) wagging when the adjacent C atom had a chlorine atom attached. This band may be ascribed to PVC [43], as well as ν(C-Cl) stretching band at 635 cm^{-1}, the methylene deformation at 1425 cm^{-1}, the methylene asymmetric stretching band at 2920 cm^{-1}, and ν(C-H) stretching bands at 2965 cm^{-1} [43].

FTIR spectra of the aged sample displayed severe modifications of the bands corresponding to PS-DVB (facedown arrows). The absorbance intensity of aromatic breathing modes and δ(C-H) band of the aromatic ring at 704 cm^{-1} dramatically decreased. The latter gave place to the unveiling of the band at 690 cm^{-1}, probably associated with the ν(C-Cl) stretching band from PVC. In the high frequency region, we observed a dramatic reduction of the absorbance

intensity of ν(O-H) around 3400 cm^{-1} accounting for the disappearance of bound water (presumably of functional sites as well), and the complete disappearance of the aromatic ν(C-H) band at 3023 cm^{-1}. The formation of a carbonyl band at 1779 cm^{-1} was observed. The modifications on the spectra were similar to changes suffered in PS subjected to photo-oxidation, which involves a classical chain radical oxidation process that is propagated by alkoxy and •OH radicals and results from the decomposition of hydroperoxydes [44].

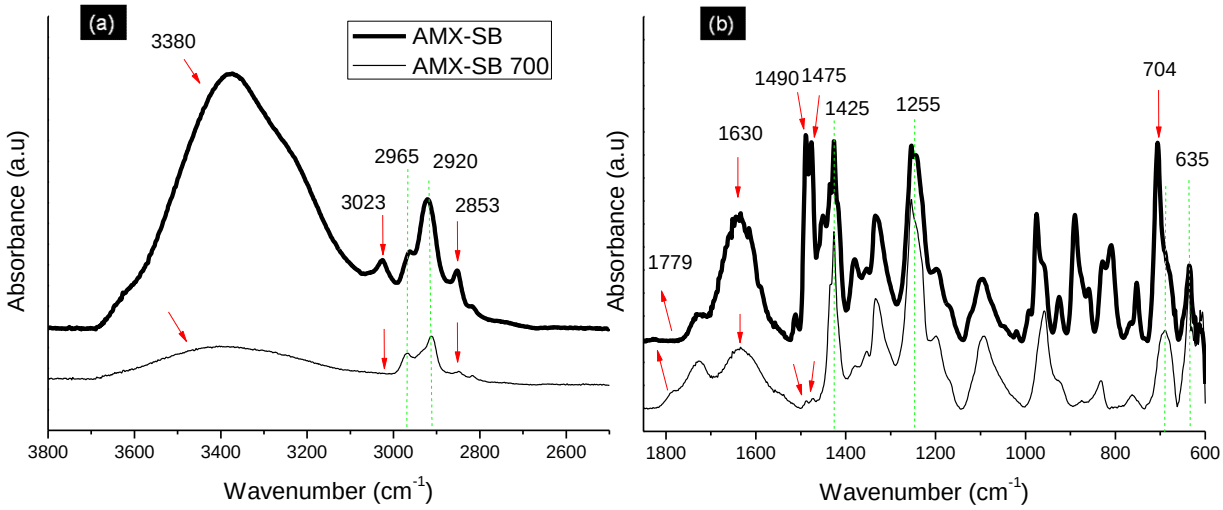

Fig. 5-4.FTIR spectra of new AMX-SB and aged sample (AMX-SB 700) after 700 h in the ageing solution: high (a) and low (b) frequency spectral regions.

On the other hand, the bands corresponding to PVC (dashed lines) did not change in the spectra. In conclusion, PS-DVB was degraded, and the image in the last row of Fig. 5-3 probably represented PVC from the semi-interpenetrating polymer network structure of the AMX-SB membrane.

Fig. 5-5 shows SEM micrographs of heterogeneous MA-41 samples. The membrane structure was considerably different from that of homogeneous AMX-SB. The MA-41 surface was not uniform, as shown by the image in the first row and column. Besides, the major part of what is possible to recognize in the surface micrographs was constituted of the polyethylene binder. In this case, zooming to a higher magnification did not permit to assess the changes in the membrane structure.

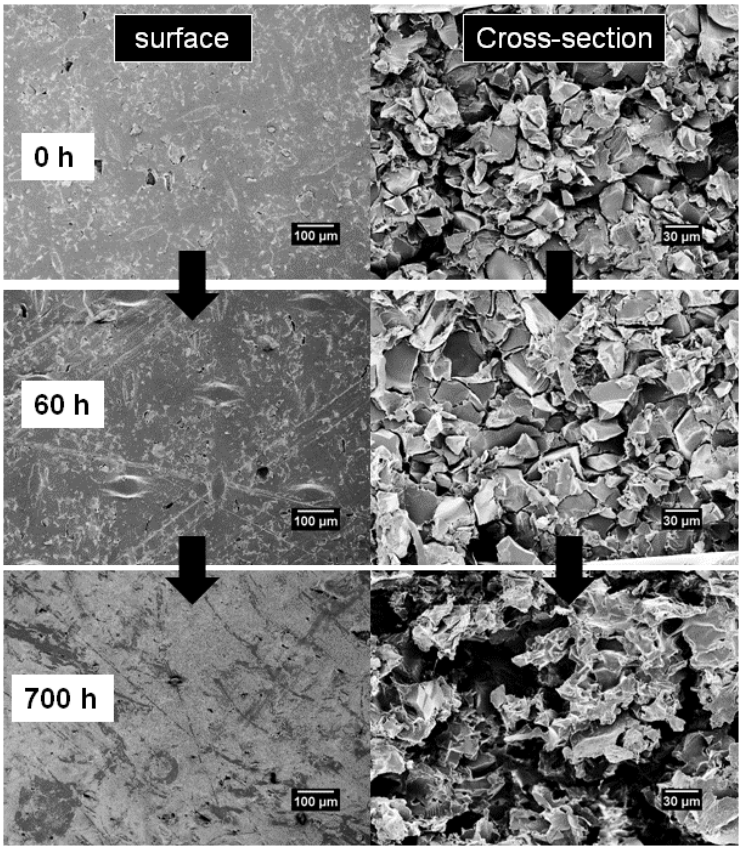

Fig. 5-5. SEM images of MA-41 surface and cross-section after 0, 60, and 700 h in the ageing solution.

The second column of Fig. 5-5 displays cross-section images of the samples. The two main parts of the membrane were clearly distinguished, *i.e.* the ion-exchange resin particles (diameter ≈30 µm) and the polyethylene binder surrounding the resin.

In the last row of the second column, the sample with 700 h of NaClO exposure, the damage of the ion-exchange resin was obvious. Particles disappeared, and they only left the polyethylene binder behind.

When trying to evaluate the FTIR spectra, we realized that it was possible to distinguish only the methylene stretching and bending absorption bands of polyethylene. No band from the ion-exchange resin could be detected clearly. Therefore, the utilization of this technique did not provide further information on the structure changes after hypochlorite exposure.

The analysis of the degradation stages by TGA may provide further insight into the degradation suffered in the membranes structure. Once again, we investigated the sample with the highest degree of degradation, *i.e.* that exposed for 700 h to NaClO.

The characteristic TGA curves for AMX-SB and MA-41 are presented in Fig. 5-6. For both new membranes, the first mass loss appeared at 60-120 °C, due to water linked to the functional sites.

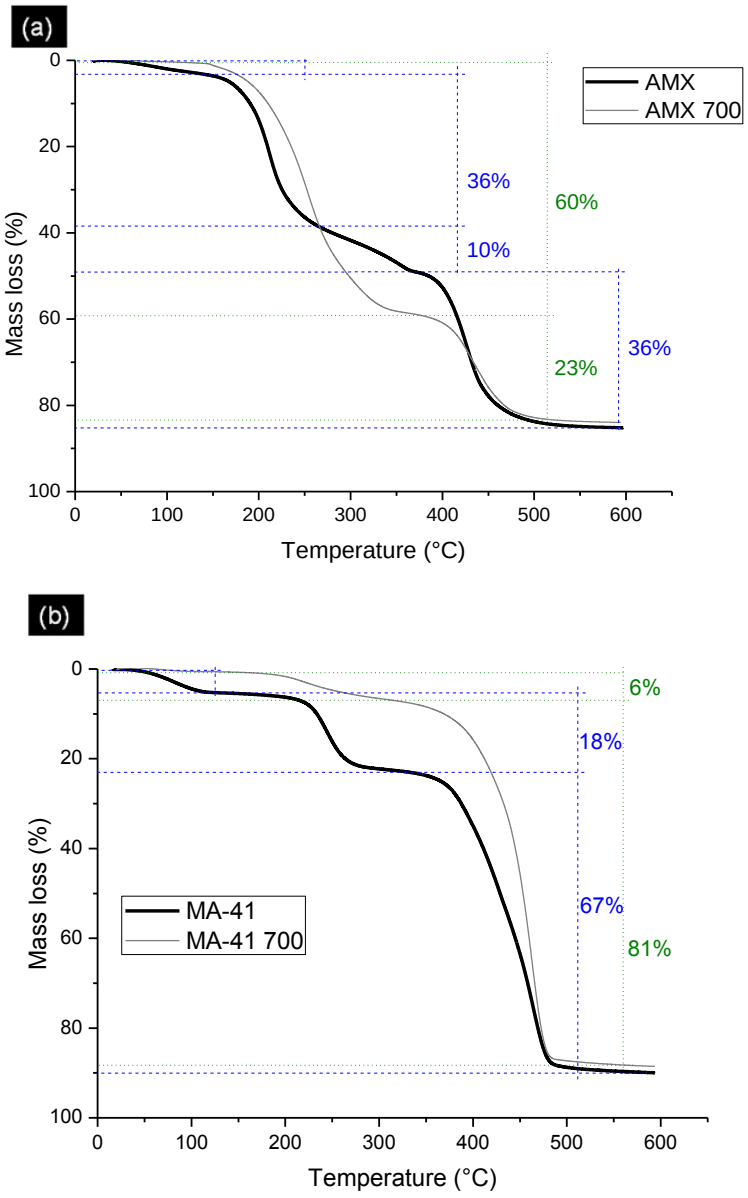

Fig. 5-6. TGA curves for the new and aged samples after 700 h in the ageing solution: AMX-SB (a), MA-41 (b).

The TGA curve for AMX-SB was highly complex as several substances formed the membrane. The ion-exchange resin was constituted of a crosslinked structure of PS and DVB substituted with quaternary ammonium ion-exchange sites, and linked water. According to

Lisa et al. [45], the thermal degradation of PS occurred in a single stage at 410 °C, except when the benzene ring was substituted. These authors indeed evaluated the thermal degradation of chloromethylated amino-substituted PS, and they found three degradation stages with different mass losses. Accordingly, thermal degradation of functional PS-DVB had to occur at least in two different steps, namely one for the quaternary ammonium sites and the other one for the PS-DVB structure.

In the literature, quaternary ammonium groups in AEMs started to degrade at 250 °C [46, 47] and represented no more than 10 % of mass loss of the studied functional polymers. Moreover, Vinodh et al. [48] found that the polymer backbone of polystyrene copolymers substituted with quaternary ammonium degraded at 460 °C.

AMX-SB also possessed two kinds of PVC, *i.e.* one of low molar mass (the polymer binder) and the other one with higher molar mass (the mechanical support) [31]. Thermal degradation of PVC has been shown by most investigators to proceed in two distinct stages [49, 50]. Up to around 360 °C, the degradation step involved dehydrochlorination to a polyene structure; this degradation step represented 65% of mass loss. Above 360 °C, the structural degradation of the backbone occurred.

AMX-SB degradation occurred in four main steps up to 85 % of mass loss. As mentioned above, the first stage from 60 to 120 °C, resulted from the removal of bound water (3 wt %). The second stage, from 160 to 270 °C, led to a mass loss of about 36 % which might correspond mostly to the dehydrochlorination of PVC. The third stage, from 270 to 370 °C, corresponded to the loss of the quaternary ammonium groups (10 wt %). The fourth degradation stage of 36 % mass loss (370-510 °C) might correspond mostly to the degradation of the PS-DVB polymer backbone as well as to that of the polyene from dehydrochlorinated PVC.

Interestingly, the TGA curve of the aged sample showed that the initial stage almost disappeared. As ion-exchange groups were degraded upon NaClO ageing, no detectable bound water was removed in TGA, hence the first and third stages disappeared. The second stage of 60 % mass loss was larger as most part of the aged sample consisted of PVC (and this was the greater stage of PVC thermal degradation), and finally the fourth stage decreased to 23 % of mass loss as the PS-DVB backbone was degraded upon ageing.

MA-41 presented three distinct stages of thermal degradation up to 90 % of mass loss. The first step was attributed to bound water which corresponded to 5% of the total mass of the

membrane. The second step from 200 to 300 °C was ascribed to the loss of quaternary ammonium groups of the resin (18 wt %), and the last stage (300-500 °C) stemmed from the degradation of the PS-DVB backbone of the resin and the polyethylene binder (67 wt %). Previous works have proven that high density polyethylene degraded in a single step from 450 °C [51].

According to Nefedova [33], the MA-41 membrane possesses from 35 to 38 % of high density polyethylene. Consequently, in the third stage which represented 67 % of mass loss, the polymer backbone of the ion-exchange membrane degraded as well.

In the TGA curve associated with aged MA-41, the first stage disappeared and the second stage severely decreased as well (from 18 to 6%), thus confirming the disappearance of bound water and ion-exchange sites. Accordingly, the aged sample was essentially formed by polyethylene, the third stage corresponding to 81% of mass loss. Obviously enough, such strong deteriorations of the membrane structure should be accompanied with significant changes in the membrane mechanical properties. In a previous work [31], it was shown that the mechanical behaviour of AEMs was influenced by its three main components, *i.e*. the functionalized ion-exchange polymer, the binder, and the mechanical support.

For the AMX-SB membrane, functionalized PS-DVB confers a high Young modulus, while PVC provides a high elongation at break [31].

Table 5-1 shows that the Young modulus, which can be related to the rigidity of a material, decreased dramatically as a function of the ageing time, as well as the breaking strength, which represents the membrane flexibility. The microscopic changes in polymer structure were well pronounced at macroscopic levels.

Meanwhile, for MA-41, with increasing ageing time, the Young modulus tended to decrease whereas the strain at break tended to increase (Table 5-1, third and fourth column). From these results, it can be concluded that the ductile behavior of the polymer membrane was enhanced with long ageing times in sodium hypochlorite. This took place as the brittle PS-DVB resin disappeared, and the aged material exhibited typical mechanical properties of polyethylene. In sharp contrast, this phenomenon was not observed for AMX-SB, as the loss of PS-DVB from the microheterogeneous structure involved a loss of the polymer binder integrity as well. Voids observed in the low magnification SEM image of aged AMX-SB (Fig. 5-3) attested for the macroscopic structural modification of the sample. It is clear that the sample aged up to 700 h does not form a uniform phase and even the polymer cloth is

exposed. Meanwhile, macroscopic modifications of aged MA-41 shown in Fig. 5-5 are not as severe as those of AMX-SB; in fact, polyethylene still constitutes a uniform phase.

t (h)	**AMX-SB**		**MA-41**	
	E (MPa)	ε (%)	E (MPa)	ε (%)
0	315.5 ± 0.9	24.8 ± 0.9	105.3 ± 0.9	41.4 ± 0.9
20	334.8 ± 1.3	25.3 ± 0.7	83.3 ± 0.5	38.0 ± 0.9
60	279.3 ± 0.2	23.9 ± 0.7	73.4 ± 0.5	39.6 ± 0.9
100	274.6 ± 0.9	23.2 ± 0.5	64.6 ± 0.3	42.6 ± 1.0
200	222.8 ± 1.8	18.7 ± 0.4	54.5 ± 0.7	47.8 ± 1.0
300	144.3 ± 0.8	5.7 ± 0.1	55.1 ± 0.2	48.1 ± 1.2
700	138.3 ± 0.5	5.7 ± 0.1	37.5 ± 0.3	60.1 ± 1.5

Table 5-1. Young modulus and strain at break of new and aged samples as a function of time in the ageing solution for AMX-SB and MA-41.

The dramatic changes in the mechanical properties observed constitute a strong argument to state that NaClO degradation is not only a surface reaction, and bulk properties of membrane changed significantly.

5.3.2. Cation-exchange membranes

The electrical conductivity of MK-40 increased sharply up to 1.6 times after 700 h of ageing, as shown by the normalized conductivity (κ_m/κ_o) in Fig. 5-1. Meanwhile, CMX-SB electrical conductivity increased up to 1.2 times and came to a standstill after 100 h of exposition. It is noteworthy that the conductivity changes of CEMs had a completely different trend from those of AEMs. From these results, one might expect that ageing of AEMs and CEMs in sodium hypochlorite solutions occurs through different mechanisms.

The equilibrium properties are shown in Fig. 5-7. CMX-SB lost 25 % of its ion-exchange capacity within 20 h of exposure in the ageing solution, and MK-40 lost up to 30 % of ion-exchange capacity within 200 h of exposure. Moreover, a gradual increase in water uptake and a slight increase of the membrane thickness where observed. The increase in CEM electrical conductivity might be linked to damage in the polymer structure. Previous

investigations on the effect of hypochlorite treatment on PSf membranes reported enlarged pore size after bleach treatment, due to partial scission of polymer chains [20].

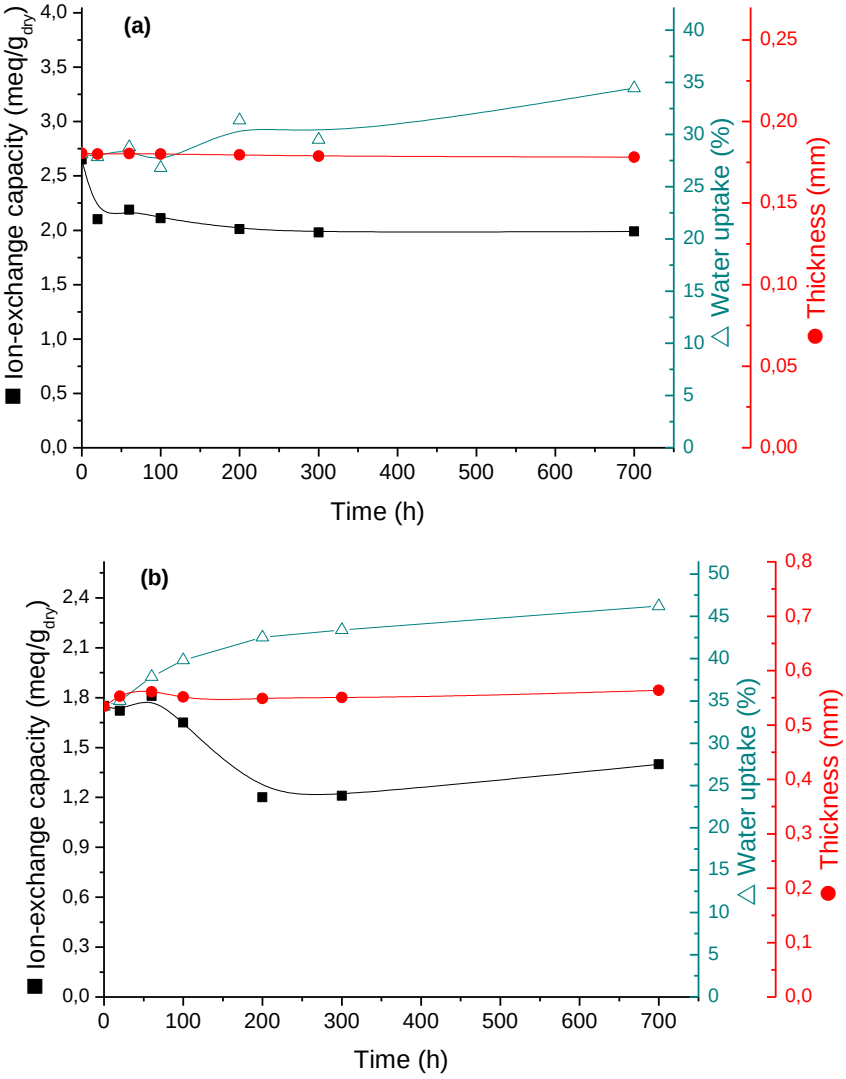

Fig. 5-7. Evolution of CEM equilibrium properties as a function of time in the ageing solution. CMX-SB (a) and MK-40 (b).

SEM images in Fig. 5-8 show CMX-SB (in the first row) had a homogeneous surface just like their AMX-SB counterparts; however, there was an ongoing loss of polymer integrity. After 60 h of exposure (second row), no cracks or defects were detectable on the low magnification image in the first column. Nevertheless, when zooming, cavities of 1µm appeared next to a possible nanoporous structure surrounded by the PVC particles. After 700 h of exposure, the

membrane surface presented macroscopic cracks, and the porosity degree was apparently higher.

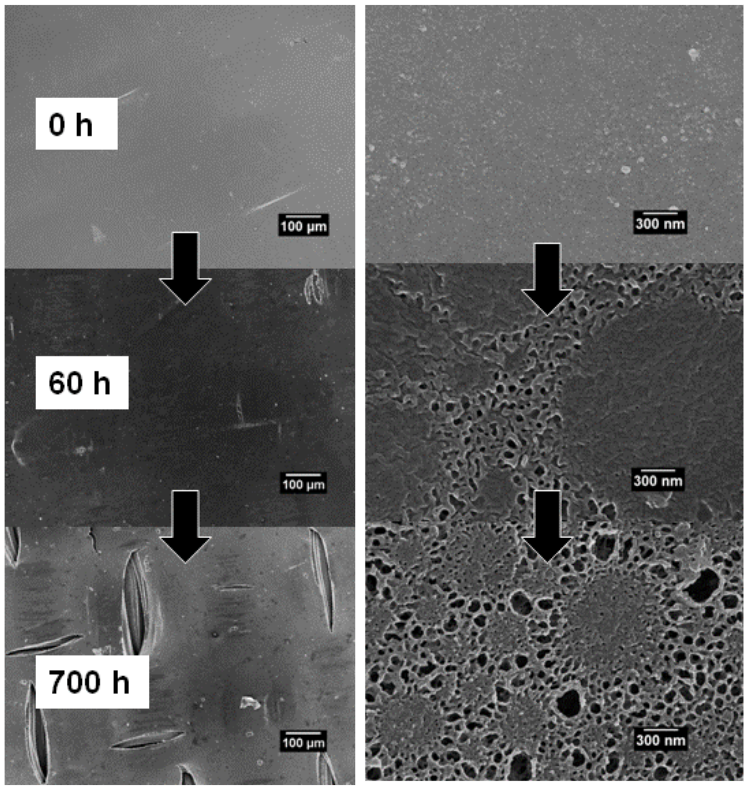

Fig. 5-8. SEM images of CMX-SB surface after 0, 60, and 700 h in the ageing solution.

The structure of aged CMX-SB had some differences from that one of aged AMX-SB. This might happen as the microscopic structure of new CMX-SB membranes might be slightly different from their AMX-SB counterparts. Both membrane types are supposed to be synthesized by the so-called "Paste Method" as explained above, with the difference lying in the last stage, when the ion-exchange groups are introduced. CEMs are treated with concentrated sulfuric acid during a few hours to introduce $-SO_3^-$ groups, while the positively charged quaternary ammonium groups of AEMs are introduced by a chloromethylation procedure, followed by a nucleophilic substitution with a tertiary amine.

In any case, the damage seemed to be different, and the formation of orifices in CEMs from an early stage of ageing was evidenced, which may account for the electrical conductivity increase.

Fig. 5-9 shows the comparison of characteristic FTIR spectra of the new CMX-SB sample and that exposed for 700 h to NaClO. The broad ν(O-H) band from bound water was present from 3000 to 3700 cm^{-1}. An aromatic ring breathing mode of PS-DVB appeared at 1649 cm^{-1}. Sharp bands located at 1010, 1038, 1124, and 1180 cm^{-1} were attributed to S-phenyl, ν(S=O), and ν(S-O) modes, corresponding to $–SO_3^-$ functional groups. Stretching bands belonging to PVC, *i.e.* ν(C-Cl) at 611 and 679 cm^{-1}, and methylene deformation at 1427 cm^{-1}, were observed as well.

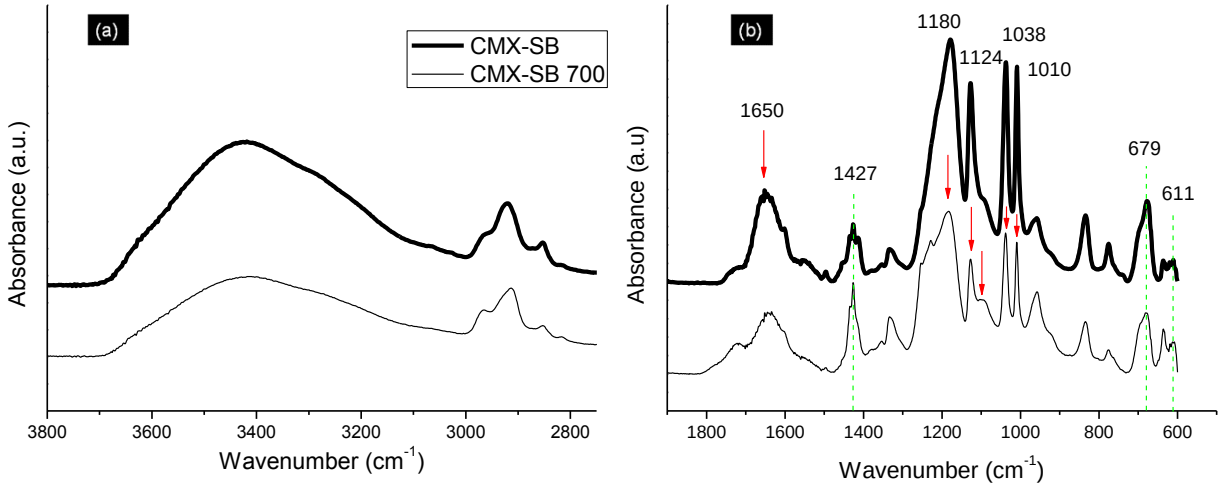

Fig. 5-9. FTIR spectra of new CMX-SB and aged sample (CMX-SB 700) after 700 h in the ageing solution: high (a) and low (b) frequency spectral regions.

The aged sample exhibited some modifications of its spectral profile, especially in the low frequency region associated with stretching and bending vibrations of the polymer skeleton and functional groups. The absorbance intensity decreased by 40-50% for bands attributed to the sulfonate groups, which indicated a partial degradation of functional sites. We might also observe a reduction of band intensity assigned to aromatic double bonds. Unlike AMX-SB spectra of aged samples, we were not able to identify the formation of the band around 1779 cm^{-1} assigned to carbonyl groups, thus confirming that ageing mechanism of CEMs in sodium hypochlorite was different from that involved AEMs.

On the other hand, the bands corresponding to PVC (dashed lines) did not suffer any noticeable change in the spectra. Accordingly, the degradation only occurred in the functionalized PS-DVB of CMX-SB.

Surface and cross-section SEM micrographs of new and hypochlorite aged MK-40 are shown in Fig. 5-10. After the hypochlorite exposure, cracks were observed in the surface images and the disappearance of some ion-exchange resin particles may be noted in the cross section micrographs. Nevertheless, it is noteworthy that the damage in MK-40 was not as pronounced as that suffered in MA-41, which lost most part of the resin particles after 700 h in the ageing solution.

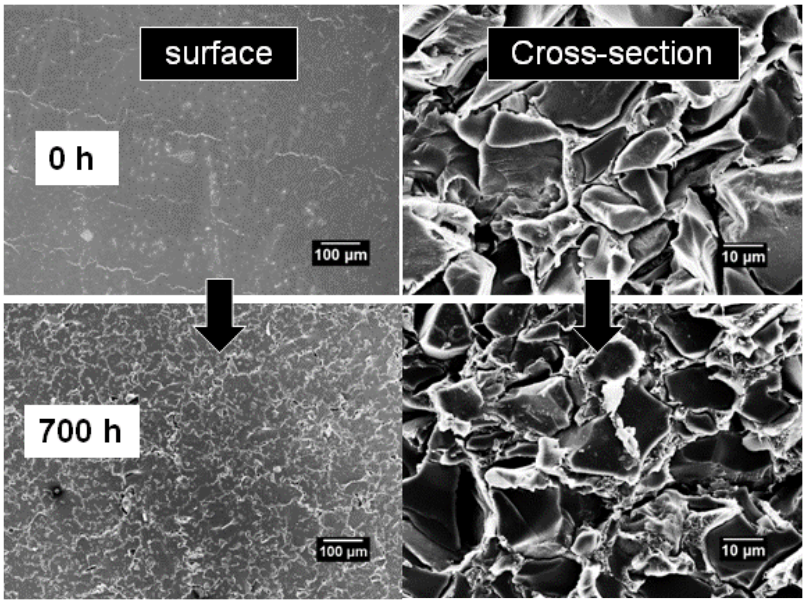

Fig. 5-10. SEM images of the MK-40 surface and cross-section after 0 and 700 h in the ageing solution.

When performing ATR-FTIR on the MK-40 surface (Fig. 5-11), it was possible to identify some stretching and bending vibrations belonging to the ion-exchange resin, and not only to the polyethylene binder like in the case of MA-41. This might be caused by a higher heterogeneity of the MK-40 surface with larger open spaces letting the ion-exchange resin particles uncovered. Furthermore, the bands belonging to the sulfonate sites possess a high absorbance intensity and are strong enough to be detected by this technique, contrary to the ν(N-C) bands corresponding to the quaternary ammonium functional sites, which are weak.

In Fig. 5-11, we could identify the methylene deformation bands of polyethylene at 1462 and 719 cm^{-1}. Due to the crystallinity of polyethylene, these bands were split, and additional bands were detected at 1473 and 729 cm^{-1}. The sharp bands located at 1010, 1039, 1126, and

1174 cm^{-1} arising from $–SO_3^-$ functional groups were also detected. The absorbance intensity of the latters decreased by almost 30 %, thus confirming damage in the ion-exchange sites.

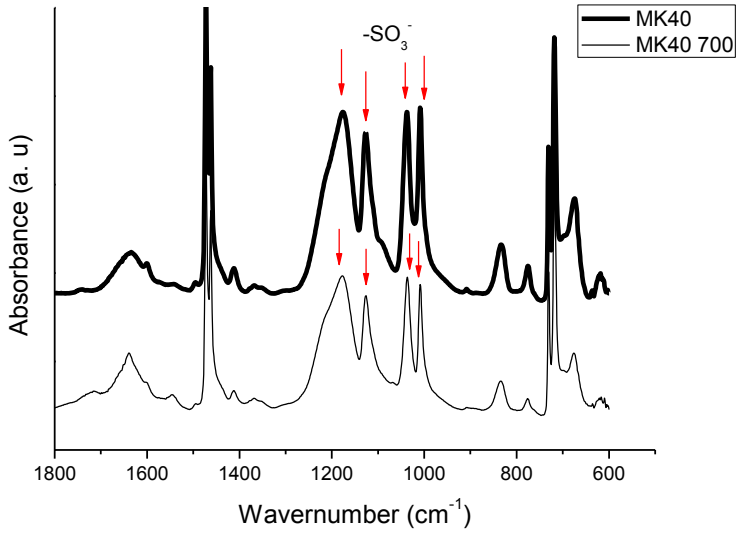

Fig. 5-11. FTIR spectra of new MK-40 and aged sample (MK-40 700) after 700 h in the ageing solution.

To obtain more facts about the structural changes undergone by the polymer membranes upon NaClO ageing, the thermal stability of CEMs was investigated by TGA (Fig. 5-12). CMX-SB degraded in four main stages up to 60 % of mass loss, as illustrated in Fig. 5-12a. The first step from 40 to 130 °C was assigned to the loss of bound water. The second stage from 180 to 250 °C was attributed to dehydrochlorination of PVC. Sulfonate sites in CEMs are known to be degraded around 250 °C [52]; accordingly, the third stage from 250 to 350 °C corresponded to degradation of the functional sites. The final stage from 350 to 450 °C corresponded to the degradation of PS-DVB and PVC backbones.

In aged CMX-SB, the first stage was reduced from 4 to 3% of mass loss, while the second stage remained almost constant (39 wt %) and the third stage decreased from 8 to 6 wt %, probably due to a partial loss of functional sites. The fourth stage varied from 18 to 20 wt % of mass loss.

MK-40 clearly showed two main stages of thermal degradation (Fig. 5-12b). The first one from 40 to 120 °C was assigned to bound water (7 wt %). The rest of the membrane (55 wt %) degraded in the second stage from 350 to 550 °C. The thermal stability of MK-40 was

lowered after the ageing process, as degradation started at a lower temperature (200 °C), probably due to a lowering of the molar mass by chain scission.

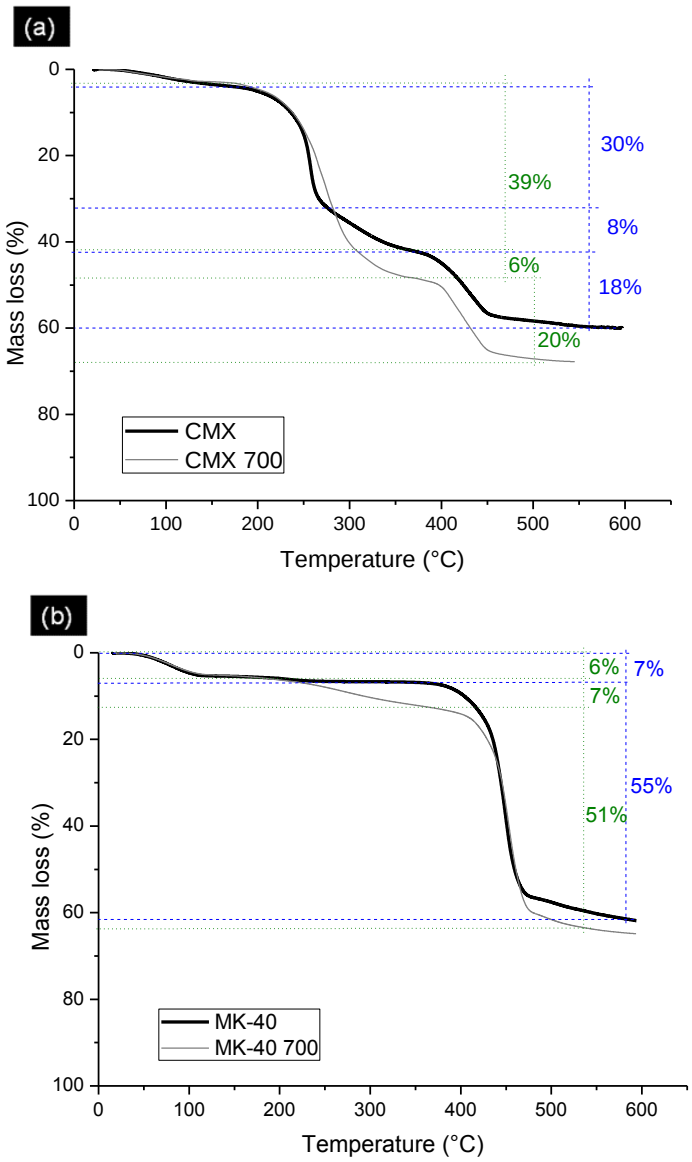

Fig. 5-12. TGA curves for the new and aged samples after 700 h in the ageing solution: CMX-SB (a), MK-40 (b).

With increasing ageing time, the Young modulus of CMX-SB tended to decrease whereas the strain at break tended to increase (Table 5-2). Therefore the ductile behavior of the polymer membrane was enhanced with long ageing times in sodium hypochlorite. This took place as

the brittle functional PS-DVB was damaged, and the aged material exhibited typical mechanical properties of PVC.

t (h)	**CMX-SB**		**MK-40**	
	E (MPa)	ε(%)	E (MPa)	ε(%)
0	244.7 ± 1.7	26.6 ± 1.0	61.4 ± 0.3	60.0 ± 1.3
20	237.1 ± 0.3	29.2 ± 0.9	63.1 ± 0.2	26.9 ± 0.7
60	227.7 ± 1.1	30.4 ± 0.8	53.4 ± 0.5	23.7 ± 0.5
100	219.1 ± 0.8	30.2 ± 1.1	46.7 ± 0.5	28.3 ± 0.4
200	200.1 ± 0.5	33.0 ± 1.0	47.7 ± 0.4	24.1 ± 0.4
300	210.0 ± 0.8	33.2 ± 1.2	43.3 ± 0.2	20.0 ± 0.7
700	183.1 ± 0.8	35.0 ± 0.9	23.0 ± 0.3	19.0 ± 0.4

Table 5-2. Young modulus and strain at break of new and aged samples as a function of time in the ageing solution for CMX-SB and MK-40.

When comparing Figs. 5-3 and 5-8 it is possible to see that damage on the macrostructure of the aged samples was less severe for CMX-SB than that suffered by AMX-SB, and this is why even if PS-DVB of the former was degraded, the sample still exhibited the mechanical properties of the polymer binder.

On the other hand, both the Young Modulus and strain at break of MK-40 decreased after hypochlorite ageing (Table 5-2, third and fourth column). Severe changes in the mechanical properties of heterogeneous MK-40 might suggest damage in the polyethylene binder, which was caused by the degradation of stabilizers or exhaustion of antioxidants probably present in the polymer. However, further investigation should be performed to confirm this hypothesis.

5.3.3. Degradation mechanisms of IEMs subjected to ageing in NaClO

Based on the overall results, it was obvious that degradation mechanisms of AEMs and CEMs in sodium hypochlorite solution were different. From infrared spectroscopy, TGA, and ion-exchange capacity measurements, it was possible to identify the degradation of ion-exchange sites in both AEMs and CEMs. This phenomenon could be caused by desulfonation or

deamination (loss of $-SO_3^-$ or - $CH_2N^+R_3$, respectively), and/or by breaking of the polymer chains.

The decrease in conductivity and membrane thickness in AEMs suggested that quaternary ammonium sites were degraded before the PS-DVB structure. In a recent study, Nouri-Nigjeh et al. [53] suggested that ketones are among the oxidation products of the tetrabutylammonium oxidation, which might explain the appearance of the C=O band in the aged AMX-SB spectra. In a second step, the polymer backbone degraded, which caused the rebound of electrical conductivity in AMX-SB after the disappearance of PS-DVB from the PVC-containing semi interpenetrating polymer network, and the loss of resin particles in MA-41.

Immersion of both AEMs and CEMs in bleach solution induces oxidation of the polymer skeleton, and hydroxyl radicals are probably involved in this oxidation. Prulho et al. [24] reported oxidation products when immersing PS in 4000 ppm free chlorine at pH = 8.

It is well known that the initiation and propagation steps in the chain radical oxidation mechanism for polymers involve the abstraction of labile hydrogen. PS has one such atom linked to the α-carbon from the aliphatic side of the chain.

Accordingly, we suggest that degradation of the IEMs took place according to the scheme presented in Fig. 5-13. For AEMs, the first step involved the degradation of the quaternary ammonium groups giving place to a non-functionalized PS-DVB. In a second step, hydroxyl radicals subtracted the α-hydrogen from PS, thus inducing chain scissions. In contrast, sulfonate groups from CEMs were not degraded directly. Hydroxyl radicals attacked the α-hydrogen from PS which resulted in chain scissions, thus dragging out some of the sulfonate groups and causing a reduction of the concentration of ion-exchange sites.

Furthermore, we did not find any proof of partial scission of C-S bond in CEMs that led to desulfonation. In this case, we might suppose that the origin of degradation was only PS-DVB chain breaking which resulted in the increase in conductivity and water uptake, along with the decrease in ion-exchange capacity.

It is noteworthy that the polymer binder did not generally suffer degradation, neither the PVC for the homogeneous membranes, nor the polyethylene of the heterogeneous ones.

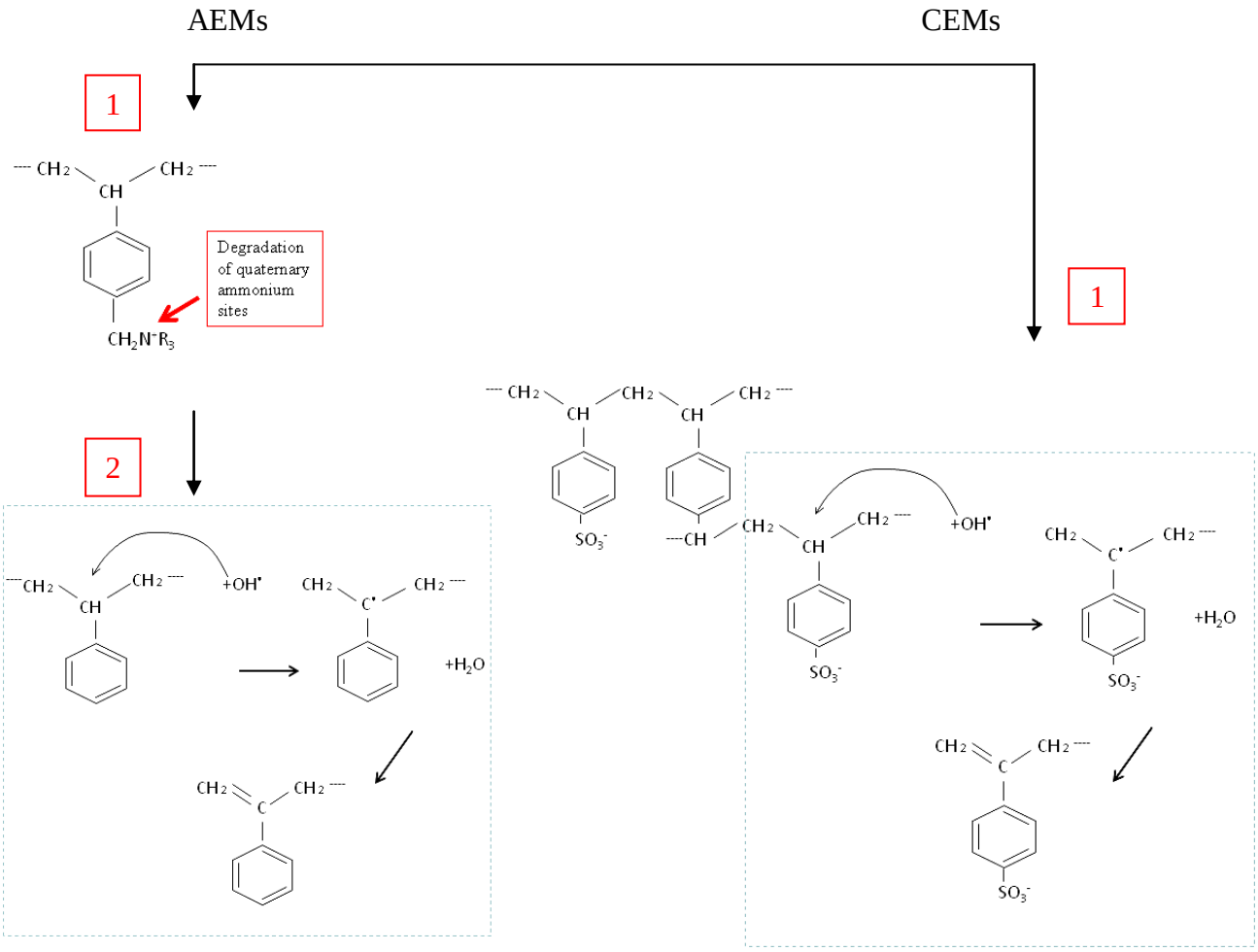

Fig. 5-13. Degradation mechanisms of AEMs and CEMs after ageing in sodium hypochlorite.

5.4. Conclusions

The effects of contact with a strong oxidizing agent on IEMs were thoroughly investigated in this paper. Their structure, properties, and long-term behavior were unveiled by means of a physico-chemical, structural, and mechanical characterization.

Ageing mechanisms appeared to be different for AEMs and CEMs. While quaternary ammonium sites of AEMs were prone to degradation by contact with NaClO, sulfonate sites were not. The loss of the nature or concentration of the quaternary ammonium sites caused a decrease in conductivity and ion-exchange capacity. Nevertheless, the second step of AEMs degradation occurred in the same manner as the sole step found for CEM degradation. PS-

DVB chains broke, due to the subtraction of a labile hydrogen atom from the aliphatic PS chain by hydroxyl radicals. The polymer chain scissions caused an increase in the conductivity and water uptake, resulting from the formation of holes and cavities forming a continuous network.

It is noteworthy that dissimilarities among the ageing mechanisms of homogeneous and heterogeneous membranes of the same type (cationic or anionic) were not found. Furthermore, differences on the physico-chemical properties after ageing were not significant. All membranes possess the same PS-DVB based functional polymer, and each type has the same functional groups. In addition, both types of polymer binders, PVC and polyethylene for homogeneous and heterogeneous membranes respectively, were resistant to attack under NaClO environment.

5.5. Acknowledgements

This investigation was realized within French-Russian laboratory "Ion-exchange membranes and related processes". The authors are grateful to CNRS, France, and to RFBR, Russia (grants 11-08-93107_CNRSL, 12-08-00188_CNRSL, 13- 8-96508r_yug), as well as to FP7 Marie Curie Actions "CoTraPhen" project PIRSES-GA-2010-269135 for financial support.

References

[1] H. Strathmann, Electrodialysis, a mature technology with a multitude of new applications, Desalination, 264 (2010) 268-288.

[2] F. Lutin, L'electrodialyse et ses nombreuses applications, L'Actualité Chimique, 327 (2009) 59-72.

[3] D.A. Vermaas, D. Kunteng, M. Saakes, K. Nijmeijer, Fouling in reverse electrodialysis under natural conditions, Water Research, 47 (2013) 1289-1298.

[4] O.M. Kattan Readi, M. Gironès, K. Nijmeijer, Separation of complex mixtures of amino acids for biorefinery applications using electrodialysis, J. Membr. Sci., 429 (2013) 338-348.

[5] M. Fidaleo, M. Moresi, Electrodialysis Applications in The Food Industry, Adv. Food Nutr. Res, 51 (2006) 265-360.

[6] A. Bukhovets, T. Eliseeva, Y. Oren, Fouling of anion-exchange membranes in electrodialysis of aromatic amino acid solution, J. Membr. Sci., 364 (2010) 339-343.

[7] N. Tanaka, M. Nagase, M. Higa, Organic fouling behavior of commercially available hydrocarbon-based anion-exchange membranes by various organic-fouling substances, Desalination, 296 (2012) 81-86.

[8] E. Ayala-Bribiesca, M. Araya-Farias, G. Pourcelly, L. Bazinet, Effect of concentrate solution pH and mineral composition of a whey protein diluate solution on membrane fouling formation during conventional electrodialysis, J. Membr. Sci., 280 (2006) 790-801.

[9] N. Cifuentes-Araya, G. Pourcelly, L. Bazinet, How pulse modes affect proton-barriers and anion-exchange membrane mineral fouling during consecutive electrodialysis treatments, J. Colloid Interface Sci., 392 (2013) 396-406.

[10] H. Strathmann, in: Ion-exchange Membrane Separation Processes, Elsevier, 2004, pp. 287-328.

[11] L. Paugam, D. Delaunay, M. Rabiller-Baudry, Cleaning efficiency and impact on production fluxes of oxidizing disinfectants on a PES ultrafiltration membrane fouled with proteins, Food Bioprod. Process., 88 (2010) 425-429.

[12] N. Porcelli, S. Judd, Chemical cleaning of potable water membranes: A review, Sep. Purif. Technol., 71 (2010) 137-143.

[13] X. Tang, S.H. Flint, R.J. Bennett, J.D. Brooks, The efficacy of different cleaners and sanitisers in cleaning biofilms on UF membranes used in the dairy industry, J. Membr. Sci., 352 (2010) 71-75.

[14] L. Paugam, D. Delaunay, M. Rabiller-Baudry, Cleaning efficiency and impact on production fluxes of oxidising disinfectants on a PES ultrafiltration membrane fouled with proteins, Food Bioprod. Process., 88 (2010) 425-429.

[15] M.E. Mansour, A. Ettori, S. Luque, J.R. Álvarez, C. Causserand, P. Aimar, Accelerated Ageing of Crosslinked Polyamide Membranes, Procedia Eng., 44 (2012) 789.

[16] C. Regula, E. Carretier, Y. Wyart, M. Sergent, G. Gésan-Guiziou, D. Ferry, A. Vincent, D. Boudot, P. Moulin, Ageing of ultrafiltration membranes in contact with sodium hypochlorite and commercial oxidant: Experimental designs as a new ageing protocol, Sep. Purif. Technol., 103 (2013) 119-138.

[17] A. Ettori, E. Gaudichet-Maurin, J.-C. Schrotter, P. Aimar, C. Causserand, Permeability and chemical analysis of aromatic polyamide based membranes exposed to sodium hypochlorite, J. Membr. Sci., 375 (2011) 220-230.

[18] E. Gaudichet-Maurin, F. Thominette, Ageing of polysulfone ultrafiltration membranes in contact with bleach solutions, J. Membr. Sci., 282 (2006) 198-204.

[19] C. Causserand, S. Rouaix, J.-P. Lafaille, P. Aimar, Ageing of polysulfone membranes in contact with bleach solution: Role of radical oxidation and of some dissolved metal ions, Chemical Engineering and Processing: Process Intensification, 47 (2008) 48-56.

[20] E. Arkhangelsky, D. Kuzmenko, V. Gitis, Impact of chemical cleaning on properties and functioning of polyethersulfone membranes, J. Membr. Sci., 305 (2007) 176-184.

[21] E. Arkhangelsky, D. Kuzmenko, N.V. Gitis, M. Vinogradov, S. Kuiry, V. Gitis, Hypochlorite Cleaning Causes Degradation of Polymer Membranes, Tribology Lett., 28 (2007) 109-116.

[22] Y.-N. Kwon, J.O. Leckie, Hypochlorite degradation of crosslinked polyamide membranes, J. Membr. Sci., 283 (2006) 21-26.

[23] K. Yadav, K. Morison, M.P. Staiger, Effects of hypochlorite treatment on the surface morphology and mechanical properties of polyethersulfone ultrafiltration membranes, Polym. Degrad. Stab., 94 (2009) 1955-1961.

[24] R. Prulho, S. Therias, A. Rivaton, J.-L. Gardette, Ageing of polyethersulfone/polyvinylpyrrolidone blends in contact with bleach water, Polym. Degrad. Stab., 98 (2013) 1164-1172.

[25] S. Rouaix, C. Causserand, P. Aimar, Experimental study of the effects of hypochlorite on polysulfone membrane properties, J. Membr. Sci., 277 (2006) 137-147.

[26] C. Causserand, S. Rouaix, J.-P. Lafaille, P. Aimar, Degradation of polysulfone membranes due to contact with bleaching solution, Desalination, 199 (2006) 70-72.

[27] L. Dammak, C. Larchet, D. Grande, Ageing of ion-exchange membranes in oxidant solutions, Sep. Purif. Technol., 69 (2009) 43-47.

[28] R. Ghalloussi, W. Garcia-Vasquez, N. Bellakhal, C. Larchet, L. Dammak, P. Huguet, D. Grande, Ageing of ion-exchange membranes used in electrodialysis: Investigation of static parameters, electrolyte permeability and tensile strength, Sep. Purif. Technol., 80 (2011) 270-275.

[29] R. Ghalloussi, W. Garcia-Vasquez, L. Chaabane, L. Dammak, C. Larchet, N. Bellakhal, Decline of ion-exchange membranes after utilization in electrodialysis for food applications, Phys. Chem. News, 65 (2012) 66-72.

[30] R. Ghalloussi, W. Garcia-Vasquez, L. Chaabane, L. Dammak, C. Larchet, S.V. Deabate, E. Nevakshenova, V. Nikonenko, D. Grande, Ageing of ion-exchange membranes in

electrodialysis: A structural and physicochemical investigation, J. Membr. Sci., 436 (2013) 68-78.

[31] W. Garcia-Vasquez, L. Dammak, C. Larchet, V. Nikonenko, N. Pismenskaya, D. Grande, Evolution of anion-exchange membrane properties in a full scale electrodialysis stack, J. Membr. Sci., 446 (2013) 255-265.

[32] Y. Mizutani, Structure of Ion Exchange Membranes, J. Membr. Sci., 49 (1990) 121-144.

[33] G.Z. Nefedova, Z.G. Klimova, G.S. Sapozhnikova, Granules and Powders, in: Pashkov (Ed.) Ion-Exchange Membranes, NIITEKhim, Moscow, 1977.

[34] AFNOR, French standard NF X 45-200, 1995.

[35] E. Gaudichet-Maurin, Caractérisation et vieillissement d'une membrane d'ultrafiltration d'eau, PhD thesis, Ecole Superieure Nationale d'Arts et Métiers, Paris, 2005.

[36] R. Lteif, L. Dammak, C. Larchet, B. Auclair, Conductivité électrique membranaire: étude de l'effet de la concentration, de la nature de l'électrolyte et de la structure membranaire, Eur. Polym. J., 35 (1999) 1187-1195.

[37] N.N. Belaid, B. Ngom, L. Dammak, C. Larchet, B. Auclair, Conductivité membranaire: interprétation et exploitation selon le modèle à solution interstitielle hétérogène, Eur. Polym. J., 35 (1999) 879-897.

[38] E.N. Komkova, D.F. Stamatialis, H. Strathmann, M. Wessling, Anion-exchange membranes containing diamines: preparation and stability in alkaline solution, J. Membr. Sci., 244 (2004) 25-34.

[39] V.I. Zabolotsky, V.V. Nikonenko, Effect of structural membrane inhomogeneity on transport properties, J. Membr. Sci., 79 (1993) 181-198.

[40] Y. Mizutani, R. Yamane, H. Ihara, H. Motura, Studies of Ion Exchange Membranes. XVI. The preparation of Ion Exchange Membranes by the "Paste Method", Bull. Chem. Soc. Jpn., 36 (1963) 361-366.

[41] Y. Mizutani, R. Yamane, H. Motomura, Studies of Ion Exchange Membranes. XXII. Semicontinuous Preparation of Ion Exchange Membranes by the “Paste Method", Bull. Chem. Soc. Jpn., 38 (1965) 689-694.

[42] Y. Mizutani, Studies of Ion Exchange Membranes. XXX. The tetrahydrofuran Extraction of the Ion-exchange Membrane and its Base Membrane Prepared by the "Paste Method", Bull. Chem. Soc. Jpn., 42 (1969) 2459-2463

[43] M. Beltrán, A. Marcilla, Fourier transform infrared spectroscopy applied to the study of PVC decomposition, Eur. Polym. J., 33 (1997) 1135-1142.

[44] S.I. Kuzina, A.I. Mikhailov, Photo-oxidation of polymers 4. The dual mechanism of polystyrene photo-oxidation: a hydroperoxide and a photochain one, Eur. Polym. J., 37 (2001) 2319-2325.

[45] G. Lisa, E. Avram, G. Paduraru, M. Irimia, N. Hurduc, N. Aelenei, Thermal behaviour of polystyrene, polysulfone and their substituted derivatives, Polym. Degrad. Stab., 82 (2003) 73-79.

[46] H. Xu, J. Fang, M. Guo, X. Lu, X. Wei, S. Tu, Novel anion exchange membrane based on copolymer of methyl methacrylate, vinylbenzyl chloride and ethyl acrylate for alkaline fuel cells, J. Membr. Sci., 354 (2010) 206-211.

[47] H. Zarrin, J. Wu, M. Fowler, Z. Chen, High durable PEEK-based anion exchange membrane for elevated temperature alkaline fuel cells, J. Membr. Sci., 394–395 (2012) 193-201.

[48] R. Vinodh, A. Ilakkiya, S. Elamathi, D. Sangeetha, A novel anion exchange membrane from polystyrene (ethylene butylene) polystyrene: Synthesis and characterization, Mater. Sci. Eng., B, 167 (2010) 43-50.

[49] A. Guyot, M. Bert, Sur la dégradation thermique du polychlorure de vinyle. VI. Etapes initiales—etude générale préliminaire, J. Appl. Polym. Sci., 17 (1973) 753-768.

[50] M.M. O'Mara, High-temperature pyrolysis of poly(vinyl chloride): Gas chromatographic-mass spectrometric analysis of the pyrolysis products from PVC resin and plastisols, J. Polym. Sci., Part A: Polym. Chem., 8 (1970) 1887-1899.

[51] H.A. Khonakdar, J. Morshedian, U. Wagenknecht, S.H. Jafari, An investigation of chemical crosslinking effect on properties of high-density polyethylene, Polymer, 44 (2003) 4301-4309.

[52] A.B. LaConti, M. Hamdan, R.C. McDonald, Mechanisms of membrane degradation, in: Handbook of Fuel Cells, John Wiley & Sons, Ltd, 2010.

[53] E. Nouri-Nigjeh, M.P. de Vries, A.P. Bruins, R. Bischoff, H.P. Permentier, Electrochemical oxidation of quaternary ammonium electrolytes: Unexpected side reactions in organic electrochemistry, Electrochem. Commun., 21 (2012) 54-57.

Conclusion Générale

Les membranes échangeuses d'ions (MEIs) sont des matériaux très complexes utilisées pour leurs perméabilités et sélectivités en fonction de la charge et/ou de la taille des espèces ioniques. L'électrodialyse est le procédé industriel le plus répandu utilisant ces MEIs. Son application dans le traitement des eaux a montré une grande longévité des MEIs. Toutefois, cette longévité est beaucoup moins importante dans les nouveaux procédés récemment développés pour le traitement des produits et sous-produits de l'industrie agroalimentaire, où les solutions traitées sont riches en matière organique et nécessitant des étapes de nettoyage chimique plus prolongées et plus agressives. Ainsi, il a été constaté des altérations, parfois sévères, en surface et dans la masse de ces membranes. La rentabilité de ces procédés et leurs impacts sur l'environnement peuvent être améliorés si on arrive à augmenter la durée de vie de ces membranes. Pour atteindre cet objectif, il nous a semblé judicieux de commencer par comprendre les origines et les mécanismes de ce vieillissement, ce qui permettrait ensuite de proposer des améliorations soit du procédé soit des matériaux.

Lors de ce travail de thèse nous avons étudié le comportement à long terme (durabilité) de différentes membranes échangeuses d'anions (MEAs) et de cations (MECs) utilisées en électrodialyse conventionnelle pour l'industrie agroalimentaire. Certaines de ces membranes sont du type homogènes et d'autres du type hétérogènes. Elles ont toutes un facteur commun qui est la nature du matériau fonctionnel échangeur d'ions : le poly(styrène-*co*-divinylebenzène). Les sites fonctionnels sont sulfoniques pour les MECs ou ammoniums quaternaires pour les MEAs. Toutefois, les structures fines des membranes homogènes et hétérogènes sont complètement différentes et n'étaient connues que partiellement et mal renseignées par les fournisseurs.

La méthodologie suivie tout au long de ce travail est basée sur la comparaison de nombreuses propriétés physico-chimiques, structurales, et mécaniques d'échantillons neufs et d'autres vieillis dans un module d'électrodialyse industriel (*in-situ*) ou selon des protocoles que nous avons mis au point en laboratoire (*ex-situ*). Les échantillons vieillis *in-situ* sont prélevés à différents moments de leur cycle de vie. Quant aux échantillons vieillis *ex-situ*, nous avons choisi, d'une part, des conditions opératoires reproductibles afin de simuler d'une manière contrôlée le vieillissement, et d'autre part, d'augmenter le nombre d'échantillons étudiés afin d'avoir une analyse plus fine. L'un des intérêts de cette double étude (*in-situ* et *ex-situ*) réside dans la comparaison des échantillons vieillis selon chaque mode. Nous avons noté une remarquable complémentarité entre les différentes techniques d'analyse et leur recoupement a permis une meilleure compréhension des mécanismes de dégradation.

Afin de mieux connaître la structure de chaque type de membrane étudiée, et d'identifier ensuite les changements survenus après leur vieillissement, nous avons démontré que :

- Les MEIs homogènes possèdent une structure formée d'un réseau semi-interpénétré de polymère, entre le polymère fonctionnel (PSt-DVB) et le PVC, un polymère thermoplastique utilisé pour améliorer la plasticité de la membrane. Une trame de PVC de poids moléculaire très important sert de support mécanique renforçant les propriétés mécaniques de l'ensemble. Il en résulte une structure qui n'est pas tout à fait homogène mais microhétérogène.

- Les MEIs échangeuses d'ions hétérogènes sont constituées de particules de résines échangeuses d'ions (de 20 à 30 µm de diamètre) du même polymère fonctionnel (PSt-DVB fonctionnalisé) reparties dans un liant en polyéthylène de haute densité. Ces dernières membranes sont également renforcées par deux trames de polyester.

L'étude du vieillissement *in-situ* des différentes MEIs utilisées dans deux procédés différents (traitement des acides organiques et déminéralisation du lactosérum) nous a permis de dégager les conclusions générales suivantes :

- Les MEAs sont beaucoup plus sensibles aux agressions externes (pendant le fonctionnement normal ou lors des phases de nettoyage) que les MECs. Par exemple, dans le traitement des acides organiques, les MECs subissent très peu de dégradation alors que les MEAs deviennent inutilisables.

- Les changements dans les propriétés de transport, et donc dans les performances des membranes, ainsi que dans les propriétés mécaniques des MEIs dépendent en grande partie des modifications survenues sur leurs microstructures. Par exemple, l'élimination du PVC liant engendre la formation de cavités de 50-200 nm de diamètre. Dans certaines de ces cavités, des molécules organiques (comme le lactose et les protéines) se trouvent piégées réduisant ainsi la perméabilité aux ions. En même temps, et pour une période prolongée de dégradation, certains pores forment un réseau de percolation augmentant ainsi le passage non sélectif d'électrolyte à travers la membrane ce qui diminue sa sélectivité. Aussi, la tenue des MEIs diminue sévèrement à cause de la dégradation du PVC et conduit à une forte perte de stabilité mécanique, ce qui rend la membrane cassante et inutilisable.

- Il est possible de conceptualiser les modifications dans la microstructure membranaire, telles que la formation de cavités et le colmatage interne, à partir d'une analyse fine des phases du modèle microhétérogène. Nous avons amélioré ce modèle afin de le rendre compatible avec les conséquences du vieillissement des MEIs.

L'effet des opérations de nettoyage sur le comportement à long terme des MEIs a fait l'objet de notre étude *ex-situ*. Ce nettoyage est effectué par des solutions acides, alcalines ou par cycles alternant les deux solutions, ou également par des solutions oxydantes de type eau de Javel. Nous avons pu dégager les conclusions suivantes :

- L'exposition des MEIs aux environnements acides et alcalins engendre une diminution progressive et irréversible de leurs performances.

- Le poly(styrène-*co*-divinylebenzène) est un polymère résistant aux environnements acides et basiques forts. La stabilité de la membrane dans ces conditions dépend alors de la résistance des polymères liants (PVC dans le cas des membranes homogènes et PE pour les membranes hétérogènes) aux pH extrêmes.

- Les sites ammonium quaternaire tendent à se dégrader en milieu alcalin.

- La stabilité des polymères liants des membranes est très importante pour la stabilité mécanique de ces matériaux.

- Les modifications de la structure des membranes homogènes entraînent des conséquences plus graves sur leurs propriétés physico-chimiques, comparées aux membranes hétérogènes.

- Les cycles de nettoyage acide-base (HCl-NaOH) effectués lors des opérations d'électrodialyse en agroalimentaire engendrent d'importantes dégradations sur les MEIs. Ces dégradations sont beaucoup plus importantes que si les MEIs sont exposées à l'acide ou à la base uniquement. L'effet du changement brutal du gonflement joue un rôle important dans la destruction et l'élimination des chaînes et des sites fonctionnels.

- Le vieillissement des membranes échangeuses d'anions homogènes utilisées en électrodialyse pour la déminéralisation du lactosérum est dû essentiellement au nettoyage chimique par les cycles HCl-NaOH.

- Le poly(styrène-*co*-divinylebenzène) se dégrade quand il est exposé à l'eau de Javel (NaClO) à cause de nombreuses ruptures de chaînes provoquées par des radicaux hydroxyles existant à pH de 7 à 9.

- Les sites sulfoniques sont résistants au vieillissement après exposition au NaClO, cependant les sites ammonium quaternaire sont très vite dégradés.

- L'utilisation de l'eau de Javel comme produit de nettoyage en électrodialyse n'est pas recommandée.

- Les résultats obtenus par vieillissement *ex-situ* sont très similaires à ceux obtenus par un vieillissement *in-situ*. Ainsi, les études *ex-situ*, sous des conditions opératoires bien choisies, constituent un excellent moyen de réalisation d'un vieillissement artificiel contrôlé.

La suite logique de ce travail, pionnier sur la thématique de la durabilité des MEIs, consiste à :

- Transposer cette étude aux membranes bipolaires qui sont formées d'une association d'une MEA et d'une MEC. Ceci permettra d'inclure les effets des ions H^+ et OH^- produits par dissociation aussi bien sur les matériaux membranaires que sur le catalyseur intra-membranaire. La vision deviendra globale et comprendra tout type d'électrodialyse.

- Modifier les cycles de nettoyage acide-base afin d'introduire une étape tampon de lavage par une solution de NaCl par exemple afin de réduire les variations brutales du gonflement des MEIs. Le cycle devient ainsi HCl – NaCl – NaOH – NaCl. Une étude d'optimisation des temps de lavage et des concentrations des solutions devient donc nécessaire.

- Evaluer les performances en matière de nettoyage de certains détergents, en synergie ou non avec des oxydants, ainsi que leurs effets sur les MEIs.

- Apporter des modifications simples sur la surface des MEIs existantes afin de réduire leur colmatage en surface et dans la masse. Ces modifications peuvent être d'ordre physique en augmentant par exemple la rugosité de la surface et par conséquent les turbulences à l'interface MEI/solution, ou d'ordre chimique en greffant de petites

molécules favorisant le passage des ions à éliminer tout en repoussant les colloïdes et protéines.

Résumé

Lors de ce travail de thèse nous avons étudié le comportement à long terme de différentes membranes échangeuses d'anions et membranes échangeuses de cations utilisées en électrodialyse conventionnelle pour l'industrie agroalimentaire. Certaines de ces membranes sont du type homogène et d'autres du type hétérogène. La méthodologie suivie tout au long de ce travail est basée sur la comparaison de nombreuses propriétés physico-chimiques, structurales et mécaniques d'échantillons neufs et d'autres vieillis dans un module d'électrodialyse industriel (*in-situ*) ou selon des protocoles que nous avons mis au point en laboratoire (*ex-situ*).

L'étude du vieillissement *in-situ* des différentes membranes échangeuses d'ions utilisées dans le traitement des acides organiques et dans la déminéralisation du lactosérum nous a permis de confirmer que les membranes échangeuses d'anions sont beaucoup plus sensibles au vieillissement que les membranes échangeuses de cations. Par ailleurs, nous avons démontré que les changements dans les propriétés de transport, et donc dans les performances des membranes, dépendent en grande partie des modifications survenues sur leur microstructure. Nous avons apporté des améliorations au modèle microhétérogène pour permettre d'interpréter et de quantifier les conséquences du vieillissement des membranes échangeuses d'ions.

L'effet des opérations de nettoyage sur le comportement à long terme des membranes échangeuse d'ions utilisées dans les opérations d'électrodialyse en agroalimentaire a fait l'objet de notre étude *ex-situ*. Ce vieillissement est effectué par des solutions acides, alcalines ou par cycles alternant les deux solutions, ou également par des solutions oxydantes de type eau de Javel. Nous avons démontré, entre autres, que les cycles de nettoyage acide-base effectués lors des opérations d'électrodialyse en agroalimentaire engendrent d'importantes dégradations sur les membranes échangeuses d'anions et que ce nettoyage est la cause essentielle du vieillissement des membranes échangeuses d'anions homogènes utilisées en électrodialyse pour la déminéralisation du lactosérum.

Une confrontation entre les résultats obtenus par les vieillissements *ex-situ* et *in-situ* nous permet de confirmer leur similarité. Ainsi, nous pouvons proposer que, sous des conditions opératoires bien choisies, les études *ex-situ* sont bien adaptées pour la réalisation d'un vieillissement artificiel contrôlé.

Mots clés : Membranes échangeuses d'ions, électrodialyse, vieillissement, déminéralisation du lactosérum , nettoyage, colmatage

Abstract

The long term behavior of anion and cation-exchange membranes used in conventional electrodialysis for food industry applications was investigated. Some of these membranes were homogeneous and some others were heterogeneous. The approach of this thesis is based upon the analysis of several physico-chemical, structural and mechanical properties of new samples and aged ones in electrodialysis stacks (*in-situ*) or under artificial ageing protocols at laboratory scale (*ex-situ*).

The *in-situ* investigation of different ion-exchange membranes used in the purification of organic acids and in whey demineralization confirmed that anion-exchange membranes are more prone to degradation than the cation-exchange membranes. It was observed, as well, that changes in the transport properties, and subsequently in the membrane performance, are dependant of the modifications of the membrane microstructure. The microheterogeneous model was improved and applied for the interpretation and quantification of the ageing consequences on ion-exchange membranes.

Assessment of the cleaning process effect on the long term behavior of ion-exchange membranes used in electrodialysis for the food industry applications was the objective of the *ex-situ* investigation. The ageing protocols were performed using acidic or alkaline solutions or by alternating both of them, as well as in oxidant bleach solutions. Among other findings, it was proven that the damage caused by the acid-base cleaning cycles provoked severe degradation to anion-exchange membranes. Furthermore this cleaning process was the main cause of ageing of homogeneous anion-exchange membranes in electrodialysis for whey demineralization.

Comparisons between results obtained by *in-situ* and *ex-situ* ageing protocols confirmed their similarity. Therefore, it may be considered that under well-chosen operation conditions, *ex-situ* investigation is a well adapted method for the artificial ageing.

Keywords: Ion-exchange membrane, eletrodialysis, ageing, whey demineralization, cleaning-in-place, fouling